THEORY OF EXPLOSIONS

by

J.H. Lee

R. Knystautas

G.G. Bach

MERL Report 69-10

APR 16 1970

Department of Mechanical Engineering

McGill University

Montreal, Canada   November 1969

PREFACE

The present report is in essence the first draft of a book entitled "Physics of Explosions" prepared by the Authors, although in its present form it is more appropriate to call it "Theory of Explosions" because the chapters on experimental observations are still in the process of preparation. The book had its genesis from a set of lecture notes that one of us (JHL) wrote while on sabbatical leave at the Institut de Mecanique des Fluides at Marseille from May to August, 1969. Professor Henri Guenoche and his students at Marseille supplied the enthusiasm and support towards the completion of the notes which then served as the zeroth draft of the book.

The Authors had been planning to write this book for the past few years but never could seem to find the time off from our research and academic work nor the inspiration to attempt such an endeavor. On the few occasions in the past that we did start to write on a particular topic, we always seemed to discover the inadequacy of the work that had been done and we ended up doing more on it. This process invariably escalated and we found ourselves studying new research problems instead. The same thing happened every time we tried to wrap up some of the past work for publication and unless we were committed to do so for a conference deadline, we couldn't seem to finish that properly either. Hence the lecture notes written practically from memory and away from the stimulation of the familiar research environment did not include many of the things we would have liked to include.

In fact it was immediately evident that the zeroth draft needed much analysis and therefore another one of us (GGB) proceeded in late August, 1969 to rework most of the analysis so that the notation and approach would conform throughout the book. Once back in the familiar

environment we could not help but make further additions to the zeroth draft on the topic of asymptotic self-similar solutions which now constitute Chapter VI.

At the completion of the theory of explosions (Chapters II to VI) it seemed appropriate to include some chapters on experimental results from our past research on explosion and implosion phenomena to round out the book somewhat. This is when RK joined in the effort and subsequently produced Chapter I which in essence summarized the chapters he is at present writing for the envisioned book on the physical aspects of explosions.

Although the majority of the material in the book had its genesis from our own research efforts, not all of it, however, is our own original work. In fact the methods of non-similar solutions which can be considered as the substance of the book such as, for example, the quasi-similarity approach, the perturbation scheme and the method of Porzel have already been developed. Our contributions mainly consist of the exploitation of these methods and their application to the specific problems in explosion and implosion physics that interest us. In the process of doing this we have made a detailed study of their validity and accuracy, in come cases extended these methods and certainly have in all cases completely reworked them over to our own satisfaction using a unified consistent approach and notation.

We regret that we cannot include numerical results of the analyses but with the academic year in full swing, it is practically imposs ble to find the time to plot and ink the couple of hundred curves required. We hope to do this during the summer months in 1970. A note of explanation is necessary to clarify the scantiness of our bibliography. We have included only those works that we are most familiar with. To compile a complete list of references on the subject is a book in itself. However we would

like to point out that we are fully aware of the many contributions in this
field and have benefited from them in our study of the subject.

To properly acknowledge the individuals who played a role in this
work we first list the direct contributions of students past and present:
B.H.K. Lee, on the study of cylindrical detonations and later on theoretical
as well as experimental work on imploding shocks and detonation waves; I.
Shanfield, on cylindrical detonations, particularly on transition phenomena;
V.A. Akinsete, on theoretical studies of collapsing bubbles; W.H. Kyong on
numerical studies of implosions; and finally W. Habashi on the propagation
of shock waves in non-uniform media. J.H.T. Wu contributed generously,
financial support from his own research grant and encouragement during the
early years of the explosion work. The freedom and the atmosphere created
by our former chairman of the Department of Mechanical Engineering, W.
Bruce, are responsible for the rapid growth of the research program. W.J.
Rae of Cornell Aeronautical Laboratories first introduced the Authors to
the various non-similar techniques and whose own work influenced greatly
the subsequent approach of the Authors. P. Savic and E. Panarella of the
National Research Council of Canada who are always such a pleasure to talk
to provided many stimulating discussions throughout the years. A.K. Oppen-
heim of the University of California, Berkeley who demonstrated such great
enthusiasm for the work and whose talents in convincing the scientific
circle of the importance of blast wave dynamics through his talks and
papers gave us a certain amount of stimulation. B.T. Wolfson, our contract
monitor from AFOSR, provided us with such great freedom to explore the
field that made contract work for the AFOSR a pleasure. The National
Research Council of Canada provided financial support for the work since
1965 through various grants under ideal conditions and absolute freedom.
The United States Air Force Office of Scientific Research joined in the

support of this work since 1967.

Our secretary Mrs. Madeleine Gagnon, who worked cheerfully through the entire manuscript under the pressure of a normal work load deserves our sincere thanks.

Finally, we express the debt to our respective families without whose continuous sacrifice our research work and the book would have been impossible.

TABLE OF CONTENTS

CHAPTER I

PHYSICS OF EXPLOSIONS

1. Introduction

In the course of the last several years the study of explosions
or explosion related phenomena has attracted unprecedented interest and
consequently a considerable following to the point where there now are
international biennial Colloquia devoted exclusively to this subject. The
full title of these is "International Colloquia on Gasdynamics of Explosions
and Reactive Systems". The first one was held in Brussels in 1967 and the
most recent one at the University of Novosibirsk in 1969. This growth of
recognition of the importance of understanding explosion processes stems
from the realization that this phenomenon is fundamental to many current
technological problems and scientific studies. To quote directly from the
preface to the Proceedings of the first Colloquium, such problems and
studies range "from internal combustion engines and rocket thrust chambers
to hypervelocity guns and nuclear as well as cosmic explosions". In fact
one need only examine the contents of the material presented at the Collo-
quia thus far to see the variety of problems which have close affinity with
the fundamental explosion phenomenon.

What then is an explosion? The term explosion in the context of
the work that is to follow describes the transient gasdynamic dispersion of
energy by the mechanism of shock waves from a concentrated source of extre-
mely high power density. An appropriately illustrative example of such a
phenomenon can be readily created on the laboratory scale. Fig. 1 displays
some spark schlieren photographs of a minute explosion created by a laser
spark in atmospheric air. In this particular example typically 1/3 joule of
energy is deposited within something like 10 nanoseconds and 0.2 mm diameter
yielding power density levels of the order of 10^{16} watts/M^3. Such rapid

SCALE 2 cm
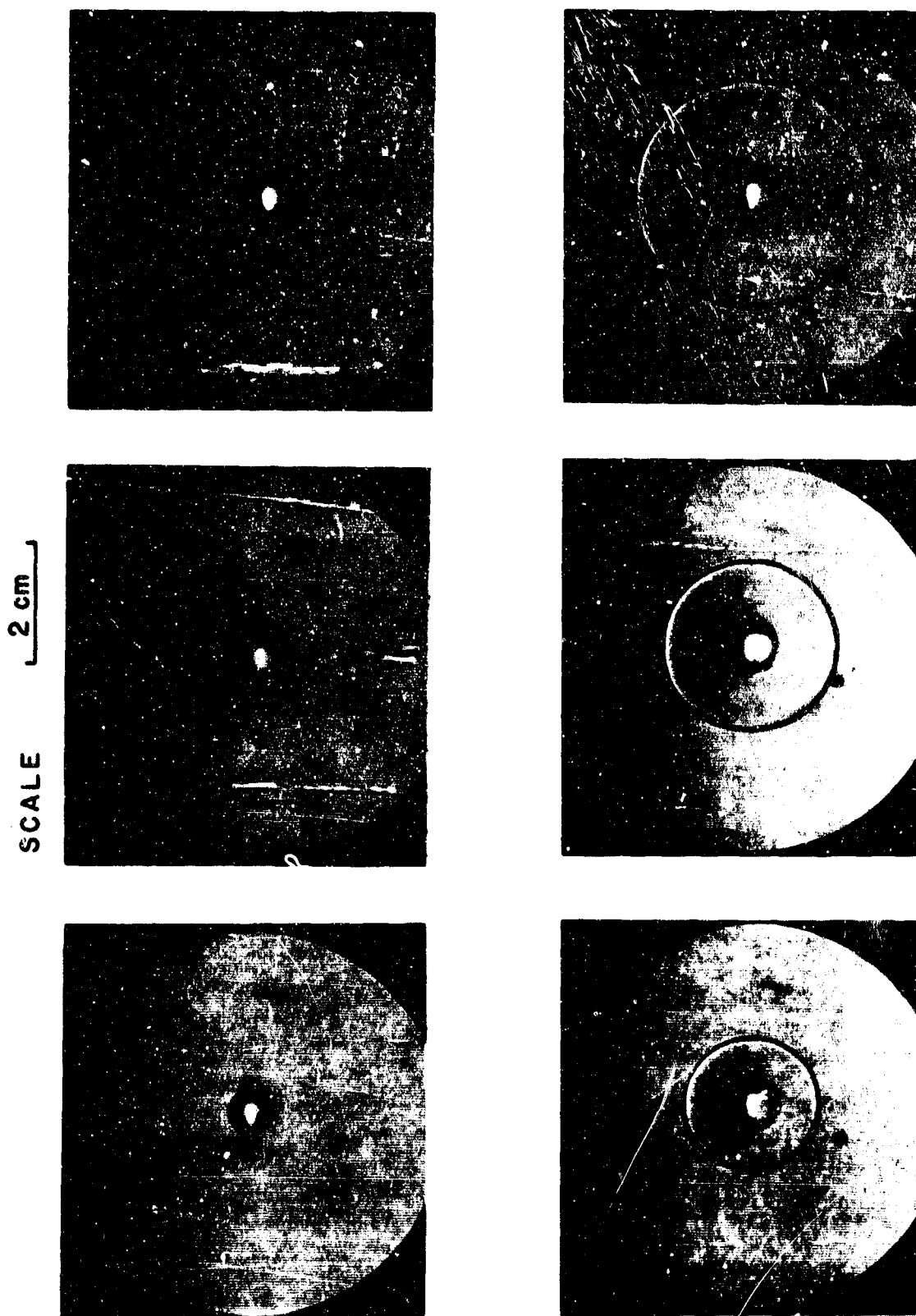
FIG. 1 SEQUENCE OF SPARK SCHLIEREN PHOTOGRAPHS ILLUSTRATING THE PROPAGATION OF A SPHERICAL BLAST WAVE FROM A LASER INDUCED SPARK IN AIR

energy deposition at a miniscule point in a gaseous medium can be achieved
by focusing the output of a Q-switched ruby laser with a very short focal
length lens. It is clearly evident from the photographs that such energy
deposition creates a plasma core which then expands and drives a spherical
shock wave ahead of it into the surrounding medium. The action of the
spherical shock wave is to disperse the virtually instantaneously created
high energy concentration of the laser spark over a wide range of the
medium. Naturally, as the shock wave diverges it is continuously trans-
ferring energy to the medium that it traverses and because it progressively
engulfs more and more of the surrounding medium one would expect that the
shock wave should attenuate or become less and less "energetic". Indeed
shock trajectory measurements plotted in Fig. 2 and shock front pressure
measurements displayed in Fig. 3 for the laser spark initiated spherical
wave described above clearly show its transient decaying character. These
then are the essential features of an explosion where dispersion of energy
from high power density sources into the surrounding medium is through the
mechanism of transient decaying shock waves or blast waves as these are
generally called. Even in the natural environment there too are evidences
of blast waves where, for example, a very common natural occurrence is the
rumble of thunder detected by humans as the passage of a "pressure wave"
over the eardrums. This is but a decayed remnant of an originally powerful
blast wave created in a localized region of the atmosphere by lightning
which is nothing more than the rapid discharge of a "meteorological conden-
ser bank".

Since the early sixties the Shock Wave Physics Group at McGill
University has been engaged in the study of the fundamental mechanisms of
gaseous detonative combustion. The close affinity between explosion pheno-
mena and such combustion was recognized at the very early stages of this
study. Such recognition was derived from extensive laboratory experiments
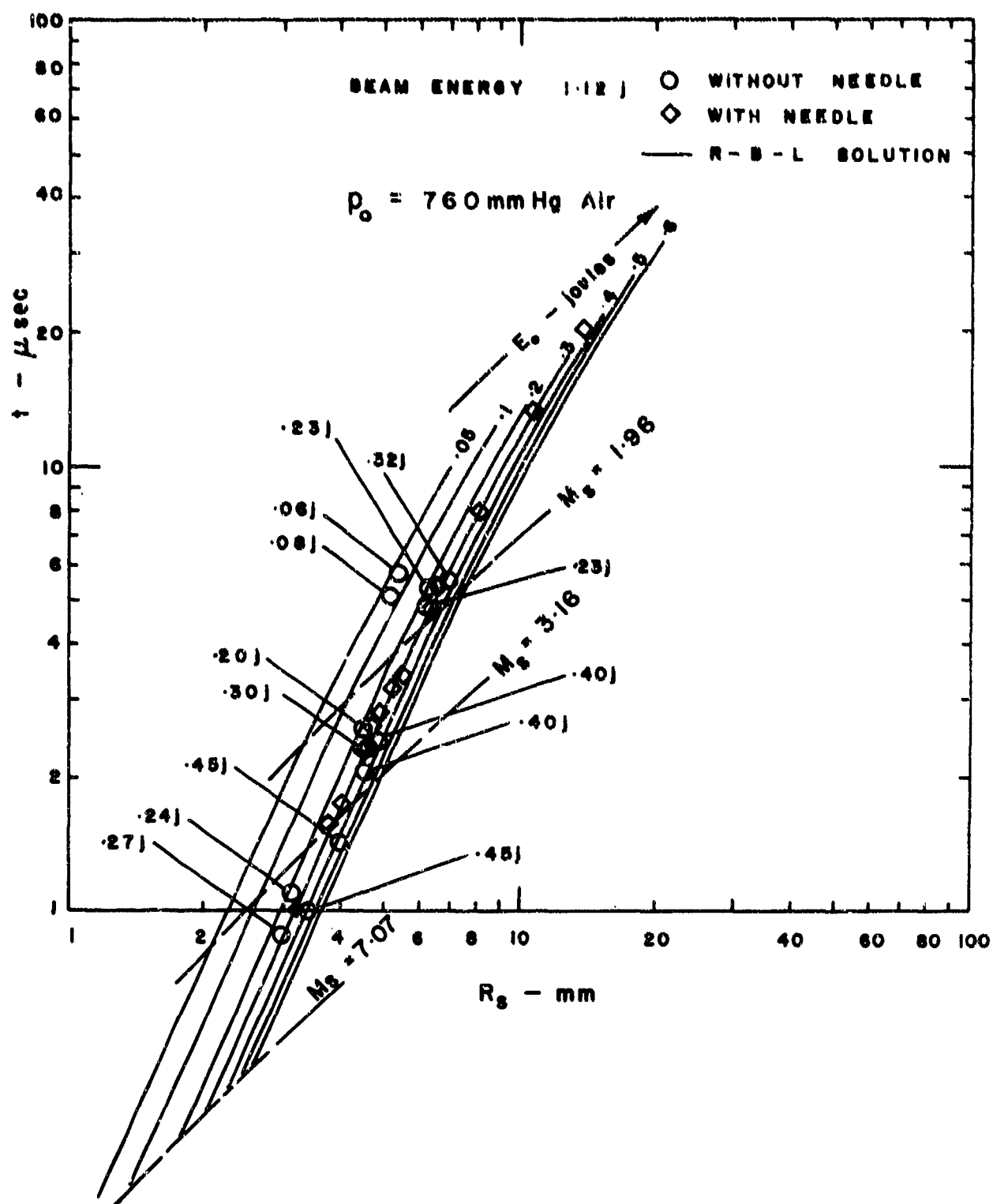
FIG. 2   LASER SPARK INDUCED BLAST TRAJECTORIES IN ATMOSPHERIC AIR
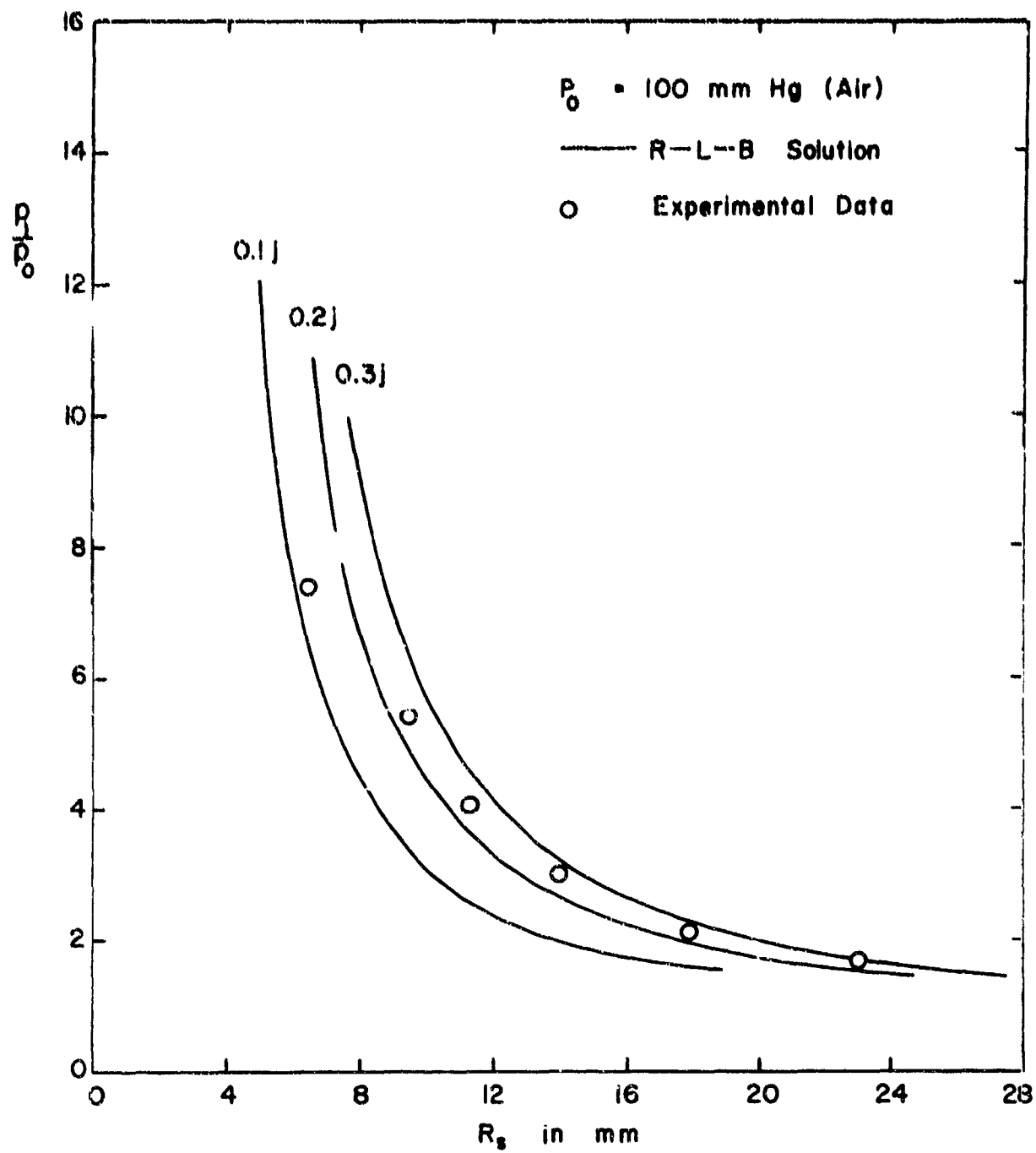
FIG. 3 DECAY OF BLAST PRESSURE WITH RADIUS FOR A SPHERICAL BLAST WAVE FROM A LASER INDUCED SPARK

in our own laboratory in those early years as well as from experimental results accumulated over the last several decades by a number of workers in this field of research. Both our work and that of these others convincingly indicate that detonative combustion invariably exhibits an inherent transient explosive character. Currently this explosion aspect has assumed such overriding importance in contributing to the understanding of the formation and propagation mechanisms of such combustion that we have seen fit to devote the present monograph to this topic and entitle it "Theory of Explosions".

At present, it is generally recognized that the transient explosive character in gaseous detonative combustion is virtually universal. It is evident not only at the inception of the detonation wave but is observed to exist even under supposedly steady propagation conditions as well. The only qualifying distinction that must be made here is that now the explosion phenomena occur in a highly volatile medium as opposed to the inert one associated with conventional explosions. In view of the additional effect of the exothermic chemical energy release, a new terminology appears in order and can be coined to describe such a process namely: chemical explo-sion.

2. Initiation and Formation of Gaseous Detonation Waves

An early inkling in our laboratory of the explosive character of gaseous detonations struck us at the time in late 1962 when we were trying to initiate diverging detonation waves. The question arose as to whether it is or is not possible to have steady diverging C-J detonation waves because from the theoretical point of view there was some uncertainty. Jouguet and Courant and Friedrichs had shown that steady diverging C-J detonations do not exist and decay as they expand. Yet, from the analyses of Taylor and Zeldovich steady diverging detonation waves can propagate, once initiated. How-

ever, the Taylor-Zeldovich model requires certain unrealistic conditions to be satisfied if C-J conditions are to be imposed. From our own point of view we felt from theoretical reasoning (Lee et al, 1965) that diverging detonations could exist at least initially only in either the overdriven state or in the weak state, more likely it being the former. Such a wave would then decay to a C-J wave asymptotically at large radius.

These notions inevitably led to experiments for which we chose the cylindrical geometry for a number of obvious conveniences. These experiments did indeed show that direct initiation of a cylindrical diverging detonation requires the impulsive or explosive release of a finite quantity of ignition energy leading, at least initially, to an overdriven wave, a blast wave of sorts in a detonating gas. Parametric measurements of the variation of initiation energy with composition and initial pressure in oxy-acetylene mixtures are displayed in Figs. 4 and 5, respectively, which are taken from the paper by Lee et al (1966) on this subject.

There had been other experiments with spherical waves by Laffitte, Manson, Zeldovich and several others all of which led to the same conclusion namely that direct initiation of such waves required the explosive release of a relatively large quantity of initiation energy. These critical energy measurements were thus catalogued for cylindrical and spherical detonation waves in a variety of mixtures using different methods of initiation. From the physical point of view these measurements appeared plausible since direct or instantaneous initiation of detonation waves, irrespective of their geometrical configuration be they planar, cylindrical or spherical, implies an impulsive and localized deposition of energy in order to guarantee a shock wave of sufficient strength for auto-ignition in the shocked medium. This is the necessary precondition for the existence of a detonation wave irrespective of its geometry. For planar waves energy must be
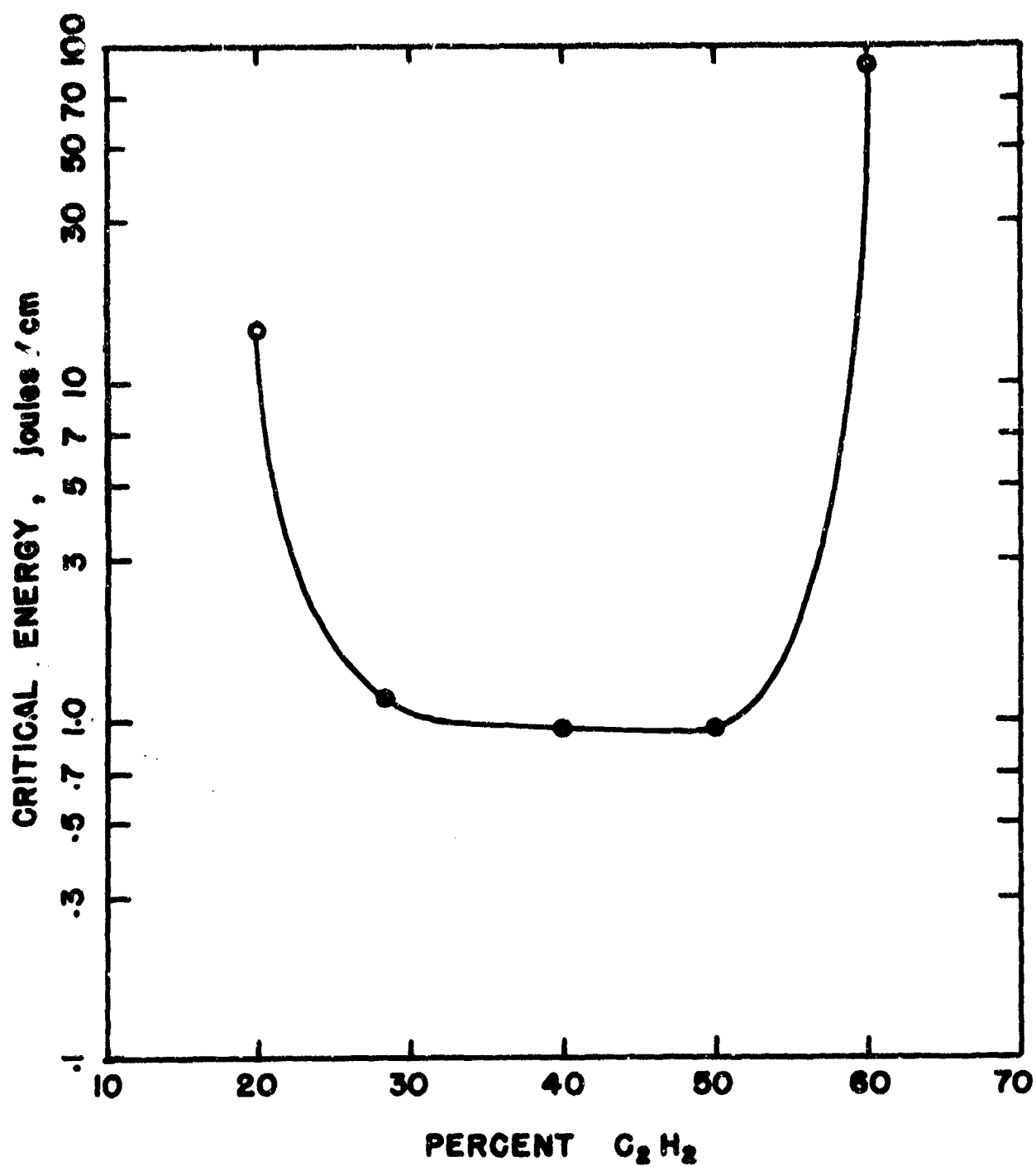
FIG. 4 DEPENDENCE OF THE CRITICAL ENERGY FOR EXPLODING WIRE IGNITION ON
THE MIXTURE COMPOSITION FOR OXY-ACETYLENE MIXTURE AT 100 mm Hg
INITIAL PRESSURE. COPPER WIRES OF 0.003 IN-DIAM ARE USED
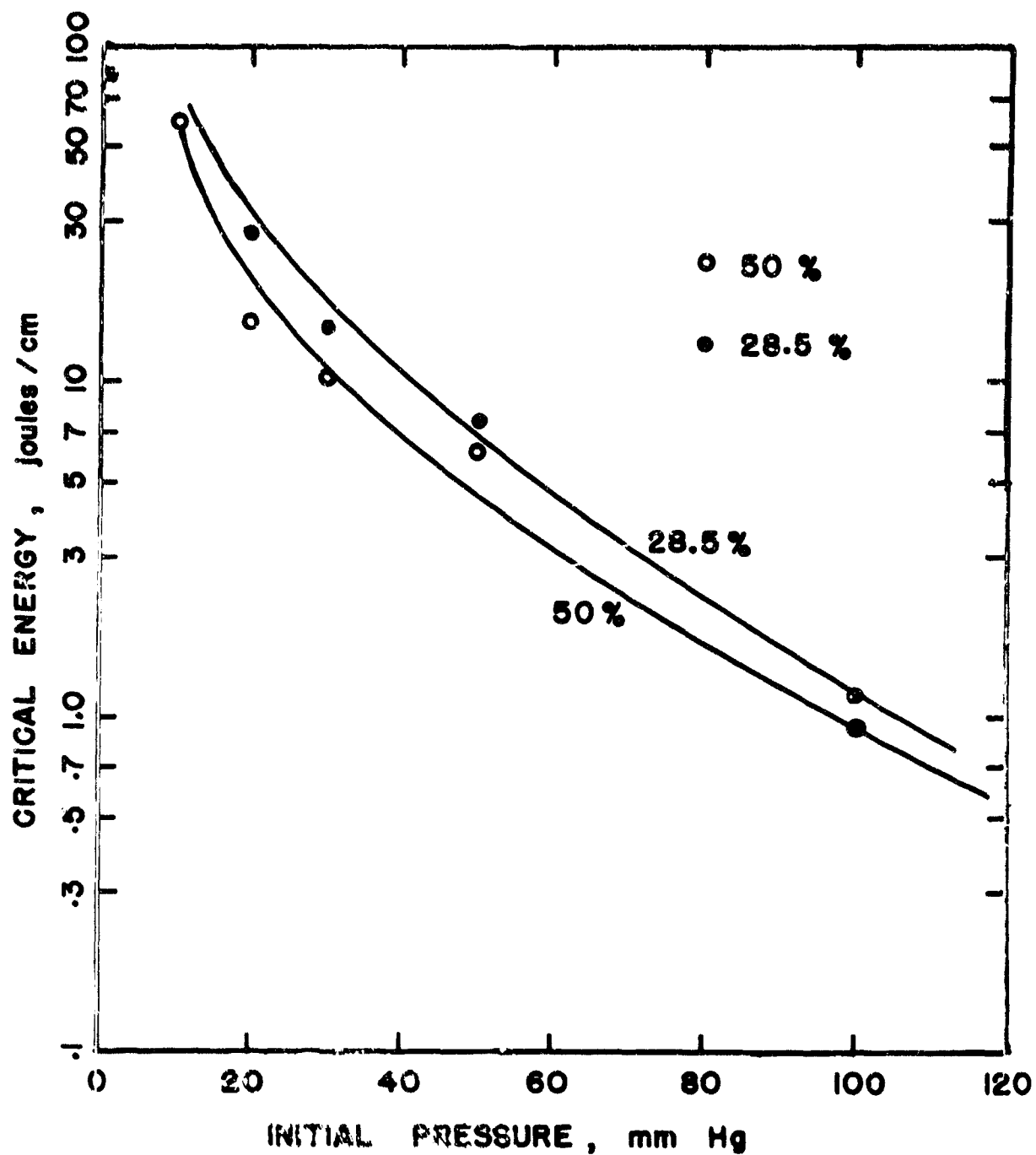
FIG. 5 DEPENDENCE OF THE CRITICAL ENERGY ON THE INITIAL PRESSURE FOR TWO
MIXTURE COMPOSITIONS.   COPPER WIRES OF 0.003 IN-DIAM ARE USED
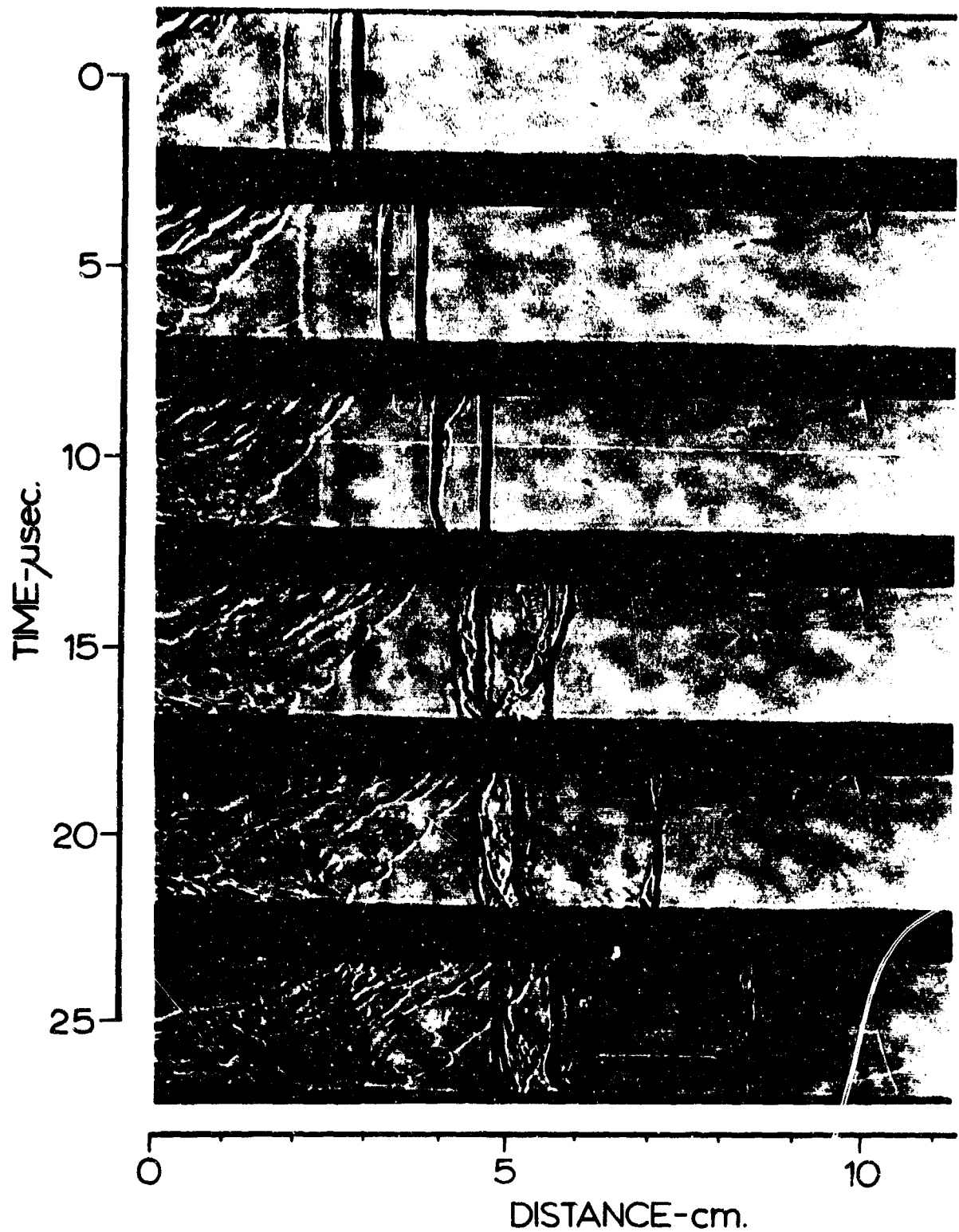
FIG. 6 A SEQUENCE OF STROBOSCOPIC LASER SCHLIEREN PHOTOGRAPHS ILLUSTRATING
TRANSITION TO A PLANAR DETONATION WAVE
(COURTESY: PROF. A.K. OPPENHEIM, BERKELEY)

supplied sufficiently rapidly to generate and drive a shock wave whose strength is at least equivalent to the corresponding C-J Mach number. For diverging detonations, the requirement is for a blast wave at a particular radius which is sufficiently strong to override the severe expansion gradient in its wake in order to maintain and sustain auto-ignition.

Experiments have shown that even where ignition is initially smooth and orderly through the mechanism of a flame, the transition from flame to detonation is nevertheless explosive. In the planar case this is beautifully evident from the by-now classical stroboscopic laser-schlieren photographs of Oppenheim, one sequence of which is displayed in Fig. 6. In these photographs the sudden forward "leap" as a result of the explosive merging of an initially slowly propagating complex of flame front and pre-cursor shock wave train to a detonation front is clearly evident. In the wake of the newly formed detonation are remnants of its violent birth in the form of transient retonation and transverse shocks. The entire transition process from flame to detonation in a linear tube is displayed more completely in Fig. 7 which is a self-luminous streak photograph obtained by Lee et al (1966) for the reinitiation of a detonation after quenching by an orifice inserted to obstruct the incident detonation wave. A laminar flame propagates from the orifice and later develops into a highly turbulent one leading to the abrupt transition to detonation. The associated retonation and transverse waves are clearly in evidence attesting to the explosive character of the process.

In geometries other than planar, transition from flame to detonation exhibits a similar explosive character in such instances as well. Lee et al (1964) report, for example, transition results for cylindrical diverging waves and here too, at least within the span of their experimental chamber, such a process appears to rely on the turbulence level of the cylindrical flame to increase the burning rate and lead to detonation.
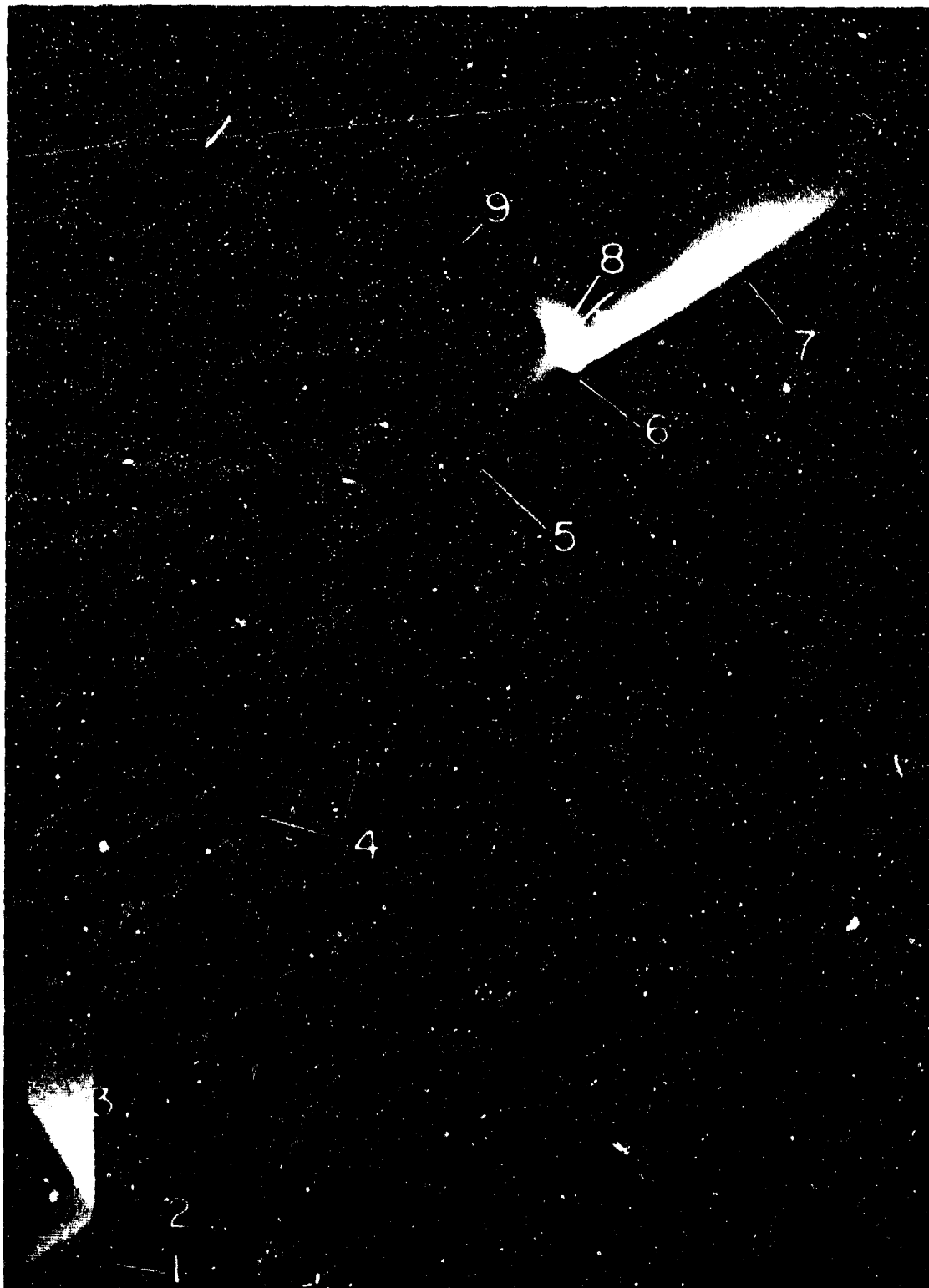
FIG 7 SELF-LUMINOUS STREAK PHOTOGRAPH OF FLAME FORMATION DOWNSTREAM OF
AN ORIFICE WITH TRANSITION TO DETONATION 1) INCIDENT DETONATION
2) ORIFICE 3) REFLECTED SHOCK 4) LAMINAR FLAME 5) TURBULENT FLAME
6) ONSET OF DETONATION 7) REGENERATED DETONATION 8) TRANSVERSE
WAVES 9) RETONATION WAVE

Nonetheless, Fig. 8 which is a self-luminous streak photograph taken directly from their work, clearly displays the random abruptness of transition. Apparently here spontaneous explosions of trapped bubbles of unburned gas in the wrinkled turbulent cylindrical flame most likely lead to detonation. This type of process appears to be quite universal to transition. For example reverting back to planar waves, Oppenheim observed several modes as to the details of the wave processes at initiation but in a general sense all these involved explosive bursts of exothermic energy in the region of shocked gas confined between the precursor wave train and the original turbulent flame front. The direct consequence of this apparently universal type of localized explosions in the reaction zone is the abrupt emergence of a self-sustaining detonation wave.

Such localized explosions at transition can perhaps be most explicitly illustrated with the sequence of spark schlieren photographs in Fig. 9 for a laser spark initiated spherical reacting wave. From this sequence it is evident that local explosions occur suddenly at isolated spots in the reaction zone forming "detonation bubbles". These then grow and, as illustrated in the streak schlieren photograph in Fig. 10, sweep around and completely engulf the shock sphere.

3. Propagation Regimes of Gaseous Detonation Waves

Broadly speaking, in planar waves one can observe one of three distinct phenomena in a gaseous medium capable of sustaining detonative combustion. First of these is a deflagration wave which in general is unstable and leads to detonation. The second phenomenon is the transient phenomenon of transition from flame to detonation. Finally the third distinguishing phenomenon is the globally steady state planar C-J detonation wave. In a sense, one can talk of propagation regimes in planar waves as being composed of the deflagrative, transition and detonation regimes.

- 14 -
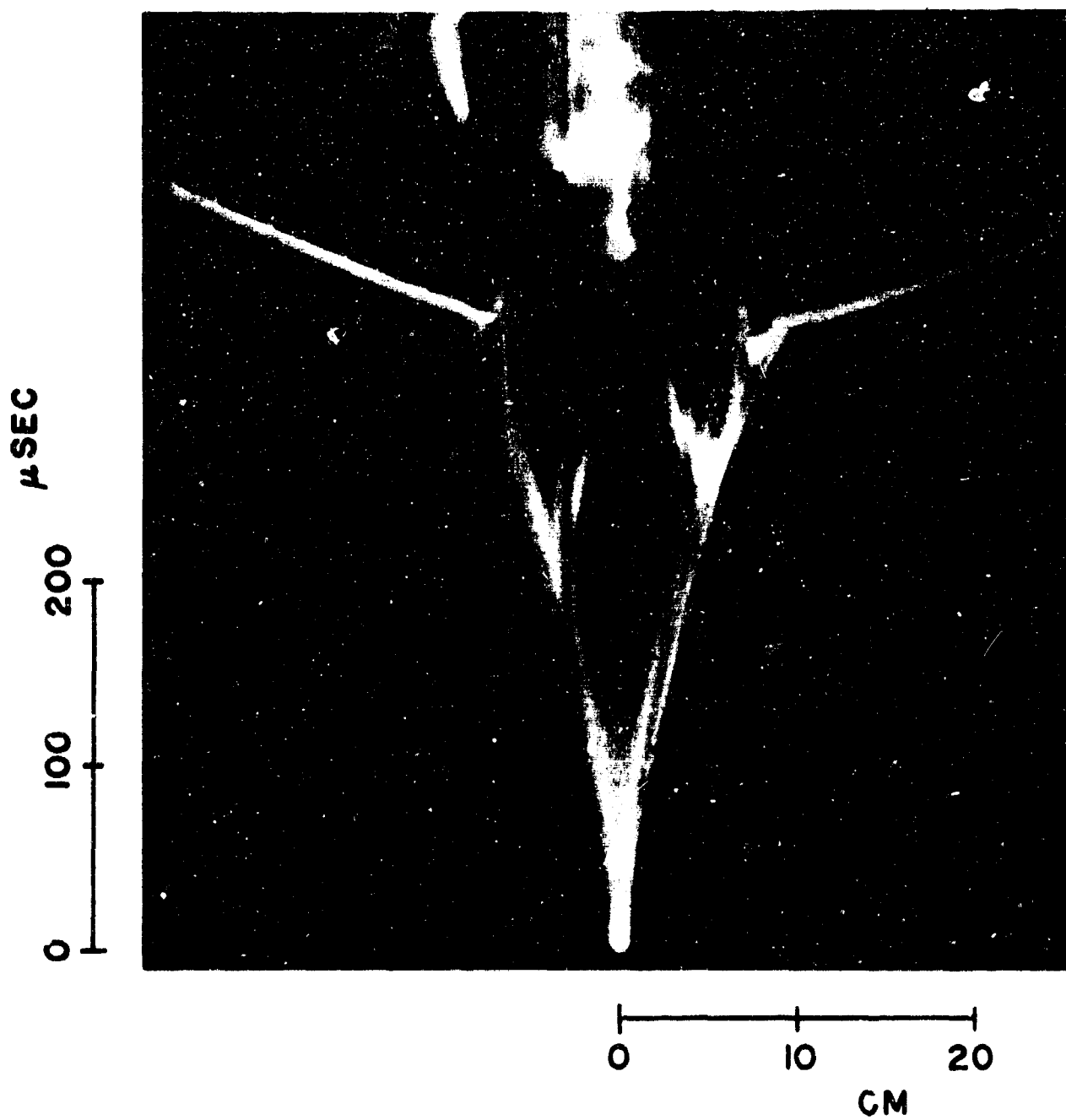
FIG. 8   SELF-LUMINOUS STREAK RECORD OF TRANSITION FROM DEFLAGRATION TO
DETONATION IN A CYLINDRICAL GEOMETRY
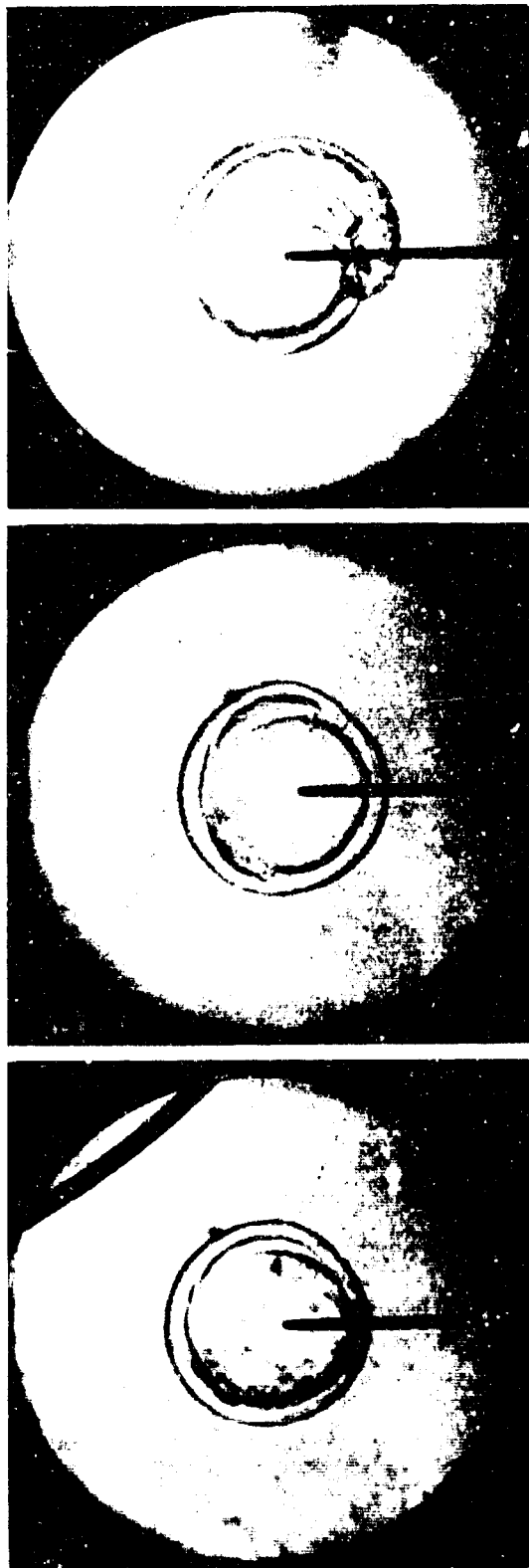
FIG. 9   SEQUENCE OF SPARK SCHLIEREN PHOTOGRAPHS ILLUSTRATING THE FORMATION OF "DETONATION BUBBLES" ON THE SPHERICAL REACTING SHOCK UNDER CONDITIONS OF RE-ESTABLISHMENT

FIG. 10 STREAK SCHLIEREN PHOTOGRAPH SHOWING THE FORMATION OF AN
ASYMMETRICAL SPHERICAL DETONATION WAVE FROM "DETONATION
BUBBLES" IN THE REACTION ZONE

However, outright categorization on the basis of some controlling parameter is not possible since the preponderance of one regime over the other depends on a number of factors such as the nature of ignition, length of tube or channel and so on.

In diverging waves there is a more definite distinction of regimes of propagation. For example, for a long time, based on the experiments by several researchers including ourselves which have already been mentioned, it was felt that there are two distinct regimes of propagation for diverging waves. Moreover, these regimes were distinguished by the magnitude of the initiation energy for a particular igniter. It was an either-or proposition in the sense that if the energy was above a certain critical value direct initiation of a diverging wave occurred and if below a deflagration wave resulted. In our later experiments with laser spark initiation of spherical waves, reported in a paper by Bach et al and in a report by Knystautas, we observed not two but three regimes of propagation based on initiation energy, most probably because we did more meticulous experiments and diagnosed them more thoroughly. These three regimes are illustrated in the streak schlieren photographs in Fig. 11 where from left to right the three regimes are: the subcritical, the critical and the supercritical initiation energy regimes. For mixtures capable of detonating but with initiation energy below the critical value for direct initiation, decoupling of the reaction front from the shock wave occurs, resulting in the decay of the initially overdriven detonation wave to a spherical deflagration wave. A typical sequence of spark schlieren records illustrating the decoupling process is shown in Fig. 12. For spark energies greater than the critical value, as is evident in Fig. 13, no decoupling of shock and the reaction front occurs. The overdriven spherical detonation wave decays continuously to a velocity of propagation corresponding to the theoretical C-J value for that medium. Unlike the previous works, which detected either a deflagration

FIG. 11 TYPICAL STREAK SCHLIEREN PHOTOGRAPHS ILLUSTRATING THE REGIMES OF PROPAGATION
OF SPHERICAL REACTING SHOCKS (MIXTURE: STOICHIOMETRIC OXY-ACETYLENE, P_o = 100 mm Hg;
IGNITION: LASER SPARK)

SCALE [2 cm]

1·6 μsec   4·8 μsec   8·0 μsec

13·0 μsec   22·5 μsec   32·3 μsec
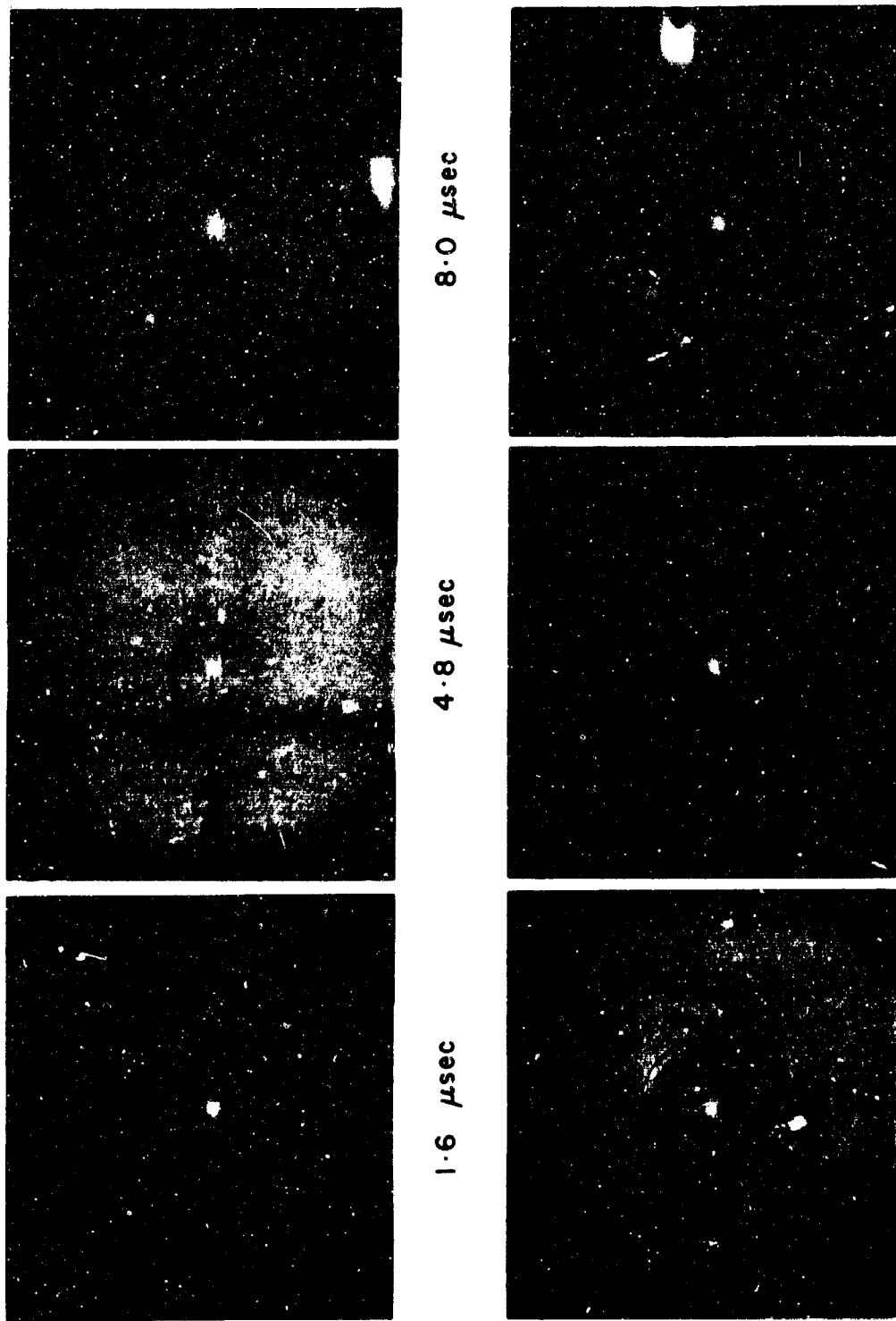
FIG. 12   SEQUENCE OF SPARK SCHLIEREN PHOTOGRAPHS ILLUSTRATING THE SPHERICAL DETONATION WAVE IN THE SUB-CRITICAL INITIATION ENERGY REGIME (MIXTURE: STOICHIOMETRIC OXY-ACETYLENE, P_o = 80 mm Hg, E_o .275 JOULES)

SCALE

2 cm

1·8 μsec

8·2 μsec
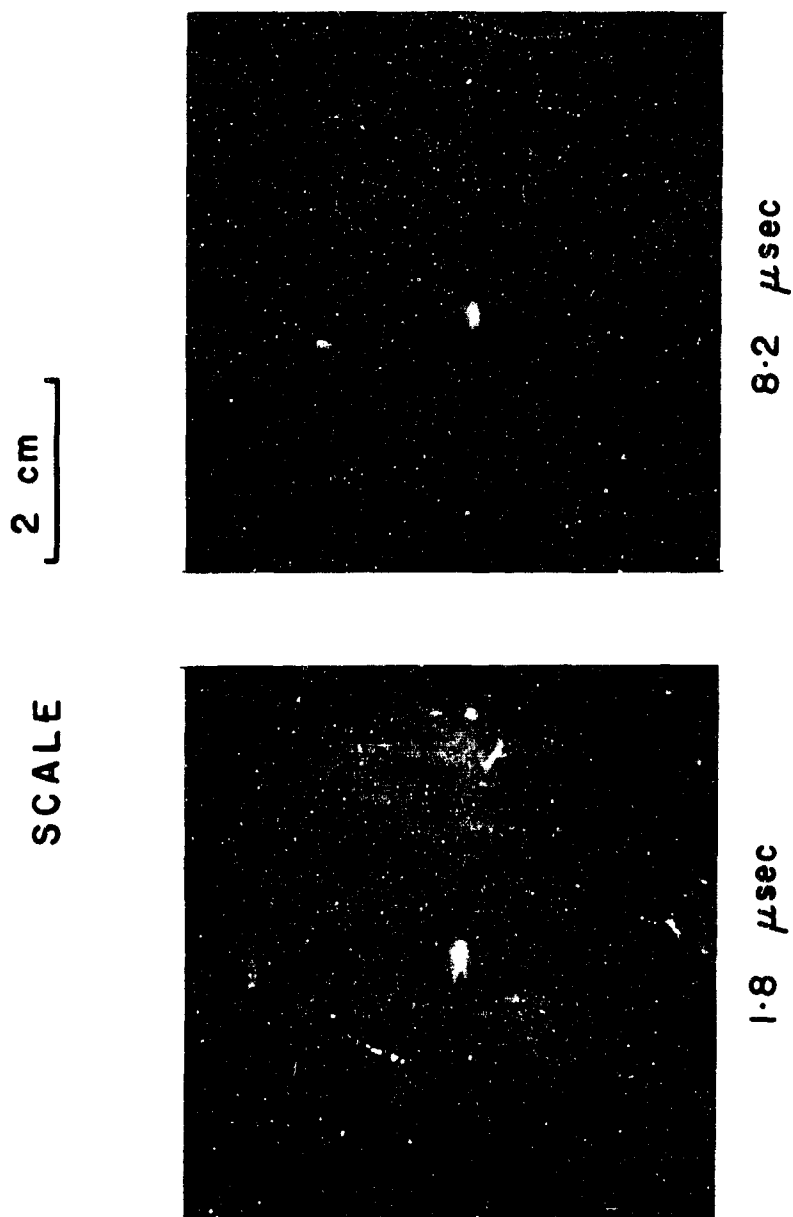
FIG. 13 SPARK SCHLIEREN PHOTOGRAPHS ILLUSTRATING THE SPHERICAL DETONATION WAVE IN THE SUPER-CRITICAL INITIATION ENERGY REGIME (MIXTURE: STOICHIOMETRIC OXY-ACETYLENE, P_o = 120 mm Hg, E_o = .3 JOULES)

or a detonation, we observed a third regime when the spark energy equalled a certain critical value. In this case, the overdriven detonation wave at first decays, and decoupling of shock and reaction zone occurs. However, unlike the subcritical energy regime, where the decoupling progresses in an exponential manner, the decoupling stops in the critical energy regime when the reaction front is a few millimeters behind the shock. Then for the next period of about 10 to 15 μ sec, the shock and the reaction front propagate as a "quasi-steady" complex at a velocity corresponding to a shock Mach number of about 3. During this period instabilities develop and the reaction front takes on a turbulent structure. At the end of this quasi-steady period, local explosions occur suddenly at isolated spots in the reaction zone forming "detonation bubbles" which then grow and completely engulf the shock sphere forming a highly asymmetrical diverging detonation wave. A typical sequence of spark schlieren photographs illustrating this detonation re-establishment phenomenon is shown in Fig. 14. The significant point about the re-establishment regime is that all at once it straddles two distinct types of reactive fronts, namely the deflagrative and the detonative fronts. In the change from one to the other one must note the emergence of a distinct non-uniform structure in the detonation as opposed to the smooth shock-reaction front complex of the deflagration. Moreover, such structure appears to emerge from localized explosions within the shock-flame complex.

4. Structure of Gaseous Detonation Waves

In recent years it has been observed that such localized explosions in fact also characterize the propagation of a supposedly stable self-sustaining detonation wave. This micro-explosive aspect of detonative combustion manifests itself in the structure of the wave. In order to appreciate the full impact of the recognition that micro-explosions and

the observed non-uniform structure in a globally stably propagating detonation wave are interrelated it is relevant at this point to trace briefly the historical evolution of detonation research as it pertains to the structure.

For a long time after the first recorded observations of a detonation wave in a tube in the days of Vieille, Berthelot, Mallard and Le Chatelier such a wave was thought to possess a uniform and unidimensional structure in which combustion occurred in the plane of the shock wave. This is the classical C-J model of a detonation wave. It was only around 1927 that the C-J concept was even slightly assailed when Campbell and Woodhead observed a helical spin associated with a detonation in a tube and a little later Campbell and Finch showed that this was inherent in the structure of the front. In the thirties, Bone, Fraser and Wheeler carried out an exhaustive exploration of spinning waves. Yet in spite of these observations the classical C-J model was still generally accepted as valid. The reason for this was that single spin waves or marginal detonations, as they were sometimes referred to, were considered distinct phenomena in themselves occurring under very restricted conditions near the limits of detonability. In fact the regular period of the spin structure suggested some form of resonant coupling with the tube dimensions and in the light of this Manson and Fay formulated the linearized acoustic wave theory for spinning waves. There followed an extensive series of experimental investigations of spinning waves extending to recent years by numerous people. The foremost among them are the works of Wagner, Duff and Schott in the West and by Soviet scientists, notably Shchelkin and his associates in Moscow and Voitzekhovskii and his collaborators at the University of Novosibirsk.

In the meantime the C-J concept of structure of "non-spinning"

waves had been modified somewhat when it was observed that a detonation wave possessed a finite reaction zone thickness. Appropriate improvements in the one-dimensional C-J theory were made when Zeldovich, Doring and Von Neumann proposed what seemed a more realistic model for the structure of a plane detonation wave. As late as the early fifties Kistiakowsky at Harvard was still carrying out comprehensive experimental studies of planar C-J detonations.

There was a traumatic turning point in the concept of detonation wave structure around the mid-fifties when White and Denisov and Troshin showed that stable C-J waves are non-existent and that in fact planar detonation waves are inherently unstable consisting of an intersecting transverse wave pattern. From their work the transverse structure of "non-spinning" planar detonation waves was deduced to be composed of elemental triple front intersections similar to that in a single spin wave which led Soloukhin to label such waves as "multihead spinning" detonation waves. Moreover it was also deduced at about this time from observations by Soloukhin with cylindrical diverging waves and by Shchelkin and Troshin and Duff and Finger with spherical waves that the transverse structure of unconfined detonation waves is uniform and indistinguishable from that in plane waves.

It was at this point that the emphasis in gaseous detonative research shifted to detailed explorations of and reasons for the wave structure since it was felt that this was the underlying key to the understanding of detonative combustion. In these early efforts a very inform-ative diagnostic tool was the smoked foil where from the "writing on the wall" so to speak, certain inferences as to the behavior of the detonation wave structure could be made. One such record, with slight modification,

is displayed in Fig. 15. This record was obtained by placing into a
circular detonation tube a smoked mylar foil with minute protuberances
punctured into the smoked side. In this manner, in addition to attaining
the by-now characteristic diamond-like pattern traced out by the oncoming
detonation wave, the local interactions of the wave with the protuberances
can be used to trace out the instantaneous detonation front orientation.
From this record it is clearly evident that the transverse diamond pattern
delineates distinctive regions of locally transient curvature. Thus even
this simple experimental record shows that what supposedly is a globally
planar front, really consists of a non-steady three-dimensional structure.

A more detailed representation of what the structure is really
composed of was reconstructed from more refined experiments by a number of
researchers and a schematic representation of the current concept is
displayed in Fig. 16. It seems that the non-uniform three-dimensional
structure of a detonation wave is composed of wave segments and that the
individual wavelets in such a multiheaded front behave similarly to
decaying blast waves in the detonating gas with periodic re-initiation
when two transverse waves collide. The attenuating nature of the wavelets
in-between collisions was confirmed experimentally by Oppenheim who did
meticulous stroboscopic laser schlieren, smoked foil and pressure measure-
ments of wavelet behavior in between collisions. The pressure history of
the wavelets is illustrated schematically in this same Fig. 16. Thus the
individual wavelets expanding from A, B and C can be considered as blast
waves initiated by impulsive energy release at the collision points. As
the wavelets expand, they decay rapidly from their initial overdriven
state to sub C-J conditions. The separation of the shock and reaction
front progressively increases as the temperature at the decaying shock
front decreases. Rejuvenation of the decaying wave occurs as the trans-
verse waves collide at A', B' and C' and the next cycle repeats again.

FIG. 15 SMOKED-FOIL RECORD OF A MULTIHEADED DETONATION AND THE WAVE FRONT GEOMETRY DEDUCED FROM IT
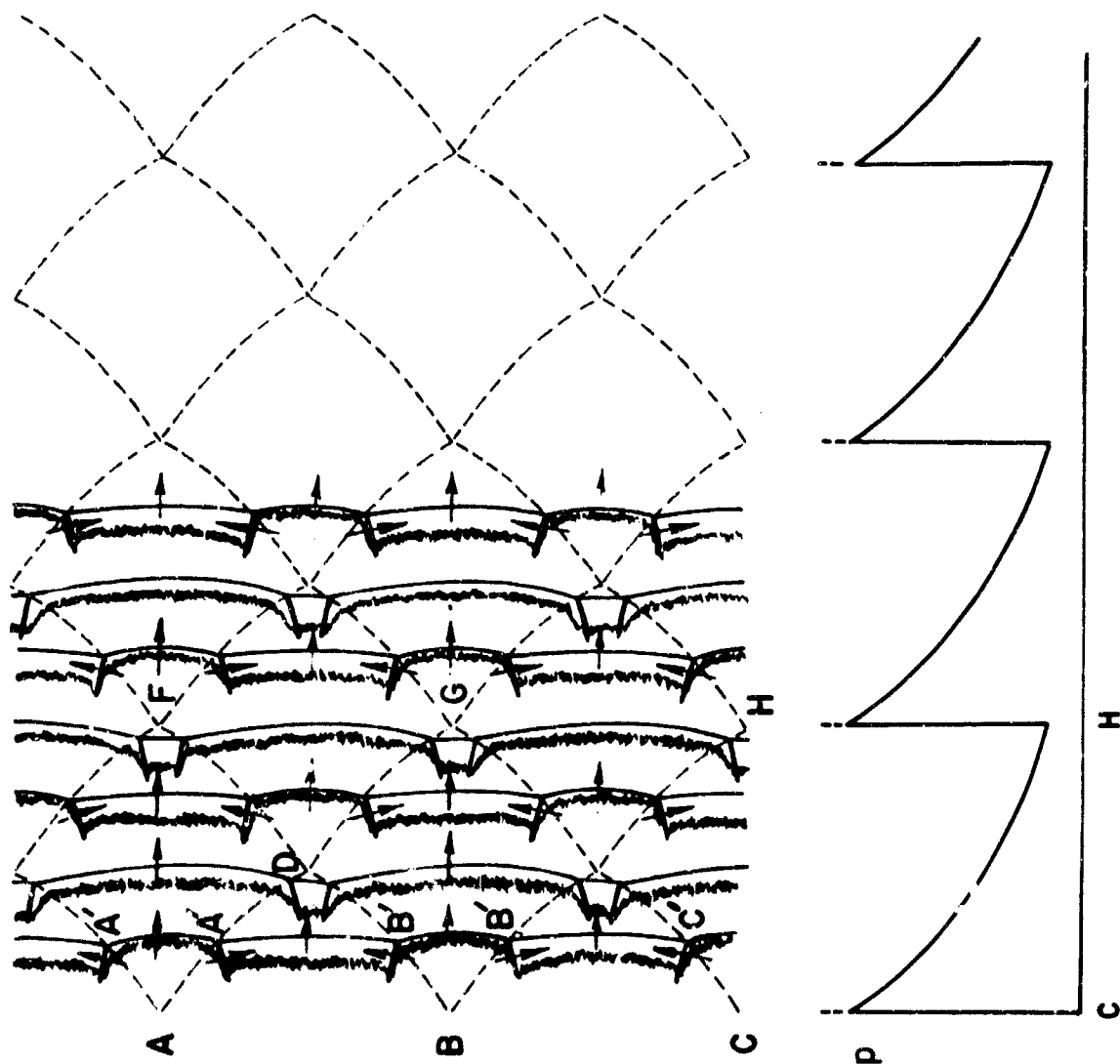
FIG. 16 SCHEMATIC ILLUSTRATING LOCAL DECAY OF A MULTIHEADED DETONATION FRONT BETWEEN COLLISIONS OF TRANSVERSE WAVES

In other words, what appears to be a globally stable detonation wave is really composed of micro-segments which "leap" along in explosive bursts and collectively account for the macroscopic motion of the front. There lies the explosion character of an otherwise steadfast phenomenon.

The question arose as to what happens in a diverging detonation wave where now there is no confinement or some characteristic length to excite resonant acoustic modes of oscillation which can lead to the regular transverse wave structure as in planar waves in tubes and channels. The first question was whether there is any structure in diverging detonation waves in the first place and if so, does the front preserve the uniform structure in view of the additional effect in that the surface area of the front continuously increases as the wave expands. To ascertain both these points we placed a soot film in our cylindrical chamber and obtained the trace displayed in Fig. 17. From this it is clearly evident that there not only is structure but that the structure is uniform proving once and for all the irrelevance of a confining resonant geometry for the existence of a regular transverse wave pattern. What this showed us is that in diverging waves there is an inherent regenerative mechanism which is locally instrumental in continuously creating new transverse waves in a progressively enlarging front. As the wave expands, the time between collisions of transverse waves also progressively increases. If no additional transverse waves are born continuously, then the multihead front fails. The continuous generation of transverse waves is the basic mechanism of propagation of diverging detonation fronts. In Fig. 18, two open shutter photographs of a cylindrical detonation wave are shown illustrating the phenomenon of failure when regeneration of transverse waves is absent and self-sustenance when there exists a continuous regeneration of transverse waves.

In view of the multitude of experiments on the structure of diverging waves there are now strong indications that the mechanism of
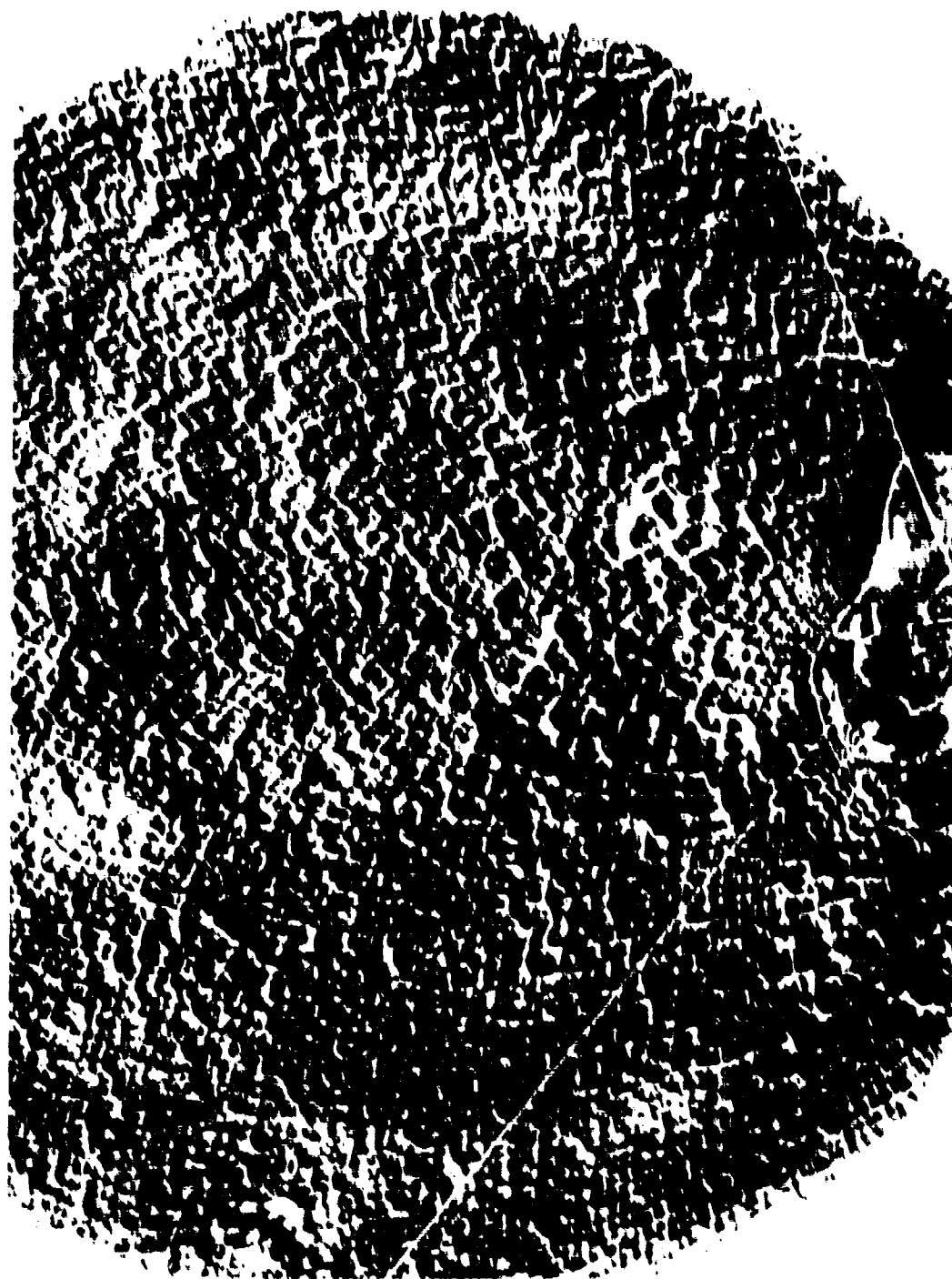
FIG. 17 SMOKED FOIL RECORD OF THE STRUCTURE OF A CYLINDRICAL DIVERGING DETONATION WAVE (MIXTURE: EQUIMOLAR OXY-ACETYLENE, $P_o = 30$ mm Hg). THE CENTER OF SYMMETRY IS LOCATED AT THE INTERSECTION OF THE RADII

FIG. 18 OPEN-SHUTTER PHOTOGRAPHS OF A SELF-SUSTAINING CYLINDRICAL DETONATION WAVE ON THE LEFT, ASSOCIATED WITH MULTIPLICATION OF TRANSVERSE WAVES AND A DECAYING WAVE ON THE RIGHT, DEVOID OF MULTIPLICATION

transverse wave regeneration is due to the formation of explosion centers in the shocked gas behind the decaying front of the blast or detonation wavelet. The spherical blast waves from these micro-explosions coalesce with the main shock front of the decaying wavelet and the subsequent wave interactions produce new transverse waves. The origin of these explosion centers is at present not completely understood but there are qualitative indications in the supporting experimental work reported by Knystautas that their origin may be associated with the sporadic nature of ignition under conditions where auto-ignition in the shock processed gas can occur.

5. The Reactive Blast Wave Model

From all that has been said so far there emerges a similarity in the phenomenological pattern in virtually all the important aspects of gaseous detonative combustion. It seems that chemical explosion in one guise or another characterizes such combustion whether one talks of direct initiation of detonation fronts, indirect creation by natural transition to detonation, the raison d'être of the non-uniform structure or the regeneration of transverse waves in diverging detonations. The pattern of all of these is that of an impulsive concentrated energy release followed by a blast wave propagating into a detonating gas.

It therefore seemed only natural to begin to study the mechanisms of formation and propagation of gaseous detonation waves from the point of view of explosion gasdynamics in detonative media. More specifically, a theoretical model, appropriately dubbed the "reacting blast wave" model, was formulated for such studies. The model is simply the classical point blast wave problem in which a finite quantity of initiation energy E_o is deposited instantaneously $\left(\dfrac{E_o}{\triangle t} \longrightarrow \infty \right)$ at time $t = 0$ at a vanishingly small point in a detonating gas. A strong spherical (or cylindrical if the source is a line) blast wave will be generated which will be followed by

chemical reactions occurring behind the shock front and such a complex will subsequently expand into the stagnant surrounding gas.

One of the important problems that can be clarified by the blast wave model is the criterion for the initiation and existence of a diverging C-J detonation wave. From the classical J-T-Z model the gasdynamic solution obtained shows a singularity in the form of an infinite expansion gradient immediately behind the C-J front. This singularity is a direct result of imposing the C-J conditions on the gasdynamic solution and for overdriven and weak detonations, the singularity does not arise. If the gasdynamic effects of initiation energy are considered as in the blast wave model, then the entire regime of propagation of the detonation wave is non-steady decaying from an initially strongly overdriven detonation near the source to a C-J wave at infinity (asymptotically). Hence no singularity in the solution arises. The implication of the blast wave model is that no steady-state diverging C-J wave exists. If one further extends this statement based on the present status of knowledge on detonative combustion, one can say that steady state C-J detonation waves always do not exist under normal conditions.

In matters other than initiation there are indications, as already discussed, that the processes responsible for the emergence of structure, its sustenance and regeneration in diverging fronts are very similar and appear to resemble point initiated blast waves in a detonating gas. It would seem that the study of the reacting blast wave model could yield some insight into the mechanisms of these processes.

These points were recognized by Lee (1965) in 1963 and the subsequent studies of the Shock Wave Physics Group essentially evolved around the problem of reacting blast waves, particularly in the understanding of the non-linear coupling mechanisms between the chemistry and a transient hydrodynamic flow field. It was recognized that all combustion

processes with high power density lead to instability and the understanding of the coupling could lead to the solution of the complex detonation process. In broad terms the research program was concerned with the study of the formation and propagation mechanisms of diverging gaseous detonation waves but essentially, in simple terms, the problem was to study what happens when a mass of highly detonable gas is processed by a shock wave whose jump conditions are sufficiently strong to result in auto-ignition of the gas medium but where such shock processing is immediately followed by a monotonic expansion in the wake of the shock. In addition, all this is occurring in a transient flow field where both the shock strength and the shock profile are changing with time. The specific problem in question is to investigate if, when and under what conditions such non-linear coupling between the kinetics of the chemical energy release and the hydrodynamics of the transient flow field can lead to a stable self-sustaining diverging gaseous detonation wave.

6. Physics of Collapsing Waves

In fact the main body of this monograph describes the details of a theoretical investigation of explosions, particularly chemical explosions. The subject matter deals with analyses of blast waves in general and more specifically their dynamics in detonative gases. However, there is also a section devoted to the analytical description of an allied problem of implosions which, as outlined in the digression below, has some phenomenological relevance to explosion phenomena in the context of detonative combustion discussed herein.

The study of collapsing wave phenomena was motivated to some extent and began when efforts were made to trace the origin of the micro-explosion centers that appear to be instrumental in the genesis, sustenance and regeneration of detonative structure. For example, some meticulously

detailed observations at transition indicate that a highly wrinkled turbu-
lent flame in the wake of the precursor shock always occurs just prior to
transition. There are actually instances which have been observed, for
example, in Oppenheim's records in planar detonation transition where
tongues of the turbulent flame leap ahead and merge with the precursor
shock conceivably trapping bubbles of unburnt gas. Subsequent collapse
of such bubbles generates implosion waves which upon reflection at the
point of focus, in turn, generate explosions. Such a process for examp'e
could explain the origin of the retonation and transverse wave phenomena
at transition since now a strong explosive wave propagates in all directions
from the center of the bubble.

Oppenheim's records suggest several modes of bubble formation at
transition in planar waves but there is one mode that is of particular
interest because a similar occurrence was observed in laser spark initiated
spherical diverging fronts. The particular mode for the formation of
trapped bubbles of unburned gas is through the multi-layered reaction zone
where in some instances ignition in a shock-flame complex additionally
occurs either right at the shock wave or else in the complex. The new
reaction front and the original flame surface then collapse onto each other.
In the spherical case Figs. 9 and 10 clearly show the multi-layered reaction
zone whereas Fig. 19 illustrates the same phenomenon in a spark schlieren
photograph of a diffracting cylindrical detonation wave.

An experimental and theoretical program was undertaken concurrent-
ly in our research group to study the dynamics of collapsing waves in the
hope of assessing their potential role in the mechanisms of detonative
combustion . Experimentally, the difficulty with these waves had always
been to generate them uniformly at a finite radius. A number of devices
were designed for this purpose exploiting the inherent stability of planar

FIG. 19 SPARK SCHLIEREN PHOTOGRAPH OF A CYLINDRICAL DETONATION WAVE
DIFFRACTING FROM A LINEAR CHANNEL AND ILLUSTRATING THE
MULTI-LAYERED REACTION ZONE

C-J detonation waves. Lee and Lee (1965) exploited this aspect and developed the so-called "deflection" plate method of initiation of implosions. They noted that because of the self-amplifying nature of converging detonation waves, first pointed out by Zeldovich in 1958, their behavior in effect is very similar to that of converging shock waves. In fact in the vicinity of the center of collapse, a converging detonation wave approaches a strong converging shock wave. Thus all the desirable effects of implosions, such as the extremely high temperatures and pressures, can just as readily be achieved through converging detonation waves. The advantages of using converging detonation waves stem from their inherent initial stability and hence ease of their initiation.

In the "deflection" plate technique of Lee, illustrated in Fig. 20, a diverging cylindrical detonation wave is used to initiate a cylindrical implosion. Symmetrical collapse was achieved and a typical self-luminous streak photograph is displayed in Fig. 21 to confirm this. Detonation velocities measured from such a streak record are found to be similar to the corresponding Chapman-Jouguet velocity of that particular mixture. No distinct acceleration of the front can be detected from these records. This, however, is not surprising since relatively large changes in the location of the C-J point on the equilibrium Hugoniot curve make only second-order changes in the detonation velocity. In these experiments a more sensitive parameter such as pressure was measured and typical detonation front pressures taken at different radii are plotted in Fig. 22. The pressure of a planar C-J detonation wave at the same initial pressure as the imploding detonation is used as the reference pressure. Also plotted in this figure is the pressure variation with radius for a strong imploding shock wave based on Guderley's similarity solution and for an imploding detonation wave based on the Chester-Chisnell-Whitham method. To be noted is the extremely
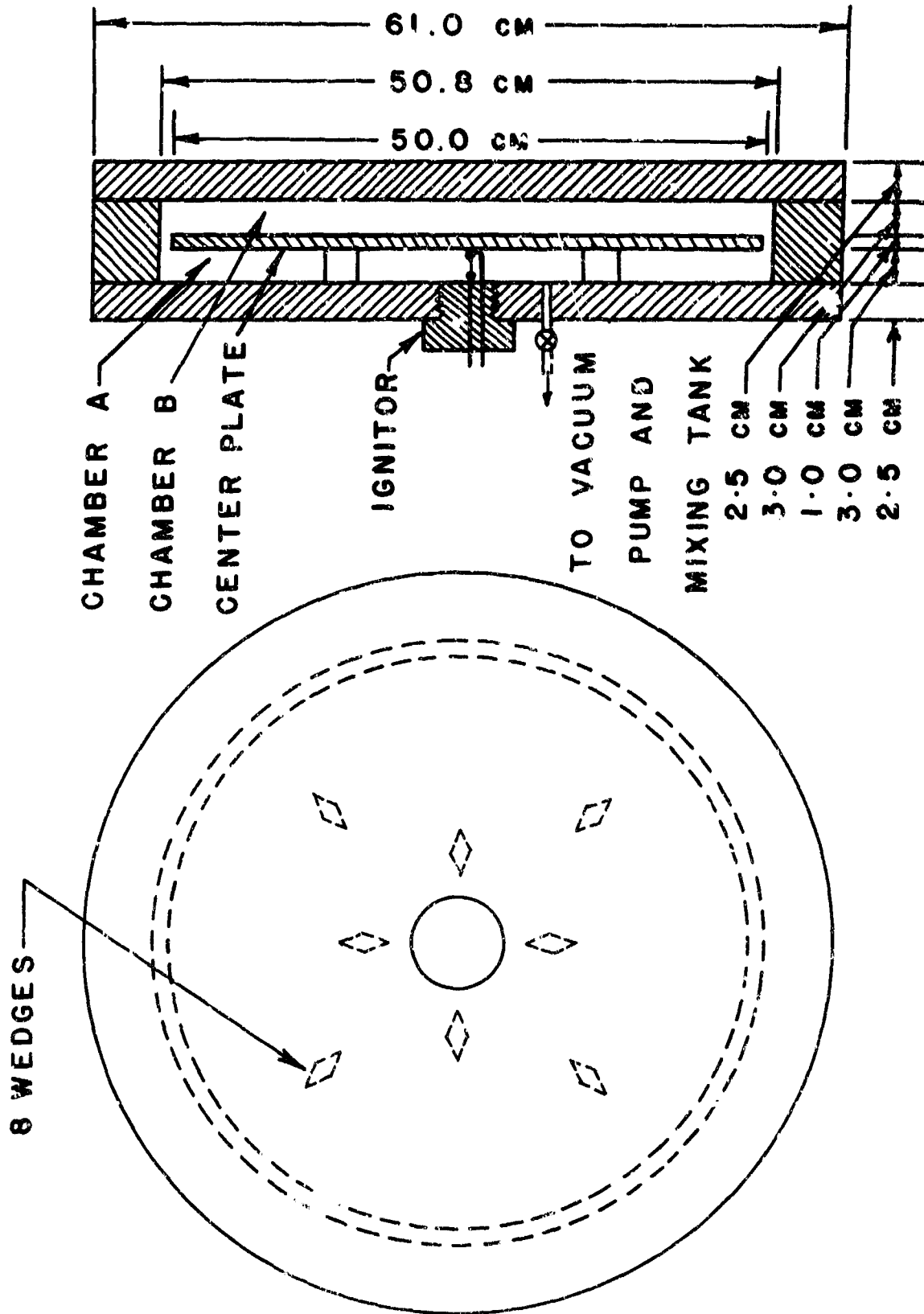
FIG. 20 SCHEMATIC OF THE "DEFLECTION PLATE" METHOD OF INITIATING IMPLODING CYLINDRICAL DETONATION WAVES
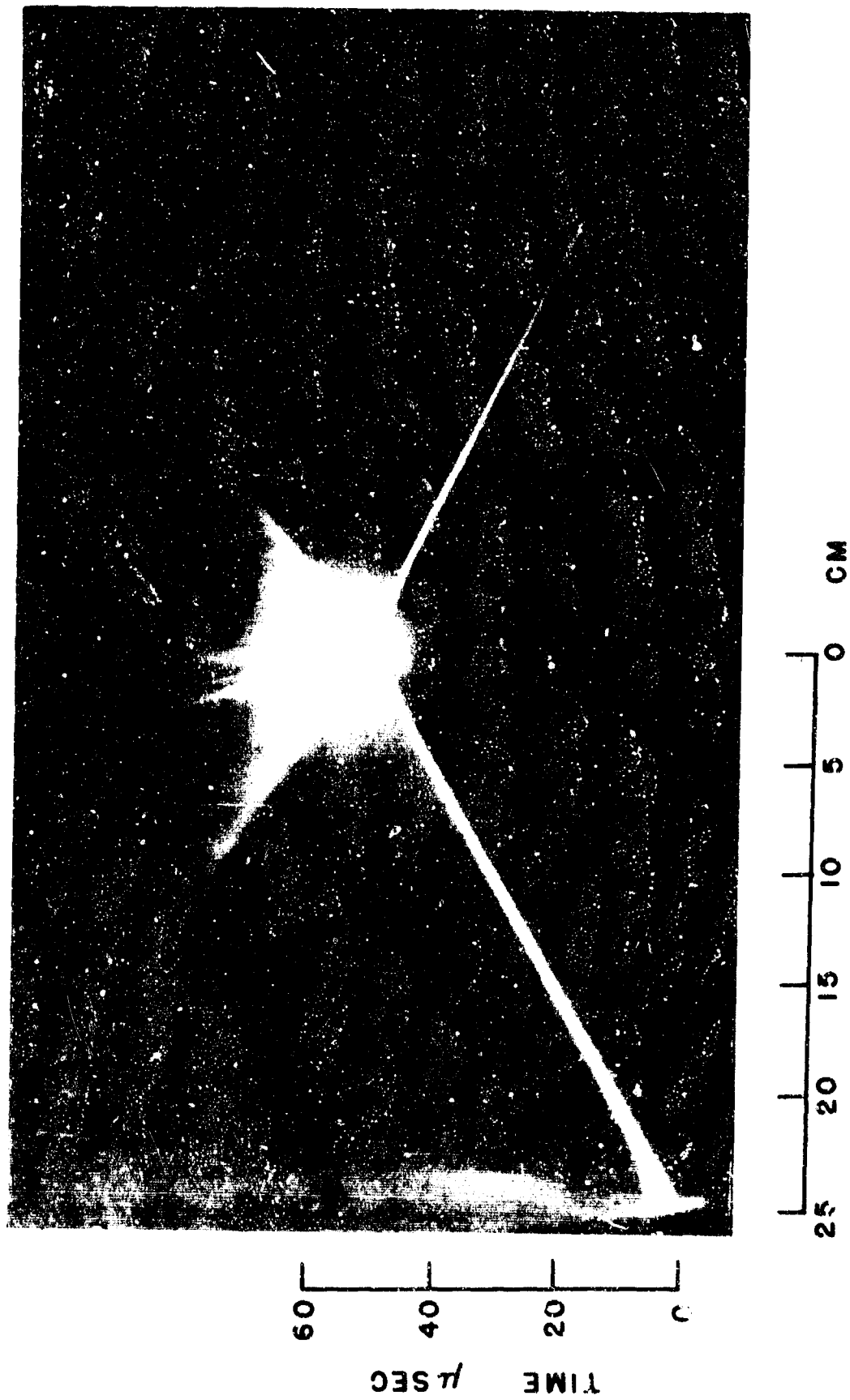
FIG. 21 SELF-LUMINOUS STREAK PHOTOGRAPH OF A CYLINDRICAL IMPLODING DETONATION WAVE (MIXTURE: EQUIMOLAR OXY-ACETYLENE. P_o = 200 mm Hg)
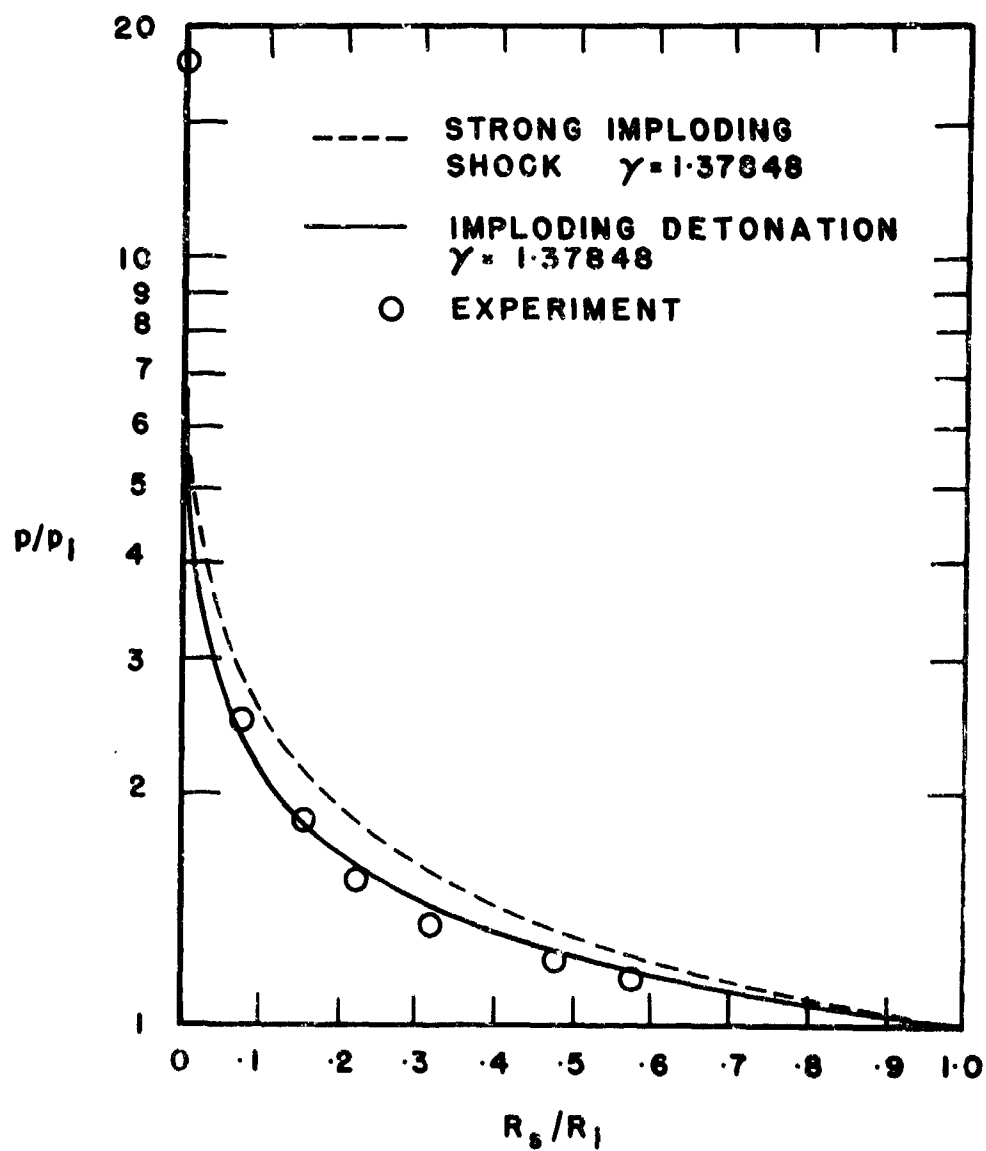
FIG. 22   VARIATION OF DETONATION PRESSURE WITH RADIUS FOR A CYLINDRICAL
IMPLODING DETONATION WAVE IN EQUIMOLAR OXY-ACETYLENE MIXTURE AT
AN INITIAL PRESSURE OF 190 mm Hg.

good agreement between theory and experiment. The important feature that
this figure clearly demonstrates is that cylindrical collapsing detonation
waves amplify as they approach the center of convergence but that significant amplification does not begin until about 1/20 of the initial radius.
This is the reason why such amplification could not be detected on the
streak photographs. However, recently Ahlborn and Hunt, in some very
accurate and detailed observations with an image converter framing camera,
have confirmed amplification of converging detonation waves from trajectory
measurements.

With the Lee "deflection" plate technique of implosion initiation
symmetrical collapse could only be achieved for relatively high initial
pressures making detailed diagnostics of the implosion wave dynamics difficult to carry out. The reason for this is that in the initial stages of
convergence where the detonation wave is forced to undergo an abrupt change
in direction, the diffraction effect was so severe that it limited their
ability to initiate stable implosions to initial pressures in excess of
1/4 atm in equimolar oxy-acetylene mixture. More important, however, the
particular geometrical arrangement of their bomb limits the practical usefulness of their technique in that it does not readily lend itself to
observation of the implosion phenomena. However, the feasibility of using
detonation was for generation of stable implosions was clearly demonstra
ted.

Subsequently a novel technique of initiation was developed by
Knystautas and Lee (1967) whereby the implosion chamber can readily be
adapted to schlieren photographic studies. The technique was suggested by
noting the stable self-sustaining nature of planar detonation waves and
the rapid attenuation of disturbances to the front. Thus it appeared fea
sible that a continuous converging detonation front could be generated by

"par bling" it up from the individual C-J wavelets.

A schematic of the implosion chamber used in these experiments is shown in Fig. 21. It consists of a cylindrical ring (2.5 cm thick, 25 cm i.d., and 40 cm o.d.) with 10 equally spaced holes, 1.3-cm diam, drilled around its periphery. At the inner periphery, the holes are smoothly flared to minimize diffraction effects and at the outer periphery, the holes are joined to a series of equal length plexiglas tubes. At the end of each tube a 1-mm spark gap is placed and these are all electrically connected in series to a 15 μF, 20-kV low inductance capacitor through a three-electrode switch. The side walls of the cylindrical chamber consist of two 2.5-cm thick steel plates with centrally located circular openings to permit the insertion of 10-cm-diam optical quality fused quartz windows.

With this method of initiation the converging detonation wave is formed from the detonation wavelets as they simultaneously emerge into the cylindrical chamber. Hence its initial wave shape is irregular and takes on a polygonal configuration. Where any two segments of the polygonal shaped detonation front collide at an angle, a reflected shock is generated extending radially into the flow behind the front. Depending on the angle between adjacent segments of the polygonal front, the reflections can either be of the "regular" or of the "Mach" type. For Chapman-Jouguet detonations in the equimolar acetylene-oxygen mixtures used in the experiments, the minimum included angle between two intersecting detonation fronts where Mach reflections occur is of the order of 100°. If the initial conditions are such that adjacent segments of the polygonal detonation front reflect regularly, the wave will collapse as a polygon preserving its initial shape without self-amplification. When more points of initiation are used, the polygonal shaped detonation front formed is such that adjacent segments generate "Mach" reflections. The difference in the strength between the Mach stem and the
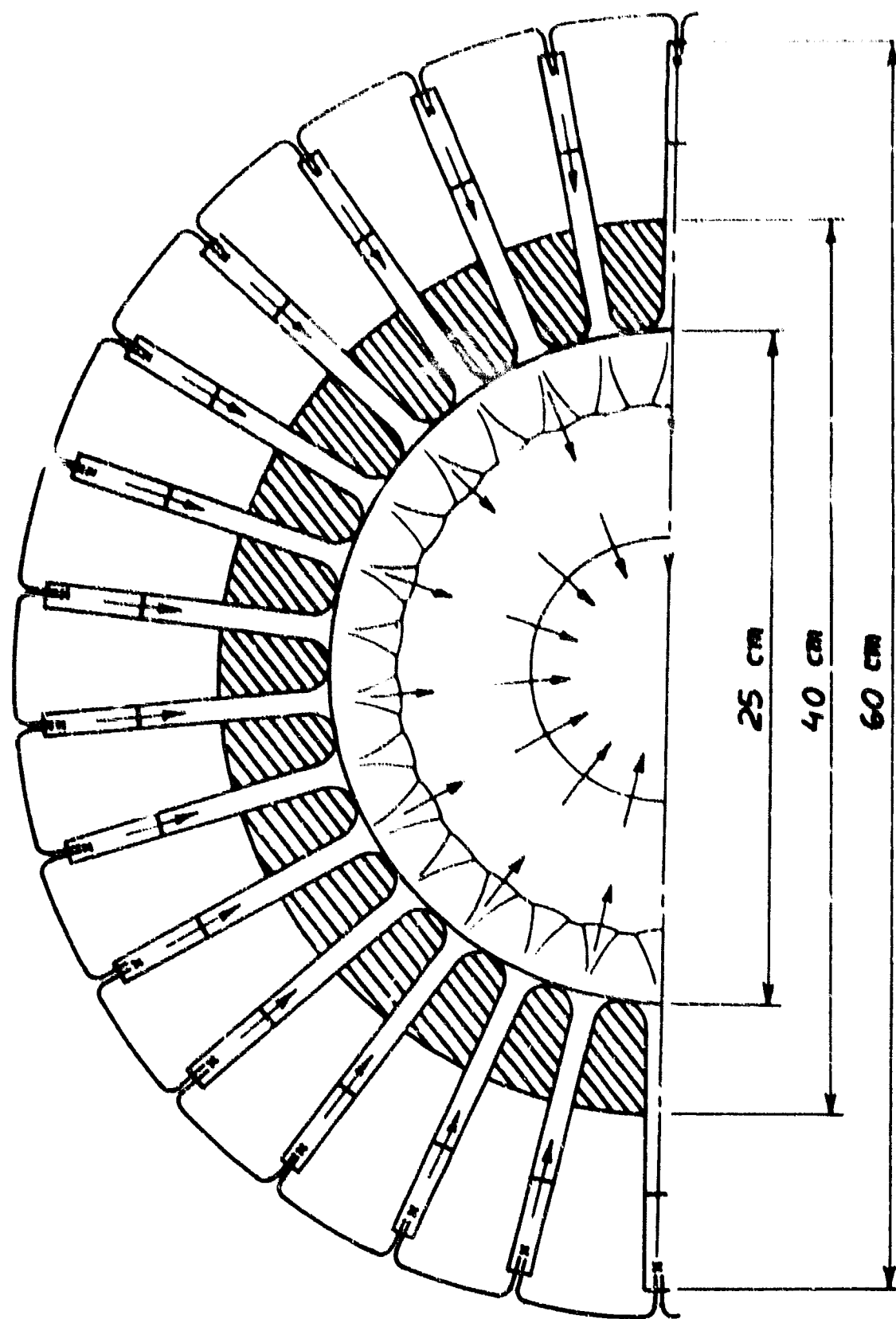
FIG. 23   SCHEMATIC ILLUSTRATING THE METHOD OF INITIATION OF CYLINDRICAL DETONATION WAVES WITH A MULTI-SPARK SYSTEM.

25 CM

40 CM

60 CM

Incident waves causes the reflected shocks to "sweep" in a direction oblique
to the radially collapsing front.

Although these Mach reflections provide a mechanism for strength-
ening the collapsing polygonal shaped detonation wave, the approach to a
smooth cylindrical form from its initial irregular shape requires that the
reflected shocks attenuate as they propagate in the tangential direction.
This attenuation of the reflected shock waves is referred to as the curva-
ture distribution mechanism by Perry and Kantrowitz. They found that for
ordinary shock waves, the attenuation decreases with increasing shock
strength accounting for the decrease in stability for strong converging
shocks. In the present case with converging detonation waves, there are
strong indications that this "curvature distribution" mechanism exists.
In the set of schlieren photographs shown in Fig. 24 taken at an initial
pressure of 100 Torr, one can observe that the polygonal shaped detonation
front does tend to approach a smooth cylindrical form as it collapses. That
the reflected shocks attenuate is indicated by their complete absence in
those parts of the front where the structure is smooth. This is perhaps
better illustrated in the photograph shown in Fig. 25 taken at a slightly
higher pressure of 120 Torr.

Owing to the poor magnification of the present schlieren system,
it is difficult to resolve the wave structure at radii smaller than 0.5 cm.
Hence, whether a true cylindrical shape is achieved in the vicinity of the
center of convergence is as yet unresolved. That stable convergence is
achieved can perhaps be hoped for on the basis that large scale vorticity
in the flow field behind the reflected shock wave (frames (h) and (i) of
Fig. 24) is absent and the presence of the extremely bright flash generated
at the collapse point. Spectroscopic measurements of temperature and pres-
sure probing in the region of the center of collapse indicated that for

FIG. 24 SPARK SCHLIEREN PHOTOGRAPHS OF AN IMPLODING CYLINDRICAL DETONATION
WAVE TAKEN AT SEQUENTIAL TIMES. EACH PHOTOGRAPH IS OF A DIFFERENT
DETONATION WAVE

FIG. 25   SINGLE FRAME SCHLIEREN PHOTOGRAPH OF AN IMPLODING CYLINDRICAL
          DETONATION WAVE

equimolar oxy-acetylene mixtures at an initial temperature and pressure of
300° K and 100 torr, the temperature and pressure at the center of collapse
of a cylindrical detonation wave are of the order of $200,000^o$ K and 130
atm, respectively.

The results of these experiments indicate that for converging
detonation waves a curvature distribution mechanism exists whereas none
exists for converging shock waves of similar initial strength. It should
be noted that the non-uniform flow structure observed is characteristic of
the particular method of initiation, where a polygonal-shaped front was
generated and transition to a smooth cylindrical front depends on the mul-
tiple shock reflections. With other methods of initiation a more uniform
flow structure should be attainable. One important point that these expe-
riments do point out is that it is possible to achieve arbitrarily high
levels of thermodynamic states in the neighborhood of the point of focus
even from collapsing polygonal waves. It is evident then that these ele-
vated thermodynamic levels are no indication that the collapse is stable
and such cumulation should not be confused with the theoretically limit-
less cumulation which can be approached with nearly perfectly symmetric
collapse. These points are particularly relevant to practical applications
of the implosion principle such as that, for example, of Glass where he has
devised a hemispherical implosion device as a driver for a hypervelocity
launcher. In his case he has applied a thin liner of solid explosive to
the inside of a hemispherical shell. A gaseous diverging detonation wave
is used to initiate the solid explosive shell thereby creating a strong im-
ploding wave which upon collapse is presumed to achieve extremely high
thermodynamic states to drive a projectile down the barrel. Glass has used
imprints on a witness-plate to assess the efficiency of his implosion device.
However, our observations in the experiments just discussed clearly indicate
that to assess the stability of the imploding wave and hence the degree of

cumulation ultimately achieved only direct measurements must be used. Indirect passive observations such as witness-plate imprints cannot distinguish one way or the other between attainment of arbitrarily limited levels of cumulation associated with nearly perfect symmetry.

Suffice it to say that currently a device is now available (although new approaches are still being explored) which is capable of producing nearly perfect symmetrical collapsing cylindrical detonation waves. A schematic diagram showing the essential features of the implosion device is shown in Fig. 26. Ignition and instantaneous detonation formation are achieved by a high energy spark discharge (i.e., 80 joules from a 10 μf capacitor at 4 KV) at the conical end of the coaxial tube. The detonation then expands in the diverging conical wave guide to form an annular detonation wave which then propagates down the straight portion of the coaxial tube towards the implosion chamber. To minimize the effects of attenuation as the detonation diffracts around the corner, the annular detonation is first amplified prior to entering the implosion chamber. This is achieved by a gradual 10° area convergence of the annular passage. Diffraction of the highly overdriven detonation wave into the implosion chamber occurs at the minimum area (i.e., 5 cm). Due to the small cross-sectional area and the highly overdriven state of the detonation wave when diffraction takes place, the attenuation and the non-uniformity it suffers have little effect on the subsequent symmetry of the imploding wave. The cylindrical implosion is essentially generated instantaneously by a powerful line source. A gradual 20° area divergence then controls the expansion of the imploding wave before it enters the constant width chamber. The implosion device is 1 meter long and the dimensions of the constant width implosion chamber are 8 cm diameter by 1 cm thick. The success of the present scheme is based on the principle that all changes in cross-sectional area are made very gradual
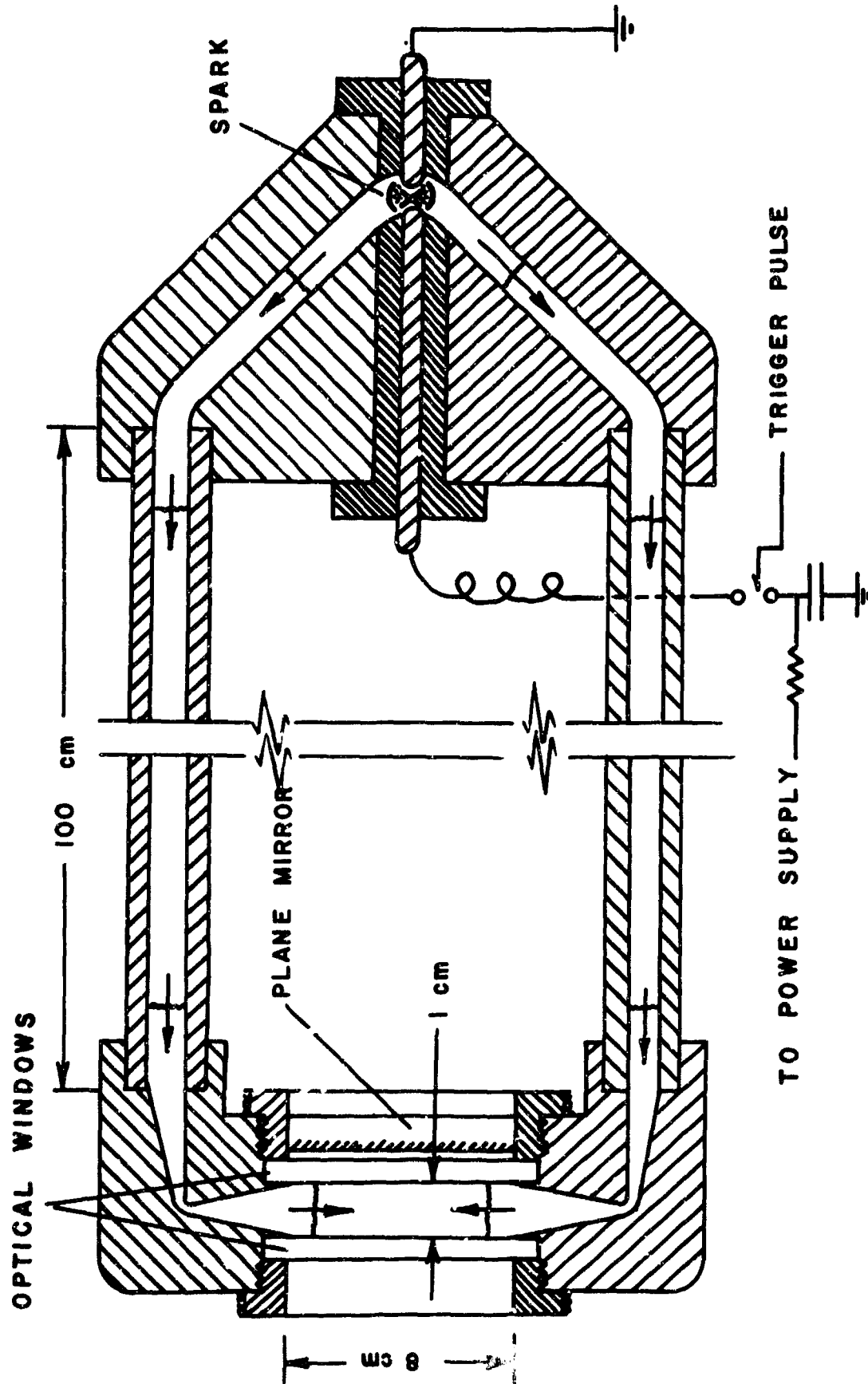
FIG. 26 SCHEMATIC DIAGRAM OF THE CYLINDRICAL IMPLOSION CHAMBER USING THE WAVE-GUIDE PRINCIPLE OF INIATION

and diffraction effects are minimized by the high amplification of the wave prior to diffraction.

A typical set of schlieren photographs of a cylindrical implosion at an initial pressure P_o = 50 torr in equimolar oxy-acetylene mixture is shown in Fig. 27. Each picture is of a different firing and the shot-to-shot jitter for the same time delay setting is within the spatial resolution ($\sim$ 1 mm) of the photographs. Note the nearly perfect cylindrical symmetry of the detonation wave at the different stages of its collapse. The center of convergence of the wave coincides with the center of symmetry of the implosion chamber within the spatial resolution of the photographs. This enables diagnostic techniques which have the probe position referenced with respect to the chamber (e.g., pressure measurements with piezoelectric transducers) to be used. The bright spot at the center of collapse signifying the high temperatures obtained is not apparent in these photographs. This is due to the very large f-stop used in the schlieren camera to prevent fogging of the film from the self-luminosity of the detonation products. It was found that such perfect cylindrical symmetry can be obtained with the present initiation scheme for initial pressures as low as 25 torr.

Within the experimental error of the time measurement of 0.5 μsec, the shock trajectory is practically a straight line, and the velocity determined from its slope corresponds to the Chapman-Jouguet velocity of the explosive. However, the shock velocity is quite an isensitive parameter since it is proportional to the square root of the slope of the Rayleigh line. Large changes in shock pressure can occur with the corresponding second order changes in shock velocity falling well within the present experimental scatter. From theoretical considerations the time exponent N of the shock trajectory (i.e., $R_s \sim t^N$) varies from unity for a Chapman-Jouguet detonation to N = .835 for a strong cylindrical shock. It would be extremely difficult to detect such small changes in the propagation law from experi-

SCALE
50 mm

t = 2·1 μsec

t = 4·5 μsec

t = 8·2 μsec

t = 10·7 μsec

t = 12·1 μsec

t = 14·1 μsec
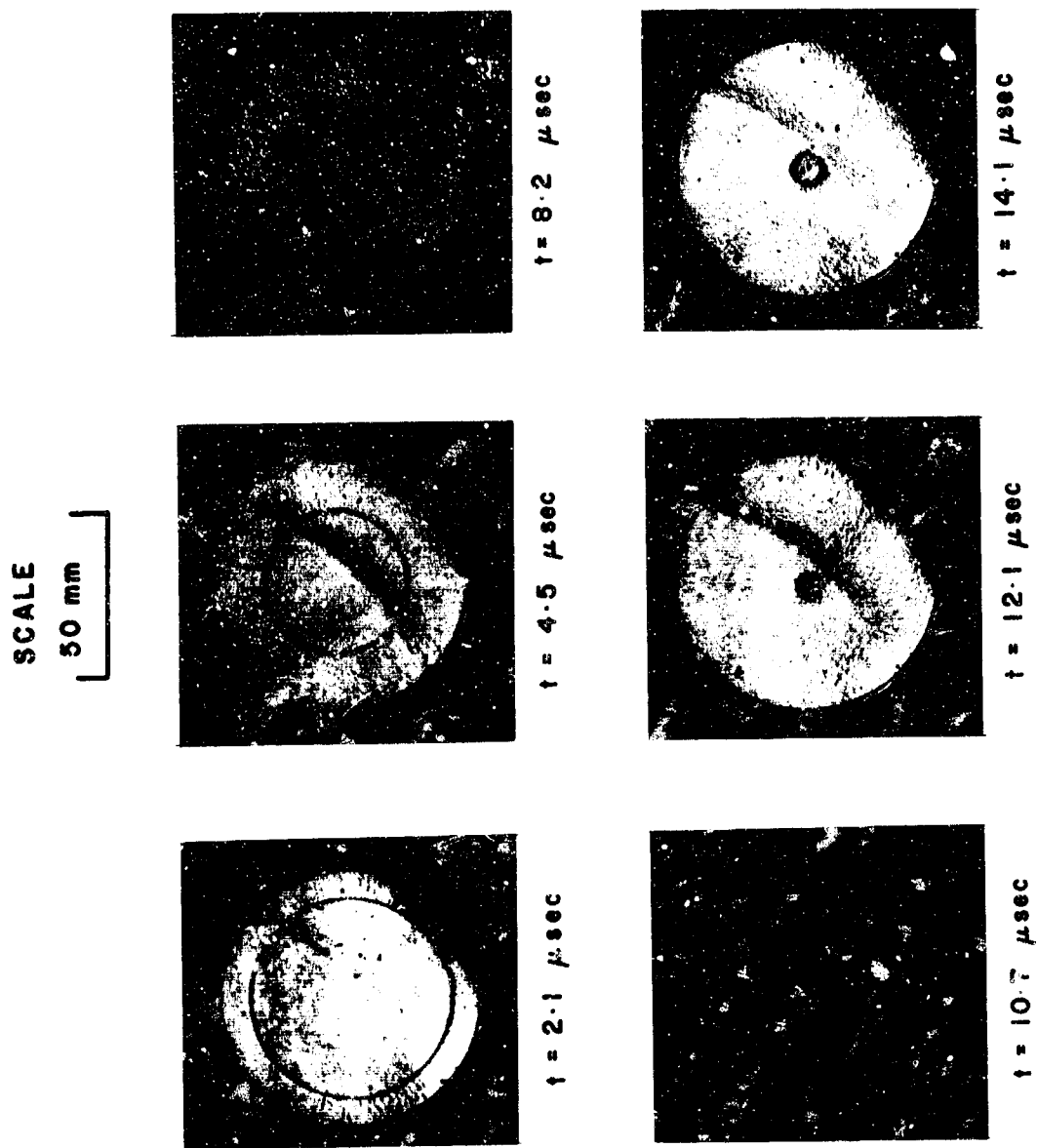
FIG. 27   SEQUENCE OF SPARK SCHLIEREN PHOTOGRAPHS OF A SYMMETRICAL CONVERGING CYLINDRICAL DETONATION WAVE

mental shock trajectories.

We repeated our previous measurements of shock pressures using a fast response barium titanate transducer (i.e., 1 μsec rise time and 3.2 mm diameter). The results confirmed those of the previous work and showed that Whitham's area rule gives an excellent prediction of the shock pressure variation with radius. The maximum shock amplification was found to occur in the small region very close to the center of convergence (i.e., $\frac{R_s}{R_o} \simeq 0.05$). Howe.er, due to the small dimension of the present implosion chamber (i.e., 8 cm diameter) and the relatively large diameter of the piezoelectric element of 3.2 mm, the present results in the interesting region of maximum amplification are inconclusive. Pressure measurements have to be repeated again in the future in a large diameter chamber with a smaller transducer giving better time and space resolutions.

It is well known that the structure of a gaseous detonation front is non-planar on a microscopic scale. The front takes on a corrugated structure with pressure waves propagating in the transverse direction to the detonation motion. From the research on detonation structure in the past decade it was found that the dimensions of the corrugation and the strength of the transverse pressure waves are directly related to the induction time of the explosive. Hence, for example, an increase in the initial pressure of the explosive, a decrease of inert diluent or over-driving the detonation by external means all tend to decrease the strength of the transverse perturbations. Fig. 28 showns a series of open-shutter photographs of the trajectories of the transverse perturbations in equimolar $C_2H_2-O_2$ mixtures in a 1 mm width flat channel. Note that the average size of the wave corrugations decreases with increasing initial pressures as indicated by the total number of transverse waves present. For equimolar $C_2H_2-O_2$ mixtures used in the present experiments at an initial pressure
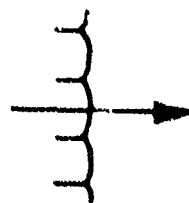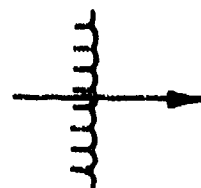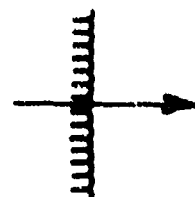
FIG. 28 OPEN-SHUTTER PHOTOGRAPHS OF A PLANAR DETONATION WAVE IN A FLAT
CHANNEL AT DIFFERENT INITIAL PRESSURES IN EQUIMOLAR OXY-ACETYLENE
MIXTURE

of 100 torr, the average dimension of the wave corrugations for a steady
planar Chapman-Jouguet detonation is of the order of 1 mm and the transverse
pressure waves are found to be weak acoustic waves propagating at the speed
of sound of the detonation products. Defining this structural instability
as micro-instability, it is interesting to observe its behavior as the deto-
nation collapses. Fig. 29 shows open-shutter photographs of an imploding
cylindrical detonation wave in a 1 mm wide chamber. Similar open-shutter
photographs of cylindrical imploding detonations have been obtained by Voit-
sekhovskii. Since the transverse perturbations propagate in the tangential
direction as the detonation wave collapses, their trajectories as indicated
in the photograph appear as logarithmic spirals. As the detonation collapses,
the number of transverse waves per unit area of the front increases. Hence,
the scale of the inhomogeneities of the front diminishes. This implies that
by the action of these transverse pressure waves, an initially corrugated
front tends to "smooth" out and approaches a pure cylindrical form of uniform
curvature. These transverse waves supply a mechanism of curvature distribu-
tion in a collapsing detonation front. As the detonation collapses, it beco-
mes progressively amplified and approaches a strong shock wave in the limit.
Since the strength of the transverse perturbations decreases as the detonation
becomes overdriven in the limit, they will decay to acoustic strength when the
wave approaches a strong shock in the vicinity of the center of collapse.

Assuming that these transverse perturbations propagate at the local
sound speed of the products, it is possible to compute their trajectories as
the detonation wave collapses. The instantaneous velocity of a transverse
perturbation is given by the equation $R_s \dot{\omega} = C_1(R_s)$ where $\dot{\omega}$ is the angular
velocity and $C_1(R_s)$ is the sound speed behind the front. The velocity of the
detonation front is given as $\dot{R}_s = -D(R_s)$ where $D(R_s)$ is the instantaneous
detonation velocity and the negative sign is chosen to denote the collapsing

P_o — 30 torr

P_o — 40 torr
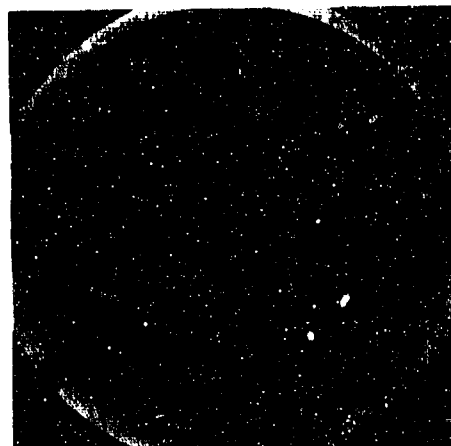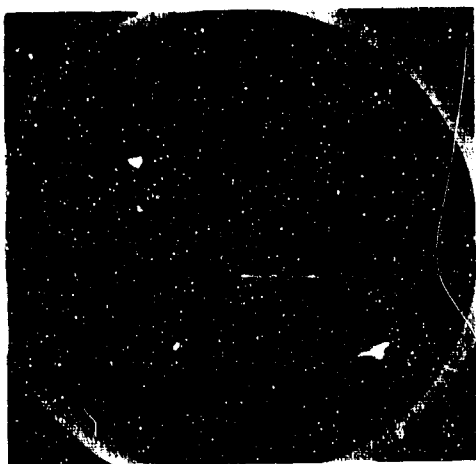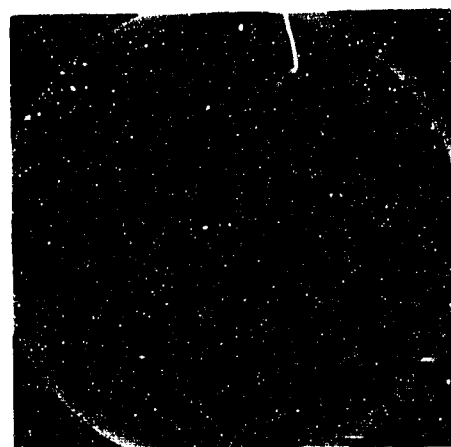
P_o — 50 torr

P_o — 60 torr

FIG. 29 OPEN-SHUTTER PHOTOGRAPHS OF A CONVERGING CYLINDRICAL DETONATION WAVE AT DIFFERENT INITIAL PRESSURES IN EQUIMOLAR OXY-ACETYLENE MIXTURE

motion. From these two relationships one obtains:

$$\omega = \pm \int_{R_o}^{R_s} \frac{C_1(R_s)}{D(R_s)} \frac{dR_s}{R_s}$$

where it is assumed that $\omega = 0$ at $R_s = R_o$. Using Whitham's simple area rule, the functions $C_1(R_s)$ and $D(R_s)$ can be determined. Hence the angular location ω of the transverse disturbance of any instantaneous shock radius R_s can be found. A plot of a few of the theoretical trajectories is shown in Fig. 30 for a range of initial pressures and agrees quite well with the experimental trajectories shown in Fig. 28.

For the perturbations on the wave generated by the initiation process, the same curvature distribution mechanisms should apply (i.e., the transverse pressure waves carry these perturbations and distribute them along the front as it collapses). It is of interest to examine the propagation of these transverse waves closely in terms of a stabilization mechanism. For a strong shock or for a constant velocity Chapman-Jouguet detonation wave, the function $\frac{C_1}{D}$ is constant, depending only on γ (i.e., $\frac{C_1}{D} = \frac{\sqrt{2\gamma(\gamma-1)}}{\gamma+1}$ for strong shocks and $\frac{C_1}{D} = \frac{\gamma}{\gamma+1}$ for C-J detonations). Integration of the above equation yields

$$\frac{R_s}{R_o} = e^{-k\omega}$$

where $k = \frac{D}{C_1}$. From this equation, we see that as $R_s/R_o \longrightarrow 0$, $\omega \longrightarrow \infty$. This means that the transverse waves sweep over the shock with increasing rapidity as the wave contracts. Hence local perturbations are distributed uniformly around the shock an infinite number of times causing the wave to regain its symmetry. In the study of stability of planar shocks, Freeman treats these transverse waves as cylindrical pulses decreasing in amplitude as they propagate. Hence they should eventually be damped out as they sweep around the shock. Viscosity can certainly provide a dissipation mechanism for these perturbations.
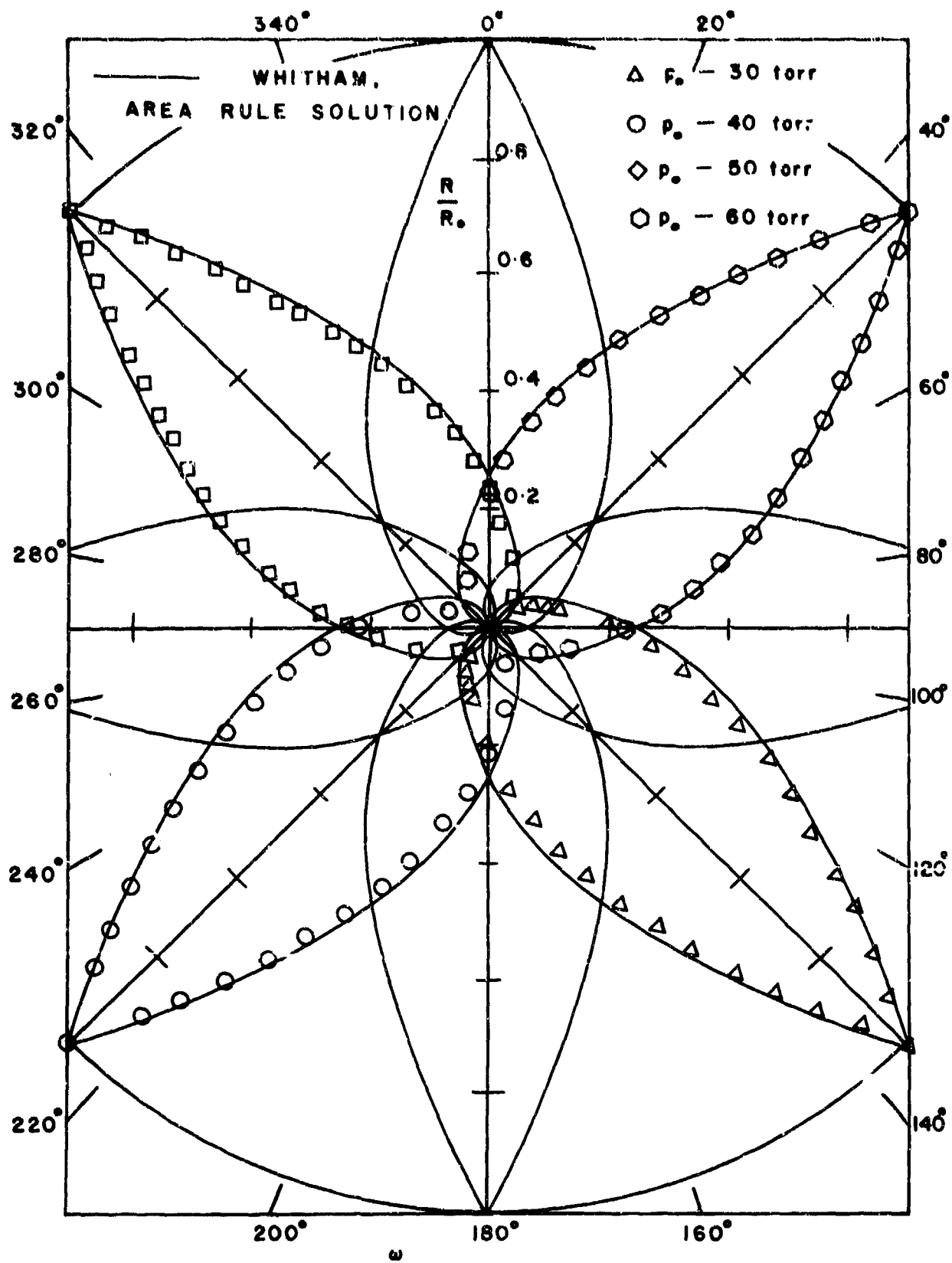
FIG. 30   THEORETICAL AND EXPERIMENTAL TRAJECTORIES OF TRANSVERSELY SWEEPING
PRESSURE DISTURBANCES ON A CONVERGING CYLINDRICAL DETONATION WAVE

A set of experiments on the decay of artificially generated
perturbations by placing a cylindrical rod in the path of the collapsing
detonation wave were performed. Figs. 31 to 33 show three sets of schlieren
photographs for the interaction of the imploding detonation wave with cylin-
drical rods of different diameter ranging from 3.2 to 9.6 mm, respectively,
together with the corresponding open-shutter photographs. The initial
pressure for these experiments is 50 torr. Two pairs of transverse waves
are generated during the interaction with the rod. The first set is formed
when the Mach shocks that ride on the surface of the cylinder meet at the
rear stagnation point of the cylinder. From Fig. 31, note that the first
set of transverse waves decays extremely rapidly and is already absent in
the first frame. The distribution of curvature by the second set of trans-
verse waves is clearly illustrated in the second frame. The detonation
wave outside the region of influence, bounded by the transverse waves re-
tains its perfect symmetry. The transverse waves damp out rather rapidly
and in the third frame the cylindrical wave regains its former symmetry.
In the second set of schlieren photographs shown in Fig. 32, the rod is
placed approximately at half the radius of the former. Note that the rate
of decay of the transverse wave is less rapid and they can still be iden-
tified in Frame 4. However, evidence that symmetry is regained towards
the very end of the collapse can be derived from the fact that the bright
spot associated with the extremely high temperature is achieved at the
centre of convergence. Also from Frame 4 of Fig. 32, one notes that the
Mach stem bounded by the second set of transverse waves takes on a curva-
ture quite close to that of the undisturbed wave indicating the existence
of a curvature distribution mechanism in the Mach reflections of converg-
ing detonation waves. In Fig. 33, a 9.6 diameter rod is used and the bright
spot obtained at the center of convergence indicated that significant focus-

SCALE
50 mm

t = 2·9 μ sec

t = 10·6 μ sec

t = 5·0 μ sec

t = 12·1 μ sec

t = 6·2 μ sec

t = 15·7 μ sec
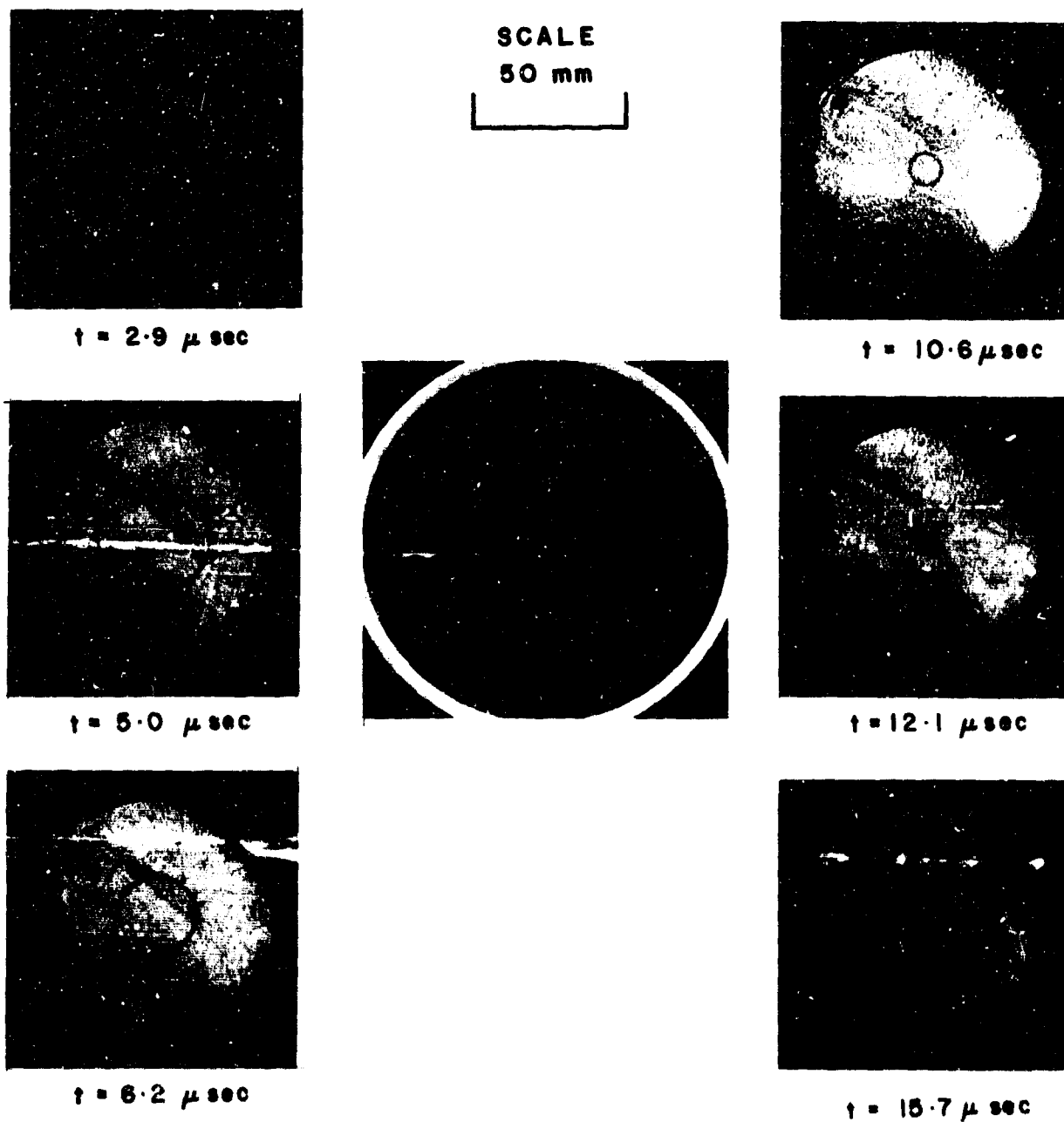
FIG. 31   SPARK SCHLIEREN AND OPEN-SHUTTER PHOTOGRAPHS ILLUSTRATING THE INFLUENCE OF
DISTURBANCES IN THE TRAJECTORY OF A CONVERGING CYLINDRICAL DETONATION WAVE
CREATED BY A 3.2 mm DIAMETER ROD NEAR THE RIM OF THE BOMB

SCALE
50 mm

t = 5·1 μsec

t = 11·2 μsec

t = 7·3 μsec

t = 12·0 μsec

t = 10·5 μsec
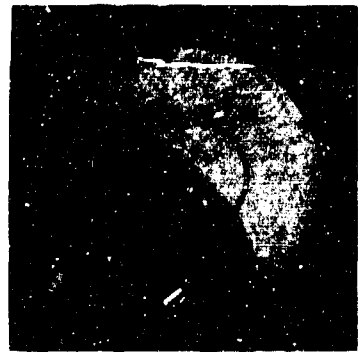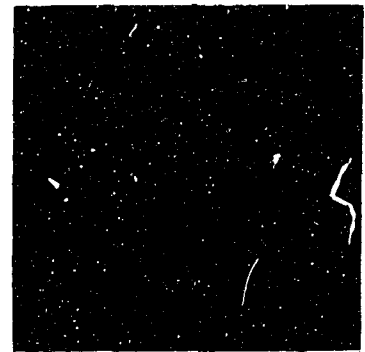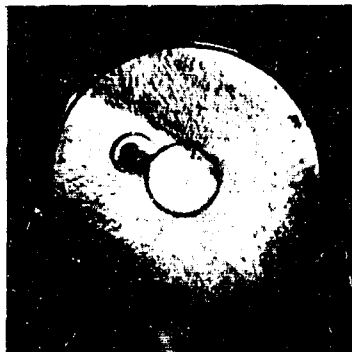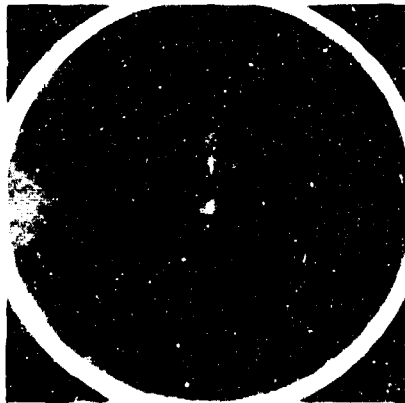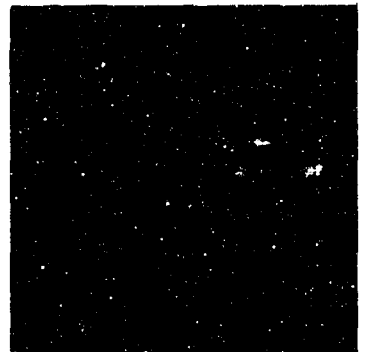
t = 15·0 μsec

FIG. 32   SPARK SCHLIEREN AND OPEN-SHUTTER PHOTOGRAPHS ILLUSTRATING THE INFLUENCE OF
DISTURBANCES IN THE TRAJECTORY OF A CONVERGING CYLINDRICAL DETONATION WAVE
CREATED BY A 3.2 mm DIAMETER ROD LOCATED AT HALF-SPAN
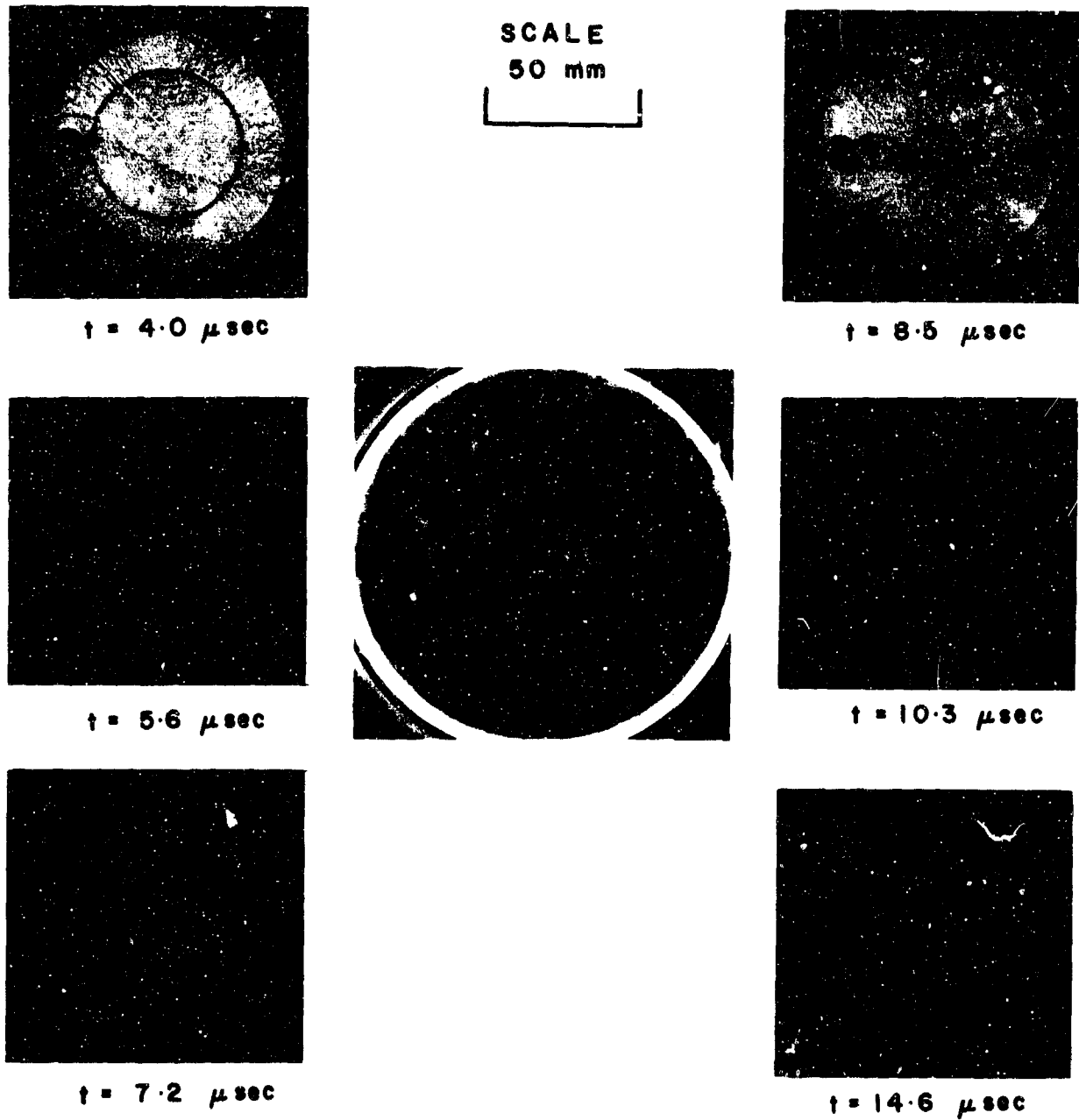
FIG. 33 SPARK SCHLIEREN AND OPEN-SHUTTER PHOTOGRAPHS ILLUSTRATING THE INFLUENCE OF DISTURBANCES IN THE TRAJECTORY OF A CONVERGING CYLINDRICAL DETONATION WAVE CREATED BY A 9.6 mm DIAMETER ROD NEAR THE RIM OF THE BOMB

ing of energy can still be achieved with such large scale perturbations. Even in this case the action of the curvature distribution mechanism is evident in re-accelerating the lagging portions of the disturbed front.

Within the spatial resolution of the present experimental records ($\sim$ 1 mm) no noticeable shift of the center of collapse was detected when the rods were used. This is in contrast to the findings of Perry and Kantrowitz, where observable shift of the bright spot occurred. However, in their case the disturbance was not generated within the implosion chamber itself but along the ramp leading to the chamber. The result may have been that the wave entered the implosion chamber asymmetrically and collapsed accordingly.

From these results attesting to the existence of an inherent stabilization mechanism in implosions there emerges a curious philosophical paradox raised recently by Zababakhin. If implosions are inherently stable, then perfectly symmetrical collapse is possible and consequently, according to current theoretical predictions, infinite temperatures and pressures can be achieved at the center of symmetry. But, as Zababakhin puts it, is it possible in nature to achieve infinite energy densities through cumulative processes among which implosions are but an example? Nature it seems is intolerant of such unbounded accumulation and tends to inject some mechanism or mechanisms to preserve finite bounds. Just as optical focusing, for example, is diffraction limited, so too is there not an upper bound to shock focusing? Zababakhin hypothesizes that although evidently cumulation occurs, infinite states, however, are not achieved. Apparently dissipation mechanisms such as viscosity and heat conductivity are not necessarily the limiting factors restricting such unbounded cumulation. He attributes this limitation to instability, loss of symmetry of the phenomenon, as he calls it. Vakhrameev has indicated that this loss of symmetry is compounded when

there is more than one degree of freedom for cummulation (e.g., implosion
into a radially diminishing density field).

To illustrate this point, Zababakhin has chosen a convincing and
appropriate example. He considers the collapse of a thin cylindrical and
slowly rotating shell of ideal fluid. There is no infinite cumulation in
this case because when the primary (radial) mode begins to experience exten-
sive cumulation, there is an energy transfer to the alternate (rotary) mode
thereby destroying the original cumulative mechanism. Thus, although infi-
nite cumulation is ruled out, this example does, nevertheless, illustrate
that the weaker the initial perturbation (i.e., the lower the angular momen-
tum in this case), the greater is the energy density ultimately reached.
The implication is that there are distinct levels to which energy densities
can ultimately accumulate. Such levels are finite and dependent on the de-
gree of initial geometrical symmetry and on the number of degrees of freedom
of cumulation.

The study just discussed indicates that converging detonations are
stable in the sense that local perturbations are distributed around the front
by transverse waves (i.e., there exists a curvature distribution mechanism).
The trajectories of these waves behave like logarithmic spirals sweeping with
increasing rapidity as the wave collapses. Rapid decay of these transverse
waves is observed experimentally provided they occur before significant cu-
mulation has begun. Whether complete resumption of symmetry is achieved or
not before collapse in an initially distorted front is uncertain. The uncer-
tainty rests in the fact that now a new (transverse) mode or a new degree of
freedom has been provided for possible energy transfer from the primary (ra-
dial) mode of convergence. The degree of symmetry that is attained now de-
pends on the initial strength of the disturbance and on the available span
of travel of the main front before collapse over which the curvature distri-
bution mechanism can act to smooth out the disturbance.

That cumulation does occur in such instances, however, is a well-confirmed and indisputable fact. The point in question here pertains to the degree of accumulation. Even in the case of strong shock wave propagating into a wedge-like channel of diminishing area Belokon et al observed considerable rise in states at the apex of the channel. In our previous work, where the initiation of cylindrical implosions was from a more or less multisided polygon, measurements indicate temperature levels of the order of $200,000^{0}$ K at the point of collapse.

The most significant conclusion of the work just described is to indicate that symmetrical collapse can be enhanced by initiating implosions in chambers of large radius so that any disturbances invariably associated with initiation have sufficient travel to attenuate or by initiating implosions with minimal perturbations in the first place. Certainly from the point of view of practical applications, the first point is particularly relevant in that large chambers are highly desirable to achieve as large a core of plasma as possible near the center of collapse. Such plasma can be utilized, say, in detonation wave lasers, among other things, for optical pumping of a ruby or neodymium rod to achieve lasing action. Currently there also are intensive efforts in our laboratory to exploit the second point pertaining to stable initiation of implosions by devising schemes of initiation with as minimal initial perturbations as possible. One approach is that of flash photolysis which has been used successfully by Wadsworth for detonation initiation. We are utilizing a Zeta-pinch device, schematically illustrated in Fig. 34, for photolytic initiation of converging cylindrical detonation waves. In this scheme an electrical energy bank is discharged rapidly through argon gas in the outer co-axial chamber and the ensuing highly luminous collapsing current sheet is exploited for optical pumping of the detonable gas in the inner chamber. Because the absorption lengths at the absorption frequencies in the detonable gases at the initial
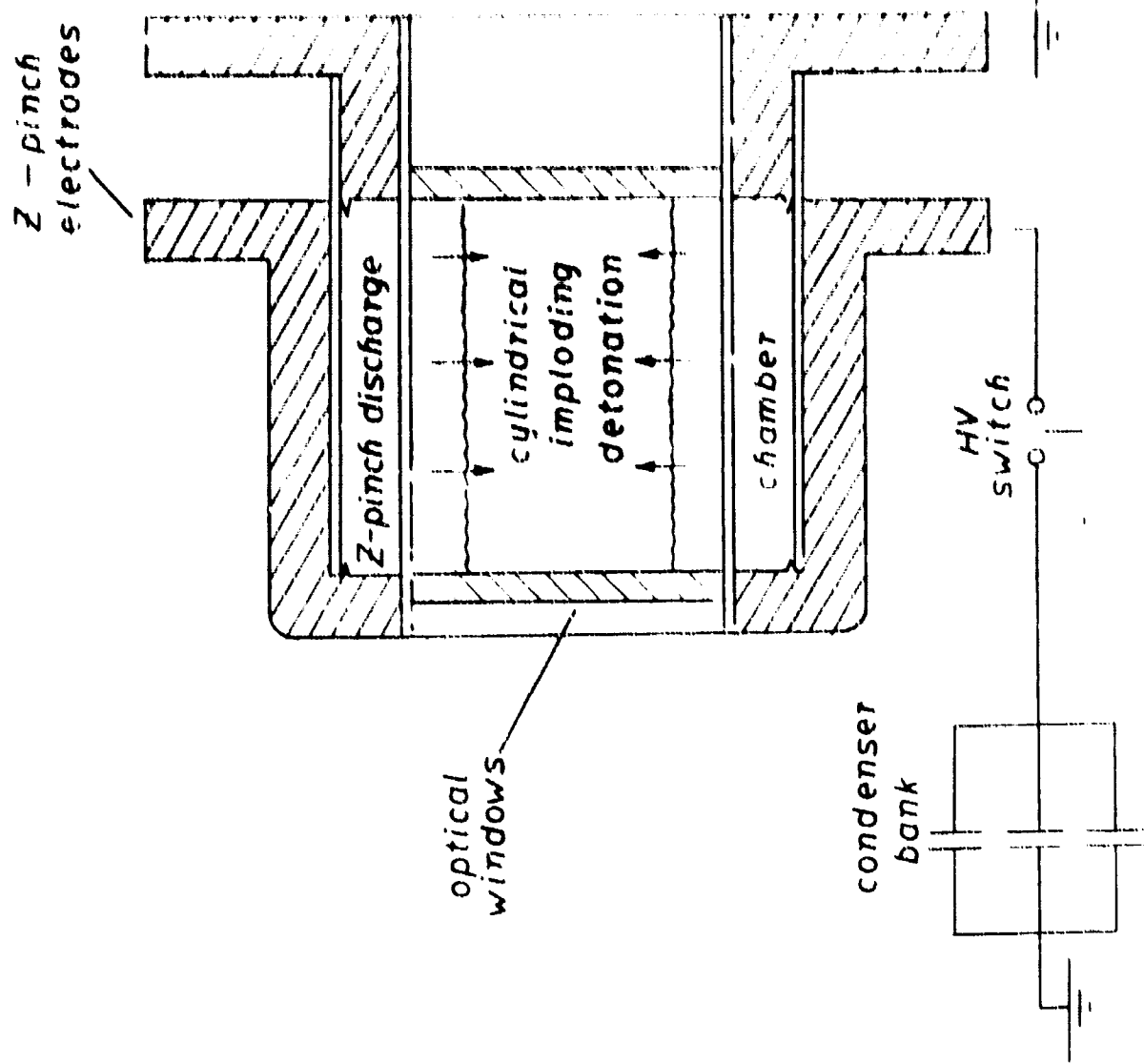
Z-pinch electrodes

Z-pinch discharge

cylindrical imploding detonation

chamber

optical windows

HV switch

condenser bank

FIG. 34

pressures used are extremely short, virtually instantaneous and uniform initiation of an implosion occurs at the periphery of the inner chamber. Preliminary exploratory results indicate that such a scheme is feasible for generation of implosions and this mode of initiation is being actively explored at the present time in our laboratory.

7. Outline of Contents

The final version of this monograph is divided into eleven chapters, five of which (Chapters 2 to 6) are presented in this report in a form that will remain intact in the final version with the missing numerical results filled in. The present Chapter 1 will be replaced by four chapters on experimental observations of various explosion phenomena. As it now stands Chapter 1 serves as a brief summary of these four chapters which are virtually complete in draft form but which came too late to be included in this report because of the necessity to meet the immediate deadline of the AFOSR grant requirements.

For these four chapters on the experimental observations of explosion phenomena, the first chapter reviews the diagnostic techniques used in shock wave physics. This includes various methods for shock wave velocity measurement, transient pressure detection by piezoelectric devices, density measurement by interferometric and other techniques, high temperature measurement by optical means, ionization by conductivity probes, etc. The second chapter deals with electrical explosion phenomena. The dynamics of shock waves from electrical spark discharges, exploding wires, laser sparks, Zeta and Theta pinches, and various types of electromagnetic shock tubes are described. Chapter 3 reviews the phenomena of chemical explosions, particularly the gaseous phase. Here the topics discussed are the transition phenomena from deflagration to detonation, mechanisms of direct initiation

of spherical detonations, instability and structure of gaseous detonation
fronts, and recent concepts of multiheaded detonation fronts and propagation
mechanisms. Chapter 4 describes the phenomena of imploding shock and deto-
nation waves. Various techniques of initiating symmetrical implosions that
we have developed are presented in detail together with the results of di-
agnostic experiments on the properties of imploding waves. The stability
of imploding waves is also treated. In these four chapters the applied
aspects of explosions and implosions are not discussed and emphasis is
placed on the physics of the phenomena.

In the remaining part of the monograph only the gasdynamic aspects
of explosions and implosions are considered. The wave front is treated in
most cases as a gasdynamic discontinuity. To provide some physical under-
standing of the transition zone of a shock or a detonation wave a chapter
has been added on the structure of shock fronts. Hence Chapter 5 reviews
first some fundamental aspects of kinetic theory of gases followed by a
study of the shock structure based on the Navier-Stokes approximation, the
thirteen moment approximation of the Boltzmann equation, the Mott-Smith
solution, and the work of Liepmann and co-workers on the BGK model. Recent
experimental results are compared to these various solutions. On detonation
structure, the Zeldovich-Doring-Neumann solution is presented.

Chapters 6 to 10 will essentially be identical to the present
Chapters 2 to 6. However numerical results will be included in the final
version together with a brief discussion of them. In view of its wide use
and success in the prediction of shock trajectories in pinch devices, a
section on the "snow-plow" model is presently being prepared to be inserted
in the chapter on implosions. A final chapter has been added on numerical
solutions of the problems illustrated in the preceeding chapters on analyti-
cal non-similar methods. We feel that this is necessary and will provide

some quantitative ideas on the accuracy of the various non-similar methods described as well as some confidence on their applicability.

CHAPTER II

BASIC EQUATIONS, BOUNDARY CONDITIONS

AND SIMILARITY TRANSFORMATIONS

The general formulation for a class of explosion problems is
presented in this Chapter. The class of problems has planar, cylindrical
or spherical symmetry. The shock or detonation front bounding the
expanding flow is treated as a discontinuity. The gas is considered to
be inviscid and non-heat-conducting. For the present formulation, no
mass, momentum and energy sources or sinks in the flow are present.

2.1 Basic Equations

Under the conditions described above, the basic conservation equations describing the one-dimensional unsteady adiabatic motion of the compressible medium can be written as:

Conservation of mass

$$\frac{\partial \rho}{\partial t} + u \frac{\partial \rho}{\partial r} + \rho \frac{\partial u}{\partial r} + j \rho \frac{u}{r} = 0 \qquad (2.1.1)$$

Conservation of momentum

$$\frac{\partial u}{\partial t} + u \frac{\partial u}{\partial r} + \frac{1}{\rho} \frac{\partial p}{\partial r} = 0 \qquad (2.1.2)$$

Conservation of energy

$$\frac{\partial e}{\partial t} + u \frac{\partial e}{\partial r} - \frac{p}{\rho^2} \left(\frac{\partial \rho}{\partial t} + u \frac{\partial \rho}{\partial r} \right) = 0 \qquad (2.1.3)$$

where j in Eq. 2.1.1 is a numerical constant with values of 0, 1, 2 for planar, cylindrical and spherical symmetry respectively. Together with the equation of state for the medium, which in general can be expressed as a function of

$$e = e(p, \rho) \qquad (2.1.4)$$

Eqs. 2.1.1 to 2.1.4 comprise a set of four non-linear partial differential equations for the four dependent variables ρ, p, u and e. Given the appropriate initial and boundary conditions, these equations can be solved numerically by using either the method of characterisics or the analogous finite difference method.

For most of the problems considered in this monograph, the medium is treated as a perfect gas with constant specific heat ratio γ. For a perfect gas, Eq. 2.1.4 takes on the form

$$e = \frac{1}{\gamma - 1} \frac{p}{\rho} \qquad (2.1.5)$$

Using Eq. 2.1.5, the internal energy e in Eq. 2.1.3 can be eliminated and an alternate form of the energy equation can be written as

$$\frac{\partial p}{\partial t} + u \frac{\partial p}{\partial r} - \frac{\gamma p}{\rho} \left(\frac{\partial \rho}{\partial t} + u \frac{\partial \rho}{\partial r} \right) = 0 \qquad (2.1.6)$$

Eq. 2.1.6 can also be written in the form

$$\left[\frac{\partial}{\partial t} + u \frac{\partial}{\partial r} \right] \frac{p}{\rho^\gamma} = 0 \qquad (2.1.7)$$

and since entropy can be written as a function of p/ρ^γ , Eq. 2.1.7 becomes

$$\frac{\partial S}{\partial t} + u \frac{\partial S}{\partial r} = 0 \qquad (2.1.8)$$

The above equation states that the entropy of each particle in the expanding flow remains constant. This complies with the original approximations that apart from the transition through the boundary (i.e., shock to detonation front), no other entropy generating sources are present in the expanding flow.

For convenience in the later analyses, a more convenient form of the energy equation is used. This is obtained by eliminating the density ρ from Eq. 2.1.6 using the continuity equation (i.e., Eq. 2.1.1). The resultant form of the energy equation becomes

$$\frac{\partial p}{\partial t} + u \frac{\partial p}{\partial r} + \gamma p \frac{\partial u}{\partial r} + \gamma j \frac{p u}{r} = 0 \qquad (2.1.9)$$

Hence for a perfect gas, Eqs. 2.1.1, 2.1.2 and 2.1.6 (or 2.1.9) constitute a set of three equations for the three dependent variables ρ , u and p .

2.2 Boundary Conditions

To obtain the boundary conditions immediately behind detonation front, consider the moving shock system below

The conservation equations across the shock front are given as

Conservation of mass

$$\rho_o \dot{R}_s = \rho_1 (\dot{R}_s - u_1) \qquad (2.2.1)$$

Conservation of momentum

$$p_o + \rho_o \dot{R}_s^2 = p_1 + \rho_1 (\dot{R}_s - u_1)^2 \qquad (2.2.2)$$

Conservation of energy

$$\frac{p_o}{\rho_o} + e_o + Q + \frac{\dot{R}_s^2}{2} = \frac{p_1}{\rho_1} + e_1 + \frac{(\dot{R}_s - u_1)^2}{2} \qquad (2.2.3)$$

where Q is the chemical energy per unit mass released at the shock. For a perfect gas the equation of state as given previously by Eq. 2.1.5 is

$$e = \frac{1}{\gamma - 1} \frac{p}{\rho} \qquad (2.1.5)$$

With the initial states (i.e. $\rho_o, p_o, e_o, \gamma_o, Q$) given, the states behind the shock can be expressed conveniently in terms of the shock Mach Number as

$$\frac{\rho_1}{\rho_o} = \frac{\gamma_o (\gamma_1 + 1)}{\gamma_1 (\gamma_o + \eta \mp S)} \qquad (2.2.4)$$

$$\frac{u_1}{\dot{R}_s} = \frac{\gamma_o - \gamma_1 (\eta \mp S)}{\gamma_o (\gamma_1 + 1)} \qquad (2.2.5)$$

$$\frac{p_1}{\rho_0 \dot{R}_s^2} = \frac{\gamma_0 + \eta \pm \gamma_1 S}{\gamma_0 (\gamma_1 + 1)} \tag{2.2.6}$$

where

$$S = \left\{ \left(\frac{\gamma_0}{\gamma_1} \cdot \eta \right)^2 - k\eta \right\}^{\frac{1}{2}} \tag{2.2.7}$$

$$k = 2 \left\{ \frac{\gamma_0 (\gamma_1 - \gamma_0)(\gamma_1 + 1)}{\gamma_1^2 (\gamma_0 - 1)} + \frac{\gamma_0^2 (\gamma_1^2 - 1)}{\gamma_1^2} q \right\} \tag{2.2.8}$$

$$q = Q/c_0^2 \tag{2.2.9}$$

$$c_0^2 = \gamma p_0 / \rho_0 \tag{2.2.10}$$

$$M_s = \dot{R}_s / c_0 \tag{2.2.11}$$

$$\eta = 1/M_s^2 \tag{2.2.12}$$

For any given shock velocity (hence shock Mach Number or η) two solutions exist corresponding to the two roots of S. For finite q, the bottom sign preceding S in Eqs. 2.2.4 to 2.2.6 yields the weak detonation solution in which the flow is supersonic behind the front and relative to it. The top sign corresponds to the strong or overdriven detonation solution where the flow is subsonic behind the front. A unique solution is obtained when the two roots of S coincide (i.e., $S=0$) and this solution is known as the Chapman-Jouguet. From entropy consider-ations, the weak detonation solution can be discarded. For the explosion

problems treated in this monograph, only the overdriven and the Chapman-Jouguet solutions are of interest and the top sign in Eqs. 2.2.4 to 2.2.6 will be used throughout. For Chapman-Jouguet detonations, S = 0 and solving for the detonation Mach Number from Eq. 2.2.7 one obtains

$$\eta_{CJ} = \frac{1}{M_{CJ}^2} = \frac{\gamma_0}{\gamma_1} + \frac{k}{2} - \left\{ \frac{\gamma_0^2}{\gamma_1^2} - 1 + k \left(\gamma_0 + \frac{k}{4} \right) \right\}^{\frac{1}{2}} \qquad (2.2.13)$$

and Eqs. 2.2.4 to 2.2.6 reduce to

$$\frac{\rho_1}{\rho_0} = \frac{\gamma_0(\gamma_1 + 1)}{\gamma_1(\gamma_0 + \eta_{CJ})} \qquad (2.2.14)$$

$$\frac{u_1}{\dot{R}_S} = \frac{\gamma_0 - \gamma_1 \eta_{CJ}}{\gamma_0(\gamma_1 + 1)} \qquad (2.2.15)$$

$$\frac{p_1}{\rho_0 \dot{R}_S^2} = \frac{\gamma_0 + \eta_{CJ}}{\gamma_0(\gamma_1 + 1)} \qquad (2.2.16)$$

For very strongly overdriven detonations when $M_S \rightarrow \infty$, $\eta \rightarrow 0$, the parameter $k \rightarrow 0$ and $S \rightarrow \gamma_0/\gamma_1$. Taking the top sign in Eqs. 2.2.4 to 2.2.6 and substituting $S = \gamma_0/\gamma_1$, we obtain the following limiting conditions for strong shocks

$$\frac{\rho_1}{\rho_0} = \frac{\gamma_1 + 1}{\gamma_1 - 1} \qquad (2.2.17)$$

$$\frac{u_1}{\dot{R}_S} = \frac{2}{\gamma_1 + 1} \qquad (2.2.18)$$

$$\frac{p_1}{\rho_0 \dot{R}_s^2} = \frac{2}{\gamma_1 + 1} \tag{2.2.19}$$

For most hydrocarbon-oxygen detonations, the Chapman-Jouguet detonation Mach Number M_{cJ} is of the order of 6 to 8. Hence $\eta_{cJ} \ll 1$ and can be neglected in Eqs. 2.2.4 to 2.2.6 without much loss in accuracy. Eqs. 2.2.4 to 2.2.6 reduce to

$$\frac{\rho_1}{\rho_0} \sim \frac{\gamma_0(\gamma_1 + 1)}{\gamma_1(\gamma_0 - S)} \tag{2.2.20}$$

$$\frac{u_1}{\dot{R}_s} \sim \frac{\gamma_0 + \gamma_1 S}{\gamma_0(\gamma_1 + 1)} \tag{2.2.21}$$

$$\frac{p_1}{\rho_0 \dot{R}_s^2} \sim \frac{\gamma_0 + \gamma_1 S}{\gamma_0(\gamma_1 + 1)} \tag{2.2.22}$$

where the parameter S now becomes

$$S \sim \frac{\gamma_0}{\gamma_1}\left[1 - 2(\gamma_1^2 - 1)\eta q \right]^{\frac{1}{2}} \tag{2.2.23}$$

In obtaining the above equation, all terms containing η are dropped except for the term containing ηq since q is of the order of M_{cJ}^2 or $1/\eta_{cJ}$, hence ηq is of the order of unity. For example for an equimolar acetylene-oxygen detonation, $M_{cJ}^2 \sim 64$ and $q \sim 50$. From Eq. 2.2.23, the Chapman-Jouguet Mach No. M_{cJ} can be obtained as

$$\eta_{cJ} = \frac{1}{2(\gamma_1^2 - 1)q} \tag{2.2.24}$$

or
$$M_{cr} = \left(2(\gamma_1^2 - 1) q \right)^{1/2}$$
(2.2.25)

and for Chapman-Jouguet detonations, Eqs. 2.2.20 to 2.2.22 reduce to

$$\frac{\rho_1}{\rho_o} = \frac{\gamma_1 + 1}{\gamma_1}$$
(2.2.26)

$$\frac{u_1}{\dot{R}_{cr}} = \frac{1}{\gamma_1 + 1}$$
(2.2.27)

$$\frac{p_1}{\rho_o \dot{R}_{cr}^2} = \frac{1}{\gamma_1 + 1}$$
(2.2.28)

For infinite strength shock waves, $\eta \to 0$, and $S \to \gamma_o/\gamma_1$, and Eqs. 2.2.20 to 2.2.22 again reduce to the limiting strong shock conditions as given previously by Eqs. 2.2.17 to 2.2.19.

For a non-detonating medium, we set $q=0$ in Eq. 2.2.8 for the parameter k and Eqs. 2.2.4 to 2.2.6 apply for the general case across a normal shock where the specific heat ratios are different on both sides of the shock to account for the change in thermodynamic states. The bottom sign in Eqs. 2.2.4 to 2.2.6 for the non-reacting medium now gives the trivial solution of no change across the shock and hence only the top sign is used. For the case of constant γ across the shock (i.e., $\gamma_o = \gamma_1 = \gamma$) the parameter $k=0$ and $S=1-\eta$. Eqs. 2.2.4 to 2.2.6 reduce to the standard Rankine-Hugoniot relationships across a normal shock in a perfect gas given as

$$\frac{\rho_1}{\rho_o} = \frac{\gamma+1}{\gamma-1+2\eta}$$
(2.2.29)

$$\frac{u_1}{R_s} = \frac{2}{\gamma+1}(1-\eta) \tag{2.2.30}$$

$$\frac{p_1}{\rho_0 R_s^2} = \frac{2}{\gamma+1}\left(1 - \frac{(\gamma-1)}{2\gamma}\eta\right) \tag{2.2.31}$$

Again for strong shocks, $M_s \rightarrow \infty$ and $\eta \rightarrow 0$. Eqs. 2.2.29 to 2.2.31 reduce to the limiting strong shock conditions given by Eqs. 2.2.17 to 2.2.19 .

For the explosion of a gas cloud in a vacuum, the boundary for the expanding flow is an escape front. The conditions at the escape front will be that the pressure, density and sound speed are all zero and the particle velocity is

$$u_e = \frac{2}{\gamma-1} c_0 \tag{2.2.32}$$

Since no mass sources are assumed to be present, the boundary condition at the center of symmetry $r=0$ will be the particle velocity $u(0,t)=0$. For piston driven explosions, the boundary condition to be satisfied at the piston surface will be the particle velocity equal to the piston velocity (i.e., $u = u_p$).

2.3 The Mass and Energy Integral

For explosion problems, the moving boundary is unknown and an extra relationship apart from the basic conservation equations is required to completely specify the problem. This extra relationship is obtained by conserving the total energy enclosed by the moving boundary at any instant of time t and is generally referred to as the energy integral. Conserving the total energy at any instant when the boundary is at $R_s(t)$, we obtain

$$E_{ext} = \int_{R_p(t)}^{R_s(t)} \rho(e + \frac{u^2}{2}) k_j r^j dr - \int_0^{R_s(t)} \rho_0(e_0 + Q) k_j r^j dr \qquad (2.3.1)$$

E_{ext} is the energy input to the flow by external means such as by an expanding piston. In general we can express E_{ext} in the following form

$$E_{ext} = E_0 R_s^\alpha(t) \qquad (2.3.2)$$

The first integral on the right hand side of Eq. 2.3.1 represents the total energy enclosed by the explosion products bounded by the front $R_s(t)$ and the piston $R_p(t)$. The second integral denotes the initial thermal and chemical energy in the gas occupying the volume from $r = 0$ to $r = R_s(t)$. Here we have assumed the initial condition that at time $t = 0$, the front $R_s(0) = 0$ and the piston $R_p(0) = 0$. The term k_j in Eq. 2.3.1 is a numerical constant having values of 1, 2π, 4π for planar $(j = 0)$ cylindrical $(j = 1)$ and spherical $(j = 2)$ symmetry. For cases in which the initial density $\rho_0 = $ constant, the second integral in Eq. 2.3.1 can be evaluated and the equation becomes

$$E_0 R_s(t)^\alpha = \int_{R_p(t)}^{R_s(t)} \rho(e + \frac{u^2}{2}) k_j r^j dr - \frac{\rho_0}{j+1} (e_0 + Q) k_j R_s(t)^{j+1}$$

$$(2.3.3)$$

For a perfect gas,

$$e_o = \frac{p_o}{(\gamma_o - 1)\rho_o}$$

and

$$c_o^2 = \gamma_o p_o / \rho_o$$

and Eq. 2.3.3 becomes

$$E_o R_s^\alpha (t) = \int_{R_p(t)}^{R_s(t)} \left[\frac{p}{\gamma_1 - 1} + \rho \frac{u^2}{2} \right] k_j r^j dr$$

$$- k_j \frac{R_s^{j+1} \rho_o c_o^2}{j+1} \left(\frac{1}{\gamma_o (\gamma_o - 1)} + \mathcal{G} \right) \tag{2.3.4}$$

where $\mathcal{G} = Q/c_o^2$. If the initial density $\rho_o = \rho_o(r)$ or particularly of the form $\rho_o = A r^\omega$, Eq. 2.3.4 takes on a different form. For example for isothermal conditions c_o^2 = constant, Eq. 2.3.4 becomes

$$E_o R_s^\alpha (t) = \int_{R_p(t)}^{R_s(t)} \left[\frac{p}{\gamma_1 - 1} + \rho \frac{u^2}{2} \right] k_j r^j dr$$

$$- k_j \frac{R_s^{j+\omega+1} A c_o^2}{j+\omega+1} \left(\frac{1}{\gamma_o (\gamma_o - 1)} + \mathcal{G} \right) \tag{2.3.5}$$

For any particular explosion problem, the solution to the basic conservation equations must also satisfy the energy integral.

Another integral relationship of importance is the mass integral. The mass integral is used in the determination of the particle trajectories from the solution in the present Eulerian formulation. To obtain the mass integral, we conserve the total mass enclosed by the expanding front at any instant of time t and this gives the relationship

$$\int_{R_p(t)}^{R_s(t)} \rho k_j r^j dr \quad - \quad \int_0^{R(t)} k_j \rho_0 r^j dr \qquad (2.3.6)$$

In the above equation we have again assumed the initial condition $R_s(o) = 0$, $R_p(o) = 0$. The first integral of Eq. 2.3.6 represents the total mass enclosed by the front at any instant while the integral on the right hand side of Eq. 2.3.6 denotes the total mass occupying the volume originally. In the absence of mass sources, the two integrals are equal. For ρ_0 = constant, the integral on the right hand side can be evaluated and Eq. 2.3.6 becomes

$$\int_{R_p(t)}^{R_s(t)} \rho r^j dr = \frac{\rho_0 R_s^{j+1}(t)}{j+1} \qquad (2.3.7)$$

If the initial density $\rho_0 = \rho_0(r) = A r^\omega$, Eq. 2.3.6 becomes

$$\int_{R_p(t)}^{R_s(t)} \rho r^j dr = \frac{A R_s^{j+\omega+1}(t)}{j+\omega+1} \qquad (2.3.8)$$

From Eq. 2.3.8, we can see that since the mass enclosed by the front must be positive and finite, the value of ω must be greater than $-(j+1)$

$$\omega \geqslant -(j+1) \qquad (2.3.9)$$

It should be noted that both the energy and the mass integral can be obtained directly by manipulation of the differential equations of motion (i.e., Eqs. 2.1.1 to 2.1.3). However it is simpler to obtain them from physical considerations as was done here. There are other integrals such as the momentum integral which can also be obtained from

the basic equations but we have not found it to be essential in the problems studied. Interested readers can refer to the work of Sedov or Korobeinikov for details of the adiabatic integral.

2.4 <u>Similarity Considerations</u>

Throughout this monograph, we shall be concerned primarily with the self-similar type of solutions. In this Section, we shall make a general investigation of the basic conservation equations and their boundary and initial conditions to establish the necessary conditions for the existence of self-similar solutions for explosion problems. Mathematically speaking, self-similar solutions are solutions in which the dependent variables are functions of a particular combination of the independent variables only. For example we can write the general solution to the basic conservation equations (i.e., Eqs. 2.1.1 to 2.1.3) in the form $\rho(r,t)$, $p(r,t)$, $u(r,t)$ and $e(r,t)$ and for self-similar solutions, they are of the form $\rho(\xi)$, $p(\xi)$, $u(\xi)$ and $e(\xi)$ where $\xi = \xi(r,t)$ is a particular combination of the independent variables r and t. If self-similar solutions exist, the number of independent variables in the differential equations is reduced by one and considerable simplifications result in obtaining the solution.

There are a number of approaches used in determining the existence of self-similar solution in a particular problem and the form of the simila-rity parameters. For example the method of dimensional analysis is used by Sedov, the group theory approach by Birkoff and Morgan, the free parameter method of Kline and Abbot, Long's method of generalized dimensional analysis, and plain common sense and experience by many others in a variety of prob-lems. All these methods in many ways are similar yielding identical end results. We have never investigated where our approach fits into the various existing methods exactly. It could well be one of the methods mentioned or a slight modification of it together with a small admixture of another approach.

Replacing the dependent and the independent variables by the following

$$\rho(r,t) = \rho_0(r)\, \mathcal{Y}\big(R_s(t),\, \xi(r,t)\big)$$

$$u(r,t) = \dot{R}_s(t)\, \phi\big(R_s(t),\, \xi(r,t)\big)$$

$$p(r,t) = \rho_0(r)\, \dot{R}_s^2(t)\, f\big(R_s(t),\, \xi(r,t)\big) \qquad\qquad (2.4.1)$$

$$e(r,t) = \dot{R}_s^2(t)\, g\big(R_s(t),\, \xi(r,t)\big)$$

$$r \;\Rightarrow\; \xi(r,t)$$

$$t \;\Rightarrow\; R_s(t)$$

where $\xi(r,t)$ is any arbitrary function of r and t to be determined later, the basic conservation equations transform to the following

Conservation of mass

$$\left(\phi + \frac{\xi_t}{R_s \xi_r}\right)\frac{\partial \mathcal{Y}}{\partial \xi} + \mathcal{Y}\frac{\partial \phi}{\partial \xi} + \phi\mathcal{Y}\left(\frac{j}{r\xi_r} + \frac{1}{\rho_0 \xi_r}\frac{\partial \rho_0}{\partial r}\right) = -\frac{1}{\xi_r}\frac{\partial \mathcal{Y}}{\partial R_s} \qquad (2.4.2)$$

Conservation of momentum

$$\left(\phi + \frac{\xi_t}{R_s \xi_r}\right)\frac{\partial \phi}{\partial \xi} + \frac{1}{\mathcal{Y}}\frac{\partial f}{\partial \xi} + \frac{\ddot{R}_s \phi}{\xi_r \dot{R}_s^2} + \frac{f}{\mathcal{Y}}\frac{1}{\rho_0 \xi_r}\frac{\partial \rho_0}{\partial r} = -\frac{1}{\xi_r}\frac{\partial \phi}{\partial R_s}$$

$$(2.4.3)$$

Conservation of energy

$$\left(\phi + \frac{\xi_t}{R_s \xi_r}\right)\frac{\partial g}{\partial \xi} + \frac{2\ddot{R}_s}{\xi_r \dot{R}_s^2}g + \frac{f}{\mathcal{Y}}\left(\frac{\partial \phi}{\partial \xi} + \frac{j\phi}{\xi_r r}\right) = -\frac{1}{\xi_r}\frac{\partial f}{\partial R_s}$$

$$(2.4.4)$$

Equation of state

$$g = \dot{R_s}^2 F(\rho_o \dot{R_s}^2 f, \rho_o \psi) \tag{2.4.5}$$

In the above equations, ξ_t and ξ_r denotes partial differentiation of $\xi(r,t)$ with respect to time t and space coordinate r respectively, $\dot{R}_s$ and $\ddot{R}_s$ denotes the first and second derivative of R_s with respect to time. In deriving the energy equation (i.e., Eq. 2.4.4), the continuity equation (i.e., Eq. 2.1.5) has been used to replace the density terms in Eq. 2.1.3. Also in the above equations we have let the initial density ρ_o be some general function of the space coordinate r. The form $\rho_o(r)$ for the existence of self-similar solutions is to be determined later.

For self-similar motions, the dependent variables are functions of a single independent variable $\xi(r,t)$ only (i.e., $\psi(\xi)$, $\phi(\xi)$, etc.) hence the right hand terms of Eqs. 2.4.2 to 2.4.4 vanish. Also all the remaining terms in the equations must be t and r independent. Hence this requires

$$\frac{\xi_t}{\dot{R}_s \xi_r} = \frac{\xi_{R_s}}{\xi_r} = f_1(\xi) \tag{2.4.6}$$

$$\frac{\ddot{R}_s}{\xi_r \dot{R}_s^2} = f_2(\xi) \tag{2.4.7}$$

$$r\xi_r = f_3(\xi) \tag{2.4.8}$$

$$\frac{1}{\rho_o \xi_r} \frac{\partial \rho_o}{\partial r} = f_4(\xi) \tag{2.4.9}$$

where the $f's$ are arbitrary functions of ξ and can be constant.

From Eq. 2.4.8, we obtain

$$\frac{d\xi}{f_3(\xi)} = \frac{dr}{r}$$

and integrating yields

$$f_5(\xi) = \ln(kr) \tag{2.4.10}$$

where k is an arbitrary function of R_s. From Eq. 2.4.10 we can write

$$\xi = f_6(kr) \tag{2.4.11}$$

From Eq. 2.4.6, we get

$$\xi_{R_s} = f_1(\xi)\xi_r = f_1(\xi)k f_6'(kr) \tag{2.4.12}$$

Differentiating Eq. 2.4.11 with respect to R_s we get

$$\xi_{R_s} = rk' f_6'(kr) \tag{2.4.13}$$

and equating Eq. 2.4.12 and 2.4.13 yields

$$\frac{rk'}{k} = f_1(\xi) \tag{2.4.14}$$

From Eq. 2.4.14, we can write

$$\xi = f_7\left(\frac{rk'}{k}\right) = f_7(rk_1) \tag{2.4.15}$$

Where $k_1 = k'/k$

Using Eq. 2.4.5 and repeating the process again we obtain

$$\frac{rk_1'}{k_1} = f_1(\xi) \tag{2.4.16}$$

and similarly

$$\xi = f_8 \left(\frac{rk_1'}{k_1} \right) = f_9 (rk_2) \qquad (2.4.17)$$

where $\quad k_2 = k_1'/k_1$

Hence we can now see the general trend that

$$\frac{k'}{k} = \frac{k_1'}{k_1} = \frac{k_2'}{k_2} = \quad \cdots \quad = \frac{k_n'}{k_n} = \cdots \qquad (2.4.18)$$

where

$$k_n = k_{n-1}'/k_{n-1} \qquad (2.4.19)$$

From Eqs. 2.4.18 and 2.4.19, we see that

$$\left(\frac{k_\infty'}{k_n} \right)' = \left(\frac{k_n'}{k_n} \right)^2 \qquad (2.4.20)$$

and solving the two above equations yields

$$\frac{k_n'}{k_n} = -\frac{1}{R_S + a_m} = \frac{k_{m-1}'}{k_{n-1}} \cdots \quad = \frac{k'}{k} \qquad (2.4.21)$$

and the constant a_n = a = a true constant. From Eq. 2.4.21, we obtain

$$k = \frac{b}{R_S + a} \qquad (2.4.22)$$

where a and b are true constants. From Eq. 2.4.22, we see that the form for ξ must be

$$\xi = G \left(\frac{rb}{R_S + a} \right) \qquad (2.4.23)$$

Going back to Eq. 2.4.7, and using Eq. 2.4.23 we get

$$\frac{\ddot{R}_S}{\dot{R}_S^2} = f_2(\xi) \frac{b}{R_S + a} G' \left(\frac{rb}{R_S + a} \right) \qquad (2.4.24)$$

Hence

$$\frac{(R_s + a)\ddot{R}_s}{b\dot{R}_s^2} = f_2(\xi) G' \tag{2.4.25}$$

In the above equation, the left hand term is a function of R_s only while the right hand side is a function of ξ only. Therefore both sides of Eq. 2.4.25 must be equal to a constant.

$$\frac{(R_s + a)\ddot{R}_s}{b\dot{R}_s^2} = constant \tag{2.4.26}$$

Since when $r = R_s$, ξ must be independent of R_s, we see by examining Eq. 2.4.23 that

$$\frac{b R_s}{R_s + a} = constant$$

and the above relationship requires the numerical constant $a = 0$. Hence Eq. 2.4.23 becomes

$$\xi = G\left(\frac{br}{R_s}\right) \tag{2.4.27}$$

There is no loss in generality by setting the constant $b = 1$ and writing

$$\xi = \frac{r}{R_s} \tag{2.4.28}$$

Eq. 2.4.26 now reduces to

$$\frac{R_s \ddot{R}_s}{\dot{R}_s^2} = constant = \theta \tag{2.4.29}$$

Solving the above equation, we obtain

$$\dot{R}_s = C R_s^\theta \tag{2.4.30}$$

Integrating Eq. 2.4.30, we get for the case $\theta \neq 1$

$$R_S = A t^{\frac{1}{1-\theta}} = A t^N \tag{2.4.31}$$

where

$$N = \frac{1}{1-\theta} \tag{2.4.32}$$

or

$$\theta = \frac{N-1}{N} \tag{2.4.33}$$

For the case where $\theta = 1$, we obtain

$$R_S = A_1 e^{c_1 t} \tag{2.4.34}$$

Hence for self-similar motion we see that the expanding front must either be a power law of time or an exponential function of time. For most of the explosion problems considered, the power law form is of interest.

We now return to Eq. 2.4.9 to determine the form for for self-similar motion. From Eqs. 2.4.9 and 2.4.8 we obtain

$$\frac{r}{\rho_o} \frac{\partial \rho_o}{\partial r} = f_{1o}'(\xi) \tag{2.4.35}$$

Since $\rho_o = \rho_o(r)$ is not a function of R_s (or time t) and $\xi = G(\frac{r}{R_S})$, the left hand side of Eq. 2.4.35 must be equal to a constant

$$\frac{r}{\rho_o} \frac{\partial \rho_o}{\partial r} = constant = \omega \tag{2.4.36}$$

Solving the above equation yields the form for $\rho_o(r)$ as

$$\rho_o(r) = A r^\omega \tag{2.4.37}$$

The form for $\rho_o(r)$ as given by Eq. 2.4.37 is the only admissable form for the existence of self-similar motion for arbitrary geometries (i.e., planar, cylindrical and spherical). For planar symmetry only, the condition given by Eq. 2.4.8 is relaxed permitting a wider choice of forms for ξ and $\rho_o(r)$. For example one may have

$$\rho_0(r) = \rho^* e^{\frac{r}{\Delta}} \qquad (2.4.38)$$

and the corresponding form for the similarity variable ξ is given as

$$\xi = (R_s - r)/\Delta \qquad (2.4.39)$$

The form given by Eqs. 2.4.38 and 2.4.39 is used by Zeldovich and Rayzer in their study of a planar explosion in an exponential atmosphere in the direction of increasing density.

Thus far we have only considered the three differential equations of motion; for self-similar solutions to exist, the equation of state (i.e., Eq. 2.4.5) must take on a particular form. The form must be such that under the similarity transformation, the equation of state does not depend on R_s (or time) explicitly. In other words, all R_s dependent terms vanish. A simple form for the equation of state satisfying this condition is

$$e = k p/\rho \qquad (2.4.40)$$

where k is a constant. Under present transformation, Eq. 2.4.40 becomes

$$g = \frac{k f}{\psi} \qquad (2.4.41)$$

For a perfect gas with constant specific heat ratio, the equation of state is of the form given by Eq. 2.4.40. In this case the constant $k = 1/(\gamma-1)$ and for a perfect gas Eqs. 2.4.40 and 2.4.41 become

$$e = \frac{1}{\gamma-1} \frac{p}{\rho}$$

$$\qquad (2.4.42)$$

$$g = \frac{1}{\gamma-1} \frac{f}{\psi}$$

A detailed study of the form of the equation of state for self-similar motion is given by Wecker and Hayes. For the majority of the problems considered in this monograph, a perfect gas is assumed.

Now we look into the boundary conditions for self-similar explosion problems. Since the self-similar solutions are not dependent on R_s explicitly, the boundary conditions must also be independent of R_s (or time). From the general relationships across a shock front given by Eqs. 2.2.4 to 2.2.8, we see that this is satisfied under two conditions. For infinite strength shock waves, Eqs. 2.2.4 to 2.2.8 reduce to Eqs. 2.2.17 to 2.2.19 and the boundary conditions are functions of γ only, hence constant. For finite strength shock waves, self-similar motion requires that the shock Mach Number M_s (hence η) must be constant throughout. Again the boundary conditions are constant under this condition. Hence for self-similar motions, we see that for the case of non-uniform shock motion, the shock strength must be infinite ($\eta \rightarrow 0$), while for finite strength shock waves, the shock motion must be uniform (η = constant).

Transforming the energy integral, Eq. 2.3.5 becomes

$$1 = y\left(\frac{I}{\eta} - \frac{1}{j+\omega+1} \left[\frac{1}{\gamma_o(\gamma_o-1)} + g \right] \right) \qquad (2.4.43)$$

where

$$I = \int_{\xi_p}^{1} \left(\frac{f}{\gamma_1-1} + \frac{4\phi^2}{2} \right) \xi^{j+\omega} d\xi \qquad (2.4.44)$$

$$y = \left(\frac{R_s}{R_o} \right)^{j+\omega+1} \qquad (2.4.45)$$

$$R_o = \left(\frac{E_o R_s^\alpha}{k_j A c_o^2} \right)^{\frac{1}{j+\omega+1}} \qquad (2.4.46)$$

y is the dimensionless shock radius while R_o is the generalized form of the characteristic explosion length. Differentiating the shock radius y with respect to η and noting that

$$R_s \frac{d}{dR_s} = \theta \dot{R}_s \frac{d}{d\dot{R}_s} = \theta m_s \frac{d}{dm_s} = -2\theta\eta \frac{d}{d\eta} \ , \qquad (2.4.47)$$

we can obtain a relationship for $y(\eta)$ as

$$\frac{dy}{d\eta} = -(j+\omega+1-\alpha) \frac{y}{2\theta\eta} \qquad (2.4.48)$$

An expression for θ can be obtained by differentiating Eq. 2.4.43 using the identity given by Eq. 2.4.47 as

$$\theta = -(j+\frac{\omega+1-\alpha}{2})\left(1 - \eta \frac{I_o}{I} \right) \qquad (2.4.49)$$

where

$$I_o = \frac{1}{j+\omega+1}\left(\frac{1}{\gamma_o(\gamma_o-1)} + \varphi \right) \qquad (2.4.50)$$

For self-similar solutions to exist, we see that the energy integral must be independent of η . This is possible under two conditions; for η = constant and for $\eta = 0$ (i.e., $m_s \rightarrow \infty$). For η = constant we see that y must be constant from Eq. 2.4.43 and from the definition of y given by Eq. 2.4.45 and 2.4.46, we obtain for y = constant

$$\alpha = j+\omega+1 \qquad (2.4.51)$$

From Eq. 2.4.49 we obtain for this case

$$\theta = 0 \qquad (2.4.52)$$

and the shock radius $R_s \sim t$. Hence for a constant velocity front driven by an expanding piston, the energy input to the flow

$E_{ext} \sim R_s^{j+\omega+1}$. For initial density ρ_o = constant

(i.e., $\omega = 0$), the energy input $E_{ext} \sim R_s^{j+1}$ which

implies a direct dependence on the rate of increase of the volume of

the shocked medium.

For a detonating medium, we can have the propagation of a

constant velocity Chapman-Jouguet wave without external energy input

mathematically, although experimentally, it has been shown that

detonation initiation always requires a finite amount of external

energy input. For this case we cannot define a characteristic explosion

length R_o since $E_o R_s^{\alpha} = 0$ and Eq. 2.4.43 can be written as

$$0 = R_s^{j+\omega+1}\left(\frac{I}{\eta_{CJ}} - \frac{1}{j+\omega+1}\left[\frac{1}{\gamma_o(\gamma_o-1)} + \xi \right]\right).$$ (2.4.53)

Since $R_s \neq 0$, we see that

$$I = \frac{\eta_{CJ}}{j+\omega+1}\left(\frac{1}{\gamma_o(\gamma_o-1)} + \xi \right) = \eta_{CJ} I_o$$ (2.4.54)

and from Eq. 2.4.49, we obtain again $\theta = 0$ corresponding to a constant

velocity front (i.e., $R_s \sim t$).

For self-similar motion where $\eta \to 0$ (i.e., $M_s \to \infty$),

we obtain from Eq. 2.4.49

$$\theta = -(j+\omega+1-\alpha)/2$$ (2.4.55)

and from Eq. 2.4.32, the time exponent N of the shock trajectory

(i.e., $R_s \sim t^N$) corresponds to

$$N = 2/(j+\omega+3-\alpha)$$ (2.4.56)

For constant energy input (i.e., $\alpha = 0$) in an initially uniform

medium (i.e., $\omega = 0$), we have the blast wave trajectory $R_s \sim t^{\frac{2}{j+3}}$.

Hence for planar, cylindrical and spherical strong blasts we have

$$R_S \sim t^{2/3} \quad , \quad R_S \sim t^{1/2} \quad \text{and} \quad R_S \sim t^{2/5} \quad \text{respectively.}$$

2.5 Similarity Equations

We shall consider a perfect gas with an initial density distribution $\rho_0 = A r^\omega$. Using the similarity transformations obtained in the previous Section,

$$\xi = \frac{r}{R_s(t)}$$

$$\phi = \frac{u}{\dot{R}_s}$$

$$f = \frac{p}{\rho_0 \dot{R}_s^2} \qquad\qquad (2.5.1)$$

$$\psi = \frac{\rho}{\rho_0}$$

the basic conservation equations (i.e., Eqs. 2.1.1 to 2.1.3) transform to the following:

Conservation of mass

$$(\phi - \xi)\psi' + \psi\phi' + (j+\omega)\psi\frac{\phi}{\xi} = 0 \qquad\qquad (2.5.2)$$

Conservation of momentum

$$(\phi - \xi)\phi' + \theta\phi + \frac{\omega f}{\xi\psi} + \frac{f'}{\psi} = 0 \qquad\qquad (2.5.3)$$

Conservation of energy

$$(\phi - \xi)\left(f' - \frac{\gamma f}{\psi}\psi'\right) + 2\theta f - (\gamma-1)\omega\frac{\phi f}{\xi} = 0 \qquad\qquad (2.5.4)$$

The alternate form of the energy equation given by Eq. 2.1.9

transforms similarly to the following

$$(\phi-\xi)f' + \gamma_1 f\phi' + 2\theta f + (\gamma_j j+\omega)\frac{f\phi}{\xi} = 0 \qquad (2.5.5)$$

The motion is bounded by the shock and the center of symmetry

$0 \leq \xi \leq 1$ or by the shock and the piston surface

$\xi_p \leq \xi \leq 1$. At the shock $\xi = 1$ (i.e., r = R$_s$), the

boundary conditions are given previously by Eqs. 2.2.4 to 2.2.8

and at the center of symmetry $\xi = 0$ (i.e., r = o) we have $\phi(o) = o$

(i.e., u = 0). At the piston surface $\xi = \xi_p$ (i.e., r = r$_p$)

the particle velocity u = u$_p$ or in the transformed coordinates, $\phi = \xi$

Solving for the derivatives γ', f' and ϕ' from Eqs. 2.5.2

to 2.5.4, we get

$$\gamma' = \frac{-\left[\{(\phi-\xi)^2 - \frac{\gamma_1 f}{4}\}(j+\omega)\frac{\phi\gamma}{\xi} - \theta\phi\gamma(\phi-\xi) + f(2\theta+\omega+\gamma_j j\frac{\phi}{\xi})\right]}{(\phi-\xi)\left[(\phi-\xi)^2 - \frac{\gamma_1 f}{4}\right]} \qquad (2.5.6)$$

$$\phi' = \frac{-\theta\phi(\phi-\xi) + \frac{f}{4}(2\theta+\omega+\gamma_j j\frac{\phi}{\xi})}{(\phi-\xi)^2 - \frac{\gamma_1 f}{4}} \qquad (2.5.7)$$

$$f' = \frac{-(\phi-\xi)\left[2\theta f +(\gamma_j j+\omega)f\frac{\phi}{\xi}\right] + \theta\gamma\phi f + \frac{\omega\gamma_1 f^2}{\xi 4}}{(\phi-\xi)^2 - \frac{\gamma_1 f}{4}} \qquad (2.5.8)$$

In the above equations, the parameter θ is known from the energy

integral(i.e., Eq. 2.4.52 and 2.4.55), hence they can be integrated

immediately using the boundary conditions at the front $\xi = 1$ by

some standard numerical integration scheme such as the Runge-Kutta method

Examining the similarity equations (i.e., Eqs. 2.5.6 to 2.5.8)
we see that there exist a number of singularities. Consideration of
these singularities is of prime importance in selecting the correct
solution. For explosion problems, the solutions belong to the so-
called first class of self-similar solutions as termed by Zeldovich
where the parameter θ is known a priori from the energy integral.
Hence the solution can be obtained immediately by integrating the
similarity equations with the boundary conditions given at the front
$\xi = 1$. However for the so-called second class of self-similar
solutions such as implosion problems, θ is not known a priori. It
is the condition that the value of θ be such that the solution be
regular at these singularities that determines the correct solution.
For this second class of self-similar motion, we have to iterate for
the correct value of θ , hence the solution, based on this criterion
of regularity at the singularity encountered in the flow domain.

From Eqs. 2.5.6 to 2.5.8, we note that there exist three
singularities

$$\xi = 0 \tag{2.5.9}$$

$$\phi = \xi \tag{2.5.10}$$

$$(\phi - \xi)^2 - \vartheta_1 f / \psi = 0 \tag{2.5.11}$$

The first singularity given by Eq. 2.4.9 occurs at the center of
symmetry $r = 0$ and this singularity always appears together with the
particle velocity ϕ (i.e., ϕ / ξ). Since symmetry demands that
$\phi \to 0$ as $\xi \to 0$, in order for f', ϕ' and ψ' to be finite, it
is necessary that $\phi \to c \xi^\alpha$ as $\xi \to 0$ with $\alpha \geq 1$. For the
problems encountered in general this condition is satisfied. For

example, the velocity profile is found to be linear near the center of
symmetry (i.e., $\alpha = 1$) for strong blast waves in an initially uniform
density medium.

The second singularity (i.e., Eq. 2.5.10) occurs when a particle
path coincides with a constant ξ line. This singularity occurs at the
piston surface or contact surface and for explosion in a non-uniform
density medium, at the vacuum edge. That the solution be regular at
this singularity requires particular values of the parameters θ , ω
and γ and will be discussed later in the specific explosion problems
considered.

The third type of singularity (i.e., Eq. 2.5.4) corresponds to
the condition when a constant ξ line coincides with a physical charac-
teristic (i.e., $\frac{dr}{dt} = u \pm c$). To demonstrate this, we see that on
a constant ξ line,

$$\frac{dr}{dt} = \xi \dot{R}_s = \frac{r}{R_s} \dot{R}_s$$

or

$$\frac{r}{R_s} = \frac{1}{\dot{R}_s} \frac{dr}{dt} = \xi$$

So the singularity

$$\left(\phi - \xi\right)^2 - \frac{\gamma f}{\gamma} = \frac{1}{\dot{R}_s^2}\left[\left(u - \frac{dr}{dt}\right)^2 - c^2\right] = 0$$

or in other words

$$\frac{dr}{dt} = u \pm c$$

This singularity is important in the study of the propagation of
Chapman-Jouguet detonations since the Chapman-Jouguet condition (i.e.,
$\dot{R}_s = u_1 + c_1$) implies that the detonation front trajectory is

a C^+ characteristic. This results in the solution being singular at $\xi = 1$ and it is this singularity that led to the questioning of the existence of steady cylindrical or spherical Chapman-Jouguet detonation waves. The singular nature of the solution for spherical Chapman-Jouguet detonations will be discussed in detail in a later Chapter. This singularity is also important in implosion problems since it occurs in the domain $1 \leq \xi \leq \infty$ of the implosion field. In fact it is the restriction that the desired solution be regular at this singularity that uniquely determines the correct physically valid solution.

It is interesting to note that an invariant can be formed from the similarity equations for arbitrary values of θ , j , ω and γ . This invariant is generally referred to as the first integral and can be derived as follows: From Eqs. 2.5.2 and 2.5.5, we obtain

$$\frac{\psi'}{\psi} + \frac{(\phi-\xi)'}{\phi-\xi} + \frac{j+\omega}{\xi} + \frac{(j+\omega+1)}{\phi-\xi} = 0 \qquad (2.5.12)$$

and

$$\frac{f'}{f} + \frac{\gamma(\phi-\xi)'}{\phi-\xi} + \frac{(\gamma j+\omega)}{\xi} + \frac{(\gamma(j+1)+\omega+2\theta)}{\phi-\xi} = 0 \qquad (2.5.13)$$

Eliminating $1/(\phi-\xi)$ from the above equations we obtain

$$\left[\gamma(j+1)+\omega+2\theta\right]\frac{\psi'}{\psi} - (j+\omega+1)\frac{f'}{f}$$

$$+ (\omega+2\theta-\gamma\omega)\frac{(\phi-\xi)'}{\phi-\xi} + \left[2\theta(j+\omega)+\omega(\gamma-1)\right]\cdot\frac{\xi'}{\xi} = 0$$

$$(2.5.14)$$

which can be integrated to yield

$$\frac{\psi^{\gamma(j+1)+\omega+2\theta}}{f^{j+\omega+1}} \cdot (\xi-\phi)^{\omega+2\theta-\gamma\omega} \cdot \xi^{2\theta(j+\omega)+\omega(\xi-1)} = k \tag{2.5.15}$$

The constant k in Eq. 2.5.15 can be evaluated using the boundary conditions at the front $\xi = 1$. For the case where the shock front propagates at a constant velocity (i.e., γ = constant and $\theta = 0$) the first integral reduces to

$$\frac{\psi^{\gamma(j+1)+\omega}}{f^{j+\omega+1}} \left(\frac{\xi}{\xi-\phi}\right)^{\omega(\xi-1)} = k \tag{2.5.16}$$

while for the case of a constant velocity shock propagating in an initially uniform me 'ium as well (i.e., $\omega = 0$) Eq. 2.5.16 reduces further to the following

$$\frac{\psi^{\gamma}}{f} = k . \tag{2.5.17}$$

From the definition of the variables f and ψ, Eq. 2.5.17 in di mensional form becomes

$$\frac{p}{\rho^{\gamma}} = constant . \tag{2.5.18}$$

This result simply states that all particles bounded by the shock have the same entropy. This is a direct consequence of the fact that the shock is of constant strength, hence the entropy increase across it is the same for each particle and since there are no further entropy sources present the entropy of each particle remains constant

throughout in the wake of the expanding shock front. For this class
of problems where the entropy remains uniform throughout the flow
field, we will refer to them as isentropic explosion problems in later
discussions. For an initially non-uniform medium (i.e., $\omega \neq 0$),
the initial entropy varies for each individual particle. Hence even
though the shock strength remains constant, the flow in the wake of
the shock is non-isentropic, but retains its initial entropy
distribution.

For constant strength shock waves (i.e., $\theta = 0$ but ω
not necessarily zero), it is more convenient to introduce a new
variable β defined as

$$\beta = \left(\frac{\gamma f}{\psi}\right)^{\frac{1}{2}} \tag{2.5.19}$$

The variable β is simply the dimensionless local sound speed.
Using Eqs. 2.5.16 and 2.5.19, we get

$$\psi \quad \left[K \left(\frac{\xi - \phi}{\xi}\right)^{\omega(\gamma-1)} \left(\frac{\beta^2}{\gamma_1}\right)^{j+\omega+1} \right]^{\frac{1}{(j+1)(\gamma-1)}} \tag{2.5.20}$$

and

$$f = \beta^2 \psi / \gamma_1 \tag{2.5.21}$$

and the three singularity equations (i.e., Eqs. 2.5.2, 2.5.3 and
2.5.5) can be reduced to two equations in ϕ and β as follows:

$$\tag{2.5.22}$$

$$\frac{2}{\gamma-1}(\phi-\xi)\beta' + \beta\phi' + j\phi\beta/\xi = 0$$

$$\frac{2}{\gamma-1}\left(\frac{\gamma(j+1)+\omega}{\gamma(j+1)}\right)\beta\beta'$$

$$+\left[(\phi-\xi)+\frac{\beta^2\omega}{\gamma(j+1)(\phi-\xi)}\right]\phi'$$

$$+\frac{\beta^2\omega}{\gamma\xi}\left(1-\frac{\phi}{(j+1)(\phi-\xi)}\right)=0$$

$$(2.5.23)$$

Solving the above equations for ϕ' and β' yields

$$\phi'=\frac{\beta^2\left(\frac{j\phi}{\xi}+\frac{\omega}{\gamma}\right)}{(\phi-\xi)^2-\beta^2}$$

$$(2.5.24)$$

$$\beta'=-\beta\left(\frac{\gamma-1}{2}\right)\frac{\left(\frac{j\phi(\phi-\xi)}{\xi}+\frac{\beta^2\omega}{\gamma(\phi-\xi)}\right)}{(\phi-\xi)^2-\beta^2}$$

$$(2.5.25)$$

For $\omega=0$, Eqs. 2.5.22 to 2.5.25 reduce respectively to the following equations

$$\frac{2}{\gamma-1}(\phi-\xi)\beta'+\beta\phi'+j\phi\beta/\xi=0$$

$$(2.5.26)$$

$$\frac{2}{\gamma-1}\beta\beta'+(\phi-\xi)\phi'\qquad=0$$

$$(2.5.27)$$

$$\phi' = \frac{j\phi\beta^2/\xi}{(\phi-\xi)^2-\beta^2} \qquad (2.5.28)$$

$$\beta' = -\left(\frac{\gamma_1-1}{2}\right) \frac{j\phi\beta(\phi-\xi)/\xi}{(\phi-\xi)^2-\beta^2} \qquad (2.5.29)$$

Once a solution for $\phi(\xi)$ and $\beta(\xi)$ has been obtained, $f(\xi)$ and $\psi(\xi)$ can be determined immediately from Eqs. 2.5.20 and 2.5.21.

Using Eqs. 2.2.4, 2.2.6 and the definition of β given by Eq. 2.5.19, the boundary condition for $\beta(1)$ at the shock front $\xi = 1$ can be obtained as

$$\beta(1) = \left(\frac{\gamma f(1)}{\psi(1)}\right)^{\frac{1}{2}}$$

$$= \frac{\gamma_1}{\gamma_0(\gamma_1+1)}\left\{(\gamma_0+\eta \pm \gamma_1 S)(\gamma_0+\eta \mp S)\right\}^{\frac{1}{2}} \qquad (2.5.30)$$

2.6 Similarity Equations in State Coordinates (Sedov's Coordinates)

The similarity coordinates we use are based on physical parameters where ϕ, f and ψ are simply the normalized particle velocity, pressure and the density respectively. As in classical gasdynamics, it is sometimes more convenient to work in state parameters using the local sound speed $c = (\gamma p/\rho)^{1/2}$ and the particle velocity u (i.e., the hodograph plane). The Russian school, after Sedov, extensively adopts these state parameters in their study of self-similar motion and in this Section we shall briefly discuss the similarity equations and boundary conditions in terms of Sedov's coordinates and point out the relationship to the similarity coordinates we adopt. The choice of coordinates is a matter of preference and although throughout later Chapters, we use only the physical coordinates in the analyses, a brief description of the alternate formalism based on state parameters is useful in better understanding of the numerous existing Russian works.

Following Sedov, we define Z and V, where Z is related to the local sound speed and V the particle velocity. To reduce the similarity equations in physical parameters (i.e., ϕ, f, ψ, ξ) into state coordinates we define

$$Z = \frac{N^2}{\xi^2} \cdot \frac{\gamma f}{\psi} \tag{2.6.1}$$

and

$$V = \frac{N}{\xi} \phi \tag{2.6.2}$$

where N is the time exponent of the shock trajectory (i.e., $R_s \sim t^N$). From Eqs. 2.6.1 and 2.6.2, we obtain

$$d \ln Z = d \ln f - d \ln \psi - 2 d \ln \xi \tag{2.6.3}$$

and

$$d\ln V = d\ln\phi - d\ln\xi \qquad (2.6.4)$$

and using Eqs. 2.6.1 to 2.6.4, the similarity equations in physical parameters given by Eqs. 2.5.2, 2.5.3 and 2.5.5 transform to the following:

Conservation of mass

$$(V-N)\frac{d\ln\psi}{d\ln V} + V(j+\omega+1)\frac{d\ln\xi}{d\ln V} + V = 0 \qquad (2.6.5)$$

Conservation of momentum

$$\frac{Z}{\gamma_1}\frac{d\ln\psi}{d\ln V} + \left[(\omega+2)\frac{Z}{\gamma_1}+V^2-V\right]\frac{d\ln\xi}{d\ln V} + \frac{Z}{\gamma_1}\frac{d\ln Z}{d\ln V} + V(V-N) = 0 \qquad (2.6.6)$$

Conservation of energy

$$(V-N)\frac{d\ln\psi}{d\ln V} + \left[2(V-1)+V(\omega+\gamma_1(j+1))\right]\frac{d\ln\xi}{d\ln V} + (V-N)\frac{d\ln Z}{d\ln V} + \gamma_1 V = 0 \qquad (2.6.7)$$

Solving the derivatives $d\ln Z/d\ln V$, $d\ln\psi/d\ln V$ and $d\ln\xi/d\ln V$ from the above equations, we obtain after considerable algebraic manipulations the following equations:

$$\frac{d\ln Z}{d\ln V} = \frac{-V[(V-N)^2-Z][2-(2+(j+1)\gamma_1(j+1))V]}{(V-N)\{V(V-1)(V-N)-Z[V(j+1)-\frac{1}{\gamma_1}(2-N(\omega+2))]\}}$$

$$- \frac{V(\gamma_1-1)}{V-N} \qquad (2.6.8)$$

$$\frac{d\ln u}{d\ln V} = \frac{-V}{V-N}\left[\frac{V(V-N)(V-1)-(j+\omega+1)V(V-N)^2+Z\{\omega V+\frac{1}{\gamma_1}(2-N(\omega+2))\}}{V(V-1)(V-N)-Z\{V(j+1)-\frac{1}{\delta_1}(2-N(\omega+2))\}}\right]$$

(2.6.9)

$$\frac{d\ln\xi}{d\ln V} = \frac{V(Z-(V-N)^2)}{V(V-1)(V-N)-Z\{V(j+1)-\frac{1}{\delta_1}(2-N(\omega+2))\}}$$

(2.6.10)

From Eqs. 2.6.9 and 2.6.10, we can eliminate $d\ln V$ and obtain

$$\frac{d}{d\ln\xi}\left[\ln(u(V-N))\right] = \frac{-V(j+\omega+1)}{V-N}$$

(2.6.11)

The above equations are identical to that given by Sedov although slightly different forms have been used by other Russian workers. Once a solution of $Z(V)$ has been obtained, $u(\xi)$, $V(\xi)$ can be found immediately from Eqs. 2.6.10 and 2.6.11. The pressure distribution $f(\xi)$ and the particle velocity $\phi(\xi)$ can be obtained from the definition of Z and V given by Eqs. 2.6.1 and 2.6.2. Rearranging these equations we get

$$f(\xi) = \frac{u Z \xi^2}{\gamma_1 N^2}$$

(2.6.12)

and

$$\phi(\xi) = \frac{\xi V}{N}$$

(2.6.13)

The singularities of the above similarity equations in $Z-V$ coordinates corresponding to those given previously by Eqs. 2.5.9

to 2.5.11 are

$$\xi = 0 \tag{2.5.9}$$

$$\phi - \xi = 0 \;\rightarrow\; (V-N) = 0 \tag{2.6.14}$$

$$(\phi - \xi)^2 - \frac{\gamma_1 f}{4} = 0 \;\rightarrow\; (V-N)^2 - Z = 0 \tag{2.6.15}$$

It should be noted that since a single integral curve $Z(V)$ can be used to represent the complete solution, it is sometimes more advantageous to work in $Z-V$ coordinates in the study of the mathematical properties of the solutions. In general the mathematical complexities involved are about the same in using either sets of coordinates.

Using the definition of Z and V and the general form of the Rankine-Hugoniot relationships for a shock given previously by Eqs. 2.2.4 to 2.2.8, the values for $Z(1)$ and $V(1)$ at the front $\xi = 1$ can be obtained as

$$V(1) = N\phi(1) = \frac{N\left(\gamma_0 - \gamma_1(\eta \mp S)\right)}{\gamma_0(\gamma_1 + 1)} \tag{2.6.16}$$

and

$$Z(1) = \frac{N^2 \gamma_1 f(1)}{4(1)} = \frac{N^2 \gamma_1^2 \left(\gamma_0 + \eta \pm \gamma_1 S\right)\left(\gamma_0 + \eta \mp S\right)}{\gamma_0^2(\gamma_1 + 1)^2} \tag{2.6.17}$$

Simplifying Eq. 2.6.17 using Eq. 2.6.16, we obtain

$$Z(1) = \left(V(1) - N\right)^2 \left[\frac{\gamma_0 + \eta \pm \gamma_1 S}{\gamma_0 + \eta \mp S}\right] \tag{2.6.18}$$

From the above equation we see that the locus of states for Chapman-Jouguet detonations lies on the parabola

$$Z(1) = (N - V(1))^2 \qquad (2.6.19)$$

since S = 0 for Chapman-Jouguet detonations. For overdriven detonations, the top sign in Eq. 2.6.18 is used while the weak detonation solution corresponds to the bottom sign.

For non-reacting shock waves (i.e., Q = 0), taking $\gamma_1 = \gamma_o = \gamma$, we have $S = 1 - \eta$ and Eq. 2.6.18 reduces to

$$Z(1) = (N - V(1))^2 \cdot \left[\frac{2\gamma - (\gamma - 1)\eta}{\gamma - 1 + 2\eta} \right] \qquad (2.6.20)$$

and using Eq. 2.2.30 for $\phi(1)$, we obtain

$$V(1) = \frac{2N}{\gamma + 1}(1 - \eta) \qquad (2.6.21)$$

Solving for η in the above equation we get

$$\eta = 1 - \frac{(\gamma + 1)}{2} \frac{V(1)}{N} \qquad (2.6.22)$$

and replacing η in Eq. 2.6.20 using Eq. 2.6.22, we obtain $Z(1)$ as a function of $V(1)$ as follows

$$Z(1) = (N - V(1))\left(N + (\frac{\gamma - 1}{2})V(1)\right) \qquad (2.6.23)$$

Eq. 2.6.23 gives the locus of states across a normal shock wave in a non-reacting medium. For infinite strength shock waves (i.e., $M_S \rightarrow \infty$, $\eta \rightarrow 0$) we have

$$V(1) \rightarrow \frac{2N}{\gamma + 1} \qquad (2.6.24)$$

$$z^2(1) = \frac{2\gamma N^2(\gamma-1)}{(\gamma+1)^2} \qquad (2.6.25)$$

For a highly detonable medium where $\eta_{cJ} << 1$, we can neglect terms of the order of η except for the term $\eta \mathcal{E}$ and we have the approximate boundary conditions given previously by Eqs. 2.2.20 to 2.2.23. Dropping the η term in Eq. 2.6.16 and solving for S , we get

$$S = \pm \frac{\gamma_0}{\gamma_1}\left[(\gamma_1+1)\frac{V(1)}{N} - 1\right] \qquad (2.6.26)$$

Dropping also the η terms in Eq. 2.6.17 and substituting S from Eq. 2.6.26, we obtain

$$Z(1) = \gamma_1 V(1)(N - V(1)) \qquad (2.6.27)$$

The above equation defines the locus of states for detonations in a highly detonable medium where $\eta_{cJ} << 1$.

The representation of shocked states on the $Z-V$ plane is illustrated below.
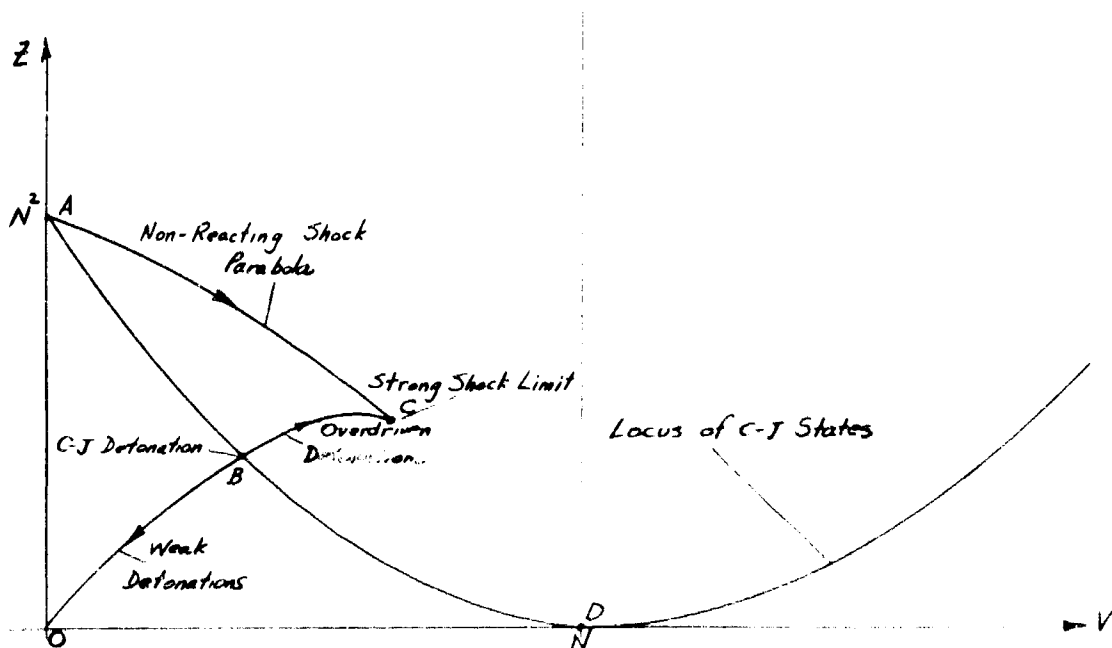
For strong shocks, the integral curve $Z(V)$ for the solution of Eq. 2.6.28 starts at point C $\left(Z(i) = 2\gamma_1 N^2 (\gamma_1 - 1)/(\gamma_1 + 1)^2, \quad V(i) = 2N/(\gamma + 1) \right)$ while for finite strength shock waves (i.e., $\eta \neq 0$), the integral curve $Z(V)$ starts on a point on the shock parabola AC given by Eq. 2.6.23. Given a particular shock Mach Number (hence η), $V(i)$ can be obtained from Eq. 2.6.21 and $Z(i)$ from Eq. 2.6.23 locating the starting point on the shock parabola AC. The locus of detonation states lie on the detonation parabola OBC given by Eq. 2.6.27. The portion of the detonation parabola BC corresponds to overdriven detonation states while the portion OB corresponds to weak detonation states. The Chapman-Jouguet states lie on the parabola ABD given by Eq. 2.6.19

The termination of the integral curves for various problems depends on the rear boundary conditions. For piston driven explosions, the condition at the piston surface is $\phi - \xi = 0$ or $V - N = 0$. Hence the integral curves terminate on the vertical line $V = N$ on the $Z - V$ plane. For freely expanding detonations, the integral curves terminate when the particle velocity $\phi = 0$ (hence $V = 0$) and the state is sonic (i.e. $Z = N^2$). Hence the integral curves for freely expanding detonations terminate at the point A where $Z = N^2$ on the Z axis. For strong point blast waves, the rear boundary conditions are that $\phi(0) = 0$ (i.e., $V = \dfrac{N}{\gamma_1}$) and since $\psi(0) = 0$ and $f(0) =$ finite, $Z \rightarrow \infty$. Hence the integral curve for strong blasts terminates on $V = N/\gamma_1$ at infinity. It can readily be shown where the various integral curves for different problems terminate once the rear boundary conditions are specified. Since the singularities of the similarity equations can be represented on the $Z - V$ plane, it is advantageous sometimes to investigate the nature of the singularities encountered by the solution using the $Z - V$ formulation. Details of the integral curves of Eq. 2.6.8 on the $Z - V$

plane are given in Sedov's book and in the sketch below, a few of them described above are illustrated.
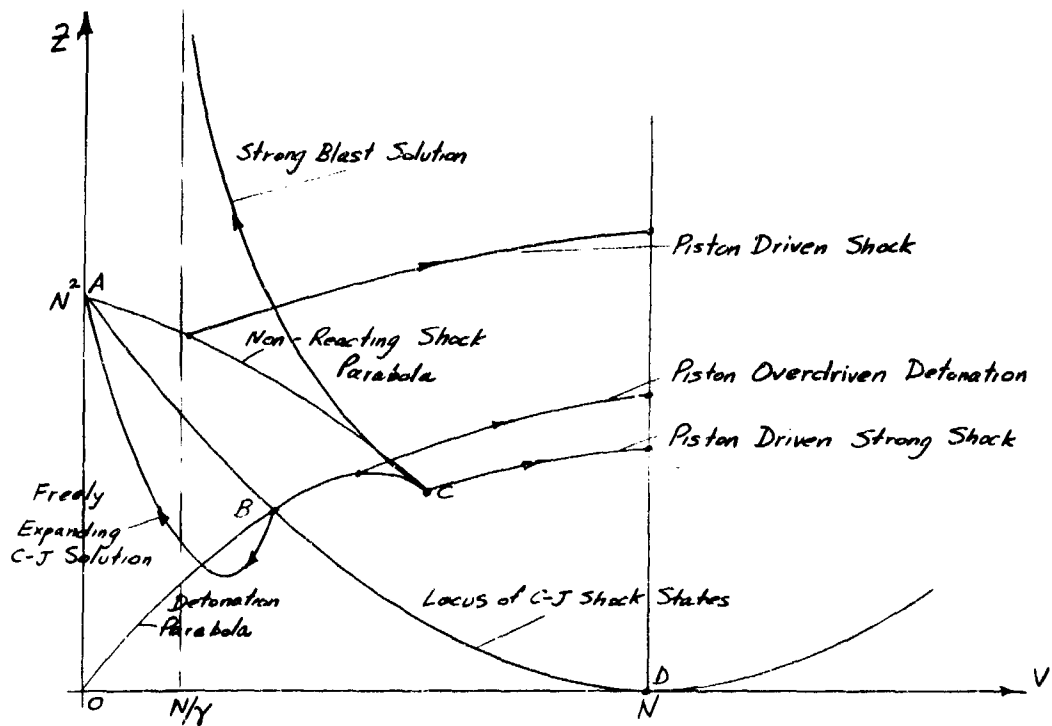
CHAPTER III

ISENTROPIC SELF-SIMILAR MOTIONS

In this Chapter we shall consider a number of explosion problems in which the gas motion   ded by the expanding shock or detonation front is isentropic. For the entire flow field to be isentropic throughout implies that the shock front propagates at a constant velocity and the entropy increase for all particles crossing the shock are identical. We shall also consider constant strength shock and detonation waves propagating into an initially non-uniform media (i.e. $\rho_o = \rho_o(r)$) although in this case the flow field is not isentropic throughout as a result of the initial non-uniformity. Also treated in this Chapter is the expansion of gas clouds into a vacuum environment.

3.1 General Solution for Planar Isentropic Self-Similar Motions

We first consider the general self-similar solution for planar isentropic flow in this section and in the following sections we shall apply this solution to the problem of explosion of a planar gas mass into a vacuum, the propagation of planar Chapman-Jouguet detonations, the shock tube problem, and for detonation driven shock waves.

For isentropic motions, the similarity equations given previously in Chapter II (i.e., Eqs. 2.5.28 and 2.5.29) are

$$\phi' = \frac{j\,\phi\beta^2/\xi}{(\phi-\xi)^2 - \beta^2} \tag{2.5.28}$$

$$\beta' = \frac{-(\tfrac{\gamma-1}{2})\,j\,\phi\beta(\phi-\xi)/\xi}{(\phi-\xi)^2 - \beta^2} \tag{2.5.29}$$

For planar motion where $j = 0$, we see that the above equations yield two possible solutions: i) we have $(\phi-\xi)^2 - \beta^2 \neq 0$ hence $\beta' = 0$, $\phi' = 0$ giving $\beta =$ constant and $\phi =$ constant and ii) $(\phi-\xi)^2 - \beta^2 = 0$ in which case β' and ϕ' are both finite. The first solution is the trivial solution corresponding to a planar piston driving a constant velocity shock or detonation wave where the fluid states are constant from the shock to the piston surface and the piston velocity is equal to the particle velocity behind the front. For the second solution we have

$$(\phi-\xi)^2 - \beta^2 = 0 \tag{3.1.1}$$

or
$$\phi \cdots \qquad \cdots \phi' \tag{3.1.2}$$

From the similarity equations for ϕ and β (i.e., Eqs. 2.5.26 and 2.5.27) we get

$$\frac{\phi'}{\beta'} = \frac{2}{\gamma-1} \frac{\phi'}{\cdots} \tag{3.1.3}$$

Substituting Eq. 3.1.2 into the above equation, we get

$$\frac{\phi'}{\beta'} = \mp \frac{2}{\gamma-1} \tag{3.1.4}$$

which can be integrated immediately to yield

$$\phi = \mp \frac{2\beta}{\gamma-1} + const. \tag{3.1.5}$$

Using Eqs. 3.1.2 and 3.1.5, we obtain the solution for $\beta(\xi)$ and $\phi(\xi)$ as

$$\beta(\xi) = \mp \frac{(\gamma-1)}{\gamma+1}(\xi-1) + \beta(1) \tag{3.1.6}$$

$$\phi(\xi) = \frac{2}{\gamma+1}(\xi-1) + \phi(1) \tag{3.1.7}$$

where

$$\phi(1) = 1 \pm \beta(1) \tag{3.1.8}$$

and $f(1)$ and $p(1)$ are the boundary condition at $\xi = 1$ which depends on the particular problem considered. Eqs. 3.1.6 and 3.1.7 give the general solution for planar one dimensional self-similar motion in an initially uniform medium.

3.2 Explosion of a Planar Gas Cloud into Vacuum

Consider initially a semi-infinite gas mass of uniform density ρ_0 and sound speed c_0 occupying the negative r half plane at time t = 0. At time $t > 0$, the gas cloud expands into the vacuum environment of the positive r half-plane. We have then a rarefaction fan the head of which propagates into the gas cloud at velocity c_0 and an escape front moving into the vacuum at $u_e = \frac{2c_0}{\gamma-1}$. In this problem $R_u = u_e$ and the corresponding boundary conditions are

$$\phi(1) = 1 \quad , \quad \beta(1) = 0 \tag{3.2.1}$$

Using Eq. 3.2.1, the constants of the general solution given previously by Eqs. 3.1.6 and 3.1.7 can be evaluated and the solution can be written as

$$\phi(\xi) = \frac{2}{\gamma+1}(\xi-1) + 1 \tag{3.2.2}$$

$$\beta(\xi) = -\frac{(\gamma-1)}{\gamma+1}(\xi-1) \tag{3.2.3}$$

Note that the negative sign must be used for β in this problem since β increases for decreasing ξ and β is always positive for it corresponds to the local thermodynamic state.

To determine the position of the head of the rarefaction fan propagating into the gas cloud ξ_r we note that at the rarefaction head the particle velocity u = 0 (hence ϕ = 0). Setting Eq. 3.2.2 to zero and solving for ξ , we get

$$\xi_r \; = \; -\left(\frac{\gamma-1}{2}\right) \qquad\qquad (3.2.4)$$

Substituting this value of ξ_r into Eq. 3.2.3, we obtain the value of $\beta(\xi_r)$ as

$$\beta(\xi_r) \; = \; \frac{\gamma-1}{2} \qquad\qquad (3.2.5)$$

Since $\beta = c/R_s = c/u_e = c(\gamma-1)/(x_o)$, we see that from Eq. 3.2.5, the value of the sound speed at the rarefaction head is equal to c_o which is consistent with the boundary condition of the problem.

To obtain the pressure and the density distribution, we use the isentropic condition

$$\frac{f}{\gamma^\gamma} \; = \; A \qquad\qquad (3.2.6)$$

and the definition of β given as

$$\beta^2 = \; \frac{\gamma f}{\gamma} \qquad\qquad (3.2.7)$$

The constant A in Eq. 3.2.6 can be evaluated readily to be

$$A \; = \; \frac{(\gamma-1)^2}{4 \delta} \qquad\qquad (3.2.8)$$

for this particular problem. From the above relationships the pressure and
the density distributions obtained are

$$p = p_0 \left[\frac{2}{\gamma+1}(1-\xi) \right]^{\frac{2\gamma}{\gamma-1}} \qquad (3.2.9)$$

$$\rho = \rho_0 \left[\frac{2}{\gamma+1}(1-\xi) \right]^{\frac{2}{\gamma-1}} \qquad (3.2.10)$$

A sketch of the variations of ϕ, β, ρ, and p are shown in the
figure below.
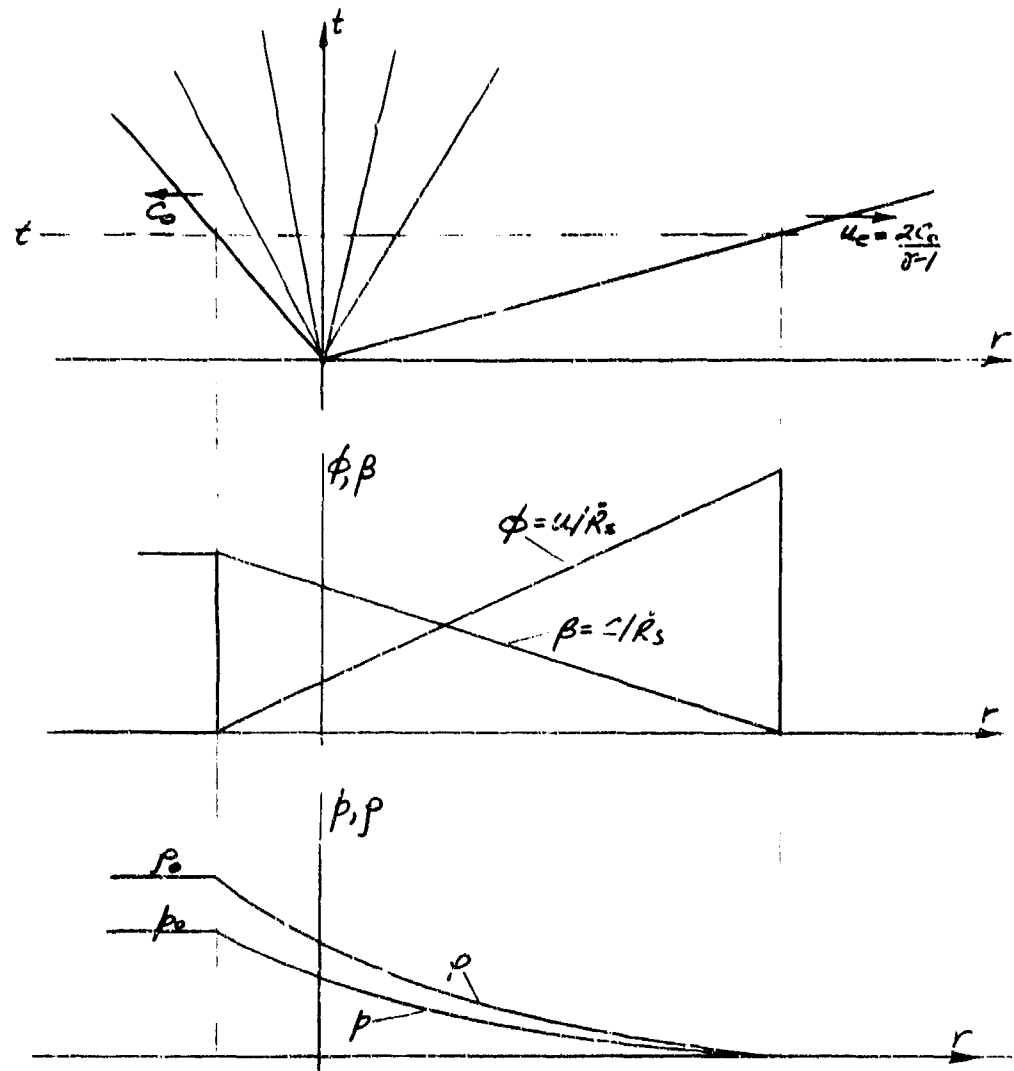
3.3 Propagation of Planar Chapman-Jouguet Detonations

In this Section we shall analyse the motion of a planar Chapman-Jouguet detonation wave originating at time $t = 0$ at $r = 0$ and propagating thereafter at its Chapman-Jouguet velocity $\dot{R}_s = \dot{R}_{sCJ}$. The isentropic motion of the combustion products in the wake of the detonation wave is described by the general solution given previously by Eqs. 3.1.6 and 3.1.7 as

$$\phi(\xi) = \frac{2}{\gamma+1}(\xi-1) + \phi(1) \tag{3.1.6}$$

$$\beta(\xi) = \frac{\gamma-1}{\gamma+1}(\xi-1) + \beta(1) \tag{3.1.7}$$

Note that the positive sign is taken in Eq. 3.1.7 in this problem since β decreases in the expansion fan behind the detonation front. The boundary conditions at the detonation front are given previously by Eqs. 2.2.15 and 2.5.30 as

$$\phi(1) = \frac{\gamma_0 - \gamma_1\eta_{CJ}}{\gamma_0(\gamma_1+1)} \tag{2.2.15}$$

$$\beta(1) = \frac{\gamma_1(\gamma_0+\eta_{CJ})}{\gamma_0(\gamma_1+1)} \tag{2.5.30}$$

where η_{CJ} is given by Eq. 2.2.13

$$\eta_{CJ} = \frac{\gamma_0}{\gamma_1} + \frac{k}{2} - \left[\frac{\gamma_0^2}{\gamma_1^2} - 1 + k\left(\gamma_0 + \frac{k}{4}\right)\right]^{\frac{1}{2}} \tag{2.2.13}$$

From Eqs. 2.2.15 and 2.2.30 we note that for $C-J$ detonations,

$$\phi(1) + \beta(1) = 1 \tag{3.3.1}$$

For a closed end tube, the rear boundary condition is $\phi(0) = 0$ or at some finite value of $\xi = \xi_0$, and the solution given by Eqs. 3.1.6 and 3.1.7 is valid in the region $\xi_0 \leq \xi \leq 1$ where $\phi(\xi_0) = 0$. Setting Eq. 3.1.6 equal to zero and solving for ξ_0 , we get

$$\xi_0 = 1 - (\frac{\gamma+1}{2})\phi(1) \tag{3.3.2}$$

For $\phi = 0$, we have $\beta = \beta(\xi_0)$ = constant and substituting Eq. 3.3.2 into Eq. 3.1.7 we obtain

$$\beta(\xi_0) = \beta(1) - (\frac{\gamma-1}{\gamma+1})\phi(1) \tag{3.3.3}$$

and using the Chapman-Jouguet condition of $\phi(1) + \beta(1) = 1$, Eq. 3.3.3 becomes

$$\beta(\xi_0) = 1 - \frac{2\gamma}{\gamma+1}\phi(1) \tag{3.3.4}$$

Using the approximate relationship for $\phi(1)$ given by Eq. 2.2.23

$$\phi(1) \sim \frac{1}{\gamma+1} \tag{2.2.27}$$

we obtain $\xi_0 \sim 0.5$. Hence the flow field behind a planer Chapman-Jouguet detonation wave consists of an expansion region immediately behind the front. A stationary zone of constant fluid properties exists at approximately half the total distance traversed by the detonation front.

For the detonation originating from an open end, the problem is considerably more complex. The expansion of the high pressure detonation

products into the low pressure inert gas drives a constant velocity shock wave in it. This problem will be treated in the next Section in connection with the shock tube problem. However if one assumes the exit pressure of the open end is constant equal to say the ambient atmospheric pressure the solution given by Eqs. 3.1.6 to 3.1.7 is still valid. The pressure decreases from the detonation front until it is equal to the exit pressure.

It should be noted that for overdriven planar detonations, $(\phi - \xi)^2 - \beta^2 \neq 0$ at the front, hence we have the simple solution where $\phi' = \beta' = 0$, $\phi(\xi) = \phi(1)$ and $\beta(\xi) = \beta(1)$ and remain constant from the detonation front to the piston surface.

3.4 The Shock Tube Problem

In this Section we shall apply the general solution for planar isentropic motion to the classical shock tube problem. Consider initially at time t = 0 a diaphram separating the negative r half space filled with a high pressure gas at $p = p_4$, $\rho = \rho_4$, $C = C_4$, $u_4 = 0$ from the positive r half space filled with a low pressure gas at $p = p_0$, $\rho = \rho_0$, $C = C_0$ and $u_0 = 0$. At $t > 0$, the diaphram is removed, a shock is formed propagating into the low pressure region while a centered rarefaction fan propagates into the high pressure gas. A contact-surface separates the shocked gas from the expanded gas in the high pressure region. The r - t diagram illustrating the wave system for the shock tube problem is shown below.

t

Tail of Rarefaction Fan

Contact Surface

Shock

Head of Rarefaction

p_4, ρ_4, C_4, γ
$u_4 = 0$

p_0, ρ_0, C_0, γ
$u_0 = 0$

r

O
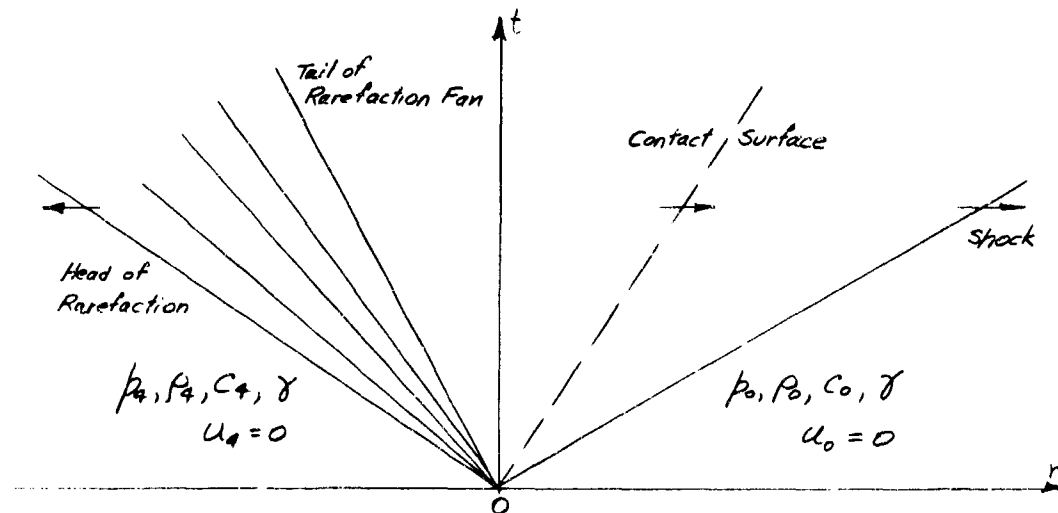
We choose the shock velocity $\dot{R}_s$ as the characteristic velocity and the similarity variable $\xi = r/R_s$. We denote the contact surface by ξ_c, the tail of rarefaction by ξ_t and the head of the fan by ξ_r. Since the shock velocity is unknown and to be determined, ξ_c, ξ_T and ξ_r are also unknown. The boundary conditions to be satisfied at the shock front $\xi = 1$ are given previously by Eqs. 2.2.30 and 2.5.30.

$$\phi(\iota) = \frac{2}{\gamma+\iota}(\iota-\eta) \tag{2.2.30}$$

$$\beta(\iota) = \left[\frac{\gamma f(\iota)}{\psi(\iota)}\right]^{\frac{1}{2}} = \frac{\iota}{\gamma+\iota}\left[(2\gamma-(\gamma-\iota)\eta)(\gamma-\iota+2\eta)\right]^{\frac{1}{2}} \tag{2.5.30}$$

From the basic equations (i.e., Eqs. 2.5.28 and 2.5.29) we see that the solution for the region bounded by the shock and the contact surface $\xi_c \leq \xi \leq \iota$ is the simple solution in which $\phi' = \beta' = 0$ and the fluid properties remain constant (i.e., $\phi(\xi) = \phi(\iota)$, $\beta(\xi) = \beta(\iota)$).

At the contact surface, the particle velocity and the pressure are continuous while the density and therefore the sound speed is discontinuous. Hence we have

$$\phi(\xi_c) = \phi(\iota) \tag{3.4.1}$$

$$f(\xi_c) = f(\iota) \tag{3.4.3}$$

The region bounded by the contact surface and the tail of the rarefaction fan $\xi_t \leq \xi \leq \xi_c$ is again uniform, hence

$$\phi(\xi_t) = \phi(\xi_c) = \phi(\iota) \tag{3.4.3}$$

$$f(\xi_t) = f(\xi_c) = f(\iota) \tag{3.4.4}$$

The expansion region of the rarefaction fan $\xi_r \leq \xi \leq \xi_t$ is described by the general solution given previously by Eqs. 3.1.6 and 3.1.7. Evaluating the constants using the boundary condition a ξ_r

$$\phi(\xi_r) = 0 \tag{3.4.5}$$

$$\beta(\xi_r) = \frac{C_4}{R_s} = \left[\frac{p_4}{p_0} \cdot \frac{\rho_0}{p_4} \eta \right]^{\frac{1}{2}} \tag{3.4.6}$$

where

$$\eta = 1/m_s^2 = c_0^2/R_s^2 \,,$$

and the subscripts 4 and 0 denote the initial high pressure and low pressure states respectively, the solution for the region $\xi_r \le \xi \le \xi_t$ can be written as

$$\phi(\xi) = \frac{2}{\gamma+1}(\xi-\xi_r) \tag{3.4.7}$$

$$\beta(\xi) = -\frac{(\gamma-1)}{\gamma+1}(\xi-\xi_r) - \xi_r \tag{3.4.8}$$

Note that the boundary condition for $\beta(\xi_r)$ can be obtained by applying the condition $(\phi-\xi)^2 - \beta^2 = 0$ at $\xi = \xi_r$ and since $\phi(\xi_r)=0$, therefore

$$\beta(\xi_r) = -\xi_r = \left[\frac{p_4}{p_0} \cdot \frac{\rho_0}{p_4} \eta \right]^{\frac{1}{2}} \tag{3.4.9}$$

From the definition of $\beta = \left(\frac{\gamma f}{\rho}\right)^{\frac{1}{2}}$ and the isentropic condition $f/\rho^\gamma =$ constant, we can express the pressure $f(\xi)$ as

$$f(\xi) = k \cdot \beta(\xi)^{\frac{2\gamma}{\gamma-1}} \tag{3.4.10}$$

Using Eqs. 3.4.8 and 3.4.9, Eq. 3.4.10 becomes

$$f(\xi) = f(\xi_r)\left[1 + \frac{(\gamma-1)}{\gamma+1}\left(\frac{\xi-\xi_r}{\xi_r}\right)\right]^{\frac{2\gamma}{\gamma-1}} \qquad (3.4.11)$$

where

$$f(\xi_r) = \frac{p_4}{\rho_0 R_s^2} = \frac{p_4}{\rho_4}\frac{\eta}{\gamma} \qquad (3.4.12)$$

Matching the pressure at the contact surface we get

$$f(\xi_t) = \frac{p_4}{\rho_4}\frac{\eta}{\gamma}\left[1 + \frac{(\gamma-1)}{(\gamma+1)}\cdot\left(\frac{\xi_t-\xi_r}{\xi_r}\right)\right]^{\frac{2\gamma}{\gamma-1}} = f(\xi_c) = f(1) \qquad (3.4.13)$$

where $f(1)$ is the pressure at the shock given previously by Eq. 2.2.31 in terms of η as

$$f(1) = \frac{2}{\gamma+1}\left(1 - \frac{(\gamma-1)}{2\gamma}\eta\right) \qquad (2.2.31)$$

From Eq. 3.4.7, we obtain ξ_t as

$$\xi_t = \xi_r + \left(\frac{\gamma+1}{2}\right)\phi(\xi_t) \qquad (3.4.14)$$

Matching the particle velocity at the contact front using Eq. 3.4.3, we get

$$\xi_t = \xi_r + \left(\frac{\gamma+1}{2}\right)\phi(1) \qquad (3.4.15)$$

where $\phi(1)$ is the boundary condition at the shock given by Eq. 2.2.30. Using Eq 3.4.9 for ξ_r, Eqs. 3.4.15 for ξ_t, Eqs. 2.2.31 and 2.2.30 for $f(1)$ and $\phi(1)$, Eq. 3.4.13 becomes

$$\frac{p_4}{\rho_4}\frac{\eta}{\gamma}\left[1 - \frac{(\gamma-1)}{(\gamma+1)}(1-\eta)\left(\frac{p_4}{\rho_4}\frac{\rho_0}{p_4}\eta\right)^{-\frac{1}{2}}\right]^{\frac{2\gamma}{\gamma-1}} = \frac{2}{\gamma+1}\left(1 - \frac{(\gamma-1)\eta}{\gamma}\right)$$

$$\frac{p_4}{p_o}\frac{\eta}{\gamma}\left[1-\frac{(\gamma-1)}{\gamma+1}(1-\eta)\frac{c_4}{c_o}\eta^{-\frac{1}{2}}\right]^{\frac{2\gamma}{\gamma-1}} = \frac{2}{\delta+1}\left(1-\frac{(\gamma-1)\eta}{2\gamma}\right)$$

(3.4.16)

Given the initial conditions (i.e., p_4/p_o, c_4/c_o, γ) the resultant shock strength can be obtained from Eq. 3.4.16.

In an identical manner, the problem of the propagation of a Chapman-Jouguet detonation driven shock can be analysed. Here we consider the negative r half space as initially filled with an explosive gas at p_4, ρ_4, c_4 and the positive r half space by an inert gas at p_o , ρ_o , c_o . At time $t = 0$, a Chapman-Jouguet detonation is initiated at $r = 0$ and propagated thereafter into the explosive where the expansion of the detonation products into the positive r half space drives a shock into it. The r - t diagram is identical to that for the shock problem except that instead of a sound wave propagating at c_4 we have a Chapman-Jouguet detonation wave. Again we denote the shock by $\xi = 1$, the contact surface separating the expanded detonation products by $\xi = \xi_c$, the tail of the rarefaction by $\xi = \xi_t$ and the Chapman-Jouguet detonation by $\xi = \xi_r$. Note that

$$\xi_r = \frac{R_{CJ}}{R_s} = \frac{\dot{R}_{CJ}}{\dot{R}_s} = -(\eta/\eta_{CJ}')^{\frac{1}{2}}$$

(3.4.17)

where

$$\eta_{CJ}' = 1/m_{CJ}'^2 = c_o^2/\dot{R}_{CJ}^2$$

(3.4.18)

m'_{cr} is not the usual Chapman-Jouguet detonation Mach number since instead of using the initial sound speed of the explosive c_4 as a reference we use the initial sound speed c_o of the inert medium.

For the region bounded by the detonation front and the tail of the rarefaction (i.e., $\xi_r \leq \xi \leq \xi_t$) we have the solution given previously by Eqs. 3.1.6 and 3.1.7. Using the appropriate boundary conditions for this problem for the constants, we get

$$\phi(\xi) = \frac{2}{\gamma+1}\left(\xi - \xi_r\right) + \phi(\xi_r) \tag{3.4.19}$$

$$\beta(\xi) = \frac{-(\gamma-1)}{\gamma+1}\left(\xi - \xi_r\right) + \beta(\xi_r) \tag{3.4.20}$$

where $\beta(\xi_r)$ and $\phi(\xi_r)$ are the conditions immediately behind the detonation front. It should be noted that the ϕ and β given by Eqs. 3.4.19 and 3.4.20 are referenced to $\dot{R}_s$ (i.e., $\phi = u/\dot{R}_s$, $\beta = c/\dot{R}_s$) instead of $\dot{R}_{cJ}$. Since the boundary conditions for ϕ , f , ψ and β for a Chapman-Jouguet detonation given previously by Eqs. 2.2.14-16 and 2.5.30 are based on $\eta_{cJ} = (c_4^2/\dot{R}_{cr}^2)$, we have to transform them for the present problem based on $\eta'_{cJ} = (c_o/\dot{R}_{cJ})^2$. Using Eq. 3.4.18 we get the following relationships.

$$\phi(\xi_r) = \xi_r \phi_{cJ} \tag{3.4.21}$$

$$f(\xi_r) = \xi_r^2 f_{cJ} \tag{3.4.22}$$

$$\psi(\xi_r) = \psi_{cJ} \tag{3.4.23}$$

$$\beta(\xi_r) = |\xi_r|\beta_{cJ} \tag{3.4.24}$$

where ϕ_{CJ} , f_{CJ} , ψ_{CJ} and β_{CJ} are as given previously by Eqs. 2.2.15, 2.2.16, 2.2.14, 2.5.30 respectively as (with $\gamma_o' = \gamma_1 = \gamma$)

$$\phi_{CJ} = \frac{1 - \eta_{CJ}}{\gamma + 1} \qquad (3.4.25)$$

$$f_{CJ} = \frac{\gamma + \eta_{CJ}}{\gamma(\gamma + 1)} \qquad (3.4.26)$$

$$\psi_{CJ} = \frac{\gamma + 1}{\gamma + \eta_{CJ}} \qquad (3.4.27)$$

$$\beta_{CJ} = \frac{\gamma + \eta_{CJ}}{\gamma + 1} . \qquad (3.4.28)$$

As in the previous problem, the region bounded by the shock and the contact front (i.e., $\xi_c \leq \xi \leq 1$) is uniform with

$$\phi(\xi) = \phi(1) = \frac{2}{\gamma + 1}(1 - \eta) \qquad (2.2.30)$$

$$\beta(\xi) = \beta(1) = \frac{1}{\gamma + 1}\left[(2\gamma - (\gamma - 1)\eta)(\gamma - 1 + 2\eta)\right]^{\frac{1}{2}} \qquad (2.5.30)$$

Since

$$\phi(\xi_t) = \phi(\xi_o) = \phi(1) , \qquad (3.4.3)$$

we obtain from Eqs. 3.4.19 and 2.2.30 the following relationship

$$\frac{2}{\gamma + 1}(\xi_t - \xi_r) + \xi_r \phi_{CJ} = \frac{2}{\gamma + 1}(1 - \eta). \qquad (3.4.29)$$

From Eq. 3.4.10 and the solution for β given by Eq. 3.4.20, we obtain the pressure distribution in the region $\xi_r \leq \xi \leq \xi_t$ as

$$f(\xi) = f(\xi_r)\left[1 - \left(\frac{\gamma - 1}{\gamma + 1}\right)\frac{(\xi - \xi_r)}{|\xi_r|\beta_{CJ}}\right]^{\frac{2\gamma}{\gamma - 1}} \qquad (3.4.30)$$

and again matching the pressure at the contact front we get

$$f(\xi_t) = f(\xi_r)\left[1 - \frac{(\gamma-1)}{\gamma+1} \cdot \frac{(\xi_t - \xi_r)}{|\xi_r|\beta_{CJ}}\right]^{\frac{2\gamma}{\gamma-1}} = f(\xi_s) = \overset{\circ}{f}(1) \qquad (3.4.31)$$

where $\overset{\circ}{f}(1)$ is the pressure of the shock given by Eq. 2.2.31. Solving for $\xi_t - \xi_r$ from Eq. 3.4.29 we get

$$\xi_t - \xi_r = (1-\eta) - \left(\frac{\gamma+1}{2}\right)\xi_r \phi_{CJ}' \qquad (3.4.32)$$

and substituting Eqs. 3.4.32 and 2.2.31 into Eq. 3.4.31, we get

$$\frac{2}{\gamma+1}\left(1 - \frac{(\gamma-1)}{2\gamma}\eta\right) = f(\xi_r)\left[1 - \frac{(\gamma-1)}{(\gamma+1)}\left(1-\eta - \left(\frac{\gamma+1}{2}\right)\xi_r \phi_{CJ}'\right)\frac{1}{|\xi_r|\beta_{CJ}}\right]^{\frac{2\gamma}{\gamma-1}} \qquad (3.4.33)$$

Eliminating $f(\xi_r)$, ξ_r, ϕ_{CJ}', β_{CJ} using Eqs. 3.4.22, 3.4.26, 3.4.17, 3.4.25 and 3.4.28, we get the following result

$$\frac{2}{\gamma+1}\left(1 - \frac{(\gamma-1)}{2\gamma}\eta\right) = \left(\frac{C_+^2 \eta}{C_0^2 \eta_{CJ}}\right)\left(\frac{\gamma + \eta_{CJ}}{\gamma(\gamma+1)}\right)\left[1 - \frac{(\gamma-1)}{\gamma + \eta_{CJ}}\left(\frac{C_0^2 \eta_{CJ}}{C_+^2 \eta}\right)^{\frac{1}{2}}\right.$$
$$\left. \cdot \left(1 - \eta + \left(\frac{1-\eta_{CJ}}{2}\right)\left(\frac{C_+^2 \eta}{C_0^2 \eta_{CJ}}\right)^{\frac{1}{2}}\right)\right]^{\frac{2\gamma}{\gamma-1}} \qquad (3.4.34)$$

For a given explosive η_{CJ} can be obtained and the solution of Eq. 3.4.34 gives the shock strength η in the inert medium.

3.5 Freely Expanding Cylindrical and Spherical Chapman-Jouguet Detonation

Here we consider the problem of a cylindrical or spherical Chapman-Jouguet detonation wave originating at time $t = 0$ from the center of symmetry $r = 0$. This problem is particularly interesting since mathematically speaking the existence of spherical C-J detonation rests on the fact that a solution to the gasdynamic equations satisfying the C-J conditions at the front can be obtained. Due to the singular nature of the solution at the C-J front, there has been some doubt on the possibility of steady state spherical C-J detonations. However this singularity is of the same nature as the assumption of a discontinuity for the detonation front. It has been found that a more serious approximation concerns the model itself which reflects the fact that a finite quantity of energy must be used to initiate the detonation initially. We shall consider the influence of this initiation energy in a later Chapter on non-similar solutions and in this Section we deal with the idealized classical model.

The basic equations as given previously for the isentropic motion behind the C-J front are

$$\phi' = \frac{j\phi\beta^2/\xi}{(\phi-\xi)^2-\beta^2} \qquad (2.5.28)$$

$$\beta' = -j\frac{(\gamma-1)}{2}\frac{\phi\beta}{\xi}\cdot\frac{(\phi-\xi)}{(\phi-\xi)^2-\beta^2} \qquad (2.5.29)$$

At the boundary we have $\phi = \phi(1)$ and $\beta = \beta(1)$ and the C-J condition requires that

$$\phi(1) + \beta(1) = 1$$

(3.5.1)

or $\qquad (\phi(1) - 1)^2 - \beta^2(1) = 0$

Since for cylindrical and spherical waves $j \neq 0$, the C-J condition results in $\phi' \to \infty$, $\beta' \to \infty$ at the front $\xi = 1$. Hence before we can proceed to integrate numerically Eqs. 2.5.28 and 2.5.29, we must seek the solution in the neighborhood of the front to avoid the singularity. Assuming a general perturbation series of the form

$$\phi(\xi) = a_0 + a_1(1-\xi)^\alpha + \cdots$$

(3.5.2)

$$\beta(\xi) = b_0 + b_1(1-\xi)^b + \cdots$$

for ϕ and β in the immediate neighborhood of the front $\xi = 1$, we have to determine the coefficients a_n and b_n and also the exponents α and b from the boundary conditions and the basic equations.

Since both ϕ and β are finite at the front, the zero order coefficients must be

$$a_0 = \phi(1)$$

(3.5.3)

$$b_0 = \beta(1)$$

and also that the exponents α and b must be positive (i.e., $\alpha, b > 0$). Differentiating Eq. 3.5.2 we obtain

$$\phi' = -a_1\alpha(1-\xi)^{\alpha-1} + -$$

(3.5.4)

$$\beta' = -b_1 b(1-\xi)^{b-1} + \cdots$$

and since $\phi' \to \infty$, $\beta' \to \infty$ as $\xi \to 1^{(-)}$, the exponents must necessarily be less than unity.

Hence we have so far established

$$0 < \alpha, b < 1 \tag{3.5.5}$$

To find the value for α and b we then substitute the perturbation expansion (i.e., Eqs. 3.5.2 and 3.5.4) into the basic equations (i.e., Eqs. 2.5.28 and 2.5.29). From Eq. 2.5.28 we obtain

$$\left\{ 2\alpha a_1^2 b_0 (1-\xi)^{2\alpha-1} + 2 a_1 \alpha b_0 b_1 (1-\xi)^{\alpha+b+1} + \cdots \right\}$$
$$-j \left\{ a_0 b_0^2 + a_1 b_0^2 (1-\xi)^\alpha + \cdots \right\} = 0 \tag{3.5.6}$$

Since j, a_0 and b_0 are finite we must have either $2\alpha - 1 = 0$ or $\alpha + b - 1 = 0$. From Eq. 3.5.5 we obtain

$$\left\{ 2b b_0 b_1^2 (1-\xi)^{2b-1} + 2b b_0 b_1 a_1 (1-\xi)^{\alpha+b-1} + \cdots \right\}$$
$$-j \left(\frac{\gamma-1}{2}\right) a_0 b_0^2 + \cdots = 0 \tag{3.5.7}$$

which requires either $2b - 1$ or $\alpha + b - 1 = 0$ for Eq. 3.5.7 to be satisfied. From investigating these conditions we see that for $\alpha = b = \frac{1}{2}$, all conditions are satisfied siumltaneously and give the correct exponent for the expansion. Putting $\alpha = b = 1/2$ into Eqs. 3.5.6 and 3.5.7 we obtain the first order coefficients as

$$a_1 = \pm \left(\frac{2j \phi(1) \beta(1)}{\gamma+1} \right)^{\frac{1}{2}} \tag{3.5.8}$$

$$b_1 = \pm \left(\frac{\gamma-1}{2}\right) \left(\frac{2j \phi(1) \beta(1)}{\gamma+1} \right)^{\frac{1}{2}} \tag{3.5.9}$$

so the solution in the immediate neighborhood of the C-J front is given by the following expressions

$$\phi(\xi) \;=\; \phi(1) \;\pm\; \left(\frac{-2j\,\phi(1)\beta(1)}{\gamma+1}\right)^{\frac{1}{2}} (1-\xi)^{\frac{1}{2}} + \cdots \tag{3.5.10}$$

$$\beta(\xi) \;=\; \beta(1) \;\pm\; \left(\frac{\gamma-1}{2}\right)\left(\frac{-2j\,\phi(1)\beta(1)}{\gamma+1}\right)^{\frac{1}{2}} (1-\xi)^{\frac{1}{2}} + \cdots \tag{3.5.11}$$

The two signs in the above equations yield two types of solutions. The positive sign gives the compression solution behind the C-J front which requires a piston to follow the cylindrical or spherical C-J wave and the negative sign gives the expansion solution. The two types of solutions are illustrated in the sketch below.
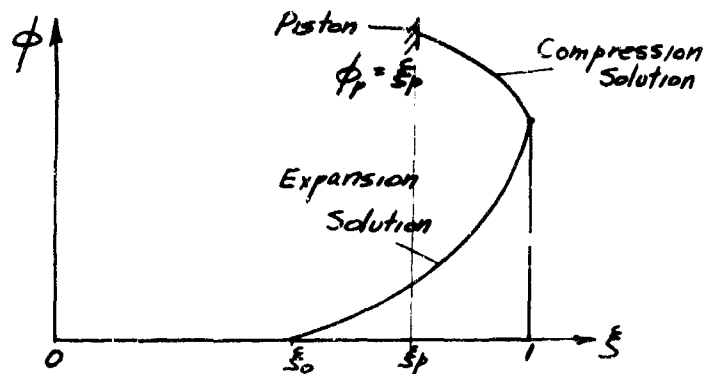
Using the perturbation expansion in the neighborhood of the front, the value of ϕ and β can be obtained at some value of ξ close to one (e.g., ξ = 0.999) and with these as starting values Eqs. 2.5.28 and 2.5.29 can be integrated numerically to obtain the solution.

Constant Velocity Detonations in a Non-Uniform Density Medium

In this Section we shall make a general analysis of the propagation of detonation waves in an initially non-uniform density medium where $\beta(r) = A r^{\omega}$. The problems treated in the previous Sections are simply particular cases of it for uniform density. For gaseous explosives, it would be difficult to obtain an initially non-uniform density under isothermal conditions in the absence of force fields. However for solid explosives this can be achieved readily and the analysis given here is of interest for solid explosives.

The basic similarity equations for an initial non-uniform medium where $\beta(r) = A r^{\omega}$ is given previously by Eqs. 2.5.24 and 2.5.25 as

$$\phi' = \frac{\beta^2\left(\frac{j\phi}{\xi} + \frac{\omega}{\gamma}\right)}{(\phi-\xi)^2 - \beta^2} \tag{2.5.24}$$

$$\beta' = \frac{-\beta\left(\frac{\gamma-1}{2}\right)\left(\frac{j\phi(\phi-\xi)}{\xi} + \frac{\beta^2\omega}{\gamma(\phi-\xi)}\right)}{(\phi-\xi)^2 - \beta^2} \tag{2.5.25}$$

And the boundary conditions at the detonation front are given by Eqs. 2.2.5 and 2.5.30 as

$$\phi(1) = \frac{1-\eta+S}{\gamma+1} \tag{2.2.5}$$

$$\beta(1) = \frac{1}{\gamma+1}\left[(\gamma+\eta+\gamma S)(\gamma+\eta-S)\right]^{\frac{1}{2}} \tag{2.5.30}$$

For Chapman-Jouguet detonations we have $s = 0$ and

$$\phi_{,\xi}(1) = \frac{-2\gamma}{\gamma+1} \qquad (3.6.1)$$

$$\beta_{,\xi}(1) = \frac{\gamma + 2\gamma}{\gamma+1} \qquad (3.6.2)$$

and the condition that

$$\phi_{,\xi}(1) + \beta_{,\xi}(1) = 1 \qquad (3.6.3)$$

For any specified initial conditions (i.e., j, γ, γ_{cT}, ω), the solution can be obtained by numerical integration of Eqs. 2.5.24 and 2.5.25 in the region $0 \le \xi \le 1$ using the boundary conditions at $\xi = 1$ given by Eqs. 3.6.1 and 3.6.2. It should be noted that the value of ω must be

$$\omega \ge -\phi(1) \qquad (2.3.9)$$

if the mass enclosed by the front is finite. For Chapman-Jouguet detonations we see that again the slopes ϕ' and β' are infinite as a result of Eq. 3.6.3. Hence to effect the numerical integration, analytical solutions in the neighborhood of the front $\xi = 1$ must first be determined. Using an identical method as in the previous Section, we get

$$\phi(\xi) = \phi(1) + a_1(1-\xi)^\alpha + \cdots$$

$$\beta(\xi) = \beta(1) + b_1(1-\xi)^b + \cdots \qquad (3.6.4)$$

and obtain the exponents α and b and the coefficients a_1 and b_1 as follows

$$\alpha = b = \tfrac{1}{2}$$

$$a_1 = \pm\left(2\beta_{cT}(1)\frac{(j\phi_{,\xi}(1) + \omega/\gamma)}{\gamma+1} \right)^{\frac{1}{2}} \qquad (3.6.5)$$

$$b_j = \pm \left(\frac{1}{\beta_i} \right) \left(\frac{-2\beta_{i\cdot} \cdot (j\phi_{(i)} + \omega r)}{\gamma + j} \right)^{\frac{1}{2}}$$

(3.6.6)

Note that for $\omega = 0$, the above equations reduce exactly to Eqs. 3.5.10 and 3.5.11 of the previous section for the uniform density case. Again two solutions exist corresponding to the positive and negative signs in Eq. 3.6.5. The positive sign gives the compression solution behind the Chapman-Jouguet front which must terminate at a piston surface. The negative sign gives the free expansion solution which terminates where the particle velocity becomes zero; at or before the center of symmetry.

To obtain the solution for Chapman-Jouguet detonations propagating in a non-uniform density medium, Eqs. 3.6.5 and 3.6.6 are first used to obtain the value of ϕ and β at some value of ξ close to unity (e.g., $\xi = 0.999$). With $\phi(.999)$ and $\beta(.999)$ as starting values, the similarity equations can then be integrated numerically using say the Runge-Kutta method.

Since an extra degree of freedom is now provided for finite ω, we see that for a particular value of ω, we can . je cylindrical or spherical Chapman-Jouguet detonations propagating in a non-uniform medium in which the solution is no longer singular at the front. From Eqs. 2.5.24 and 2.5.25, we note that for the particular value of

$$\omega = - \gamma j \phi_{(1)}$$

(3.6.7)

the numerator vanishes at the front as well as the denominator. Hence ϕ' and β' are finite. To obtain the solution numerically for this case, we must again seek solutions in the immediate neighborhood of the detonation front since both ϕ' and β' are indeterminate. Writing the solution in the following perturbation form

- 120 -

$$\phi(\xi) = \phi_1(1) + a_2(1-\xi) + \cdots$$

$$\beta(\xi) = \beta_1(1) + b_2(1-\xi) + \cdots \tag{3.6.8}$$

and substituting into Eqs. 2.5.24 and 2.5.25 we obtain the coefficients a_2 and b_2 as

$$a_2 = \frac{j\beta_1(1)(a_2 + \phi_1(1))}{2(a_2 + b_2 + 1)} \tag{3.6.9}$$

$$b_2 = \frac{-(\gamma-1)j}{4} \frac{\left[2\phi_1(1)(a_2 + b_2 + 1) - \beta_1(1)(a_2 + \phi_1(1))\right]}{(a_2 + b_2 + 1)} \tag{3.6.10}$$

In obtaining Eqs. 3.6.9 and 3.6.10, use has been made of the Chapman-Jouguet condition (i.e., Eq. 3.6.3) and the critical value for ω given by Eq. 3.6.7 Using Eq. 3.6.9, Eq. 3.6.10 can be written as

$$b_2 = -j\left(\frac{\gamma-1}{2}\right)\phi_1(1) + \left(\frac{\gamma-1}{2}\right)a_2 \tag{3.6.11}$$

and substituting Eq. 3.6.11 for b_2 in Eq. 3.6.10, we get a quadratic equation for a_2 as follows

$$a_2^2 + a_2\left[\frac{2-j-\gamma j\phi_1(1)}{\gamma+1}\right] - j\frac{\phi_1(1)\beta_1(1)}{\gamma+1} = 0 \tag{3.6.12}$$

Therefore two roots can be obtained for a_2, hence b_2 as before. The two roots yield two possible solutions, again one is a compression solution terminating at a piston surface and the other is a free expansion solution terminating when the particle velocity is zero. To start the numerical integration of Eqs. 2.5.24 and 2.5.25, the perturbation expressions given by Eqs. 3.6.8 and 3.6.10 are used to determine ϕ and β at some value of ξ

close to unity (e.g., ξ = .99) and integration proceeds from ξ = .99
for decreasing values of ξ until the solution terminates at either ϕ = ξ
for the compression case and ϕ = 0 for the expansion case.

From Eqs. 3.6.5 and 3.6.6 we note that

$$\omega \gtrless -j\gamma\phi_{cj}(1) \qquad (3.6.13)$$

for Chapman-Jouguet detonations to exist. For

$$\omega < -j\gamma\phi_{cj}(1) \qquad (3.6.14)$$

we cannot have Chapman-Jouguet detonations since the roots are imaginary
in Eq. 3.6.5. We could, however, have a constant velocity overdriven or
weak detonation wave in which $\phi(1) + \beta(1) \neq 1$. Since weak detonations
are ruled out from entropy considerations we have then for $\omega < -j\gamma\phi_{cj}(1)$,
a constant velocity overdriven detonation wave. For any specified value
of the initial conditions (i.e., j, γ, η, ω) Eqs. 2.5.24 and 2.5.25 can
be integrated immediately using the boundary conditions given by Eqs. 2.2.5
and 2.5.30. Now, no singularities exist at the front and the solution is
regular there. It is interesting to note that contrary to the initially
uniform density case, we can have a constant velocity overdriven detonation
wave in an initially non-uniform density medium without any piston motion.
The rate of amplification as a result of the density decrease just balances
the rate of decay of an otherwise non-supported overdriven detonation in
this case.

For a particular value of ω there exists a very simple solution
to Eqs. 2.5.24 and 2.5.25 in the form of linear profiles for ϕ and β.

$$\phi(\xi) = \phi(1)\xi$$
$$\beta(\xi) = \beta(1)\xi \qquad (3.6.15)$$

for detonations in a non-uniform medium. To determine what the value of ω is for such a solution to exist, we substitute Eq. 3.6.15 into Eqs. 2.5.24 and 2.5.25 and evaluating at the detonation front $\xi = 1$ we get

$$\phi(1) = \frac{2}{(\gamma-1)(j+1)+2} \qquad (3.6.16)$$

$$\beta^2(1) = \frac{\phi(1)(\phi(1)-1)^2}{(j+1)\phi(1)+\omega/\gamma} \qquad (3.6.17)$$

Using the approximate form for the boundary conditions given by Eqs. 2.2.21 and 2.5.30 as

$$\phi(1) = \frac{1+S}{\gamma+1} \qquad (2.2.21)$$

$$\beta^2(1) = \frac{\gamma(1+S)(\gamma-S)}{(\gamma+1)^2} \qquad (2.5.30)$$

where

$$S = \left(1 - 2(\gamma^2-1)\eta g\right)^{1/2} \qquad (2.2.23)$$

we can solve for the value of ω as

$$\omega = \frac{-(\gamma+1)(j+1)}{2+(\gamma-1)(j+1)} \qquad (3.6.18)$$

For the spherical symmetry, we see that Eq. 3.6.18 becomes

$$\omega = \frac{-3(\gamma+1)}{3\gamma-1} \qquad (3.6.19)$$

which corresponds to that given by Sedov.

For values of $\omega < -(\gamma+1)(j+1)/[2+(\gamma-1)(j+1)]$ the solution demonstrates the existence of a hole in the center at $\xi = \xi_h$ where $\phi(\xi_h) = \xi_h$. In other words, the detonation drags the mass outwards faster than the rarefaction can kick it back. Starting at the detonation front the solution terminates at $\xi = \xi_h$ where $\phi(\xi_h) = \xi_h$ and $\beta(\xi_h) = 0$.

3.7 Piston Driven Constant Velocity Shocks and Detonations

Here we consider the problem of a constant velocity front (shock or detonation) driven by a constant velocity expanding piston in an initially uniform density medium. At time $t = 0$ both the shock and the piston originate at the origin $r = 0$ and at later times both propagate at a constant velocity $\dot{R}_s$ (shock) and $\dot{R}_p$ (piston). Since the shock and piston velocities are constant, their respective trajectories are given as $R_s = \dot{R}_s t$ and $R_p = \dot{R}_p t$. Under the Hayes and Tsien hypersonic similitude law, the flow field corresponding to a steadily expanding cylindrical piston corresponds to the two dimensional hypersonic steady flow field past a slender cone. Since the shock propagates at a constant velocity into an initially uniform medium, the non-steady flow behind the front is isentropic. The basic equations governing the self-similar motion of the shocked states as given previously by Eqs. 2.5.28 and 2.5.29 are

$$\phi' = \frac{j\phi\beta/\xi}{(\phi-\xi)^2-\beta^2} \tag{2.5.28}$$

$$\beta' = -\frac{(\gamma-1)}{2}\frac{j\phi\beta(\phi-\xi)/\xi}{(\phi-\xi)^2-\beta^2} \tag{2.5.29}$$

We shall first consider the case of an inert medium and the boundary conditions at the shock front $\xi = 1$ are given as

$$\phi(1) = \frac{2(1-\eta)}{\gamma+1} \tag{2.2.30}$$

$$\beta(1) = \left\{ \frac{2\gamma}{(\gamma-1)^2} (\gamma-1+2\eta)(1-(\frac{\gamma-1}{2\gamma})\eta) \right\}^{1/2} \qquad (3.7.1)$$

The solution terminates at the piston surface ($r = R_p$, $\xi = \xi_p$) where
the particle velocity matches the piston velocity ($u = \dot{R}_p$, $\phi(\xi_p) = \xi_p$).
A word must be said about the specification of the initial conditions for
this particular problem. In general, it is convenient to specify the
piston velocity $\dot{R}_p$ and to obtain the solution in this case we have to
first assume a shock velocity $\dot{R}_s$. With $\dot{R}_p$ and $\dot{R}_s$ known $\xi_p = \frac{R_p}{R_s} = \frac{\dot{R}_p}{\dot{R}_s}$ can
be found. With the shock velocity $\dot{R}_s$ known, the shock Mach number $\dot{R}_s/c_0$
and $\eta = 1/m_s^2$ can be obtained and Eqs. 2.2.30 and 3.7.1 yield the
boundary conditions $\phi(1)$ and $\beta(1)$ at the shock. The basic equation can
now be integrated. The correct solution will be obtained when the
assumed value of the shock velocity yields a solution that satisfies
the condition at the piston surface (i.e., $\phi(\xi_p) = \xi_p$). In general we
have to iterate for the correct shock velocity for a given piston
velocity.

However if we were to do the inverse problem and specify the
shock velocity leaving the corresponding piston velocity to be
determined by this solution, no iteration is necessary. We simply
integrate the basic equation from the shock $\xi = 1$ until $\phi = \xi$. The
piston velocity $\dot{R}_p$ can then be found immediately for the value of
the shock velocity specified.

In general, the separation between the piston surface and
the shock front is relatively small for strong shock waves (i.e., $M_s \gg 1$,
$\eta \ll 1$). Hence an approximate solution can be obtained (at least
accurate in the neighborhood of the shock) by expanding the values of

$\phi(\xi)$ and $\beta(\xi)$ in a power series in $(1-\xi)$ as follows

$$\phi(\xi) = \sum_{n=0}^{\infty} \phi^{(n)}(1-\xi)^n = \phi^{(o)} + \phi^{(1)}(1-\xi) + \cdots \qquad (3.7.2)$$

$$\beta(\xi) = \sum_{n=0}^{\infty} \beta^{(n)}(1-\xi)^n = \beta^{(o)} + \beta^{(1)}(1-\xi) + \cdots \qquad (3.7.3)$$

The zeroth order coefficients $\phi^{(o)}$ and $\beta^{(o)}$ can readily be evaluated using the boundary conditions at the shock given by Eqs. 2.2.30 and 3.7.1 as

$$\phi^{(o)} = \phi(1) = \frac{2}{\gamma+1}(1-\eta) \qquad (3.7.4)$$

$$\beta^{(o)} = \beta(1) = \left\{ \frac{2\gamma}{(\gamma+1)^2}(\gamma-1+2\eta)(1-\frac{(\gamma-1)}{2\gamma}\eta) \right\}^{\frac{1}{2}} \qquad (3.7.5)$$

Substituting the perturbation expressions of Eqs. 3.7.2 and 3.7.3 into the basic equations and equating coefficients of the terms in similar powers in $(1-\xi)$ we can readily obtain the higher order coefficients $\phi^{(1)}$ and $\beta^{(1)}$. The solution in the neighborhood of the shock can now be written as

$$\phi(\xi) = \phi(1) - \frac{j\phi(1)\beta^2(1)}{(\phi(1)-1)^2 - \beta^2(1)}(1-\xi) + \cdots \qquad (3.7.6)$$

$$\beta(\xi) = \beta(1) - \frac{\frac{(\gamma-1)}{2}j\phi(1)\beta(1)(\phi(1)-1)}{(\phi(1)-1)^2 - \beta^2(1)}(1-\xi) + \cdots \qquad (3.7.7)$$

Where $\phi^{(1)}$ and $\beta^{(1)}$ are given by Eqs. 3.7.4 and 3.7.5.

The solution for $\phi(\xi)$ for piston driven planar, cylindrical and spherical shocks are illustrated below
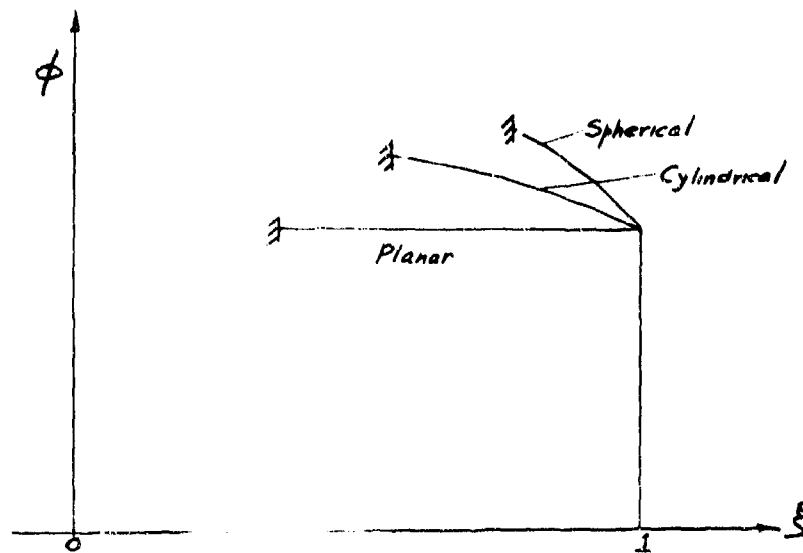
It is interesting to note that for cylindrical and spherical piston driven shocks the particle velocity increases behind the shock to the piston surface while for the planar case, it remains constant throughout. The additional isentropic compression behind the shock is a result of the area divergence effect for cylindrical and spherical symmetry.

We proceed next to the situation when the medium is detonable and the front is a detonation wave. We see in Section 3.5 that for cylindrical or spherical Chapman-Jouguet detonations, there exist two possible solutions, a free expansion solution and a compression solution.
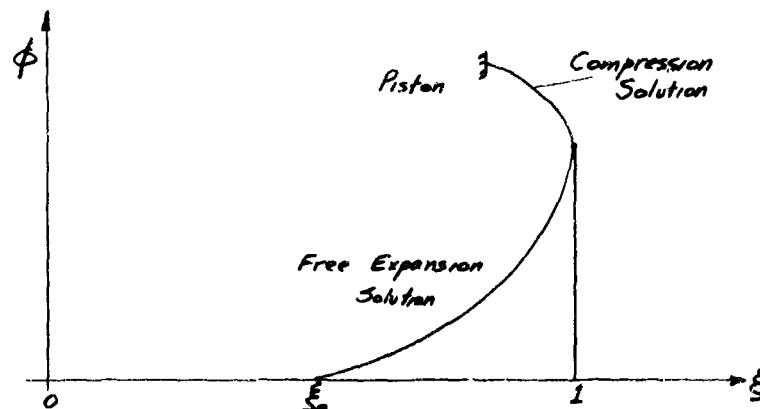
For the compression solution, the solution must terminate at a piston surface where $\phi = \xi$. Denoting the particular piston velocity which yields a Chapman-Jouguet detonation as ϕ_{pc} we have for piston velocities $\phi_p > \phi_{pc}$

an overdriven detonation. For overdriven detonations, the solution is regular at the front. Using the boundary conditions for a detonation wave given by Eqs. 2.2.5 and 2.5.30

$$\phi(1) = \frac{1 - \eta + S}{\gamma + 1} \qquad (2.2.5)$$

$$\beta(1) = \frac{1}{\gamma + 1} \left\{ (\gamma + \eta + \gamma S)(\gamma + \eta - S) \right\}^{\frac{1}{2}} \qquad (2.5.30)$$

the basic equations can readily be integrated until $\phi = \xi$ when the piston surface is reached. The solution for the overdriven detonation case is similar to that for a non-reacting shock where $\phi(\xi)$ and $\beta(\xi)$ increase continuously from the front to the piston surface.

For piston velocities $\phi_p < \phi_{pc}$, we have then a piston trailing behind a Chapman-Jouguet detonation front. Since the motion of the Chapman-Jouguet front is independent of the conditions in its wake, there can exist a second shock wave in the detonation products as a result of the additional energy output by the piston. We assume the existence of a steady shock wave in the product gases and proceed to seek the solutions for this condition. The r-t diagram for this condition is illustrated below
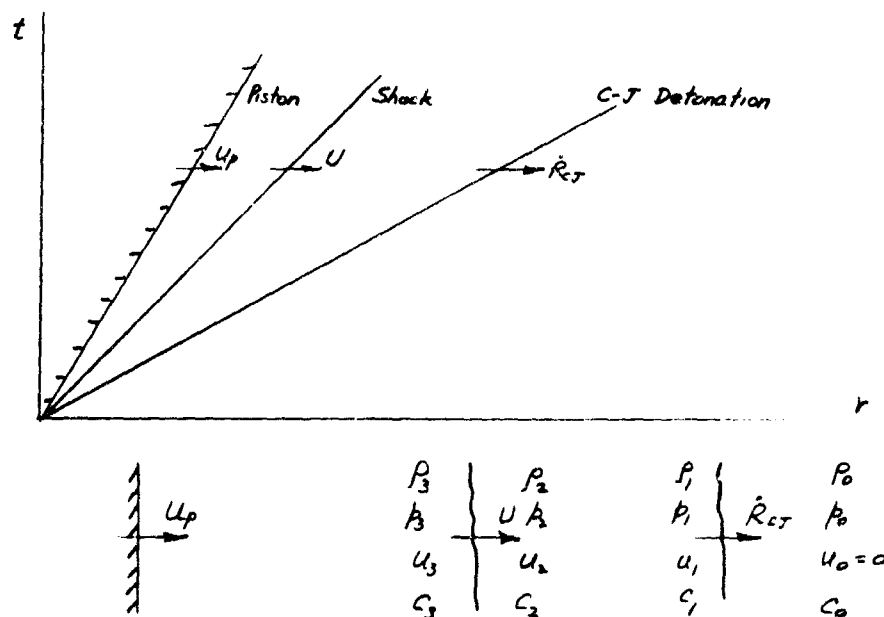
We denote the subscript 0 for the initial state of the explosive, 1 for the states immediately behind the Chapman-Jouguet detonation, 2 for the conditions immediately in front of the second shock and 3 for the states behind it. Writing the conservation equations of mass momentum and energy across the second shock, we have

$$\rho_3 \quad \xleftarrow{U-u_3} \quad \left\{ \quad \xrightarrow{U-u_2} \quad \rho_2 \right.$$
$$p_3 \qquad\qquad\qquad p_2$$
$$etc. \qquad\qquad\qquad etc.$$

$$\rho_2(U-u_2) = \rho_3(U-u_3) \tag{3.7.8}$$

$$p_2 + \rho_2(U-u_2)^2 = p_3 + \rho_3(U-u_3)^2 \tag{3.7.9}$$

$$e_2 + \frac{p_2}{\rho_2} + \frac{(U-u_2)^2}{2} = e_3 + \frac{p_3}{\rho_3} + \frac{(U-u_3)^2}{2} \tag{3.7.10}$$

From Eq. 3.7.8 we obtain

$$\frac{\rho_2}{\rho_3} = \frac{U-u_3}{U-u_2} \tag{3.7.11}$$

and since the density ratio across the shock is given in terms of the shock Mach number $M_S (\text{or } \eta_S)$ as

$$\frac{\rho_2}{\rho_3} = (\gamma - 1 + 2\eta_S)/(\gamma + 1) \tag{3.7.12}$$

where

$$\eta_S = \frac{c_2^2}{(U-u_2)^2} = \frac{\beta^2}{(\frac{z}{S_S} - \rho_2)^2} \tag{3.7.13}$$

Noting that

$$\xi_s = \frac{r_s}{R_s} = \frac{Ut}{\dot{R}_{cJ}t} = \frac{U}{\dot{R}_{cJ}} \tag{3.7.14}$$

$$\beta_2 = \frac{C_2}{\dot{R}_{cJ}} \tag{3.7.15}$$

$$\phi_2 = \frac{u_2}{\dot{R}_{cJ}} \tag{3.7.16}$$

$$\phi_3 = \frac{u_3}{\dot{R}_{cJ}} \tag{3.7.17}$$

$$\phi_p = \frac{u_p}{\dot{R}_{cJ}} \quad , \tag{3.7.18}$$

equating Eq. 3.7.11 with 3.7.12 yields

$$\frac{\xi_s - \phi_3}{\xi_s - \phi_2} = \frac{\gamma - 1 + 2\eta_s}{\gamma + 1} \tag{3.7.19}$$

To obtain the solution for a cylindrical or spherical piston following a Chapman-Jouguet detonation front, we first determine the boundary condition at $\xi = 1$ using Eqs. 3.6.1 and 3.6.2

$$\phi_{cJ}(1) = \frac{1 - \eta_{cJ}}{\gamma + 1} \tag{3.6.1}$$

$$\beta_{cJ}(1) = \frac{\gamma + \eta_{cJ}}{\gamma + 1} \tag{3.6.2}$$

From the perturbation expansions given by Kqs. 3.5.10 and 3.5.11

$$\phi(\xi) = \phi(1) \pm \left(\frac{-2j\phi(1)\beta(1)}{\gamma+1} \right)^{\frac{1}{2}} (1-\xi)^{\frac{1}{2}} + \cdots \qquad (3.5.10)$$

$$\beta(\xi) = \beta(1) \pm \left(\frac{-2j\phi(1)\beta(1)}{\gamma+1} \right)^{\frac{1}{2}} (\frac{\gamma-1}{2})(1-\xi)^{\frac{1}{2}} + \cdots \qquad (3.5.11)$$

we obtain the starting conditions for ϕ and β at some value of ξ close to unity (e.g., $\xi = 0.999$). We next integrate the basic equations (i.e., Eqs. 2.5.28 and 2.5.29) until some desired value of ξ_s (hence the strength of the second shock wave) is reached. With β_2, ϕ_2, and ξ_s known, η_s can now be evaluated and the conditions behind the second shock wave determined using Eqs. 2.2.30 and 3.7.1.

$$\phi(\xi_s) = \frac{2}{\gamma+1} (1-\eta_s) \qquad (2.2.30)$$

$$\beta(\xi_s) = \left\{ \frac{2\gamma}{(\gamma+1)^2} (\gamma-1+2\eta_s)(1 - (\frac{\gamma-1}{2\gamma})\eta_s) \right\}^{\frac{1}{2}} \qquad (3.7.1)$$

With ϕ and β behind the second shock wave determined, Eqs. 2.5.28 and 2.5.29 can be integrated further until the piston surface where $\phi = \xi$ is reached. A qualitative illustration of the solution is shown in the sketch below
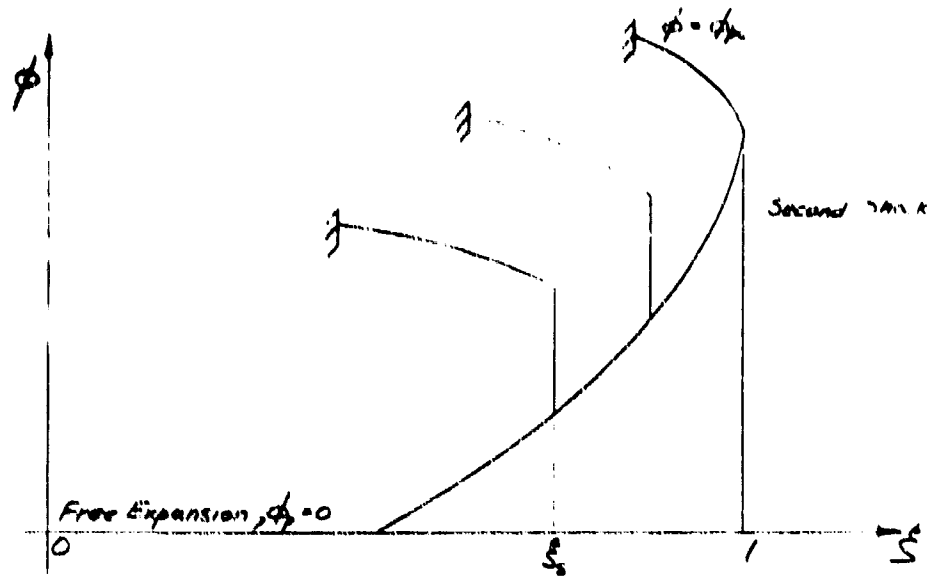
It should be noted that the free expansion solution is not influenced by the piston motion from the Chapman-Jouguet front $\xi = 1$ to the second shock wave $\xi = \xi_s$. After the second shock, the solution changes from an expansion solution to a compression solution and it terminates at the piston surface $\phi = \xi$.

Let us investigate the variation of the strength of the second shock wave with different piston velocities. We note that when the piston velocity $\phi_p = \phi_{pc}$ (the critical piston velocity for Chapman-Jouguet detonations), the second shock wave vanishes and a smooth compression solution is obtained from the front to the piston. For zero piston velocity $\phi_p = 0$, again the second shock vanishes and we have the free expansion solution throughout. Between these two limits (i.e., $0 \le \phi_p \le \phi_{pc}$) we have a second shock wave in the flow field. Let us first of all investigate the planar case (i.e., $j = 0$). For planar Chapman-Jouguet waves, the free expansion solution is given previously in Section 3.3 by Eqs. 3.1.6 and 3.1.7 as

- 140 -

$$\phi(\xi) = \frac{2}{\gamma+1}(\xi-1) + \phi(1) \tag{3.1.6}$$

$$\beta(\xi) = \frac{\gamma-1}{\gamma+1}(\xi-1) + \beta(1) \tag{3.1.7}$$

From Eq. 3.7.13, the Mach number of the second shock can be obtained as

$$M_S = \frac{U-u_2}{C_2} = \frac{\xi_s-\phi_2}{\beta_2} \tag{3.7.20}$$

Substituting Eqs. 3.1.6 and 3.1.7 into the above equation, we get

$$M_S = \frac{\xi_s - \left[\frac{2}{\gamma+1}(\xi_s-1) - \phi(1)\right]}{\frac{\gamma-1}{\gamma+1}(\xi_s-1) + \beta(1)} \tag{3.7.21}$$

Using the Chapman-Jouguet condition $\phi(1)+\beta(1)=1$, Eq. 3.7.21 reduces to the following

$$M_S = 1 \tag{3.7.22}$$

Hence we see that for the planar case, the secondary shock wave is always a compressional Mach wave irrespective of the piston velocity. The piston motion simply reduces the expansion fan behind the front. This is illustrated in the sketch below.
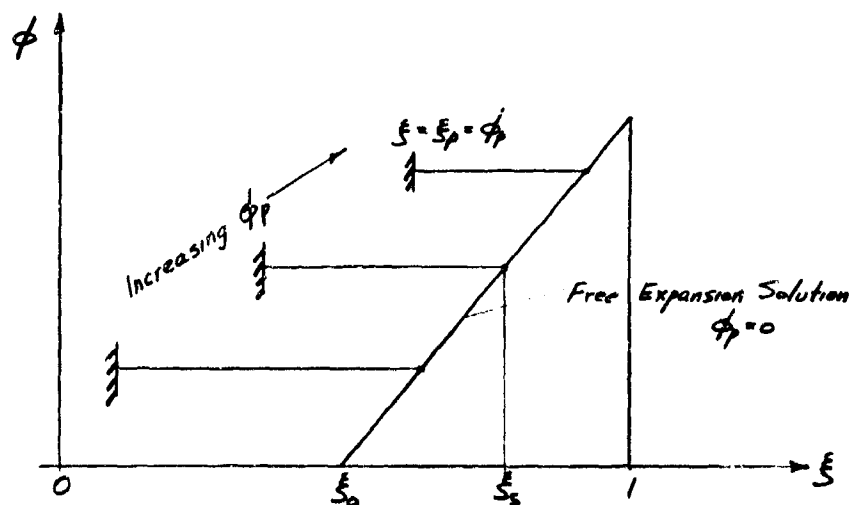
For cylindrical and spherical symmetry, we can only investigate analytically the strength of the second shock wave near the front where we have the solution given by Eqs. 3.5.10 and 3.5.11 as

$$\phi(\xi) = \phi(1) - \left(\frac{2j\phi(1)\beta(1)}{\gamma+1}\right)^{\frac{1}{2}}(1-\xi)^{\frac{1}{2}} + \cdots \tag{3.5.10}$$

$$\beta(\xi) = \beta(1) - \left(\frac{\gamma-1}{2}\right)\left(\frac{2j\phi(1)\beta(1)}{\gamma+1}\right)^{\frac{1}{2}}(1-\xi)^{\frac{1}{2}} + \cdots \tag{3.5.11}$$

and in the vicinity of $\xi = \xi_0$ where $\phi \to 0$ and $\beta \to$ constant and the solution can be expressed as

$$\phi(\xi) = \phi^{(1)}(\xi - \xi_0) + \cdots \tag{3.7.23}$$

$$\beta(\xi) = \beta^{(0)} + \beta^{(1)}(\xi - \xi_0) + \cdots \tag{3.7.24}$$

For the Mach number of the second shock in the vicinity of the Chapman-Jouguet front $\xi = 1$, we substitute Eqs. 3.5.10 and 3.5.11 into Eq. 3.7.20 and obtain

$$M_s = \frac{\xi_s - \phi(1) + \left(\frac{2j\phi(1)\beta(1)}{\gamma+1}\right)^{\frac{1}{2}}(1-\xi_s)^{\frac{1}{2}}}{1 - \phi(1) - \left(\frac{\gamma-1}{2}\right)\left(\frac{2j\phi(1)\beta(1)}{\gamma+1}\right)(1-\xi_s)^{\frac{1}{2}}} \tag{3.7.25}$$

From the above equation we see that as $\xi_s \to 1$, $M_s \to 1$ and the second shock degenerates into a compressional Mach wave. As ξ_s decreases, the strength of the second shock increases.

In the vicinity of $\xi_s = \xi_0$, M_s can be obtained by substituting Eqs. 3.7.23 and 3.7.24 into Eq. 3.7.20 as

$$M_s = \frac{\xi_s - \phi^{(1)}(\xi_s - \xi_0)}{\xi_0 + \beta^{(1)}(\xi_s - \xi_0)} \tag{3.7.25}$$

Again as $\xi_S \to \xi_o$, $M_S \to 1$ and the second shock degenerates into a
compressional Mach wave propagating at the local speed of sound. We
see therefore the strength of the second shock wave at first increases
to a maximum rapidly from the front and then decreases again to a Mach
wave as $\xi_S \to \xi_o$ and $\phi_p \to o$. A qualitative sketch of the variation of
the strength of the second shock wave with ξ_S is shown below
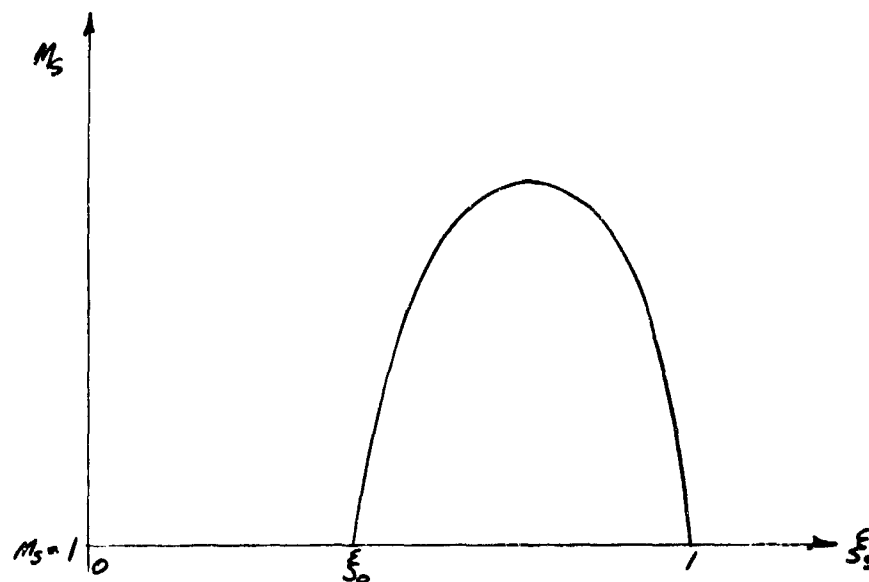
3.8 Expansion of a Gas Cloud into a Vacuum

In this Section, we shall consider the isentropic expansion
of a finite gas cloud into a vacuum environment. This problem finds
application in astrophysical problems dealing with the dynamics of
cosmic gas clouds and is also of some current interest in the problem
of rocket exhaust into a vacuum.

For an initially uniform density finite gas mass bounded
by $0 \leq r \leq R_0$, similarity solutions are not possible due to the
presence of a characteristic length R_0 . However for planar symmetry,
the basic equations are invariant under a coordinate transformation
of $r \rightarrow r - R_0$ hence self-similar solutions are possible and are
given previously in Section 3.2. For an initially non-uniform finite
gas mass, self-similar solutions are possible for particular distribu-
tions of the initial states in the gas mass. We shall try to nd these
particular initial distributions for this problem in this Section by
examining the basic equations under specified initial and boundary
conditions in a manner similar to that of Section 2.4.

The initial and boundary conditions specified are as follows:

for $t \leq 0$, $0 \leq r \leq R_0$

$$u = 0 \tag{3.8.1}$$

$$p = p(r) , \quad p(R_0) = 0 \tag{3.8.2}$$

$$\rho = \rho(r) , \quad \rho(R_0) = 0 \tag{3.8.3}$$

for $\quad t > 0,$

$$u(0,t) = 0 \qquad\qquad (3.8.4)$$

$$p(R_e,t) = 0 \qquad\qquad (3.8.5)$$

$$\rho(R_e,t) = 0 \qquad\qquad (3.8.6)$$

where $R_e(t)$ is the position of the escape front. We seek similarity solutions of the following form

$$\phi(\xi) = \frac{u(r,t)}{\dot{R}_e(t)} \qquad\qquad (3.8.7)$$

$$\psi(\xi) = \frac{\rho(r,t)}{F(R_e)} \qquad\qquad (3.8.8)$$

$$f(\xi) = \frac{p(r,t)}{G(R_e)} \qquad\qquad (3.8.9)$$

where $\quad \xi = r/R_e \qquad\qquad (3.8.10)$

and $F(R_e)$ and $G(R_e)$ are arbitrary functions to be determined. Using Eqs. 3.8.7 to 3.8.10 the basic conservation equations of mass momentum and energy (i.e., Eqs. 2.1.1, 2.1.2 and 2.1.9) transform to the following equations:

$$\frac{1}{\psi}\left[(\phi\cdot\xi)\psi' + \psi\phi' + j\frac{\phi\psi}{\xi}\right] = -\frac{R_e}{F}\frac{dF}{dR_e} \qquad\qquad (3.8.11)$$

$$(\phi - \xi)\phi' + \frac{Re \ddot{R}e}{\dot{R}_e^2}\phi + \frac{G}{F}\frac{f'}{\psi} = 0 \tag{3.8.12}$$

$$\frac{1}{f}\left[(\phi - \xi)f' + \gamma f \phi' + \gamma \frac{f\phi}{\xi}\right] = -\frac{Re}{G}\frac{dG}{dRe} \tag{3.8.13}$$

where the primed quantities denote differentation with respect to the similarity parameter ξ. Examining Eqs. 3.8.11 and 3.8.13 we see that the left hand side are functions of ξ while the right hand side are functions of Re. Hence for self-similar solutions we must have

$$\frac{Re}{F}\frac{dF}{dRe} = k_1 = const. \tag{3.8.14}$$

$$\frac{Re}{G}\frac{dG}{dRe} = k_2 = const. \tag{3.8.15}$$

The solution of Eqs. 3.8.14 and 3.8.15 yields the functional forms for F and G as

$$F = A Re^{k_1} \tag{3.8.16}$$

$$G = B Re^{k_2} \tag{3.8.17}$$

where A and B are chosen such that the boundary conditions for $f(\xi)$ and $\psi(\xi)$ are

$$f(1) = \psi(1) = 0 \tag{3.8.18}$$

$$f(0) = \phi(0) = 1 \tag{3.8.19}$$

Substituting Eqs. 3.8.16 and 3.8.17 into Eq. 3.8.12, we get

$$(\phi - \xi)\phi' + \frac{B}{A} \frac{R_e^{k_2 - k_1}}{\bar{R}_e^2} \frac{f'}{\psi} + \frac{R_e \ddot{R}_e}{\bar{R}_e^2} \phi = 0 \tag{3.8.20}$$

Examining the above equation we see that for self-similar solutions
to be possible, we must have

$$\frac{f'}{\psi} = \alpha \phi \tag{3.8.21}$$

$$\frac{\alpha B}{A} \frac{R_e^{k_2 - k_1}}{\bar{R}_e^2} + \frac{R_e \ddot{R}_e}{\bar{R}_e^2} = \beta \tag{3.8.22}$$

where α and β are constants. Using Eqs. 3.8.21 and 3.8.22, Eq.
3.8.20 now becomes

$$(\phi - \xi)\phi' - \beta\phi = 0 \tag{3.8.23}$$

The boundary condition for ϕ is given as

at $\quad r = R_e (\xi = 1), \quad u = \dot{R}_e, \quad \phi(1) = 1 \tag{3.8.24}$

at $\quad r = 0 (\xi = 0), \quad u = 0, \quad \phi(0) = 0 \tag{3.8.25}$

Depending on the value of the arbitrary constant β, we can have an
infinite number of solutions. For example if we set $\beta = 0$, we obtain
from Eq. 3.8.23 the solution for ϕ as

$$\phi = \xi \tag{3.8.26}$$

Substituting Eq. 3.8.26 into Eqs. 3.8.11 and 3.8.13, we obtain

$$k_1 = -(j+1) \tag{3.8.27}$$

$$k_2 = -\gamma(j+1) \tag{3.8.28}$$

Note that Eqs. 3.8.11 and 3.8.13 cannot be used to determine ψ and f since they are homogeneous in ψ and f. Hence we must use Eq. 3.8.21 which can be written using Eq. 3.8.26 as

$$\frac{f'}{\psi} = \alpha \xi \tag{3.8.29}$$

For isentropic motion $p/\rho^\gamma = C$ and using Eqs. 3.8.8, 3.8.9, 3.8.16, 3.8.17, 3.8.27 and 3.8.28, we obtain

$$\frac{p}{\rho^\gamma} = \frac{B}{A^\gamma} \frac{f}{\psi^\gamma} = C \tag{3.8.30}$$

Therefore

$$\frac{f}{\psi^\gamma} = constant \tag{3.8.31}$$

and from the boundary condition for f and ψ (i.e., Eqs. 3.8.18 and 3.8.19), we see that the constant in the above equation is unity

$$\frac{f}{\psi^\gamma} = 1 \tag{3.8.32}$$

Substituting Eq. 3.8.32 into 3.8.21, we obtain a differential equation for f as

$$df = \alpha \xi f^{\frac{1}{\gamma}} d\xi \tag{3.8.33}$$

which can readily be integrated to yield

$$f = C_1 (1 + k\xi^2)^{\frac{\gamma}{\gamma-1}} \tag{3.8.34}$$

The constant C_1 and K can be evaluated using the boundary conditions for f given by Eqs. 3.8.18 and Eq. 3.8.34 becomes

$$f = (1-\xi)^{\frac{\gamma}{\gamma-1}}$$

(3.8.35)

From Eq. 3.8.32, we get the solution for ψ as

$$\psi = (1-\xi^2)^{\frac{1}{\gamma-1}}$$

(3.8.36)

Substituting Eq. 3.8.35 and 3.8.36 into Eq. 3.8.32, the constant α is evaluated to be

$$\alpha = \frac{-2\gamma}{\gamma-1}$$

(3.8.37)

To determine the velocity of the escape front $\dot{R}_e$ as a function of R_e, we use Eq. 3.8.22 with $\beta = 0$, $\alpha = -2\gamma/(\gamma-1)$ and $k_2 - k_1 = -(\gamma-1)(j+1)$ which then gives the following equation

$$\ddot{R}_e = \dot{R}_e \frac{d\dot{R}_e}{dR_e} = \frac{2\gamma}{\gamma-1} \cdot \frac{B}{A} \cdot R_e^{-(\gamma-1)(j+1)-1}$$

This equation is immediately integrated to yield

$$\frac{\dot{R}_e^2}{2} = \varkappa - \frac{2\gamma}{(\gamma-1)^2(j+1)} \cdot \frac{B}{A} R_e^{-(\gamma-1)(j+1)}$$

(3.8.38)

The constant $\varkappa$ must be chosen so that at $R_e = R_o$, $\dot{R}_e = 0$. Defining c_o as the local sound speed at the origin at time $t = 0$, one has

$$c_o^2 = \frac{\gamma p(0,0)}{\rho(0,0)} = \gamma \frac{A}{B} R_o^{-(\gamma-1)(j+1)}$$

(3.8.39)

Using Eq. 3.8.39, Eq. 3.8.38 may be written

$$\frac{d\bar{R}_e}{d\bar{t}} = \frac{2}{\gamma-1} \cdot \frac{1}{(j+1)^{\frac{1}{2}}} \left(1 - \bar{R}_e^{-(j+1)(\gamma-1)}\right)^{\frac{1}{2}}$$

(3.8.40)

where $\quad \bar{R}_e = R_e / R_0$ $\qquad$ (3.8.41)

$$\bar{t} = c_0 t / R_0 \qquad (3.8.42)$$

Note that the front starts out at rest and steadily accelerates as the gas cloud expands.

$\qquad$ The trajectory of the escape front can be obtained by integrating Eq. 3.8.40 as

$$\frac{2}{(\gamma-1)} \cdot \frac{\bar{t}}{(j+1)^{1/2}} = \int_1^{\bar{R}_e} \frac{d\bar{R}_e}{(1 - \bar{R}_e^{-(j+1)(\gamma-1)})^{1/2}} \qquad (3.8.43)$$

For certain values of the combination of j and γ, the integral of Eq. 3.8.43 can be expressed in closed form. As was found by Mirels and Mullens, this can be done when N_0 is an integer where N_0 is defined as

$$N_0 = 2/((j+1)(\gamma-1)) \qquad (3.8.44)$$

For example Eq. 3.8.43 becomes

$$N_0 = 1 \quad : \quad \frac{1}{(j+1)^{1/2}} \cdot \frac{2}{\gamma-1} \bar{t} = (\bar{R}_e^2 - 1)^{1/2} \qquad (3.8.45)$$

$$N_0 = 2 \quad : \qquad = \bar{R}_e^{\frac{1}{2}}(\bar{R}_e - 1)^{\frac{1}{2}} + \ln\left[(\bar{R}_e - 1)^{\frac{1}{2}} + \bar{R}_e^{\frac{1}{2}}\right] \qquad (3.8.46)$$

$$N_0 = 3 \quad : \qquad = (\bar{R}_e^{2/3} + 2)(\bar{R}_e^{2/3} - 1)^{1/2} \qquad (3.8.47)$$

Eq. 3.8.45 includes the case $j = 2$, $\gamma = 5/3$. Eq. 3.8.46 includes the
cases $j = 1$, $\gamma = 3/2$ and $j = 2$, $\gamma = 4/3$ and Eq. 3.8.47 includes the
cases $j = 0$, $\gamma = 5/3$, $j = 1$, $\gamma = 4/3$ and $j = 2$, $\gamma = 11/9$.

In the asymptotic limit for long times when $\bar{R}_e^{-(j+1)(\gamma-1)} \ll 1$,
Eq. 3.8.43 reduces to the following form

$$\bar{R}_e \sim \frac{1}{(j+1)^{\frac{1}{2}}} \cdot \frac{2}{\gamma-1} \bar{t} \qquad (3.8.48)$$

and the velocity in the asymptotic limit is given by the equation

$$\dot{\bar{R}}_e \sim \frac{1}{(j+1)^{\frac{1}{2}}} \cdot \frac{2}{\gamma-1} \qquad (3.8.49)$$

For the planar case ($j = 0$), the velocity of the escape front is identical
to that associated with the expansion of an initially uniform gas cloud
into a vacuum. As pointed out by Mirels and Mullens, the escape front
velocity is alway equal to $\dot{\bar{R}}_e = \frac{2}{\gamma-1}$, irrespective of geometry for an
initially uniform medium since at $t = 0$, the flow in the vicinity of
$r = R_e$ behaves as though it is planar (i.e., $j = 0$). Hence the limiting
edge achieves the limiting velocity of $\dot{\bar{R}}_e = 2/(\gamma-1)$ and is unaffected by
the subsequent expansion of the remainder of the gas.

For cylindrical and spherical symmetry, the escape front
velocity is alway less than the planar case by the factor $1/(j+1)^{\frac{1}{2}}$.
Mirels and Mullens reasoned that in the present case the particles at the
leading edge of the expansion have no energy at $t = 0$ and subsequently
are accelerated by the particles at and near the energy corresponding to
the condition $t = r = 0$ to drive the front to the limiting velocity of
$\dot{\bar{R}}_e = 2/(\gamma-1)$. With increasing values of j, the area divergence effect
increases and there are fewer particles at the front initially having
energies at or near the value at $t = r = 0$. Hence the front is acceler-
ated to lower velocities as j increases.

In dimensional form the solution to the present problem can be
written as

$$u = \dot{R}_e(t) \frac{r}{R_e} \tag{3.8.50}$$

$$\rho = A R_e^{-(j+1)} \left(1 - \left(\frac{r}{R_e}\right)^2\right)^{\frac{1}{\gamma-1}} \tag{3.8.51}$$

$$p = B R_e^{-\gamma(j+1)} \left(1 - \left(\frac{r}{R_e}\right)^2\right)^{\frac{\gamma}{\gamma-1}} \tag{3.8.52}$$

while the escape front velocity $\dot{R}_e$ and the trajectory $R_e(t)$ are given by Eqs. 3.8.40 and 3.8.43.

CHAPTER IV

NON-ISENTROPIC SELF-SIMILAR MOTION -

THE STRONG BLAST WAVE PROBLEM

4.1 General Considerations

In this Chapter we shall discuss the self-similar motion of the propagation of non-uniform shock waves. By non-uniformity, we mean that the shock strength is time dependent, hence the entropy increase for different fluid particles crossing the shock front at different times will be different. Therefore we called this class of self-similar motion non-isentropic as contrasted to the class of self-similar isentropic motion with a uniform shock front discussed in the previous Chapter. However we note that although different fluid particles possess different entropies, they retain their initial values after crossing the shock in their subsequent motion behind the front. Hence this class of problems should properly be termed as particle isentropic self-similar motion.

Due to the restrictions imposed by similarity the shock front must necessarily be of infinite strength (i.e., $M_S \rightarrow \infty$, $\eta \rightarrow 0$). However in practice, the strong shock approximation is found to be quite adequate for shock strengths above 3 (i.e., $p/p_0 > 3$).

We shall consider two problems in this class of self-similar motion; the strong blast problem and the problem of strong shock waves driven by a non-uniform expanding piston. We place particular emphasis on the blast wave problem because of its fundamental importance and wide applicability to various fields involving explosion problems that interest us. In spite of the restrictions imposed by self-similarity, the solution often serves as a zero order approximation to various complex problems and we can always perturb this basic solution to account for the various non-similar effects.

The non-similar technique to perturb the basic strong blast
solution to account for different non-similar effects such as counter-
pressure, heat release by chemical reactions, and a non-similar form of
the equation of state will be described in detail in the next Chapter.
Mathematically, the strong blast solutions are also of great interest
since we can write them in closed analytical forms permitting a detailed
study of the influence of various physical parameters (such as the
specific heat ratio γ of the medium) on the properties of the solution.
The piston problem is of interest to aerodynamicists since under the
similitude law of Hayes and Tsien, the hypersonic flows over blunt-nosed
slender bodies are equivalent to motion generated by a cylindrical piston.
The piston path in the r - t plane is analogous to the body shape in the
x - y plane. Actually the strong blast solution is a special case of the
piston problem in which the piston simply imparts an impulse to the
medium. In the hypersonic analogy, this corresponds to the steady
flow past a blunt-nosed straight cylindrical body. Since apart from
the initial instant when a finite quantity of energy is imparted to
the medium and no further energy input to the flow subsequently, the
strong blast solution is often referred to as the constant energy
solution. However these two problems differ only mathematically since
the solution for the particular case of constant energy input can be
written in closed forms.

For the physical problem we consider initially, a finite
quantity of energy E_o to be released in a time t_o in a finite volume
of dimension R_i in a medium at rest. This can correspond to a small
change of high explosive energy content E_o , of dimension R_i and
burning time t_o . We assume that the energy is released sufficiently
rapidly to generate a strong shock wave in the medium. At later times
the shock expands dissipating its energy to an ever increasing mass

hence it attenuates. This decaying shock wave is what is conventionally called a blast wave.

To obtain the solution for the above problem we have to integrate the set of partial differential equations of motion by some numerical means as was done by Von Neuman and later Brode. For analytical solutions to be possible we have to make the following idealizations. We shrink the size of the energy source to a plane, line or point depending on the symmetry considered (i.e., $R_i \to O$), and we also let $t_o \to O$. This then eliminates the characteristic length R_i and the characteristic time to make self-similar solutions possible. The idealization implies an energy source of infinite power density (i.e., $\frac{E_o}{k_j t_o R_i^{j+1}} \to \infty$). The explosions of fine metal wires by very low inductance capacitor discharge, laser induced air sparks and nuclear detonators are typical line and point energy sources of extremely high power densities approaching the idealized requirement. At any rate, providing the shock is still sufficiently strong at a radius $R_s \gg R_i$ and in a time $t \gg t_o$, the self-similar solution is found to give an accurate description of the processes.

The strong blast similarity solution was obtained numerically by G.I. Taylor and the closed form solution by Von-Neuman, Sedov, Kynch, J.L. Taylor and Sakurai. For the sake of completeness we shall reformulate the problem in this Section and give the derivation of the exact solution in closed forms in the next Section followed by a parametric study of the properties of the solution.

As given previously in Chapter II, the similarity equations in terms of the variable ξ where

$$\xi = r/R_s(t) \qquad (4.1.1)$$

can be written as

$$(\phi - \xi)\psi' + \psi\phi' + (j+\omega)\frac{\phi\psi}{\xi} = 0 \qquad (4.1.2)$$

$$(\phi - \xi)\phi' + \frac{1}{\psi}f' + \theta\phi + \frac{\omega f}{\xi\psi} = 0 \qquad (4.1.3)$$

$$(\phi - \xi)f' + \gamma f\phi' + 2\theta f + (\gamma j + \omega)\frac{f\phi}{\xi} = 0 \qquad (4.1.4)$$

where

$$\theta = \frac{R_s \ddot{R}_s}{\dot{R}_s^2} \qquad (4.1.5)$$

The primed quantities denote differentiation with respect to ξ and the dimensionless density ψ, particle velocity ϕ and pressure f are given by

$$\psi = \frac{\rho}{\rho_0} \quad , \quad \phi = \frac{u}{\dot{R}_s} \quad , \quad f = \frac{p}{\rho_0 \dot{R}_s^2} \qquad (4.1.6)$$

For generality, we assume the medium to have an initial density distribution given by

$$\rho_0 = Ar^\omega \qquad (4.1.7)$$

Since the non-uniform density medium is of interest in astrophysical problems and the inclusion of Eq. 4.1.7 does not require special mathematical treatment, we shall retain this throughout the discussion. It should be noted that the ω used here is opposite in sign to that of Sedov. In Sedov's analysis, the initial density distribution is given by $\rho_0 = Ar^{-\omega}$.

Since $R_s > 0$, then the sign of the parameter θ defined in Eq. 4.1.5 is positive or negative depending on whether the shock is accelerating or decelerating. For the present problem, θ is negative

and is referred to sometimes as the shock decay coefficient.

As discussed generally in Chapter II, the existence of similarity solutions to Eqs. 4.1.2 to 4.1.4 requires that θ be constant. The value of θ can be obtained from consideration of the energy integral. As derived in Chapter II, the energy integral can be written as

$$1 = y\left(\frac{I}{\eta} - I_o\right) \tag{4.1.8}$$

where

$$I = \int_0^1 \left(\frac{f}{\gamma-1} + \phi^2\frac{\psi}{2}\right)\xi^{j+\omega}d\xi \tag{4.1.9}$$

$$I_o = \frac{1}{j+\omega+1} \cdot \frac{1}{\gamma(\gamma-1)} \tag{4.1.10}$$

$$y = \left(\frac{R_s}{R_o}\right)^{j+\omega+1} \tag{4.1.11}$$

$$R_o = \left(\frac{E_o}{k_j A C_o^2}\right)^{\frac{1}{j+\omega+1}} \tag{4.1.12}$$

$$\eta = \frac{C_o^2}{\dot{R}_s^2} \tag{4.1.13}$$

Differentiating Eq. 4.1.8 with respect to R_s and using the identity

$$R_s\frac{d}{dR_s} = -2\theta\eta\frac{d}{d\eta} \tag{4.1.14}$$

we get the following expression for θ

$$\theta = -\left(\frac{j+\omega+1}{2}\right)\left(1-\eta\frac{I_o}{I}\right) \tag{4.1.15}$$

From the above equation, we see that for θ = constant, we can either have η = constant or η = 0. For η = constant the front propagates at a constant velocity and problems of this class are described in the preceeding Chapter. For strong shocks we obtain from Eq. 4.1.15 the value of θ to be

$$\theta = -(j+\omega+1)/2 \qquad (4.1.16)$$

The numerical value for θ is determined once the geometry j and the value of ω is specified. For θ = constant, the solution of Eq. 4.1.5 yields the shock radius time dependence as

$$R_S = K t^{\frac{1}{1-\theta}} = K t^N \qquad (4.1.17)$$

where

$$N = \frac{1}{1-\theta} = \frac{2}{j+\omega+3} \qquad (4.1.18)$$

Hence for an initially uniform medium (i.e., ω = 0), we have the trajectory of the blast wave given as

$$R_S = K t^{2/5}, \quad j = 2, \qquad \text{spherical}$$

$$\qquad\qquad\qquad\qquad\qquad\qquad\qquad (4.1.19)$$

$$R_S = K t^{\frac{1}{2}}, \quad j = 1, \qquad \text{cylindrical}$$

$$R_S = K t^{2/3}, \quad j = 0, \qquad \text{planar}$$

Substituting Eq. 4.1.17 into the energy integral, we can obtain the constant K of the shock trajectory in terms of the initial conditions and the solution as

$$K = \left[\frac{E_o}{N^2 I k_j A} \right]^{N/2} \qquad (4.1.20)$$

where N is given by Eq. 4.1.18, and I by Eq. 4.1.9 which is determined by the similarity solution itself.

Hence for given initial conditions, and the value of θ determined from Eq. 4.1.16, the similarity equations (i.e., Eqs. 4.1.2 to 4.1.4) can be integrated numerically starting at the shock front ($\xi = 1$) with the boundary conditions given by the following relationships.

$$\psi(1) = \frac{\gamma+1}{\gamma-1} \quad , \quad \phi(1) = f(1) = \frac{2}{\gamma+1} \qquad (4.1.21)$$

The flow is bounded by the shock and the center of symmetry (i.e., $0 \le \xi \le 1$). From the solution for $\psi(\xi)$, $\phi(\xi)$ and $f(\xi)$, the integral I can be evaluated, hence K can be found from Eq. 4.1.20 completing the solution of the problem.

It should be noted that for physically valid solutions, the value of ω must be greater than $-(j+1)$ (i.e., $\omega > -(j+1)$). From the mass integral derived previously in Chapter II

$$\int_0^1 \psi \xi^{j+\omega} d\xi = \frac{A R_s^{j+\omega+1}}{j+\omega+1} , \qquad (4.1.22)$$

we see that the total mass enclosed by the shock front is finite only when

$$\omega > -(j+1) \qquad (4.1.23)$$

For $\omega \le -(j+1)$, we cannot deposit finite energy into the system at the origin such that $\eta^{I_0}/I \rightarrow 0$ and $\theta \rightarrow -(j+\omega+1)/2$. For the consideration of systems where $\omega \le -(j+1)$, similarity solutions therefore require $E_0 \rightarrow \infty$ in a particular manner such that $\eta^{I_0}/I \rightarrow 0$. The study of such systems can only be of mathematical interest and if in fact they do exist, the special circumstances of them actually arising must lead to a separate specialized analysis.

4.2 Closed Form Expressions for the Constant Energy Solution

As was stated in the previous Section, it is often faster to simply integrate the similarity equations numerically on the computer to determine the constant energy solution for strong blast waves. However it was found that for this particular value of $\theta = -(j+\omega+1)/2$ for the constant energy solution, the similarity equations can be integrated analytically to yield closed form expressions for the solution. Although these closed form expressions are somewhat implicit in nature and it is rather difficult to recover the original variables from them, they serve an important purpose in the study of the dependence of the properties of the solutions on the parameters ω, j and γ .

As derived in Chapter II, the first integral obtained from the continuity and energy equation is given as

$$\frac{\psi^{\gamma(j+1)+\omega+2\theta}(\xi-\phi)^{\omega+2\theta-\gamma\omega}\,\xi^{2\theta(j+\omega)+\omega(\gamma-1)}}{f^{j+\omega+1}} = k$$

(2.5.15)

For the particular value of θ in the constant energy solution (i.e., $\theta = -(j+\omega+1)/2$) the first integral becomes

$$\frac{\psi^{(\gamma-1)(j+1)}}{f^{j+\omega+1}(\xi-\phi)^{j+1+\gamma\omega}\,\xi^{(j+\omega)(j+\omega+1)-\omega(\gamma-1)}} = k$$

(4.2.1)

Using the boundary conditions at the front for strong shocks (i.e., Eq. 4.1.21), the constant k can be evaluated as

$$K = \left\{ \frac{(\gamma+1)^{\gamma+1}}{2(\gamma-1)^{\gamma}} \right\}^{j+\omega+1} \tag{4.2.2}$$

To obtain the second integral, we first multiply the continuity equation (i.e., Eq. 4.1.2) by $\phi^2/2$, the momentum equation (i.e., Eq. 4.1.3) by $\phi\psi$ and the energy equation (i.e., Eq. 4.1.4) by $1/(\gamma-1)$. Adding the resultant equations and rearranging yields

$$\left[(\phi-\xi)i' + (\phi-\xi)'i + (j+\omega)\frac{(\phi-\xi)i}{\xi} \right]$$

$$+ \left[\phi'f + f'\phi + (j+\omega)\frac{f\phi}{\xi} \right]$$

$$+ (2\theta + j + \omega + 1)i = 0 \tag{4.2.3}$$

where
$$i = \frac{f}{\gamma-1} + \frac{\phi^2\psi}{2}$$

In the particular case where $\theta = -(j+\omega+1)/2$, Eq. 4.2.3 can be integrated and we get the following expression

$$\xi^{j+\omega}\left[(\phi-\xi)i + \phi f \right] = const. \tag{4.2.4}$$

Evaluating the constant of integration using the strong shock conditions at the front (i.e., Eq. 4.1.21) it is found to be zero. Hence Eq. 4.2.4 can be written as

$$(\phi-\xi)\left(\frac{f}{\gamma-1} + \frac{\phi^2\psi}{2} \right) + \phi f = 0 \tag{4.2.5}$$

It should be noted that unlike the first integral (i.e., Eq. 4.2.1) which is valid for arbitrary values of θ, the second integral (i.e.,

Eq. 4.2.5 exists for the particular value of $\theta = -(j+\omega+1)/2$ only.

To complete the solution of the problem we have to obtain one more expression since there are three dependent variables ψ, ϕ and f. To obtain the third integral, we use the derivative of ϕ expression derived in Chapter II (i.e., Eq. 2.5.7) which is given as

$$\phi' = \frac{-\theta\phi(\phi-\xi) + \frac{f}{\psi}(2\theta+\omega+\frac{1}{2}f/\xi)}{(\phi-\xi)^2 - \gamma f/\psi} \qquad (2.5.7)$$

From the second integral we can express f/ψ as a function of ϕ and ξ as

$$\frac{f}{\psi} = \frac{-(\gamma-1)}{2}\frac{\phi^2(\phi-\xi)}{(\gamma\phi-\xi)} \qquad (4.2.6)$$

Substituting Eq. 4.2.6 into Eq. 2.5.7 and using the value of $\theta = -(j+\omega+1)/2$, we obtain the following equation

$$\phi' = -\frac{\phi}{\xi} \cdot \frac{(\gamma j(\gamma-1)\phi^2 - \phi\xi[(j+1)(2\gamma-1)+\omega] + (j+\omega+1)\xi^2)}{(\gamma(\gamma+1)\phi^2 - 2(\gamma+1)\phi\xi + 2\xi^2)} \qquad (4.2.7)$$

The above equation may be conveniently transformed by defining a new variable P as

$$P = \phi/\xi \qquad (4.2.8)$$

In terms of P, Eq. 4.2.7 becomes

$$-\frac{d\xi}{\xi} = dP\left(\frac{A_1}{P} + \frac{A_2}{P\cdot\alpha_1} + \frac{A_3}{P\cdot\alpha_2}\right) \qquad (4.2.9)$$

where

$$A_1 = \frac{2}{j+\omega+3} = N \qquad (4.2.10)$$

$$A_3 = \frac{-(\gamma-1)}{j+1+\gamma(\omega+3)-2} \qquad (4.2.11)$$

$$A_2 = \frac{\gamma+1}{2\gamma(\gamma-1)(j+1)} - A_1 - A_3 \qquad (4.2.12)$$

$$\alpha_1 = \frac{j+\omega+3}{2+(j+1)(\gamma-1)} \qquad (4.2.13)$$

$$\alpha_2 = \frac{1}{\gamma} \qquad (4.2.14)$$

Eq. 4.2.9 can be integrated immediately to yield

$$\frac{K_3}{\xi} = \left(\frac{\phi}{\xi}\right)^{A_1}\left(\frac{\phi}{\xi}-\alpha_1\right)^{A_2}\left(\frac{\phi}{\xi}-\alpha_2\right)^{A_3} \qquad (4.2.15)$$

Again the constant of integration K_3 can be evaluated using the strong shock conditions at the front $\xi = 1$ as

$$K_1 = \frac{2^{A_1} \left[\dfrac{(j+1)(\gamma \cdot 3) - 2(\gamma - 1) - \omega(\gamma + 1)}{2 + (j+1)(\gamma - 1)} \right]^{A_2} \cdot \left(\dfrac{\gamma - 1}{\gamma} \right)^{A_3}}{(\gamma + 1)^{A_1 + A_2 + A_3}}$$

$$(4.2.16)$$

with the A_1, A_2 and A_3 given by Eqs. 4.2.10 to 4.2.12. Upon examination of the above equation, we see that the term

$$\frac{(j+1)(\gamma \cdot 3) - 2(\gamma - 1) - \omega(\gamma + 1)}{2 + (j+1)(\gamma - 1)}$$

comes from the middle term $\phi(1) - \alpha_1$, in Eq. 4.2.15. Defining a critical value of ω as

$$\omega_c = \frac{(j+1)(\gamma \cdot 3) - 2(\gamma - 1)}{\gamma + 1}$$

$$(4.2.17)$$

we see that

$$\phi(1) - \alpha_1 < 0 \qquad if \quad \omega > \omega_c$$

$$(4.2.18)$$

and $\quad \phi(1) - \alpha_1 > 0 \qquad if \quad \omega < \omega_c$

$$(4.2.19)$$

From the above equations, it is evident that the third integral as given by Eq. 4.2.15 represents the condition for $\omega < \omega_c$ and $\phi(1) - \alpha_1 > 0$. For $\omega > \omega_c$, the third integral should be written as

$$K_3^* = \left(\oint \right)^{A_1} \left(\alpha_1 - \oint \right)^{A_2} \left(\oint - \alpha_2 \right)^{A_3}$$

$$(4.2.20)$$

where

$$K_3^* = \frac{2^{A_1}\left[\dfrac{\omega(\gamma-1) + 2(\gamma-1) - (j+1)(\gamma-3)}{2+(j+1)(\gamma-1)}\right]^{A_2}\left(\dfrac{\gamma-1}{\gamma}\right)^{A_3}}{(\gamma+1)^{A_1+A_2+A_3}}$$

<div align="right">(4.2.21)</div>

and the value of A_1, A_2, A_3, α_1 and α_2 are as given before by Eqs. 4.2.10 to 4.2.14.

The simplest way to obtain the solution for the variables ϕ, f and ψ from the three integrals derived is to first use the third integral given by Eq. 4.2.15 or Eq. 4.2.20 depending on whether $\omega < \omega_c$ or $\omega > \omega_c$, and solve for ξ in terms of ϕ/ξ. Having done this, f and ψ may be found from the first and the second integrals.

From the first and second integrals, we get

$$\frac{\psi^{(\gamma-1)(j+1)}}{f^{j+\omega+1}} = \left[\frac{(\gamma+1)^{\gamma+1}}{2(\gamma-1)^\gamma}\right]^{j+\omega+1}(\xi-\phi)^{j+1+\gamma\omega}\cdot\xi^{(j+\omega)(j+\omega+1)-\omega(\gamma-1)}$$

and

$$\frac{f}{\psi} = \frac{(\gamma-1)}{2}\,\frac{\phi^2(\xi-\phi)}{(\gamma\phi-\xi)}$$

and solving for ψ by eliminating f, we obtain

$$\psi^{(\gamma-2)(j+1)-\omega} = \left[\frac{(\gamma+1)^{\gamma+1}}{4(\gamma-1)^{\gamma+1}}\cdot\frac{\phi^2}{(\gamma\phi-\xi)}\right]^{j+\omega+1}\cdot$$

$$\cdot\,\xi^{(j+\omega)(j+\omega+1)-\omega(\gamma-1)}\cdot(\xi-\phi)^{2(j+1)+\omega(\gamma+1)}\,.$$

<div align="right">(4.2.22)</div>

Providing $\omega \neq (\gamma-2)(j+1)$, we can solve for ψ immediately from the above equation and obtain

$$\psi = \left\{ \frac{(\gamma+1)^{\gamma+1}}{4(\gamma-1)^{\gamma-1}} \cdot \frac{\phi^2}{(\gamma\phi-\xi)} \right\}^{\frac{j+\omega+1}{(\gamma-2)(j+1)-\omega}} \cdot (\xi-\phi)^{\frac{2(j+1)+\omega(\gamma+1)}{(\gamma-2)(j+1)-\omega}}$$

$$\times \xi^{\frac{(j+\omega)(j+\omega+1) - \omega(\gamma-1)}{(\gamma-2)(j+1)-\omega}}$$

$$(4.2.23)$$

Substituting the above equation into the third integral (i.e., Eq. 4.2.6) we get an expression for f as follows

$$f = \frac{\gamma-1}{2} \cdot \left\{ \frac{(\gamma+1)^{\gamma+1}}{4(\gamma-1)^{\gamma-1}} \right\}^{\frac{j+\omega+1}{(\gamma-2)(j+1)-\omega}} \cdot \left\{ \frac{\phi^2}{\gamma\phi-\xi} \right\}^{\frac{j+\omega+1}{(\gamma-2)(j+1)-\omega}+1}$$

$$\times (\xi-\phi)^{\frac{2(j+1)+\omega(\gamma+1)}{(\gamma-2)(j+1)-\omega}+1} \cdot \xi^{\frac{(j+\omega)(j+\omega+1)-\omega(\gamma-1)}{(\gamma-2)(j+1)-\omega}}$$

$$(4.2.24)$$

For $\omega = (\gamma-2)(j+1)$, we cannot solve for ψ from Eq. 4.2.22. In fact for this particular value of ω, the first integral (i.e., Eq. 4.2.22) and the third integral (i.e., Eq. 4.2.15) are identical reducing the number of available analytical expressions by one. For this particular case, methods other than the one described above must be used to solve the problem.

It is possible to express the solutions obtained in a more compact form than that presented. Defining the following parameters

$$T_1 = \frac{1}{\phi(1)} \cdot \frac{\phi}{\xi}$$

$$T_2 = \frac{1}{\phi(1) - 1} \cdot \left(\frac{\phi}{\xi} - 1 \right)$$

$$T_3 = \frac{1}{\gamma \phi(1) - 1} \left(\frac{\gamma \phi}{\xi} - 1 \right) \qquad (4.2.25)$$

$$T_4 = \frac{1}{\frac{\phi(1)}{\alpha_1} - 1} \left(\frac{\phi}{\alpha_1 \xi} - 1 \right)$$

where $\phi(1) = 2/(\gamma+1)$ is the boundary value of ϕ at the shock and α_1 is defined previously by Eq. 4.2.13. It is seen that T_1, T_2, T_3 and T_4 all equal unity at the front $\xi = 1$. In terms of the T's defined by Eq. 4.2.25, the third integral can be written as

$$\xi = T_1^{\frac{-2}{j+\omega+3}} \; T_3^{\frac{\gamma-1}{j+1+2(\gamma-1)+\gamma\omega}} \; T_4^{-A_2} \qquad (4.2.26)$$

where A_2 is given previously by Eq. 4.2.12 as

$$A_2 = \frac{\gamma+1}{2+(\gamma-1)(j+1)} - \frac{2}{j+\omega+3} + \frac{\gamma-1}{j+1+\gamma(\omega+2)-2} \qquad (4.2.12)$$

The expression for the density ψ given by Eq. 4.2.23 becomes

$$\frac{\psi}{\psi(1)} = T_2^{\frac{2(j+1)+\omega(\gamma+1)}{d_1}} \; T_3^{\frac{j+\omega+1}{j+1+2(\gamma-1)+\gamma\omega}} \cdot T_4^{\frac{-A_2(j+\omega+1)(j+\omega+3)}{d_1}} \qquad (4.2.27)$$

where

$$d_1 = (\gamma-2)(j+1) - \omega \qquad (4.2.28)$$

If instead ρ/ρ_S , where ρ_S is the value of ρ at the shock front, is desired it can be obtained simply by multiplying Eq. 4.2.27 through by ξ^ω . Hence

$$\frac{\rho}{\rho_S} = \frac{\psi}{\psi_{(1)}} \xi^\omega \qquad (4.2.29)$$

where ξ is given by Eq. 4.2.26.

For the pressure f , Eq. 4.2.6 can be written in terms of the T's by inspection as

$$\frac{f}{f_{(1)}} = T_1^2 T_2 T_3^{-1} \frac{\psi}{\psi_{(1)}} \xi^2 \qquad (4.2.30)$$

where ξ and $\psi/\psi_{(1)}$ are given above by Eqs. 4.2.26 and 4.2.27 respectively. Similarly, if p/p_S where p_S is the value of the pressure at the shock front is desired, it can be obtained by multiplying Eq. 4.2.30 by ξ^ω.

$$\frac{p}{p_S} = \frac{f}{f_{(1)}} \xi^\omega \qquad (4.2.31)$$

The temperature distribution can also be written as

$$\frac{T}{T_S} = \frac{f}{f_{(1)}} \cdot \frac{\psi_{(1)}}{\psi} \qquad (4.2.32)$$

We can also obtain the Lagrangian coordinate for the fluid particles as follows: A particle whose original position was at r_o when the shock was at r_o will be at later time at r when the shock position is at R_s. Since the entropy of the particle remains constant we can write

$$\frac{p(r, R_S)}{\rho^\gamma(r, R_S)} = \frac{p(r_0, r_0)}{\rho^\gamma(r_0, r_0)} \tag{4.2.33}$$

Using the definition of $f(\xi) = p(r, R_S)/(\rho_0(r) \dot{R}_S^2)$ and

$\psi = \rho(r)/\rho_0(r)$, Eq. 4.2.33 becomes

$$\frac{f}{\psi^\gamma} = \frac{f(1)}{\psi(1)^\gamma} \left[\frac{\rho_0(r)}{\rho_0(r_0)} \right]^{\gamma-1} \frac{\dot{r}_0^2}{\dot{R}_S^2} = \frac{f(1)}{\psi(1)^\gamma} \left(\frac{r}{r_0} \right)^{\omega(\gamma-1)} \frac{\dot{r}_0^2}{\dot{R}_S^2} \tag{4.2.34}$$

From the energy integral given by Eq. 4.1.8 which for strong blast waves can be written as

$$1 = y \frac{I}{\eta} = \left(\frac{R_S}{R_0} \right)^{j+\omega+1} I \frac{\dot{R}_S^2}{c_0^2} ,$$

we obtain

$$\dot{R}_S^2 = \frac{c_0^2 R_0^{j+\omega+1}}{I R_S^{j+\omega+1}} .$$

Hence

$$\frac{\dot{r}_0^2}{\dot{R}_S^2} = \left(\frac{R_S}{r_0} \right)^{j+\omega+1}$$

and Eq. 4.2.34 can be written as

$$\frac{f}{\psi^\gamma} = \frac{f(1)}{\psi(1)^\gamma} \left(\frac{r}{r_0} \right)^{\omega(\gamma-1)} \left(\frac{R_S}{r_0} \right)^{j+\omega+1}$$

or alternatively as

$$\frac{f}{4^\gamma} = \frac{f_{(1)}}{4_{(1)}^\gamma} \left(\frac{R_s}{r}\right)^{j+\omega+1} \left(\frac{r}{r_o}\right)^{j+\gamma\omega+1}$$

Solving for r/r_o from the above equation yields

$$\frac{r}{r_o} = \left[\frac{f}{f_{(1)}} \left(\frac{4_{(1)}}{4}\right)^\gamma \xi^{j+\omega+1} \right]^{\frac{1}{j+\gamma\omega+1}} \tag{4.2.35}$$

Eq. 4.2.35 can also be written as

$$\frac{r_o}{R_s} = \left[\frac{f_{(1)}}{f} \left(\frac{4}{4_{(1)}}\right)^\gamma \xi^{\omega(\gamma-1)} \right]^{\frac{1}{j+\gamma\omega+1}} \tag{4.2.36}$$

and the solution for $f/f_{(1)}$, $4/4_{(1)}$ and ξ are given by Eqs. 4.2.30, 4.2.27 and 4.2.26 respectively.

To obtain a solution with specified values for ω , j and γ , one assigns a value for ϕ/ξ which then determines the value of the T's. Once the T's are known, all the variables can then be found from the expressions given above. For the particle velocity ϕ itself, we can use the first of Eq. 4.2.25 and obtain

$$\frac{u}{u_s} = \frac{\phi}{\phi_{(1)}} = T_1 \xi \tag{4.2.37}$$

The analytical expressions given for the solution of the strong blast problem are valid for arbitrary values of the density exponent ω (except for the critical value of $\omega = (\gamma-2)(j+1)$). For the solution of the case with initially uniform density, we simply equate ω to zero in all the expressions given in this Section.

4.3 The Strong Blast Solution in $Z-V$ Coordinates

Although the choice of variables is a matter of preference, it would be interesting to describe the constant energy solution in terms of the state variables (i.e., Z and V) used by Soviet scientists as well as many Western investigators. As discussed in Chapter II, the similarity equations in $Z-V$ coordinates are given as

$$\frac{dz}{dV} = \frac{-V\left[(V-N)^2-z\right]\left[2-\left((j+1)(\gamma-1)+2\right)V\right]}{(V-N)\left\{V(V-1)(V-N)-z\left[V(j+1)-\frac{1}{\gamma}(2-N(\omega+2))\right]\right\}} - \frac{\gamma(\gamma-1)}{V-N} \quad (2.6.8)$$

$$\frac{d\ln\psi}{d\ln V} = \frac{-V}{V-N}\cdot\left[\frac{V(V-1)(V-N)-(j+\omega+1)V(V-N)^2+z\left(\omega V+2-N(\omega+2)\right)}{V(V-1)(V-N)-z\left(V(j+1)-\frac{1}{\gamma}(2-N(\omega+2))\right)}\right] \quad (2.6.9)$$

$$\frac{d\ln\xi}{d\ln V} = \frac{V\left(z-(V-N)^2\right)}{V(V-1)(V-N)-z\left(V(j+1)-\frac{1}{\gamma}\left(2-N(\omega+2)\right)\right)} \quad (2.6.10)$$

where Z and V are defined as

$$z = \frac{N^2}{\xi^2}\frac{\gamma f}{\psi} \quad (2.6.1)$$

$$V = \frac{N\phi}{\xi} \quad (2.6.2)$$

Once a solution for $Z(V)$ has been obtained ψ , ξ , f , ϕ can be found from Eqs. 2.6.9, 2.6.10, 2.6.1 and 2.6.2 respectively.

The strong shocks the boundary conditions at the front are given by

$$Z(1) = \frac{2\gamma N^2(\gamma-1)}{(\gamma+1)^2} \qquad (2.6.25)$$

$$V(1) = \frac{2N}{\gamma+1} \qquad (2.6.24)$$

and the value of the exponent N is

$$N = \frac{2}{j+w+3} \qquad (4.1.18)$$

for the strong blast constant energy solution. With the value of N given by Eq. 4.1.8 and the boundary conditions for $Z(1)$ and $V(1)$ by Eqs. 2.6.24 and 2.6.25, the integral curve $Z(V)$ can be obtained by integrating numerically Eq. 2.6.8. However for the particular value of N for the constant energy solution, a closed form solution for $Z(V)$ can be obtained. To get this solution, the simplest way is to use the second integral derived in the previous Section as

$$\frac{f}{4} = \frac{\gamma-1}{2} \frac{\phi^2(\xi-\phi)}{(\gamma\phi-\xi)} . \qquad (4.2.6)$$

Writing the above equation in terms of Z and V, we get

$$\frac{\gamma N^2 f}{\xi^2 4} = \frac{(\frac{\gamma-1}{2})\left(\frac{N\phi}{\xi}\right)^2\left(1-\frac{N\phi}{\xi}\cdot\frac{1}{N}\right)}{\left[\left(\frac{N\phi}{\xi}\right)\frac{1}{N}-\frac{1}{\gamma}\right]}$$

and simplifying, we obtain the following result

$$Z = \left(\frac{\gamma-1}{2}\right) \frac{V^2(N-V)}{(V-N/\gamma)} \qquad (4.3.1)$$

The above equation is identical to that given by Sedov (Eq. 14.6 on page 261 of Sedov's book) where Sedov uses δ instead of N and his

ω is opposite in sign to ours (we let ω carry its own sign). In fact the complete analytical solution comprises the three integrals derived in the previous Section. Expressing the complete solution in z-V coordinates we transform 4.2.23 to 4.2.36 with V as a parameter.

From Eq. 4.2.25, we obtain

$$
\left.
\begin{aligned}
\tau_1 &= \frac{V}{V(1)} \\[6pt]
\tau_2 &= \left(\frac{V}{N}-1\right)\Big/\left(\frac{V(1)}{N}-1\right) \\[6pt]
\tau_3 &= \left(\frac{\gamma V}{N}-1\right)\Big/\left(\frac{\gamma V(1)}{N}-1\right) \\[6pt]
\tau_4 &= \left(\frac{V}{\alpha_1 N}-1\right)\Big/\left(\frac{V(1)}{\alpha_1 N}-1\right)
\end{aligned}
\right\} \tag{4.3.2}
$$

where α_1 is defined by Eq. 4.2.13 as

$$
\alpha_1 = \frac{j+3}{2+(j+1)(\gamma-1)} \tag{4.2.13}
$$

Eq. 4.2.26 for ξ now becomes

$$
\xi = \tau_1^{-N}\, \tau_3^{\frac{\gamma-1}{j+1+2(\gamma-1)+\omega\gamma}}\, \tau_4^{-A_2} \tag{4.3.3}
$$

where A_2 is given by Eq. 4.2.12 as

$$
A_2 = \frac{\gamma+1}{2+(\gamma-1)(j+1)} - N + \frac{\gamma-1}{j+1+\gamma(\omega+3)-2} \tag{4.2.12}
$$

The expression for the density ψ from Eq. 4.2.27 becomes

$$\frac{\psi}{\psi(1)} = \tau_2^{-\frac{(A_2)+\omega \gamma(1)}{d_1}} \cdot \tau_3^{\frac{j+\omega}{j+\omega(\gamma-1)+j\omega}} \tau_4^{-\frac{A_2(j+\omega-k j+\omega s)}{d_1}} \tag{4.3.4}$$

where d_1 is defined by Eq. 4.2.28 as

$$d_1 = \nu_0\ 2)(j+1) - \omega \tag{4.2.28}$$

and A_2 by Eq. 4.2.12. Similarly Eqs. 4.2.29, 4.2.30, 4.2.32, 4.2.36 and 4.2.37 become

$$\frac{\rho}{\rho_s} = \frac{\psi}{\psi(1)} \xi^{\omega} \tag{4.2.29}$$

$$\frac{f}{f(1)} = \tau_1^2 C_2 \tau_3^{-1} \frac{\psi}{\psi(1)} \xi^2 \tag{4.3.5}$$

$$\frac{p}{p_s} = \frac{f}{f(1)} \xi^{\omega} \tag{4.2.31}$$

$$\frac{T}{T_s} = \frac{f}{f(1)} \frac{\psi(1)}{\psi} \tag{4.2.32}$$

$$\frac{\dot{o}}{R_s} = \left[\frac{f(1)}{f} \left(\frac{\psi}{\psi(1)}\right)^{\gamma} \xi^{\omega(\gamma-1)} \right]^{\frac{1}{j+1+\omega\gamma}} \tag{4.2.36}$$

and

$$\frac{u}{u_s} = \tau_1 \xi \ . \tag{4.3.6}$$

The above equations are identical to those given by Sedov.

4.4 Parametric Study of the Constant Energy Solution

Since the constant energy solution can be written in closed analytical form, we can readily make an investigation on the interesting dependence of the solution on the various parameters ω, j and γ. We shall first of all consider the most common case encountered in practice, that of an initially uniform density medium ($\omega = 0$, $\rho_0 = $ constant).

For $\omega = 0$, the first two integrals given previously can be written as

$$\frac{\psi}{f}^{\gamma-1} = \frac{(\gamma+1)^{\gamma+1}}{2(\gamma-1)^\gamma}(\xi-\phi)\xi^j \qquad (4.4.1)$$

$$\frac{f}{\psi} = \frac{j-1}{2} \cdot \frac{\phi^2(\xi-\phi)}{\gamma\phi\cdot\xi} \qquad (4.4.2)$$

while the third integral has two forms depending on whether $(j+1)(\gamma-3) - 2(\gamma-1)$ is greater than or less than zero

$$\frac{\left(\frac{\phi}{\xi}\right)^{\frac{2}{j+3}}\left(\frac{j+3}{2+(j+1)(\gamma-1)} - \frac{\phi}{\xi}\right)^{A_2}}{\left(\frac{\phi}{\xi} - \frac{1}{\gamma}\right)^{\frac{\gamma-1}{j+1+2(\gamma-1)}}} \quad \dots \quad \frac{k_3}{\xi} \qquad (4.4.3)$$

for $(j+1)(\gamma-3) - 2(\gamma-1) < 0$

$$\left(\frac{\psi}{\xi}\right)^{j+1}\left(\xi - \frac{j+1}{2+(\gamma-1)(j+1)}\right)^{A_2} \qquad k_4$$

$$\left(\xi - \psi\right)^{\frac{j+1}{j+1+\gamma(j+1)}} \qquad \xi \qquad (4.4.4)$$

for $(j+1)(\beta-1) - 2(\beta+1) > 0$

where $A_2 = \frac{\gamma+1}{2+(\gamma-1)(j+1)} - \frac{2}{j+3} + \frac{\gamma-1}{j+1+\gamma(j+1)}$ (4.4.5)

and $k_3 = 2^{\frac{2}{j+1}}\left|\frac{(\gamma-1)(j+1)-2(\gamma-1)}{2+(j+1)(\gamma-1)}\right|^{A_2}\left(\frac{\gamma}{\gamma-1}\right)^{\frac{j+1}{j+1+\gamma(j+1)}}$

$$(\gamma+1)^{\frac{j+1}{j+1+\gamma(j+1)}} \qquad (4.4.6)$$

As described previously, the solution is obtained by first determining ξ as a function of ϕ/ξ from Eq. 4.4.3 or 4.4.4. Then Eqs. 4.4.1 and 4.4.2 are used to solve for f and ψ.

Eliminating f from Eq. 4.4.1 using Eq. 4.4.2, we obtain

$$\psi^{\gamma-2} = \frac{(\gamma+1)^{\gamma+1}}{4(\gamma-1)^{\gamma-1}} \frac{\phi^2(\xi-\phi)^2\xi^j}{(\gamma\phi-\xi)} \qquad (4.4.7)$$

from which ψ is evaluated at once providing $\gamma \neq 2$. The $\gamma = 2$ case corresponds to the general special case of $\omega = (\gamma-2)(j+1)$ mentioned previously in Section 4.2 and the solution cannot be determined by the procedures outlined in this Chapter. In fact if $\gamma = 2$, Eq. 4.4.7 reduces to the second integral given by Eq. 4.4.3. Hence an additional relationship must be found in order to determine the solutions for the three variables ϕ, f and ψ.

For $\gamma \neq 2$, the solution of Eq. 4.4.7 for the density yields

$$\psi = \left[\frac{(\gamma+1)^{\gamma+1}}{4(\gamma-1)^{\gamma-1}} \right]^{\frac{1}{\gamma-2}} \cdot \left[\frac{\phi^2 (\xi-\phi)^2 \xi^j}{(\gamma\phi \xi)} \right]^{\frac{1}{\gamma-2}} \tag{4.4.8}$$

Substituting the above equation into Eq. 4.4.2 for ψ yields the following relationship for the pressure f

$$f = \frac{\theta_2}{2}\xi \cdot \left[\frac{(\gamma+1)^{\gamma+1}}{4(\gamma-1)^{\gamma-1}} \right]^{\frac{1}{\gamma-2}} \left[\frac{\phi^{2(\gamma-1)}(\xi-\phi)^{\gamma}\xi^j}{(\gamma\phi-\xi)^{\gamma-1}} \right]^{\frac{1}{\gamma-2}} \tag{4.4.9}$$

For the planar and cylindrical cases (i.e., $j = 0$ and 1 respectively), the term $(j+1)(\gamma-3)-2(\gamma-1) = -(\gamma+1)$ and -4. For the spherical case $(j+1)(\gamma-3)-2(\gamma-1) = \gamma-7$.

Hence we see immediately that the third integral has the form given by Eq. 4.4.3 for $j = 0$ and 1 for all values of γ, and for $j = 2$ with $\gamma < 7$. For the case $j = 2$ and $\gamma > 7$, the second form given by Eq. 4.4.4 is used.

For the particular case of $j = 2$ and $\gamma = 7$, the solution takes on a very simple form. In this case, the constant of integration of the third integral K_3 given by Eq. 4.4.6 is zero and Eq. 4.4.4 yields the solution for ϕ as

$$\phi = \frac{\xi}{7} \tag{4.4.10}$$

Using the above solution for $\phi(\xi)$, Eqs. 4.4.8 and 4.4.9 yield the solutions for ψ and f as

$$\psi = \frac{4}{3}\xi \qquad\qquad (4.4.11)$$

$$f = \frac{\xi^3}{4} \qquad\qquad (4.4.12)$$

Hence for $j = 2$ and $\gamma = 7$, the particle velocity ϕ and the density ψ are linear with ξ, decreasing from its value at the shock to zero at the center of symmetry. The pressure distribution f is a cubic function of ξ also decreasing from its value at the shock to zero at the center in contrast with the cases for arbitrary values of γ where the pressure f is finite at the center of symmetry $\xi = 0$.

Before examining the solutions for the two cases where $(j+1)(\gamma-3)-2(\gamma-1)$ is less than and greater than zero, it is appropriate to mention that a close study of the integrals reveals that for the case $(j+1)(\gamma-3)-2(\gamma-1) < 0$, the particle velocity ϕ behaves like ξ as $\xi \to 0$ at the center of symmetry. For the case where $(j+1)(\gamma-3)-2(\gamma-1) > 0$, ϕ behaves like ξ at some finite value of $\xi = \xi_0$. This implies that for the second case, $(\phi-\xi) \to 0$ at some finite $\xi = \xi_0$, hence ξ_0 is a vacuum-gas boundary.

Let us now look at the solution for the first case where $(j+1)(\gamma-3)-2(\gamma-1) < 0$. This corresponds to $j = 0, 1$ for arbitrary values of γ and $j = 2$ with $\gamma < 7$. For this case, we have $\phi \to$ constant $\cdot \xi$ near $\xi = 0$, which implies that the solution exists for the entire range of $0 \le \xi \le 1$. The asymptotic solution for the variables ϕ, f and ψ as $\xi \to 0$ can be written as

$$\phi = \phi_0 \xi + \phi_1 \xi^{S_2} + \cdots$$

$$f = f_0 \xi^{\delta_1} + f_1 \xi^{\delta_2} + \cdots$$

(4.4.13)

$$\psi = \psi_0 \xi^{\beta} + \psi_1 \xi^{A} + \cdots$$

Substituting the above expression for ϕ with the third integral (i.e., Eq. 4.4.3), it is seen that in order to satisfy the integral,

$$\phi_0 = \frac{1}{\gamma} \quad \text{or} \quad \frac{j+3}{2+(j+1)(\gamma-1)}$$

(4.4.14)

It turns out that $\phi_0 = \frac{1}{\gamma}$ since the other alternative yields an unsatisfactory value for the exponent s_2 since $s_2 > 1$. The exponent s_2 is found to be

$$s_2 = \frac{(j+1)}{\gamma-1} + 3$$

(4.4.15)

and the coefficient ϕ_1 is

$$\phi_1 = \left\{ \left(\frac{1}{\gamma} \right)^{\frac{2}{j+3}} \left(\frac{j+3}{2+(j+1)(\gamma-1)} - \frac{1}{\gamma} \right)^{A_2} \cdot \frac{1}{K_3} \right\}^{\frac{j+1+2(\gamma-1)}{\gamma-1}}$$

(4.4.16)

where A_2 and K_3 are given by Eqs. 4.4.5 and 4.4.6. Substituting the expressions for f and ψ into Eqs. 4.4.8 and 4.4.9

$$\psi_0 = \left[\frac{(\gamma+1)^{\gamma+1}}{4(\gamma-1)^{\gamma-3}\gamma s \phi_1} \right]^{\frac{1}{\gamma-2}}$$

(4.4.17)

$$g_1 = 0 \tag{4.4.18}$$

$$f_0 = \frac{(\gamma-1)^2}{2\gamma^4} \frac{u_0}{\phi_1} \tag{4.4.19}$$

$$p_1 = \frac{j+1}{\gamma-1} \tag{4.4.20}$$

$$g_2 = p_1 + 2 \tag{4.4.21}$$

where ϕ_1 is given by Eq. 4.4.16. Using Eqs. 4.4.14 to 4.4.21, the solutions near the center of symmetry can now be written as

$$\phi = \frac{\xi}{\gamma} + \phi_1 \xi^{\frac{j+1}{\delta-1}+3} + \cdots$$

$$\psi = \left[\frac{(\gamma+1)^{\gamma+1}}{4(\delta-1)^{\gamma-3}\gamma^5 \phi_1} \right]^{\frac{1}{\gamma-2}} \xi^{\frac{j+1}{\gamma-1}} + \cdots \tag{4.4.22}$$

$$f = \frac{(\gamma-1)^2 u_0}{2\gamma^4 \phi_1} + f_1 \xi^{\frac{j+1}{\delta-1}+2} + \cdots$$

For some order of magnitude, let us take the case of spherical blasts in air (i.e., $j = 2$, $\gamma = 1.4$). Eq. 4.4.22 can be written as

$$\phi = \frac{\xi}{1.4} + \phi_1 \xi^{\frac{21}{2}} + \cdots$$

$$\psi = u_0 \xi^{15/2} + \cdots \tag{4.4.23}$$

$$f = f_0 + f_1 \xi^{19/2} + \cdots$$

Note that the powers of ξ in the above equations are very large. Since $0 < \xi < 1$, we see that the particle velocity is almost linear, the pressure almost constant while the density is near zero for a substantial distance from the center of symmetry to the shock since the first term dominates. The density profile indicates that most of the mass is concentrated in the neighborhood of the shock front - especially so for lower values of γ. For example if say $\gamma < 1.1$, the density profile becomes

$$\psi = \psi_0 \, \xi^{30} + \cdots$$

$$(4.4.24)$$

and since $\xi \leq 1$, we see that ψ decreases extremely rapidly behind the shock front to vanishingly small for $\xi < 1$. This led Cheryni to propose the Newtonian approximation for treating blast waves yielding quite accurate results for $\gamma \sim 1$. For the second case where

$$(j+1)(\gamma-3) - 2(\gamma-1) > 0 \quad , \text{ (i.e., for } j = 2 \text{ and } \gamma > 7 \text{), the}$$

third integral takes on the second form given by Eq. 4.4.4. Upon further examination, it is seen that it is impossible to achieve $\phi(0) = 0$ and therefore we have $\phi \to \xi_0$. The solution exists for the domain $\xi_0 \leq \xi \leq 1$ and for $\xi < \xi_0$, we have a vacuum cavity. Physically this means that the shock drags the mass away from the center faster than the rarefaction waves can accelerate it back in the opposite direction.

Near the gas-vacuum boundary $\xi = \xi_0$, the solutions have the forms given as

$$\phi = \xi_0 + \phi_1^* (\xi - \xi_0) + \cdots$$

$$\psi = \psi_0^* (\xi - \xi_0)^{\frac{2}{\gamma - 2}} + \cdots$$

$$f = f_0^* (\xi - \xi_0)^{\frac{\gamma}{\gamma - 2}} + \cdots$$

(4.4.25)

where the cavity diameter ξ_0 and the coefficient ϕ_1^* can be obtained by substituting the above expressions into the third integral. ξ_0 is given as

$$\xi_0 = \frac{k_3 \left(\frac{\gamma - 1}{\gamma} \right)^{\frac{\gamma - 1}{2\gamma + 1}}}{\left(1 - \frac{5}{3\gamma - 1} \right)^{A_2}}$$

(4.4.26)

ϕ_1^* , f_0^* and ψ_0^* are not given here but can be obtained readily using the integrals as before. For high values of γ, ψ practically suffers a jump, rising from zero at the boundary ξ_0 to some finite value at $\xi \sim \xi_0$ very rapidly.

For $\omega \neq 0$, we again have two cases. In order to correspond to the $\omega = 0$ solution given previously we shall denote the first case for $\omega > \omega_c$ and the second case for $\omega < \omega_c$ where

$$\omega_c = \frac{(j+1)(\gamma - 3) - 2(\gamma - 1)}{\gamma + 1}$$

(4.4.27)

For j = 0, 1 and 2, $\omega_c = -1$, $-\frac{4}{\gamma + 1}$ and $\frac{\gamma - 7}{\gamma + 1}$ respectively. From the mass integral, we see that $\omega > -(j+1)$ if the mass enclosed by the shock front is to be finite. Hence case 2 ($\omega < \omega_c$)

is only permitted for cylindrical (j = 1) and spherical (j = 2) symmetry.

For the first case $\omega > \omega_c$, we see again that $\phi(o) = 0$ and the solution exists for the entire domain $0 \leq \xi \leq 1$. Using the three integrals (i.e., Eqs. 4.2.20, 4.2.1 and 4.2.6) we obtain the solutions for ϕ , f and ψ near the center of symmetry $\xi = 0$ as

$$\phi = \frac{1}{\gamma}\xi + \phi_1 \xi^{\frac{j+\omega+1}{\gamma-1} + \omega + 3} + \cdots$$

$$f = f_o \xi^{-\omega} + f_1 \xi^{\frac{j+\omega+1}{\gamma-1} + 2} + \cdots \qquad (4.4.28)$$

$$\psi = \psi_o \xi^{\frac{j+\omega+1}{\gamma-1}} + \cdots$$

where

$$\phi_1 = \left[\left(\frac{1}{\gamma}\right)^{\frac{2}{j+\omega+3}} \left(\frac{j+\omega+3}{2+(j+1)(\gamma-1)} - \frac{1}{\gamma}\right)^{A_2} \cdot \frac{1}{K_3^*} \right]^{\frac{j+1+\frac{2(\gamma-1)+\gamma\omega}{\gamma-1}}} $$

$$(4.4.29)$$

and A_2 and K_3^* are given by Eqs. 4.2.12 and 4.2.21. f_o and ψ_o are obtained as

$$f_o = \frac{(\gamma-1)^2 \psi_o}{2\gamma^4 \phi_1} \qquad (4.4.30)$$

$$\psi_o = \left[\frac{(\gamma+1)^{\gamma+1}}{4(\gamma-1)^{\gamma-1}\phi_1\gamma^3} \right]^{\frac{j+\omega+1}{(\gamma-2)(j+1)-\omega}} \left(\frac{\gamma-1}{\gamma}\right)^{\frac{2(j+1)+\omega(\gamma-1)}{(\gamma-2)(j+1)-\omega}} \qquad (4.4.31)$$

- 183 -

It can be seen that for $\omega = 0$, the above equations reduce to those given previously by the uniform density case (i.e., Eq. 4.4.22). Note that the pressure f goes to infinity as $\xi^{-\omega}$ since the leading term in the expression for f in Eq. 4.4.28 behaves like $\xi^{-\omega}$. This is a result of the way the pressure f is defined.

$$f = \frac{p}{\rho_0 \dot{R}_s^2}$$

and since $\rho_0 = A r^{\omega}$, this places a $\xi^{-\omega}$ in the leading term for f. If we were to use p/p_s where p_s is the pressure at the shock then

$$\frac{p}{p_s} = \frac{f_0}{f(1)} = \frac{(\gamma+1)}{2} f_0$$

where f_0 is given by Eq. 4.4.30 and will then be finite.

For the case $\omega = \omega_c = [(j+1)(\gamma-3) - 2(\gamma-1)]/(\gamma+1)$, which can be physically meaningful for cylindrical ($j = 1$) and spherical geometry, the constant K_3 (i.e., Eq. 4.2.16) becomes zero and the particle velocity is linear in ξ

$$\phi = \frac{2\xi}{\gamma+1} \tag{4.4.32}$$

The pressure f and the density ψ take on the simple forms which are obtained from Eqs. 4.2.23 and 4.2.24 as

$$\psi = \frac{\gamma+1}{\gamma-1} \xi^{\frac{4j}{\gamma+1}} \tag{4.4.33}$$

$$f = \frac{2}{\gamma+1} \xi^{\frac{4j}{\gamma+1}+2} \tag{4.4.34}$$

As was pointed out earlier the physically allowable limits on ω (i.e., $\omega > -(j+1)$) permit the above solutions to be meaningful only for cylindrical and spherical geometrics. For the planar case $j = 0$ and putting $\omega = \omega_c = -1$, it becomes evident by examining the density

profile given by Eq. 4.4.33 that

$$\psi = \frac{\gamma+1}{\gamma-1} = \text{constant throughout}$$

This means that if before the explosion we have mass M within a distance of R_s and after the explosion when the shock is at R_s, we now have a mass $\frac{\gamma+1}{\gamma-1}M$. This means we have more mass than we started out with. This type of behavior is typical for values of

$$\omega \leq -(j+1)$$

Of course if $\omega = -1$ for $j = 0$, the mass M is infinite so that the argument breaks down, but it illustrates the non-physical nature of the solution when $\omega \leq -(j+1)$.

For the second case where $\omega < \omega_c$, a vacuum cavity is formed at the center and the solution exists in the region $\xi_o \leq \xi \leq 1$ where ξ_o is the gas-vacuum boundary. Using the third integral given by Eq. 4.2.15 the cavity radius ξ_o is obtained as

$$\xi_o = k_3 \left(\frac{\gamma-1}{\gamma} \right)^{\frac{\gamma-1}{j+1+2(\gamma-1)+\omega\gamma}} \left(1 - \frac{j+3+\omega}{2+(j+1)(\gamma-1)} \right)^{-A_2} \quad (4.4.35)$$

Where k_3 and A_2 are given by Eqs. 4.2.16 and 4.2.12 respectively. The solution in the neighborhood of $\xi = \xi_o$ is found to be

$$\phi = \xi_o + \phi_1^*(\xi - \xi_o) + \cdots$$

$$\psi = \psi_o^{\prime*}(\xi - \xi_o)^{\frac{2(j+1)+\omega(\gamma+1)}{(\gamma-2)(j+1)-\omega}} + \cdots \quad (4.4.36)$$

$$f = f_o^*(\xi - \xi_o)^{\frac{2(j+1)+\omega(\gamma+1)}{(\gamma-2)(j+1)-\omega}} + \cdots$$

where the coefficients d_1^*, d_b^* and f_c^* can be found by substituting the above expressions into Eqs. 4.2.15, 4.2.23 and 4.2.24. It is interesting to note the general behavior of ψ and f near the cavity by examining the exponents of them in Eq. 4.4.36. It is seen that the density goes to zero for $\omega > -2(j+1)/(\gamma+1)$, finite for $\omega = -2(j+1)/(\gamma+1)$ and goes to infinity if $\omega < -2(j+1)/(\gamma+1)$. The pressure f always goes to zero however, if $\omega > -(\gamma+1)$, which is in the physically meaningful range for ω.

From the foregoing analysis, it is seen that the three integrals derived are extremely useful in generally describing the behavior of the solution with varying γ, j and ω . However due to their implicit nature, it is often more convenient to simply integrate the similarity equations directly on the computer.

4 5 Piston Driven Strong Shock Waves

We shall study in this Section the gas motion behind an
expanding shock wave driven by a piston in its wake. Since the expanding
piston is continuously doing work on the gas, energy is being added to
the flow continuously also. For self-similar motion it is necessary
that the energy input be of the form

$$E = E_o R_s^{2\alpha} \tag{4.5.1}$$

In fact, the strong blast problem treated in the previous Sections of
this Chapter is but a special case of Eq. 4.5.1 in which $\alpha = 0$ and
$E = E_o$ (i.e., the constant energy solution). For the case in which
$\omega = 0$ (i.e., uniform initial density) and $\alpha = j+1$, we have a
uniformly expanding shock wave (i.e., M_s = constant, η = constant)
driven by a constant velocity expanding piston. This case is treated in
Chapter III on isentropic self-similar problems since the entropy is
uniform throughout the flow field. We shall consider here only the
case where $\omega = 0$ since it is of more practical interest in connection
with the inviscid hypersonic flow past blunt-nosed slender bodies.

For $\omega = 0$, the expression for θ derived previously in Chapter
II is given as

$$\theta = - \frac{(j+1-\alpha)}{2}\left(1 - \eta\frac{I_o}{I}\right) \tag{2.4.49}$$

where

$$I_o = \frac{1}{j+1}\left(\frac{1}{\gamma(\gamma-1)} + g\right) \tag{2.4.50}$$

Since self-similar solution requires θ to be time independent, we see
from Eq. 2.4.49 that only for the case with $\alpha = j+1$ where $\theta = 0$,
the shock strength can be finite and arbitrary. For $\alpha \neq j+1$,
it is necessary that the shock strength be infinite (i.e., $\eta \to 0$)

so that the time dependent term drops out.

The shock trajectory for self-similar motion is given as

$$R_S \sim t^N$$

where $\qquad N = \dfrac{1}{1-\theta} = \dfrac{2}{j+3-\alpha}$ $\qquad\qquad$ (4.5.2)

Hence for $\alpha = 0$ and $\theta = -(j+1)/2$, we have $R_S \sim t^{\frac{2}{j+3}}$ which is the strong blast solution described in the previous Section. For $\alpha = j+1$, $\theta = 0$ and $N = 1$ and we have $R_S \sim t$, a uniformly expanding shock wave of constant strength followed by a uniformly expanding piston. For arbitrary values of α , $R_S \sim t^{\frac{2}{j+3-\alpha}}$ and for self-similar motion, the piston path must correspond to a similarity line (i.e., constant ξ line) hence $R_p \sim t^{\frac{2}{j+3-\alpha}}$ also where R_p is the piston path.

From physical considerations, α cannot be arbitrary, but has to be limited to a permissible range. In other words, the piston path cannot be arbitrary at least not if self-similar solutions were to exist. For example $\alpha = 0$ corresponds to a finite energy released at the initial instant, and if $\alpha < 0$, we see immediately from Eq. 4.5.1 that the energy input at the initial instant is infinite, and at later times, energy is being extracted from the flow. It is difficult to imagine a physical situation corresponding to this case. For $\qquad \alpha > j+1 \qquad$, we see from Eq. 4.5.2 that $N > 1$, hence the shock velocity is zero at the initial instant and accelerates as it expands. Although this situation cannot be ruled out from physical considerations because we can have hypersonic flows over concave bodies, we would not expect the flow over concave bodies to exhibit similarity properties. Besides, the zero strength shock wave property

contradicts the formulation since the entire analysis is based on strong shock approximation (i.e., $\eta \to 0$). Hence from physical arguments, α must be between the limits

$$0 \le \alpha \le j+1$$
$$-(j+1)/2 \le \theta \le 0 \tag{4.5.3}$$
$$2/(j+3) \le N \le 1 \ .$$

A sketch illustrating the shock and piston trajectories for various values of α are shown below
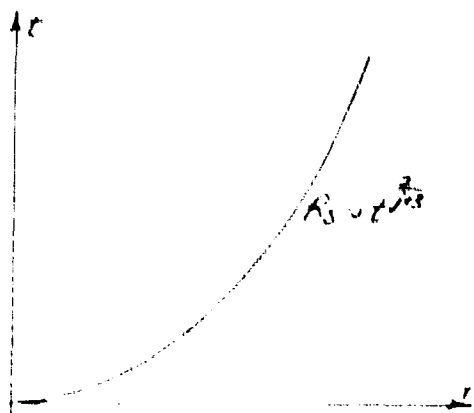
Zero piston velocity, constant
energy solution $\alpha = 0$

$\alpha < j+1$
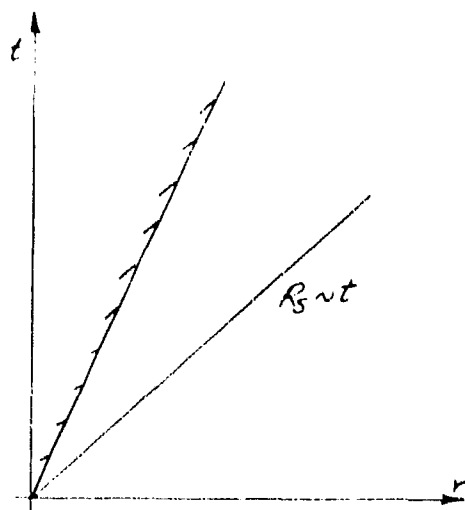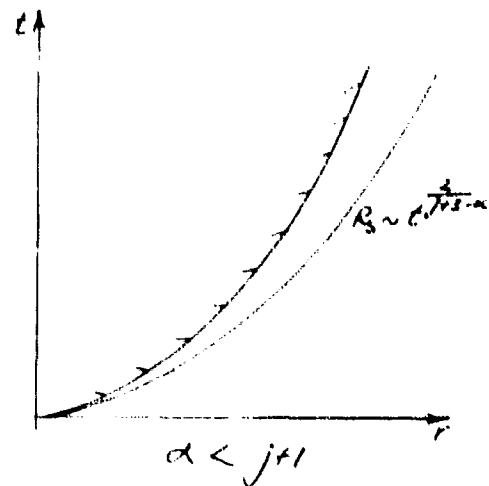
$\alpha = j+1$
constant shock velocity
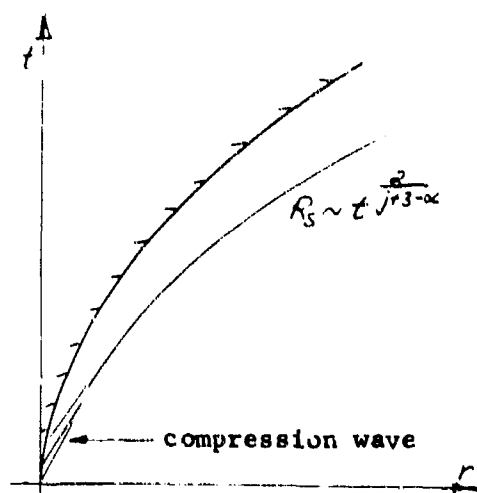
$\alpha > j+1$
no self-similar solution

For any piston path (i.e., body shape) $x_p \sim r^{\nu}$ within the limits specified by Eq. 4.5.3, θ can be found directly from Eq. 2.4.55

$$\theta = -\left(\frac{j+1-\alpha}{2}\right) = \frac{N-1}{N} \tag{2.4.55}$$

With the value of θ known, the similarity equations

$$\psi' = \frac{\left[(\phi-\xi)^2 - \frac{\gamma f}{4}\right]\frac{j\phi\psi}{\xi} - \theta\phi\psi(\phi-\xi) + (2\theta + \frac{\nu j\phi}{\xi})f}{(\phi-\xi)\left[(\phi-\xi)^2 - \frac{\gamma f}{4}\right]} \tag{4.5.4}$$

$$\phi' = \frac{-\theta\phi(\phi-\xi) + \frac{f}{4}(2\theta + \frac{\nu j\phi}{\xi})}{(\phi-\xi)^2 - \frac{\gamma f}{4}} \tag{4.5.5}$$

$$f' = \frac{-(\phi-\xi)(2\theta f + \frac{\nu j f\phi}{\xi}) + \theta\gamma\phi f}{(\phi-\xi)^2 - \frac{\gamma f}{4}} \tag{4.5.6}$$

can be integrated immediately with the boundary conditions at the shock $\xi = 1$ given as

$$\psi(1) = \frac{\gamma+1}{\gamma-1} , \quad \phi(1) = f(1) = \frac{2}{\gamma+1} \tag{4.5.7}$$

The solution terminates at the piston surface where $\phi - \xi = 0$.

From Eq. 4.5.4, we see that the boundary condition at the

piston surface $\phi - \xi = 0$ corresponds to a singularity. Let us investigate the behavior of the solution in the neighborhood of the piston surface. Rearranging the first integral obtained previously in Section 2.5, we obtain for the case $\omega = 0$

$$f^{\frac{2\theta + \gamma(j+1)}{j+1}} \frac{(\phi \cdot \xi)^{\frac{-2\theta}{2\theta + \gamma(j+1)}} \xi^{\frac{-2\theta}{2\theta + \gamma(j+1)}}}{\psi} = constant$$

(4.5.8)

As we approach the piston surface $(\phi - \xi) \rightarrow 0$, the density $\psi \rightarrow (\phi - \xi)^{\frac{-2\theta}{2\theta + \gamma(j+1)}}$ since the right hand side of Eq. 4.5.8 is a finite constant. Hence for the density to be finite, we must have

$$\frac{-2\theta}{2\theta + \gamma(j+1)} > 0$$

(4.5.9)

From the above equation, we get

$$\theta < - \frac{\gamma(j+1)}{2}$$

and

$$N > \frac{2}{c^2 + \gamma(j+1)}$$

(4.5.10)

Eq. 4.5.10 specifies the limit for N if the density at the piston surface is to be finite. For any real gas $\gamma > 1$ and the limits imposed by physical arguments given by Eqs. 4.5.3 satisfies Eq. 4.5.10. In practice the limits are set by Eq. 4.5.3 from physical considerations.

CHAPTER V

NON-SIMILAR SOLUTIONS FOR BLAST WAVES

In this Chapter, we shall present some methods for obtaining analytical solutions to explosion problems where the requirements for the existence of self-similar solutions discussed previously in Chapter II are not satisfied. We shall illustrate these non-similar techniques by treating the problem of point, line or planar blast waves in a detonating gas. Although in this particular problem, the non-similar effects arise from counter-pressure effects (i.e., influence of the initial internal energy of the medium) and from the energy released by chemical reactions at the front, the underlying concepts of these non-similar methods can be applied to account for other non-similar effects such as from a non-similar form of the equation of state or from the presence of a characteristic length in other problems. We shall present the analysis in a generalized form and the particular case of blast wave propagation in an inert medium with counterpressure effects can be reduced from the present generalized formulation by simply taking the chemical energy $Q = O$.

The model is identical to that for the blast wave problem treated in the preceeding Chapter in which at time t = 0, a finite amount of energy E_0 is deposited in a detonating gas. Consider the ratio of the total chemical and initial thermal energy of the gas enclosed by the shock front to the source of energy E_0

$$\mathcal{E} = \frac{\rho_0 k_j R_s^{j+1} (Q + e_0)}{E_0}$$

For early times when R_s is small, $\mathcal{E} << 1$ and $E_0 >> \rho_0 k_j R_s^{j+1} (Q + e_0)$. Hence the flow is dominated by the source energy E_0 which is constant and the solution is self-similar and is in fact the constant energy strong blast

solution given in the previous Chapter. At later times, the shock radius becomes significant and the total chemical and thermal energies enclosed by the front (i.e., $\beta k_j R_s^{j+1}(Q + e_o)$) can no longer be neglected as compared to E_o. The shock strength is now finite and hence the boundary conditions as well as the energy integral become time dependent and self-similar solutions are no longer possible. We shall present the various non-similar techniques for obtaining solutions in this finite shock strength non-similar regime.

We shall describe three non-similar methods: the perturbation method developed by Sakurai and independently by Melnikova. The local similarity or quasi-similarity method developed by Oshima and the power law density profile method first proposed by Porzel and developed by Rae and the authors. Of these three methods, the perturbation scheme is perhaps the most rigorous mathematically and yields excellent results for relatively high shock Mach Numbers. However due to the asymptotic nature of the perturbation expansions, they diverge rapidly and become quite inaccurate for low strength shock waves. The quasi-similar method of Oshima yields a solution for any particular value of shock Mach Number specified and less effort is involved in getting the solution. However it gives fairly good results only for the intermediate shock strength regime where the local similarity approximation is adequate. As pointed out by Oshima himself the method works best in conjunction with the perturbation scheme for the high shock strength regime. A serious drawback of the quasi-similar technique is that mass is not conserved. Hence flow distributions particularly particle velocity trajectories are very poorly described as compared to quantities such as the shock trajectory. The density profile method gives surprisingly good results for the entire range of shock strengths in spite of its simplicity. It is perhaps the most useful non-similar method for this particular problem. However it lacks generality and can only be

applied to problems if the density distribution can adequately be described by a simple power law.

5.1 The Non-Similar Equations

For non-similar problems, the exact differential equations of motion must be used. They are as given previously Eqs. 2.1.1, 2.1.2 and 2.1.9 as follows:

$$\frac{\partial \rho}{\partial t} + u \frac{\partial \rho}{\partial r} + \rho \frac{\partial u}{\partial r} + j \frac{\rho u}{r} = 0 \tag{2.1.1}$$

$$\frac{\partial u}{\partial t} + u \frac{\partial u}{\partial r} + \frac{1}{\rho} \frac{\partial p}{\partial r} = 0 \tag{2.1.2}$$

$$\frac{\partial p}{\partial t} + u \frac{\partial p}{\partial r} + \gamma p \frac{\partial u}{\partial r} + \gamma j \frac{pu}{r} = 0 \tag{2.1.9}$$

For convenience in obtaining analytical solutions, we make the following transformation based on the parameters used previously in similarity analyses.

$$\rho(r,t) \longrightarrow \rho_o \psi(\xi, R_s(t)) \tag{5.1.1}$$

$$u(r,t) \longrightarrow \dot{R}_s(t) \phi(\xi, R_s(t)) \tag{5.1.2}$$

$$p(r,t) \longrightarrow \rho_o \dot{R}_s^2 f(\xi, R_s(t)) \tag{5.1.3}$$

$$r \longrightarrow \xi = r/R_s(t) \tag{5.1.4}$$

$$t \longrightarrow R_s(t) \tag{5.1.5}$$

$R_s(t)$ and $\dot{R}_s(t)$ are the instantaneous shock position and shock velocity

respectively. We assume the initial density ρ_o of the medium to be constant for the sake of simplicity although the inclusion of $\rho_o(r) = A r^{-w}$ only involves slight modifications of the equations, the analyses remain identical.

Using the above defined parameters Eqs. 2.1.1, 2.1.2 and 2.1.9 become

$$(\phi - \xi)\frac{\partial \psi}{\partial \xi} + \psi \frac{\partial \phi}{\partial \xi} + j \frac{\psi \phi}{\xi} = -R_s^2 \frac{\partial \psi}{\partial R_s} \qquad (5.1.6)$$

$$(\phi - \xi)\frac{\partial \phi}{\partial \xi} + \theta \phi + \frac{f}{\psi}\frac{\partial f}{\partial \xi} = -R_s \frac{\partial \phi}{\partial R_s} \qquad (5.1.7)$$

$$(\phi - \xi)\frac{\partial f}{\partial \xi} + \gamma f \frac{\partial \phi}{\partial \xi} + \gamma j \frac{\phi f}{\xi} + 2\theta f = -R_s \frac{\partial f}{\partial R_s} \qquad (5.1.8)$$

where $\qquad \theta = R_s \ddot{R}_s / \dot{R}_s^2 .$ $\qquad\qquad\qquad (5.1.9)$

It should be noted that Eqs. 5.1.6 to 5.1.8 are exact and no approximations have been made other than a transformation of dependent and independent variables. They remain a set of three non-linear partial differential equations as the original set of equations in dimensional form (i.e., Eqs. 2.1.1, 2.1.2 and 2.1.9). Depending on the method of analysis, it is sometimes more convenient to use the shock Mach Number M_s or $\eta = 1/M_s^2$ as the independent variable rather than the shock radius $R_s(t)$. To use the shock Mach Number as the independent variable we use the identity

$$R_s \frac{\partial}{\partial R_s} = \theta \dot{R}_s \frac{\partial}{\partial \dot{R}_s} = \theta M_s \frac{\partial}{\partial M_s} = -2\theta \eta \frac{\partial}{\partial \eta} \qquad (5.1.10)$$

and simply replace the right hand side of Eqs. 5.1.6 to 5.1.8 by the desired form in Eq. 5.1.10.

The energy integral and the shock radius - shock strength relationship given previously in Chapter II for constant energy (i.e., $\alpha = 0$) and uniform initial density (i.e., $\omega = 0$) are as follows:

$$ y\left/\frac{1}{\eta}\right. = \mathcal{f}_{s}\left(\frac{1}{I(1+\alpha)}, \gamma\right) \tag{5.1.11} $$

where

$$ I = \int_{0}^{1}\left(\frac{f}{\gamma-1} + \frac{\psi\phi^2}{2}\right)\xi^{j}d\xi \tag{5.1.12} $$

$$ y = \left(\frac{R_s}{R_o}\right)^{j+1} \tag{5.1.13} $$

$$ R_o = \left(\frac{E_o}{k_j\rho_o C_o^2}\right)^{\frac{1}{j+1}} = \left(\frac{E_o}{k_j\gamma p_o}\right)^{\frac{1}{j+1}} \tag{5.1.14} $$

$k_j = 1, 2\pi, 4\pi$ for $j = 0, 1, 2$ respectively and

$$ \frac{dy}{d\eta} = -(j+1)y/\theta\eta \tag{5.1.15} $$

The boundary conditions at the front $\xi = 1$ for the general case taking $\gamma_o = \gamma_1 = \gamma$ are given as

$$ \psi(1,\eta) = \frac{\gamma+1}{\gamma+\eta-S} \tag{5.1.16} $$

$$\phi(\cdot,\eta) = \frac{?\cdot S}{?\cdot?} \tag{5.1.17}$$

$$f(\cdot,\eta) = \frac{?\cdot\eta\cdot?S}{\gamma(\gamma+1)} \tag{5.1.18}$$

where

$$S = \left[(1-\eta)^2 - k\eta\right]^{\frac{1}{2}} \tag{5.1.19}$$

$$k = 2(\gamma^2-1)\phi \tag{5.1.20}$$

In the above equations, the sign for overdriven solution is considered only since the blast wave started out as an infinite strength shock and decays asymptotically to a Chapman-Jouguet detonation. Eqs. 5.1.16 to 5.1.18 can be expressed in a more convenient form as follows· From Eq. 5.1.19, we note for Chapman-Jouguet detonations (i.e., $\eta \to \eta_{cr}$) the parameter $S \to 0$ and solving for K as a function of η_{cr}, we get

$$K = \frac{(1-\eta_{cr})^2}{\eta_{cr}} \tag{5.1.21}$$

Substituting Eq. 5.1.21 for K in Eq. 5.1.19 and simplifying yields

$$S = \left[\left(1 - \frac{\eta}{\eta_{cr}}\right)(1 - \eta\,\eta_{cr})\right]^{\frac{1}{2}}$$

Defining

$$\eta' = \eta/\eta_{cr}$$

Eqs. 5.1.16 to 5.1.19 can be rewritten in the following form:

$$q(1,\eta') = \frac{\eta'}{\eta_{cr}\eta'} S \tag{5.1.22}$$

$$g(1,\eta') = 1 - \frac{\eta'\eta_{cr} + S}{\gamma + 1} \tag{5.1.23}$$

$$f(1,\eta') = \frac{\gamma + \eta_{cr}\eta' + \gamma S}{\gamma(\gamma+1)} \tag{5.1.24}$$

$$S = \left[(1-\eta')(1-\eta_{cr}^2\eta') \right]^{\frac{1}{2}} \tag{5.1.25}$$

To reduce the above equations for the non-reacting case (i.e., $q = 0$) we simply take $\eta_{cr} = 1$.

In terms of η' instead of η, we note that the basic equations remain identical while the energy integral becomes

$$1 = y\left[\frac{I}{\eta'\eta_{cr}} - \frac{1}{j+1}\left(\frac{1}{\gamma(\gamma-1)} + q \right) \right] \tag{5.1.26}$$

and the shock radius - shock strength relationship stays in the same form.

5.2 Perturbation Solution in $\eta' = \eta/\eta_{cr}$

The flow field is bounded by the shock and the center of symmetry $0 \leq \xi \leq 1$ while $0 \leq \eta' \leq 1$. For early times, $\eta' \ll 1$ and we seek solutions to Eqs. 5.1.6 to 5.1.8 of the following form

$$
\phi(\xi, \eta') = \sum_{n=0}^{\infty} \phi_n(\xi) \eta'^{n} = \phi_0(\xi) + \phi_1(\xi)\eta' + \cdots
$$

$$
f(\xi, \eta') = \sum_{n=0}^{\infty} f_n(\xi) \eta'^{n} = f_0(\xi) + f_1(\xi)\eta' + \cdots
$$

$$
\psi(\xi, \eta') = \sum_{n=0}^{\infty} \psi_n(\xi) \eta'^{n} = \psi_0(\xi) + \psi_1(\xi)\eta' + \cdots
$$

(5.2.1)

From the energy integral (i.e., Eq. 5.1.26) we note that the left hand side is a constant equal to unity. Hence as $\eta' \to 0$, y must approach the form $y \to A\eta'$ as $\eta' \to 0$. Therefore the correct expansion for $y(\eta')$ is given as

$$
y(\eta') = \sum_{n=1}^{\infty} A_n \eta'^{n} = A_1 \eta' + A_2 \eta'^2 + A_3 \eta'^3 + \cdots
$$

(5.2.2)

Using the above equation and the definition of θ given by Eq. 5.1.9, we obtain the perturbation expression for $\theta(\eta')$ as

$$
\theta(\eta') = \sum_{n=1}^{\infty} \theta_n \eta'^{n} = \theta_0 + \theta_1 \eta' + \theta_2 \eta'^2 + \cdots
$$

(5.2.3)

where

$$
\theta_0 = -(j+1)/2
$$

(5.2.4)

$$
\theta_1 = \frac{(j+1)}{2} \frac{A_2}{A_1}
$$

(5.2.5)

$$
\theta_2 = (j+1)\left(\frac{A_3}{A_1} - \frac{A_2^2}{A_1^2} \right)
$$

(5.2.6)

$$
\theta_3 = \frac{(j+1)}{2}\left(4\left(\frac{A_2}{A_1}\right)^3 - \frac{7A_2 A_3}{A_1^2} + \frac{3A_4}{A_1} \right)
$$

(5.2.7)

The boundary conditions at the front $\xi = 1$ given by Eqs. 5.1.22 to 5.1.25 can readily be expanded in ascending power of η'. Substituting the perturbation expressions given by Eqs. 5.2.1, 5.2.2 and 5.2.3 into the basic conservation equations (i.e., Eqs. 5.1.6 to 5.1.8) the energy integral (i.e., Eq. 5.1.26) and expanding the boundary conditions given by Eqs. 5.1.22 to 5.1.25 in ascending powers of η', and sorting out the terms of the same powers in η', we get for:

Zeroth order in η'

(5.2.8)

$$(\phi_0 - \xi)\, u_0' + u_0\, \phi_0' = -j\, u_0\, \phi_0/\xi$$

$$(\phi_0 - \xi)\, \phi_0' + \frac{f_0'}{u_0} = -\theta_0\, \phi_0 \qquad (5.2.9)$$

$$(\phi_0 - \xi)\, f_0' + \gamma f_0\, \phi_0' = -\left(2\theta_0 f_0 + \gamma j f_0 \phi_0/\xi\right) \qquad (5.2.10)$$

$$A_1 = \frac{\eta_{CJ}}{I_0} \qquad (5.2.11)$$

$$I_0 = \int_0^1 \left(\frac{f_0}{\gamma-1} + \frac{\phi_0^2 u_0}{2}\right)\xi^j d\xi \qquad (5.2.12)$$

$$\theta_0 = -\frac{(j+1)}{2} \qquad (5.2.4)$$

and the boundary conditions at the shock front $\xi = 1$

$$u_0(1) = \frac{\gamma+1}{\gamma-1} \quad , \quad \phi_0(1) = f_0(1) = \frac{2}{\gamma+1} \qquad (5.2.13)$$

Note that the zeroth order equations and their boundary conditions are identical to the classical strong blast similarity solution given in the previous Chapter. For first order in η' we have

First Order in η'

$$(\phi_0 - \xi)\psi_1' + \psi_0\phi_1' = -[\psi_1(\phi_0' + j + 1) + \phi_1\psi_0' + j(\psi_0\phi_1 + \psi_1\phi_0)/\xi]$$

(5.2.14)

$$(\phi_0 - \xi)\phi_1' + \frac{1}{\psi_0}f_1' = -[\phi_1(\phi_0' - \theta_0) + \theta_1\phi_0 - \psi_1 f_0'/\psi_0^2]$$

(5.2.15)

$$(\phi_0 - \xi)f_1' + \gamma f_0\phi_1' = -[\gamma f_1\phi_0' + \phi_1 f_0' + 2\theta_1 f_0 + \gamma j(f_0\phi_1 + f_1\phi_0)/\xi]$$

(5.2.16)

$$A_2 = (\eta_{CJ}kA_1 - A_1 I_1)/I_0$$

(5.2.17)

where

$$k = \frac{1}{j+1}\left(\frac{1}{\gamma(\gamma-1)} + \frac{9}{8}\right)$$

(5.2.18)

$$I_1 = \int_0^1\left(\frac{f_1}{\gamma-1} + \frac{\psi_1\phi_0^2}{2} + \psi_0\phi_0\phi_1\right)\xi^j d\xi$$

(5.2.19)

$$\theta_1 = -\theta_0 A_2/A_1$$

(5.2.5)

With the boundary condition at $\xi = 1$ given as

$$\psi_1(1) = -\frac{(\gamma+1)}{2(\gamma-1)^2}(1 + \eta_{CT})^2$$

(5.2.20)

$$\phi_1(1) = -\frac{(1 + \eta_{CJ})^2}{2(\gamma + 1)} \tag{5.2.21}$$

$$f_1(1) = \frac{\left(\eta_{CJ} - \gamma\left(\frac{1 + \eta_{CJ}^2}{2}\right)\right)}{\gamma(\gamma + 1)} \tag{5.2.22}$$

Second Order in η'

$$(\phi_0 - \xi)\psi_2' + \psi_0\phi_2' = -\left[\psi_2(\phi_0' + 2(j+1)) + \psi_1\phi_1'\right. \tag{5.2.23}$$
$$+ \phi_1\psi_1' + \phi_2\psi_0' - 2\psi_1\theta_1$$
$$\left. + j(\psi_0\phi_2 + \psi_1\phi_1 + \psi_2\phi_0)/\xi\right]$$

$$(\phi_0 - \xi)\phi_2' + \frac{f_2'}{\psi_0} = -\left[\phi_2(\phi_0' + \frac{3}{2}(j+1)) + \phi_1\phi_1'\right. \tag{5.2.24}$$
$$- \theta_1\phi_1 + \theta_2\phi_0 - \psi_1 f_1'/\psi_0^2$$
$$\left. + f_0'\left(\frac{\psi_1^2}{\psi_0} - \psi_2\right)/\psi_0^2\right]$$

$$(\phi_0 - \xi)f_2' + \gamma f_0\phi_2' = -\left[f_2(\gamma\phi_0' + j + 1) + \gamma f_1\phi_1'\right. \tag{5.2.25}$$
$$+ \phi_1 f_1' + \phi_2 f_0' + 2\theta_2 f_0$$
$$\left. + \gamma j(f_0\phi_2 + f_1\phi_1 + f_2\phi_0)/\xi\right]$$

$$A_3 = \left(\eta_{CT} A_2 k - A_1 I_2 - A_2 I_1 \right) / I_0 \qquad (5.2.26)$$

$$I_2 = \int_0^1 \left(\frac{f_2}{\gamma-1} + \frac{\psi_2 \phi_0^2}{2} + \frac{\psi_0 \phi_1^2}{2} \right.$$

$$\left. + \psi_1 \phi_1 \phi_0 + \psi_0 \phi_0 \phi_2 \right) \xi^j d\xi \qquad (5.2.27)$$

$$\theta_2 = (j+1) \left(\frac{A_3}{A_1} - \left(\frac{A_2}{A_1} \right)^2 \right) \qquad (5.2.28)$$

with the following boundary conditions at the front $\xi = 1$

$$\psi_2(1) = \frac{\gamma+1}{8(\gamma-1)^3} \left(2(1+\eta_{CT})^4 \right. \qquad (5.2.29)$$

$$\left. -(\gamma-1)(1-\eta_{CT}^2)^2 \right)$$

$$\phi_2(1) = -\frac{(1-\eta_{CT}^2)^2}{8(\gamma+1)} \qquad (5.2.30)$$

$$f_2(1) = \phi_2(1) \qquad (5.2.31)$$

For the third order in η' we have

Third Order in η'

$$(\phi_0 - \xi)\psi_3' + \psi_0\phi_3' = -\Big[\psi_3(\phi_0' - 6\theta_0) + \psi_2(\phi_1' - 4\theta_1)$$

$$+ \psi_1(\phi_2' - 2\theta_2) + \phi_3\psi_0' + \phi_2\psi_1' \qquad (5.2.32)$$

$$+ \phi_1\psi_2' + j\big(\psi_0\phi_3 + \psi_1\phi_2$$

$$+ \psi_2\phi_1 + \psi_3\phi_0\big)/\xi\Big]$$

$$(\phi_0 - \xi)\phi_3' + \frac{1}{\psi_0}f_3' = -\Big[\phi_3(\phi_0' - 5\theta_0) + \phi_2(\phi_1' - 3\theta_1)$$

$$+ \phi_1(\phi_2' - \theta_2) + \theta_3\phi_0$$

$$-\frac{\psi_1 f_2'}{\psi_0^2} + \frac{f_1'}{\psi_0^2}\left(\frac{\psi_1^2}{\psi_0} - \psi_2\right) \qquad (5.2.33)$$

$$-\frac{f_0'}{\psi_0^2}\left(\frac{\psi_1^3}{\psi_0^2} - \frac{2\psi_1\psi_2}{\psi_0} + \psi_3\right)\Big]$$

$$(\phi_0 - \xi)f_3' + \gamma f_0\phi_3' = -\Big[f_3(\gamma\phi_0' - 4\theta_0) + f_2(\gamma\phi_1' - 2\theta_1)$$

$$+ \gamma f_1\phi_3' + 2\theta_3 f_0 + \phi_3 f_0' + \phi_2 f_1'$$

$$+ \phi_1 f_2' + \gamma j\big(f_0\phi_3 + f_1\phi_2 \qquad (5.2.34)$$

$$+ f_2\phi_1 + f_3\phi_0\big)/\xi\Big]$$

$$A_4 = (\eta_{cJ}A_3 k - A_1 I_3 - A_2 I_2 - A_3 I_1)/I_0 \qquad (5.2.35)$$

$$I_3 = \int_0^1 \left(\frac{f_3}{\gamma-1} + \mathcal{U}_1 \frac{\phi_1^2}{2} + \mathcal{U}_3 \frac{\phi_0'^2}{2} + \mathcal{U}_6 \phi_0 \phi_3 \right.$$
$$\left. + \mathcal{U}_0 \phi_1 \phi_2 + \mathcal{U}_1 \phi_0 \phi_2 + \mathcal{U}_2 \phi_0 \phi_1 \right) \xi^j d\xi \qquad (5.2.36)$$

$$\theta_3 = \frac{j+1}{2} \left(4 \left(\frac{A_2}{A_1} \right)^3 - \frac{7 A_2 A_3}{A_1^2} + \frac{3 A_4}{A_1} \right) \qquad (5.2.37)$$

with the following boundary conditions at the front $\xi = 1$

$$\mathcal{U}_3(1) = \frac{(\gamma+1)}{16(\gamma-1)^4} \left[-(\gamma-1)^2 (1-\eta_{cJ}^2)^2 (1+\eta_{cJ}^2) \qquad (5.2.38) \right.$$
$$+ 2(\gamma-1)(1+\eta_{cJ})^2 (1-\eta_{cJ}^2)^2$$
$$\left. - 2(1+\eta_{cJ})^6 \right]$$

$$(5.2.39)$$
$$\phi_3(1) = - \frac{(1-\eta_{cJ}^2)^2 (1+\eta_{cJ}^2)}{16(\gamma+1)}$$

$$f_3(1) = \phi_3(1) \qquad (5.2.40)$$

It should be noted that the present perturbation expressions are asymptotic in nature and do not converge. In fact very little is gained by taking higher orders in η' above the third order. In Sakurai's original work, the analysis has been carried out to first order in η' only and he termed it the second approximation with the classical similarity solution for strong blasts being the first approximation. In his work on hypersonic blunt body flows, Swigart extended the analysis to the third approximation (i.e., the second order solution in the present

work) and gave results for the particular case of cylindrical symmetry
(j = 1) in air (= 1.4) only. Swigart's work indicates that for shock
Mach Numbers below 3 , the third order correction, particularly for
the density, is a significant percentage of the first and second order
terms. It appears worthwhile to carry out the analysis to higher
orders as is done here to obtain better results for the density profiles.
However for quantities such as the shock trajectory, the higher order
solutions in fact overcorrects it and the second order solution gives the
best results.

To complete the solution, we shall derive the expression for the
shock trajectory. Using Eqs. 5.2.2 and 5.2.3 and the identity $\dot{R}_S = \dfrac{dR_s}{dt}$,
we can have the following equation for the shock trajectory

$$\frac{c_o t}{R_o} = B_1\, \eta'^{\frac{j+3}{2(j+1)}}\left(1 + B_2\,\eta' + B_3\,\eta'^2 + B_4\,\eta'^3 + \cdots\right)$$

where

$$B_1 = \frac{2\,\eta_{cJ}^{\frac{1}{2}}\,A_1^{\frac{1}{j+1}}}{j+3}$$

$$B_2 = \frac{A_2(j+2)(j+3)}{A_1(j+1)(3j+5)}$$

$$B_3 = \frac{(2j+3)(j+3)\left(\dfrac{A_3}{A_1} - j\,A_2^2/(2A_1^2(j+1))\right)}{(j+1)(5j+7)}$$

$$B_4 = \frac{(3j+4)(j+3)\left(\dfrac{A_4}{A_1} - \dfrac{j A_2 A_3}{A_1^2(j+1)} + \dfrac{j(2j+1)A_2^3}{A_1^3\,6(j+1)^2}\right)}{(j+1)(7j+9)}$$

and the A's are given previously by Eqs. 5.2.11, 5.2.17, 5.2.26 and 5.2.35.

From the zeroth order equation and its boundary conditions we see that the zeroth order solution is the classical constant energy solution of Taylor, Von-Neuman and Sedov discussed in the previous Chapter. To obtain the zeroth order solution numerically, Eqs. 5.2.8 to 5.2.10 are integrated with the conditions at $\xi = /$ given by Eq. 5.2.13 using the value of $\theta = -(\dot{}/\ddot{})$ From this solution $\bar{I}_o$ and $A_/$ can then be determined from Eqs. 5.2.12 and 5.2.11 respectively.

For the first and higher order solutions the equations cannot be integrated directly since θ_n is as yet unknown. An iteration procedure can be used to arrive at the correct solution using the condition of zero parti- cle velocity at the center of symmetry as a criterion (i.e., $\phi_n(o) = O$). For example, to obtain the first order solution, a trial value of A_2 is assumed and $\theta_/$ can be determined from Eq. 5.2.5. The first order differential equations are then integrated numerically with this value of $\theta_/$, and the boundary conditions given by Eqs. 5.2.20 to 5.2.22 at $\xi = /$. The correct solution will be obtained when the assumed value of A_2, hence $\theta_/$, gives a solution with the particle velocity at the center of symmetry equal to zero (i.e., $\phi_/(o) = O$). As a check, the new value of A_2 computed from the energy integral (i.e., Eqs. 5.2.17 and 5.2.19) using the solution obtained must also agree with the initial assumed value. It should be noted that either the zero particle velocity at $\xi = O$ criterion or the energy integral criterion (assumed value of A_2 satisfies Eqs. 5.2.17 and 5.2.19) alone is sufficient to determine the correct solution. However it was found that the particle velocity at the center of symmetry is by far more sensitive than the energy integral to very small variations in θ_n as θ_n approaches its correct value. Hence very high accuracies in the solutions can be obtained using the $\phi_n(o) = O$ criterion for the iteration.

We found that using the "regula-falsi" iteration scheme with an accuracy limit of $|A_n(\omega)| \leq 10^{-9}$, rapid convergence is obtained with double precision on the IBM 360. Numerical integration is by the Runge-Kutta method with a step size $\Delta \xi = .001$.

5.3 Perturbation Solution in $y = \left(\frac{R_s}{R_o}\right)^{j+1}$

The analysis given in the previous Section is based on the perturbation parameter η'. It should be noted that other parameters can be used as well and although they yield identical results since they must be related, the accuracy to the same order in the perturbation parameter should be based on this accuracy of the particular quantities desired. In this Section we give the analysis using the dimensionless shock radius $y = \left(R_s/R_o\right)^{j+1}$ as the perturbation parameter since initially $y << 1$.

Examining again the energy integral given by Eq. 5.1.11, we see that as $y \to 0$, $1/\eta$ must approach $\frac{F_o}{y}$. Hence the expansion for $\eta(y)$ must be of the following form

$$\eta(y) = \frac{y}{F_o + F_1 y + F_2 y^2 +} = \frac{y}{\sum_0 F_n y^n} \tag{5.3.1}$$

From the above equation, we can obtain the expansion for $\theta(y)$ as

$$\theta(y) = \sum_0^\infty \theta_n y^n = \theta_0 + \theta_1 y + \theta_2 y^2 + \cdots \tag{5.3.2}$$

where

$$\theta_0 = -\frac{(j+1)}{2} \tag{5.3.3}$$

$$\theta_1 = -\theta_0 F_1/F_o \tag{5.3.4}$$

$$\theta_2 = \theta_0 \left(\left(\frac{F_1}{F_o}\right)^2 - \frac{2F_2}{F_o} \right) \tag{5.3.5}$$

Using now y as the independent variable replacing η' , the basic conservations (i.e., Eqs. 5.1.6 to 5.1.9) become

$$(\phi - \xi)\frac{\partial u}{\partial \xi} + u\frac{\partial \phi}{\partial \xi} + j\frac{\phi u}{\xi} = -(j+1)y\frac{\partial u}{\partial y} \qquad (5.3.6)$$

$$(\phi - \xi)\frac{\partial \phi}{\partial \xi} + \theta\phi + \frac{1}{u}\frac{\partial f}{\partial \xi} = -(j+1)y\frac{\partial \phi}{\partial y} \qquad (5.3.7)$$

$$(\phi - \xi)\frac{\partial f}{\partial \xi} + \gamma f\frac{\partial \phi}{\partial \xi} + 2\theta f + \gamma j\frac{f\phi}{\xi} = -(j+1)y\frac{\partial f}{\partial y} \qquad (5.3.8)$$

Writing the solutions to the above equations in the following perturbation form

$$\phi(\xi,y) = \sum_{0}^{\infty} \phi_m(\xi)y^n = \phi_0(\xi) + \phi_1(\xi)y + \cdots$$

$$f(\xi,y) = \sum_{0}^{\infty} f_m(\xi)y^n = f_0(\xi) + f_1(\xi)y + \cdots \qquad (5.3.9)$$

$$u(\xi,y) = \sum_{0}^{\infty} u_m(\xi)y^n = u_0(\xi) + u_1(\xi)y + \cdots$$

and substituting them together with the perturbation for $\theta(y)$ given by Eq. 5.3.2 into the basic equations (i.e., 5.3.6 to 5.3.8) and the energy integral given by Eq. 5.1.11, we obtain after sorting out terms of the same order of magnitude in y the following equations.

Zeroth order in y

$$(\phi_0 - \xi)\psi_0' + \psi_0\phi_0' = -j\phi_0\psi_0/\xi \tag{5.3.10}$$

$$(\phi_0 - \xi)\phi_0' + \frac{1}{\psi_0}f_0' = -\theta_0\phi_0 \tag{5.3.11}$$

$$(\phi_0 - \xi)f_0' + \gamma f_0\phi_0' = -\left(2\theta_0 f_0 + \gamma j f_0\phi_0/\xi\right) \tag{5.3.12}$$

$$F_0 = 1/I_0 \tag{5.3.13}$$

$$I_0 = \int_0^1 \left(\frac{f_0}{\gamma-1} + \phi_0^2\frac{\psi_0}{2}\right)\xi^j d\xi \tag{5.3.14}$$

$$\theta_0 = -(j+1)/2 \tag{5.3.15}$$

First order in y

$$(\phi_0 - \xi)\psi_1' + \psi_0\phi_1' = -\left[\psi_1(\phi_1' - 2\theta_0) + \phi_1\psi_0' + j(\phi_0\psi_1 + \phi_1\psi_0)/\xi\right] \tag{5.3.16}$$

$$(\phi_0 - \xi)\phi_1' + \frac{1}{\psi_0}f_1' = -\left[\phi_1(\phi_0' - \theta_0) - \theta_1\phi_0 - \psi_1 f_0'/\psi_0^2\right] \tag{5.3.17}$$

$$(\phi_0 - \xi)f_1' + \gamma f_0\phi_1' = -\left[\gamma f_1\phi_0' + \phi_1 f_0' + 2\theta_1 f_0 + \gamma j(f_0\phi_1 + f_1\phi_0)/\xi\right] \tag{5.3.18}$$

$$F_1 = \left[\frac{1}{j+1}\left(\frac{1}{\gamma(\gamma-1)} + \frac{k}{2(j^2-1)}\right) - F_0 I_1\right]/I_0 \tag{5.3.19}$$

$$I_1 = \int_0^1 \left(\frac{f_1}{\gamma - 1} + \phi_0 \phi_1 u_0 + \phi_0^2 \frac{u_1}{2} \right) \xi^j d\xi \tag{5.3.20}$$

$$\theta_1 = -\phi_0 F_1 / F_0 \tag{5.3.21}$$

Second order in y

$$(\phi_0 - \xi) u_2' + u_0 \phi_2' = -\Big[u_2 (\phi_0' - 4\theta_0) + u_1 \phi_1' + \phi_1 u_1' $$
$$+ \phi_2 u_0' + j (\phi_0 u_2 + \phi_1 u_1 \tag{5.3.22}$$
$$+ \phi_2 u_0) / \xi \Big]$$

$$(\phi_0 - \xi) \phi_2' + \frac{1}{u_0} f_2' = -\Big[\phi_2 (\phi_0' - 3\theta_0) + \phi_1 (\phi_1' + \theta_1) $$
$$+ \theta_2 \phi_0 - u_1 f_1' / u_0^2 $$
$$+ f_0' (u_1^2 / u_0 - u_2) / u_0^2 \Big] \tag{5.3.23}$$

$$(\phi_0 - \xi) f_2' + \gamma f_0 \phi_2' = -\Big[f_2 (\gamma \phi_0' - 2\theta_0) + f_1 (\gamma \phi_1' + 2\theta_1) $$
$$+ 2\theta_2 f_0 + \phi_1 f_1' + \phi_2 f_0' $$
$$+ \gamma j (f_0 \phi_2 + f_1 \phi_1 + f_2 \phi_0) / \xi \Big] \tag{5.3.24}$$

$$F_2 = -(F_0 I_2 + F_1 I_1) / I_0 \tag{5.3.25}$$

$$I_2 = \int_0^1 \left(\frac{f_2}{\gamma-1} + \phi_0^2 \frac{u_2}{2} + \phi_1^2 \frac{u_0}{2} \right.$$
$$\left. + \phi_0 (\phi_1 u_1 + \phi_2 u_0) \right) \xi^j d\xi \qquad (5.3.26)$$

$$\theta_2 = \theta_0 \left(\left(\frac{F_1}{F_0}\right)^2 - \frac{2F_2}{F_0} \right) \qquad (5.3.27)$$

Using the perturbation expression for $\eta(y)$ given by Eq. 5.3.1, the boundary conditions can be expanded in powers of y and we get the following results corresponding to the different orders in y.

Zeroth order in y

$$u_0(1) = \frac{\gamma+1}{\gamma-1} \qquad (5.3.28)$$

$$\phi_0(1) = f_0(1) = \frac{2}{\gamma+1} \qquad (5.3.29)$$

First order in y

$$u_1(1) = -\frac{(\gamma+1)(k+4)}{2F_0(\gamma-1)^2} \qquad (5.3.30)$$

$$\phi_1(1) = -\frac{(k+4)}{2F_0(\gamma+1)} \qquad (5.3.31)$$

$$f_1(1) = -\frac{\left[2(\gamma-1) + \gamma k\right]}{2F_0 \gamma(\gamma+1)} \qquad (5.3.32)$$

Second order in y

$$\psi_2(1) = \frac{(\gamma+1)(k+4)}{2F_0^2(\gamma-1)^2}\left(F_1 + \frac{k+4}{2(\gamma-1)} - \frac{k}{4}\right) \qquad (5.3.33)$$

$$\phi_2(1) = \frac{(k+4)(4F_1 - k)}{8F_0^2(\gamma+1)} \qquad (5.3.34)$$

$$f_2(1) = \frac{8F_1(\gamma-1) - \gamma k(k+4 - 4F_1)}{8\gamma(\gamma+1)F_0^2} \qquad (5.3.35)$$

The zeroth order solution recovers the similarity strong blast solution. With the zeroth order solution known, I_0 hence F_0 can be determined. With F_0 known the first order boundary conditions can now be evaluated. Using an assumed value of θ_1 , the first order differential equation can be integrated and we iterate for the correct value of θ_1 , hence the solution, by demanding the rear boundary condition at the center (i.e., $\phi_1(0)=0$) to be satisfied as described in the preceding Section.

The expression for the shock trajectory can be determined in a manner identical to that for the case of using η' as the perturbation parameter in the preceeding Section. It can be written as

$$\frac{C_0 t}{R_0} = \frac{y^{\frac{j+3}{2}}}{\sqrt{F_0}} \left(\frac{2}{j+3} - \frac{F_1}{F_0} \frac{y}{(3j+5)} \right.$$

$$\left. + \left(\frac{3}{8}\left(\frac{F_1}{F_0}\right)^2 - \frac{F_2}{2F_0} \right) \cdot \frac{2y^2}{5j+7} \right)$$

(5.3.36)

5.4 Oshima's Quasi-Similar Method

In this Section, we shall discuss the quasi-similar or the local similarity method first used by Oshima in the study of cylindrical blast waves from exploding wires, generalized by Lewis to planar as well as spherical symmetry with applications to hypersonic blunt body flows and extended by Lee to detonating gases in the study of detonation initiation. The quasi-similar method was also used by Rae to investigate the material impact problem where departure from similarity arises from the equation state for solid media.

The basic conservation equation (i.e., Eqs. 5.1.6 to 5.1.8) in terms of ξ and $\eta' = \eta/\eta_{c\sigma}$ as independent variables are given as

$$(\phi - \xi) \frac{\partial \psi}{\partial \xi} + \psi \frac{\partial \phi}{\partial \xi} + j \frac{\phi \psi}{\xi} = 2 \theta \eta' \frac{\partial \psi}{\partial \eta'} \tag{5.4.1}$$

$$(\phi - \xi) \frac{\partial \phi}{\partial \xi} + \theta \phi + \frac{1}{\psi} \frac{\partial f}{\partial \xi} = 2 \theta \eta' \frac{\partial \phi}{\partial \eta'} \tag{5.4.2}$$

$$(\phi - \xi) \frac{\partial f}{\partial \xi} + \gamma f \frac{\partial \phi}{\partial \xi} + \gamma j \frac{f \phi}{\xi} + 2 \theta f = 2 \theta \eta' \frac{\partial f}{\partial \eta'} \tag{5.4.3}$$

From experimental observations, it was found that the density distribution ψ for nearly equal shock strengths have similar features. In other words, the solution for $\psi(\xi, \eta')$ in the narrow range of shock strength can be approximated by the form

$$\psi(\xi, \eta') = \psi_1(\xi) \cdot \psi_2(\eta') \tag{5.4.4}$$

Differentiating the above equation with respect to η' we get

$$\left(\frac{\partial \ln \psi}{\partial \eta'}\right)_{\xi} = \frac{\partial \ln \psi_2(\eta')}{\partial \eta'} = F(\eta') = \frac{\partial \ln \psi(1)}{\partial \eta'} \qquad (5.4.5)$$

Where $\psi(1)$ is the value at the front $\xi = 1$. Assuming quasi-similarity for the pressure and particle velocity distributions as well, we can write

$$\left(\frac{\partial \ln f}{\partial \eta'}\right)_{\xi} = \frac{\partial \ln f(1)}{\partial \eta'} \qquad (5.4.6)$$

$$\left(\frac{\partial \ln \phi}{\partial \eta'}\right)_{\xi} = \frac{\partial \ln \phi(1)}{\partial \eta'} \qquad (5.4.7)$$

Eqs. 5.4.5 to 5.4.6 are called the quasi-similar approximations. Using the boundary conditions given previously by Eqs. 5.1.22 to 5.1.25

$$\psi(1, \eta') = \frac{\gamma + 1}{\gamma + \eta_{CJ}\eta' - S} \qquad (5.1.22)$$

$$\phi(1, \eta') = \frac{1 - \eta_{CJ}\eta' + S}{\gamma + 1} \qquad (5.1.23)$$

$$f(1, \eta') = \frac{\gamma + \eta_{CJ}\eta' + \gamma S}{\gamma(\gamma + 1)} \qquad (5.1.24)$$

$$S = \left[(1-\eta')(1-\eta_{cJ}^2 \eta') \right]^{1/2} \qquad (5.1.25)$$

we can evaluate the derivatives and Eqs. 5.4.5 to 5.4.7 become

$$\frac{\partial \ln \mathcal{U}}{\partial \ln \eta'} = \frac{-\left[\eta' \eta_{cJ} + \frac{\eta'}{2S}\left(1 - \eta' \eta_{cJ}^2 + \eta_{cJ}^2 (1-\eta') \right) \right]}{(\gamma + \eta_{cJ}\eta' - S)} \qquad (5.4.8)$$

$$\frac{\partial \ln \phi}{\partial \ln \eta'} = \frac{-\left[\eta' \eta_{cJ} + \frac{\eta'}{2S}\left(1 - \eta' \eta_{cJ}^2 + \eta_{cJ}^2 (1-\eta') \right) \right]}{(1 - \eta' \eta_{cJ} + S)} \qquad (5.4.9)$$

$$\frac{\partial \ln f}{\partial \ln \eta'} = \frac{\left[\eta' \eta_{cJ} - \frac{\eta' \gamma}{2S}\left(1 - \eta' \eta_{cJ}^2 + \eta_{cJ}^2 (1-\eta') \right) \right]}{\gamma + \eta_{cJ}\eta' + \gamma S} \qquad (5.4.10)$$

For the non-reacting case where q = 0, $S = 1-\eta$ and $\eta_{cJ} = 1$, the above equations reduce to

$$\frac{\partial \ln \mathcal{U}}{\partial \ln \eta'} = \frac{-2\eta}{\gamma - 1 + 2\eta} \qquad (5.4.11)$$

$$\frac{\partial \ln \phi}{\partial \ln \eta} = \frac{-\eta}{1-\eta} \tag{5.4.12}$$

$$\frac{\partial \ln f}{\partial \ln \eta} = \frac{-\eta(\gamma-1)}{2\gamma - \eta(\gamma-1)} \tag{5.4.13}$$

which are identical to those obtained by Oshima.

Using the above equations for the derivatives of ϕ, f, ψ with respective to η, the non-similar equations given by Eqs. 5.4.1 to 5.4.3 become

$$(\phi-\xi)\psi' + \psi\phi' + j\phi\frac{\psi}{\xi} = \Lambda_1 \psi \tag{5.4.14}$$

$$(\phi-\xi)\phi' + \frac{j}{\psi} f' = \Lambda_2 \phi \tag{5.4.15}$$

$$(\phi-\xi)f' + \gamma f\phi' + \gamma j\frac{f\phi}{\xi} = \Lambda_3 f \tag{5.4.16}$$

where the prime quantities denote differentiation with respect to ξ and the Λ_S are defined as

$$\Lambda_1 = \frac{-2\theta\left[\eta'\eta_{cr} + \frac{\eta'}{2S}\left(1-\eta_{cr}^2\eta' + \eta_{cr}^2(1-\eta')\right)\right]}{\gamma + \eta_{cr}\eta' - S} \tag{5.4.17}$$

$$\Lambda_2 = -\theta \left\{ \frac{2\left[\eta'\eta_{cr} + \frac{\gamma'}{2S}\left(1 - \gamma'\eta_{cr}^2 + \eta_{cr}^2(1-\eta')\right)\right]}{1 - \gamma'\eta_{cr} + S} + 1 \right\} \quad (5.4.18)$$

$$\Lambda_3 = -2\theta \left\{ \frac{\eta'\eta_{cr} - \frac{\eta'}{2S}\left(1 - \gamma'\eta_{cr}^2 + \eta_{cr}^2(1-\eta')\right)}{\gamma + \gamma'\eta_{cr} + \gamma S} + 1 \right\} \quad (5.4.19)$$

Similarly the $\Lambda's$ for the non-reacting case can be written as follows using Eqs. 5.4.11 to 5.4.13 for the derivatives.

$$\Lambda_1 = \frac{-4\theta\eta}{\gamma - 1 + 2\eta} \quad (5.4.20)$$

$$\Lambda_2 = -\theta\left(\frac{2\eta}{1-\eta} + 1\right) \quad (5.4.21)$$

$$\Lambda_3 = -2\theta\left(\frac{(\gamma-1)\eta}{2\gamma - \eta(\gamma-1)} + 1\right) \quad (5.4.22)$$

Hence for any specified shock strength (i.e., the value of η'), Eqs. 5.4.14 to 5.4.16 become a set of ordinary differential equations. Assuming a value of θ, these equations can be integrated numerically using

the boundary conditions at the front $\xi = 1$ computed from Eqs. 5.1.22 to
5.1.25. An iteration procedure is necessary for arriving at the correct
solution which satisfies the rear boundary conditions at the center of
symmetry (i.e., $\phi(o) = 0$).

It will be shown later that the quasi-similar approximation
yields solutions that do not conserve the total mass enclosed by the
front (i.e., the mass integral). Therefore the profiles themselves are
in error and iterating for the correct solution using the boundary
condition of zero particle velocity at the center in this case is quite
inaccurate for certain values of η'. It was found that using the
energy integral criterion for determining the correct solution (i.e.,
demanding that the solution satisfies the energy integral) yields better
results.

An expression for θ can be obtained by differentiating the
energy integral (i.e., Eq. 5.1.25) with respect to η'. Using Eq. 5.1.15
and solving for θ , we get

$$\theta = -(\tfrac{j+1}{2})\left(1 - \frac{C\eta'}{I}\right)\Big/\left(1 - \frac{\eta'}{I}\frac{dI}{d\eta'}\right) \qquad (5.4.23)$$

$$C = \frac{1}{j+1}\left(\frac{1}{\gamma(\gamma-1)} + g\right) \qquad (5.4.24)$$

$$I = \int_0^1 \left(\frac{f}{\gamma-1} + \frac{\phi^2 \gamma}{2}\right)\xi^j d\xi \qquad (5.4.25)$$

It should be noted that the quasi-similar approximation cannot be applied
to functions which consist of the sum of two other functions (e.g.,

$I(\eta') = I_1(\eta') + I_2(\eta'))$. However it can be applied to fur ions consisting of the products of other functions (i.e., $F(\eta') = F_1(\eta') \cdot F_2(\eta')$). Therefore to use the quasi-similar approximation to evaluate $dI/d\eta'$, we must first write

$$\frac{\eta'}{I} \frac{dI}{d\eta'} = \frac{\eta'}{I}\left(\frac{dI_1}{d\eta'} + \frac{dI_2}{d\eta'}\right) \tag{5.4.26}$$

where

$$I_1 = \int_o^1 \frac{f}{\gamma-1} \xi^j d\xi \tag{5.4.27}$$

$$I_2 = \int_o^1 \frac{u\phi^2}{2} \xi^j d\xi \tag{5.4.28}$$

Using Eqs. 5.4.5 to 5.4.7 and Eqs. 5.4.8 to 5.4.10, Eq. 5.4.26 becomes

$$\frac{\eta'}{I} \frac{dI}{d\eta'} = \frac{1}{I}\left(G_1(\eta')\int_o^1 \frac{f}{\gamma-1} \xi^j d\xi + G_2(\eta')\int_o^1 \frac{u\phi^2}{2}\xi^j d\xi\right) \tag{5.4.29}$$

where

$$G_1(\eta') = \frac{\eta'\eta_{cr} - \frac{\gamma\eta'}{2S}\left(1-\eta'\eta_{cr}^2 + \eta_{cr}^2(1-\eta')\right)}{\gamma + \eta'\eta_{cr} + \gamma S} \tag{5.4.30}$$

$$G_2(\eta') = -\left(\eta'\eta_{cr} + \frac{\eta'}{2S}\left[1-\eta'\eta_{cr}^2 + \eta_{cr}^2(1-\eta')\right]\right) \cdot \tag{5.4.31}$$

$$\cdot \left(\frac{1}{\gamma+\eta'\eta_{cr}-S} + \frac{1}{\gamma+\eta'\eta_{cr}+\gamma S}\right)$$

For the non-reacting case, $G_1(\eta')$ and $G_2(\eta')$ reduce to the following

$$G_1(\eta) = \frac{-(\gamma-1)\eta}{2\gamma-(\gamma-1)\eta} \qquad (5.4.32)$$

$$G_2(\eta) = -2\eta\left(\frac{1}{\gamma-1+2\eta} + \frac{1}{2\gamma-(\gamma-1)\eta}\right) \qquad (5.4.33)$$

We can use Eq. 5.4.31 to iterate for the correct solution as follows:
We again assume a value for θ and integrating the basic equations we can
determine the integrals I, I_1 and I_2. From Eq. 5.4.31, we can compute a
new value of θ based on the solutions obtained from the assumed value of
θ . We then iterate until the two values of θ are matched to a desired
accuracy.

We can obtain the first integral of the quasi-similar equations by
an identical manner as described previously in Section 2.5 for the similarity
equations. Multiplying the continuity equation (i.e., Eq. 5.4.1) by
$\left[(\phi-\xi)\psi\right]^{-1}$ and the energy equation (i.e., Eq. 5.4.3) by $\left[(\phi-\xi)f\right]^{-1}$
and rearranging the results, we get the following pair of equations

$$\frac{\psi'}{\psi} + \frac{(\phi-\xi)'}{\phi-\xi} + \frac{j+1-\Lambda_1}{\phi-\xi} + \frac{j}{\xi} = 0 \qquad (5.4.34)$$

$$\frac{f'}{f} + \frac{\gamma(\phi-\xi)'}{\phi-\xi} + \frac{\gamma(j+1)-\Lambda_3}{\phi-\xi} + \frac{\gamma j}{\xi} = 0 \qquad (5.4.35)$$

Eliminating the $\phi - \xi$ term in the above equations we get

$$\chi_2 \frac{f'}{f} - \chi_1 \frac{\psi'}{\psi} + (\gamma\chi_2 - \chi_1)\frac{(\phi-\xi)'}{\phi-\xi} + (\gamma j \chi_2 - j\chi_1)\frac{1}{\xi} = 0 \qquad (5.4.36)$$

which can be integrated immediately to yield

$$\frac{f^{\chi_2}(\phi-\xi)^{\gamma\chi_2-\chi_1} \xi^{j(\gamma\chi_2-\chi_1)}}{\psi^{\chi_1}} = K_1(\eta') \qquad (5.4.37)$$

where

$$\chi_1 = \gamma(j+1) - \Lambda_3 \qquad (5.4.38)$$

$$\chi_2 = j+1 - \Lambda_1 \qquad (5.4.39)$$

and the Λ's are given previously by Eqs. 5.4.17 to 5.4.19. Eq. 5.4.37 can be arranged in a more convenient form as

$$\psi^\gamma \left[\psi(\xi-\phi)\xi j \right]^\delta = k_2(\eta') f \qquad (5.4.40)$$

where

$$\delta = -(\gamma\chi_2 - \chi_1)/\chi_2 = \frac{\gamma\Lambda_1 - \Lambda_3}{j+1 - \Lambda_1} \qquad (5.4.41)$$

and k_2 evaluated using the boundary conditions at the front $\xi = 1$ is given as

$$k_2(\eta') = \left(\frac{\gamma+1}{\gamma + \eta'\eta_{cr} - S} \right)^\gamma \frac{\gamma(\gamma+1)}{\gamma + \eta'\eta_{cr} + \gamma S} \qquad (5.4.42)$$

For the non-reacting case, the first integral reduces to

$$\psi^\gamma \left[\psi(\xi-\phi)\xi j \right]^{\frac{4\theta\gamma\left(\frac{1}{2\gamma-(\gamma-1)\eta} - \frac{\eta}{\gamma-1+2\eta}\right)}{j+1 + \frac{4\theta\gamma}{\gamma-1+2\eta}}}$$

$$= \left(\frac{\gamma+1}{\gamma-1+2\eta} \right)^\gamma \frac{\gamma(\gamma+1)}{2\gamma-(\gamma-1)\eta} f \qquad (5.4.43)$$

An alternate method for obtaining the solution was proposed by
Oshima in a later paper at the Second Conference on Exploding Wire Phenomena*
utilizing the first integral. Following Oshima, we introduce two new
variables

$$J = \xi - \phi \tag{5.4.44}$$

$$k = 1 - (\xi - \phi)^2 \frac{\psi}{\gamma f} \tag{5.4.45}$$

From the quasi-similar equations of momentum and energy we get

$$\phi' = \frac{\phi(\phi-\xi)\Lambda_2 - \frac{f}{\psi}(\Lambda_3 - \gamma j \phi/\xi)}{(\phi-\xi)^2 - \frac{\gamma f}{\psi}} \tag{5.4.46}$$

Using the definition of the variables given by Eqs. 5.4.44 and 5.4.45
Eq. 5.4.46 can be transformed to the following

$$\frac{dJ}{d\xi} = A + \frac{1}{k}\left(B - j\frac{J}{\xi}\right) + \frac{C\xi}{J}\left(1 - \frac{1}{k}\right) \tag{5.4.47}$$

where
$$A = 1 - \Lambda_2 \tag{5.4.48}$$

$$B = \Lambda_2 - \frac{\Lambda_3}{\gamma} + j \tag{5.4.49}$$

$$C = \Lambda_2 \tag{5.4.50}$$

* Readers should be careful in using the equations given in this paper for
it contains a tremendous amount of errors probably due to misprints.

From the quasi-similar equations of continuity and energy we get the following pair of equations:

$$\frac{\psi'}{\psi} = \frac{1}{\phi - \xi}\left(\Lambda_1 - \phi' - j\frac{\phi}{\xi}\right)$$ (5.4.51)

$$\frac{f'}{f} = \frac{1}{\phi \cdot \xi}\left(\Lambda_3 - \gamma\phi' - \gamma j\frac{\phi}{\xi}\right)$$ (5.4.52)

Using Eqs. 5.4.44, 5.4.45, 5.4.51 and 5.4.52, we obtain

$$\frac{dk}{d\xi} = \frac{1-k}{J}\left[D - (\gamma+1)\frac{dJ}{d\xi} - j(\gamma+1)\frac{J}{\xi}\right]$$ (5.4.53)

where
$$D = j(\gamma-1) + \Lambda_1 - \Lambda_3$$ (5.4.54)

The $\Lambda's$ in Eqs. 5.4.48 to 5.4.50 and 5.4.54 are given previously by Eqs. 5.4.17 to 5.4.19 for the reacting case ($\mathcal{Q} \neq 0$) and by Eqs. 5.4.20 to 5.4.22 for the non-reacting case ($\mathcal{Q} = 0$). For the non-reacting case, the coefficients A, B, C and D can be written as

$$A = 1 + \frac{(1+\eta)\theta}{1-\eta}$$ (5.4.55)

$$B = \left[\frac{-(1+\eta)}{1-\eta} + \frac{4}{2\gamma-\eta(\gamma-1)}\right]\theta + j$$ (5.4.56)

$$C = -\frac{(1+\eta)\theta}{1-\eta} \qquad (5.4.57)$$

$$D = j(\gamma-1) + \theta\left[\frac{4\gamma}{2\gamma-(\gamma-1)\eta} - \frac{4\eta}{\gamma-1+2\eta}\right] \qquad (5.4.58)$$

The boundary conditions for the new variables at the front $\xi = 1$ and the center of symmetry $\xi = 0$ can readily be obtained from the Rankine-Hugoniot relationships given by Eqs. 5.1.22 to 5.1.24 as

$$J(1) = \frac{\gamma + \eta_{CJ}\eta' - S}{\gamma + 1} \qquad (5.4.59)$$

$$K(1) = \frac{\delta(\gamma+1)}{\gamma + \eta'\eta_{CJ} + \gamma S} \qquad (5.4.60)$$

$$J(0) = 0 \qquad (5.4.61)$$

$$K(0) = 1 \qquad (5.4.62)$$

For the non-reacting case Eqs. 5.4.59 and 5.4.60 reduce to

$$J(1) = \frac{\gamma-1+2\eta}{\gamma+1} \qquad (5.4.63)$$

$$K(1) = \frac{(\gamma+1)(1-\eta)}{2\gamma-(\gamma-1)\eta} \qquad (5.4.64)$$

For every specified value of η' , the boundary conditions at the front can be determined from Eqs. 5.4.59 and 5.4.60 (or Eqs. 5.4.63 and 5.4.64 for the non-reacting case). Assuming an arbitrary value of θ , Eqs. 5.4.47 and 5.4.53 can be integrated and we iterate for θ until a solution satisfying the boundary conditions at the center of symmetry given by Eqs. 5.4.61 and 5.4.62 has been obtained. Once a solution for $J(\xi)$ and $k(\xi)$ has been determined, Eqs. 5.4.44, 5.4.45 and the first integral (i.e., Eq. 5.4.37) can be used to recover the original variables ϕ , f and ψ .

Examining the numerical solution for $J(\xi)$ led Oshima to suggest the following approximate form,

$$J(\xi) = \alpha\xi + \beta\xi^{n} \tag{5.4.65}$$

Substituting the above equation into Eq. 5.4.46 and using the boundary conditions given by Eqs. 5.4.59 and 5.4.61, the coefficients α and β and the exponent n can be determined as

$$\alpha = \frac{A+B}{j+1} \tag{5.4.66}$$

$$\beta = J(1) - \alpha \tag{5.4.67}$$

$$n = \left(\frac{dJ(1)}{d\xi} - \alpha\right)/\beta \tag{5.4.68}$$

Where A, B, J(1) are given by Eqs. 5.4.48, 5.4.49 and 5.4.59 respectively and $dJ(1)/d\xi$ can be evaluated using Eq. 5.4.47 and the Rankine-Hugoniot

equations at the front.

Substituting Eq. 5.4.65 into the differential equation for k (i.e., Eq. 5.4.53) and integrating, we get the solution for $k(\xi)$ as

$$K(\xi) = 1 - (1 - K(1)) \left(\frac{J(\xi)}{J(1)} \right)^{\gamma + 1 + \frac{D}{\alpha(n-1)}} \cdot \xi^{j(\gamma-1) - \frac{nD}{\alpha(n-1)}} \qquad (5.4.69)$$

where $K(1)$ is given by Eq. 5.4.60 and D by Eq. 5.4.58. Using Eqs. 5.4.51 and 5.4.52 we can obtain the solution for $\psi(\xi)$ and $f(\xi)$ as

$$\psi(\xi) = \psi(1) \left(\frac{J(\xi)}{J(1)} \right)^{\frac{\Lambda_1 - (\gamma+1)}{\alpha(n-1)}} \cdot \xi^{\frac{-n(\Lambda_1 - (\gamma+1))}{\alpha(n-1)} - j}$$

$$(5.4.70)$$

$$f(\xi) = f(1) \left(\frac{J(\xi)}{J(1)} \right)^{\frac{\Lambda_3 - \gamma(j+1)}{\alpha(n-1)}} \cdot \xi^{\frac{-n(\Lambda_3 - \gamma(j+1))}{\alpha(n-1)} - \gamma j}$$

$$(5.4.71)$$

Once the solution $\phi(\xi)$, $\psi(\xi)$ and $f(\xi)$ are determined, the integral I given by Eq. 5.1.12 can be evaluated and from the energy integral the dimensionless shock radius $y = (R_s / R_0)^{j+1}$ can be determined. With $y(\eta')$ known, the shock trajectory can readily be determined from the relationship

$$\frac{c_0 t}{R_0} = \int_0^y \frac{\eta^i \, dy}{(j+1) y^{j/(j+1)}} \qquad (5.4.72)$$

As pointed out earlier, the quasi-similarity approximation yields results that do not conserve the total mass enclosed by the shock front. Although quite good results can be obtained for quantities such as the shock trajectory since the total energy is conserved (i.e., energy integral satisfied), the distributions, particularly the particle paths can be in considerable error. To demonstrate this, we multiply the

quasi-similar continuity equation (i.e., Eq. 5.4.14) by $\xi^{\dot{J}}$ and rearranging
we get the following result

$$
\frac{d}{d\xi}\left[\Psi\xi^j(\phi-\xi)\right] + \Psi\xi^j\left[j+1-\Lambda_1\right] = 0 \tag{5.4.73}
$$

and integrating the above equation yields

$$
\int_0^1 \Psi\xi^j d\xi = \frac{-\Psi(1)(\phi(1)-1)}{j+1-\Lambda_1} \tag{5.4.74}
$$

where $\Psi(1)$ and $\phi(1)$ are the density and the particle velocity at the
front $\xi=1$ given by Eqs. 5.1.22 and 5.1.23 respectively. From the
relationship of mass conservation across the shock,

$$
\rho_0 \dot{R}_s = \rho_1(\dot{R}_s - u_1)
$$

$$
1 = \frac{1}{\Psi(1)}(1-\phi(1))
$$

or
$$
\frac{1}{\Psi(1)}(1-\phi(1)) = -1
$$

Eq. 5.4.74 becomes

$$
\int_0^1 \Psi\xi^j d\xi = \frac{\Psi^2(1)}{j+1-\Lambda_1} \tag{5.4.75}
$$

For mass to be conserved we see that the mass integral derived previously,
in Section 2.3

$$
\int_0^1 \Psi\xi^j d\xi = \frac{1}{j+1} \tag{5.4.76}
$$

must be satisfied. Comparing the quasi-similar mass integral (i.e.,

5.4.75) with Eq. 5.4.76, we note that the magnitude of the error depends on Λ_1. As pointed out by Rae, for spherical blast in air at a shock strength $\eta = 1/4$ (i.e., $M_s \simeq 2$), the error based on the results computed by Lewis is found to be as much as 50 percent.

It should be noted that unlike the perturbation solution, the quasi-similar solutions satisfy the boundary conditions at the front exactly and yield also a good estimate of the slope of the various fluid properties at the shock. For blast waves the mass is concentrated near the front except for very low shock Mach Numbers, therefore the quasi-similar approximation gives good prediction for quantities, such as the shock trajectory, that depend on integrated values of the solution in spite of the fact that the distributions themselves are in considerable error further downstream of the shock. For the moderate shock strength regime where the quasi-similar approximation is good, the distributions behave properly except in the region very close to the center of symmetry.

5.5   The Method of Porzel

A rather powerful method for obtaining analytical non-similar solutions to the blast wave problem can be developed based on the power law density profile approximation first suggested by Porzel. It was proposed originally by Porzel to account for departure from ideal-gas behavior in nuclear explosions and later adapted by Zaker to obtain non-similar solutions for strong point explosions in solids. The essence of Porzel's method is to assume the density profile behind the strong spherical blast wave to be of the form

$$\rho = \rho_1 \left(\frac{r}{R_S}\right)^{\beta} \tag{5.5.1}$$

where ρ_1 is the density at the shock and the exponent is time dependent and can be related to the density ratio using the conservation of total mass (i.e., mass integral) as

$$\beta = 3\left(\frac{\rho_1}{\rho_0} - 1\right) \tag{5.5.2}$$

From the continuity and momentum equation the particle velocity and the pressure profile are determined as

$$u = u_1 r/R_S \tag{5.5.3}$$

$$p = p_1 \left(\frac{r}{R_S}\right)^{\beta + 2} \tag{5.5.4}$$

The shock trajectory is determined from an energy balance equation using the so called waste heat concept.

Rae extended Porzel and Zaker's works and derived the various distributions behind the shock in a general form valid for finite shock

strengths. He also pointed out the important fact that if the equation
of state is specified, the internal energy distribution can be obtained
from it directly without using the waste heat concept to account for the
available and the unavailable portions of the shock energy for useful
work. With the internal energy distribution known, the energy integral
can be used to obtain the variation of shock strength with shock radius
and also the shock trajectory. Following Rae, Lee further extended the
analysis and applied it to the problem of blast wave propagation in a
detonating gas to account for non-similar effects arising from counter-
pressure and energy released by chemical reactions. Porzel's method was
also later applied by Bach and Lee to account for non-similar effects
arising from the equation of state in their study of shock propagation
in solid media.

It should be noted that a similar attempt has been made by
Sakurai to obtain an analytical solution valid for the entire propaga-
tion regime of blast waves in a perfect gas. In Sakurai's work, a
linear velocity profile (i.e., Eq. 5.5.3) was first assumed. To obtain
the density profile, it was necessary to further assume that the
derivative of the density with respect to the Shock Mach Number in
the continuity equation can be neglected. This assumption is true only
for relatively strong shocks and considerable errors are involved in the
low shock Mach Numbers regime. The rest of Sakurai's analysis is similar
to ours and the energy integral is used to determine the shock trajectory.

The essential steps in the following analysis on Porzel's
method is to assume a power law density profile behind the blast wave
the exponent of which is determined from the mass integral. This then
enables the particle velocity profile to be obtained from the differential
equations of mass conservation. With the forms for the density and
particle velocity profiles known the momentum equation can be integrated

to determine the pressure profile. Substituting these profiles into the energy integral then yields a first order differential equation for the dependence of the parameter $\theta(\eta')$ on the shock strength. The integration of this equation then completes the solution of the problem.

Writing down again the non-similar equations, the energy integral and the boundary conditions as given previously in Section 5.4, we have for the basic conservation equations

$$(\phi - \xi)\frac{\partial \psi}{\partial \xi} + \psi\frac{\partial \phi}{\partial \xi} + j\frac{\phi\psi}{\xi} = 2\theta\eta'\frac{\partial \psi}{\partial \eta'} \qquad (5.4.1)$$

$$(\phi - \xi)\frac{\partial \phi}{\partial \xi} + \theta\phi + \frac{1}{\psi}\frac{\partial f}{\partial \xi} = 2\theta\eta'\frac{\partial \phi}{\partial \eta'} \qquad (5.4.2)$$

$$(\phi - \xi)\frac{\partial f}{\partial \xi} + \gamma f\frac{\partial \phi}{\partial \xi} + 2\theta f + \gamma j\frac{f\phi}{\xi} = 2\theta\eta'\frac{\partial f}{\partial \eta'}, \qquad (5.4.3)$$

the energy integral given as

$$1 = y\left[\frac{I}{\eta_{cr}\eta'} - \frac{1}{j+1}\left(\frac{1}{\gamma(\gamma-1)} + \theta\right)\right], \qquad (5.1.26)$$

and the boundary conditions at the front $\xi = 1$ given by the following equations

$$\psi(1,\eta') = \frac{\gamma+1}{\gamma + \eta_{cr}\eta' - S} \qquad (5.1.22)$$

$$\phi(1,\eta') = \frac{1 - \eta_{cr}\eta' + S}{\gamma + 1} \qquad (5.1.23)$$

$$f(1,\eta') = \frac{\gamma + \eta_{cr}\eta' + \gamma S}{\gamma(\gamma + 1)} \qquad (5.1.24)$$

$$S = \left[(1-\eta')(1-\eta_{cr}^2\eta')\right]^{1/2} \qquad (5.1.25)$$

On examining the basic equations, it can be seen that the continuity equation (i.e., Eq. 5.4.1) contains only two dependent variables, the density ψ and the particle velocity ϕ . Hence by assuming the solution for one of them the other can be obtained by solving the continuity equation. In Sakurai's analysis, the particle velocity profile was assumed instead of the density, hence the solution of the continuity equation for the density ψ requires a further approximation that the term $2\Theta\eta'\frac{\partial\psi}{\partial\eta'}$ is small. However this term is of the same order of magnitude as the other terms in Eq. 5.4.1 for low shock strengths. Hence the results of Sakurai become increasingly inaccurate as $\eta' \to 1$. If the density profile is assumed, then Eq. 5.4.1 reduces to a first order linear ordinary differential equation which can be solved immediately for the particle velocity profile ϕ without further approximations. Following Porzel and Rae we assumed the density profile to be of the form

$$\psi(\xi,\eta') = \psi(1,\eta')\xi^{a(\eta')} \qquad (5.5.5)$$

Using the solution for $\psi(\xi,\eta')$ given above, the exponent $a(\eta')$ can be
determined from the mass integral (i.e., Eq. 5.4.70) as

$$a(\eta') = (j+1)(\psi(1,\eta') - 1) \tag{5.5.6}$$

Note that for the spherical case, Eq. 5.5.6 reduces to the form used
originally by Porzel (i.e., Eq. 5.5.2). From Eqs. 5.5.5 and 5.5.6, we
see that the density profile is completely specified for every local
shock Mach Number.

      With the density profile known, its derivatives with respect
to ξ and η' can readily be evaluated. Substituting these into Eq.
5.4.1, we obtain the following differential equation for ϕ :

$$\frac{\partial \phi}{\partial \xi} + (a+j)\frac{\phi}{\xi} = a + \frac{2\theta\eta}{\psi(1,\eta')}\left(1+(j+1)\psi(1,\eta')\ln\xi\right).$$

$$\cdot \frac{d\psi(1,\eta')}{d\eta'} \tag{5.5.7}$$

Solving Eq. 5.5.7 subject to the boundary condition that $\phi(0,\eta') = 0$,
we get the following result

$$\phi(\xi,\eta') = \phi(1,\eta')\xi(1 - \textcircled{H}\ln\xi) \tag{5.5.8}$$

where

$$\textcircled{H} = \frac{-2\theta\eta'}{\phi(1,\eta')\psi(1,\eta')}\frac{d\psi(1,\eta')}{d\eta'} \tag{5.5.9}$$

From Eq. 5.5.8, we see that unlike the density profile which is completely
specified for any local shock Mach Number, the particle velocity profile
cannot be explicitly determined since it contains the parameter $\theta(\eta')$
which is as yet unknown. In Sakurai's analysis, the velocity profile
is considered to be linear hence the term $\textcircled{H}$ is neglected. Under this
approximation the particle velocity profile becomes

$$\phi(\xi, \eta') = \phi(1, \eta') \xi \tag{5.5.10}$$

which is also completely determined for any specified value of η' . The present exact form given by Eq. 5.5.8 reduces to the linear form given by Eq. 5.5.10 in the strong shock limit (i.e., $\eta' \to 0$).

Substituting the density and the particle velocity profiles given by Eqs. 5.5.5 and 5.5.8 into the momentum equation (i.e., Eq. 5.4.2) we obtain

$$f(\xi, \eta') = -\int \left[\left[-2\theta\eta'\xi \left(\frac{d\phi(1,\eta')}{d\eta'} - \frac{d}{d\eta'} \left(\phi(1,\eta') \Theta \right) \ln \xi \right) \right. \right.$$

$$\left. + (\phi - \xi)\phi(1,\eta')\left(1 - \Theta - \Theta \ln \xi \right) + \theta\phi \right].$$

$$\left. \cdot \psi(1,\eta') \xi^{a(\eta')} d\xi \right] \qquad + C(\eta').$$

$$\tag{5.5.11}$$

The above equation can be integrated directly and to evaluate the constant of integration $C(\eta')$, we use the boundary conditions at the front for $f(1,\eta')$ given by Eq. 5.1.24. After some algebraic manipulations, the pressure distribution $f(\xi, \eta')$ can be written as

$$f(\xi, \eta') = f(1, \eta') + f_2(\xi^{a+2} - 1)$$

$$+ f_3\left(\xi^{a+2}\left[(a+2)\ln\xi - 1\right] + 1\right)$$

$$+ f_4\left(2 - \xi^{a+2}\left[(a+2)^2 \ln^2\xi - 2(a+2)\ln\xi + 2\right]\right)$$

$$(5.5.12)$$

where

$$f(1, \eta') = \frac{\gamma + \eta_{c\tau}\eta' + \gamma S}{\gamma(\gamma+1)}$$

$$f_2 = \frac{\mathcal{U}(1,\eta')}{(a+2)}\left[(1-\Theta)\left(\phi(1,\eta') - \phi^2(1,\eta')\right)\right.$$

$$\left. -\theta\left(\phi(1,\eta') - 2\eta'\frac{d\phi(1,\eta')}{d\eta'}\right)\right] \qquad (5.5.13)$$

$$f_3 = \frac{\mathcal{U}(1,\eta')}{(a+2)^2}\left[\theta\left(\Theta\phi(1,\eta') - 2\eta'\frac{d}{d\eta'}\left(\Theta\phi(1,\eta')\right)\right)\right.$$

$$\left. -\Theta\phi(1,\eta') - \Theta^2\phi^2(1,\eta') + 2\Theta\phi^2(1,\eta')\right] \qquad (5.5.14)$$

$$f_4 = \frac{\Theta^2\phi^2(1,\eta')\mathcal{U}(1,\eta')}{(a+2)^3} \qquad (5.5.15)$$

In the strong shock limit when $\eta' \to 0$, the pressure profile simplifies to the following form

$$f(\xi, 0) = f(1, 0) + \frac{\psi(1, 0) \phi(1, 0)}{(a+2)} \left(\xi^{a+2} - 1 \right) \cdot$$

$$\cdot \left(1 - \phi(1, 0) - \Theta(0) \right)$$

(5.5.16)

where $f(1, 0)$, $\psi(1, 0)$ and $\phi(1, 0)$ are the conditions at the shock in the limit $\eta' \to 0$ which can be written as

$$\psi(1, 0) = \frac{\gamma + 1}{\gamma - 1} \quad , \quad f(1, 0) = \phi(1, 0) = \frac{2}{\gamma + 1}$$

(5.5.17)

Eq. 5.5.16 for the pressure profile is identical to that given by Sakurai. Summarizing, we see that in Sakurai's analysis, the profiles are always assumed to take on the simplified form valid only in the limit of strong shock as $\eta' \to 0$. However these limiting forms were used to consider the propagation regime where the shock strength is finite. Hence in the weak shock regime, Sakurai's approximate solution becomes quite inaccurate.

From Eq. 5.5.12 to 5.5.15, we note that the pressure profile requires not only the value of $\Theta(\eta')$ but also its first derivative to be known before it can be evaluated.

To complete the solution, the functional relationship between Θ and η' must be determined. Substituting the density, particle velocity and the pressure profiles (i.e., Eqs. 5.5.5, 5.5.8 and 5.5.12) into the energy integral (i.e., Eq. 5.1.26) and solving for , we obtain the following equation

$$\frac{d\Theta}{d\eta'} = F(\Theta, \eta')$$

(5.5.18)

where $F(\theta, \eta')$ is given as

$$F(\theta,\eta') = \left[-\frac{1}{2\eta'} + \frac{\phi(1,\eta')}{2\eta'}(2+(j+1)(\gamma-1)) + \frac{(a+j+3)}{\eta'\psi(1,\eta')} \right.$$

$$\left. - \frac{(a+j+3)\phi(1,\eta')\psi(1,\eta')}{4\eta'^2\psi'(1,\eta')} \right]$$

$$+ \theta\left[\frac{2+(j+1)(\gamma-1)}{a+j+3}\frac{\psi'(1,\eta')}{\psi(1,\eta')} - \frac{1}{2\eta'} + \frac{\psi'(1,\eta')}{\psi(1,\eta')} - \left(\frac{\psi'(1,\eta')}{\psi(1,\eta')}\right)'\frac{\psi(1,\eta')}{\psi'(1,\eta')} \right]$$

$$+ \frac{1}{\theta}\left[\frac{(a+j+3)^2}{4\eta'^2\psi'(1,\eta')}\left((\gamma-1)g\eta'\eta_{cJ} - \phi(1,\eta') \right) \right.$$

$$\left. + \frac{(a+j+3)\phi(1,\eta')}{4\eta'^2\psi(1,\eta')} - \frac{(a+j+3)(j+1)(\gamma-1)\phi^2(1,\eta')\psi(1,\eta')}{8\eta'^2\psi'(1,\eta')} \right] \quad (5.5.19)$$

$$+ \frac{(j+1)(\gamma-1)(a+j+3)^2\eta_{cJ}}{4\eta'\psi'(1,\eta')\theta_y}$$

For the non-reacting case, $F(\theta,\eta')$ reduces to

$$F(\theta,\eta) = \left[-\frac{1}{2\eta} + \frac{\phi(1,\eta)}{2\eta}(2+(\gamma-1)(j+1)) + \frac{(D_1+4\eta)}{2\eta(\gamma+1)} \right.$$

$$\left. + \frac{(D_1+4\eta)(1+\eta)}{8\eta^2(\gamma+1)} \right]$$

$$+ \theta\left[-\frac{1}{2\eta} + \frac{2(2+(\gamma-1)(j+1))}{D_1+4\eta} \right] + \frac{1}{\theta}\left[\frac{(D_1+4\eta)^2\phi(1,\eta)}{8\eta^2(\gamma+1)} \right.$$

$$- \frac{(D_1+4\eta)\phi(1,\eta)}{8\eta^2\psi(1,\eta)} + \frac{(\gamma-1)(j+1)(D_1+4\eta)\phi^2(1,\eta)}{16\eta^2} \right]$$

$$- \frac{(\gamma-1)(j+1)(D_1+4\eta)^2}{8\eta\theta_y(\gamma+1)}$$

$$(5.5.20)$$

$$D_1 = \gamma(j+3) + (j-1) \tag{5.5.20}$$

In the above equation, the relationship for the dependence of the shock radius y on the shock strength η' is unknown. Hence the differential equation for $y(\eta')$ given previously by Eq. 5.1.15

$$\frac{dy}{d\eta'} = \frac{-(j+1)}{2} \frac{y}{\theta \eta'}, \tag{5.1.15}$$

must be used. Eqs. 5.5.19 and 5.1.15 constitute a pair of first order differential equations for $\theta(\eta')$ and $y(\eta')$ which can be integrated by standard numerical methods such as the Runge-Kutta scheme. The boundary conditions are at $\eta'=0$.

$$\theta(0) = \theta_o \quad , \quad y(0) = 0 \tag{5.5.21}$$

However one notes that both Eqs. 5.5.19 and 5.1.15 are singular at $\eta'=0$ since the boundary condition states that $y(0)=0$. Hence the slopes are indeterminate (i.e., $\frac{d\theta(0)}{d\eta'} = \frac{0}{0}$, $\frac{dy(0)}{d\eta'} = \frac{0}{0}$). Therefore to perform the numerical integration, it is necessary to evaluate both θ and y at some small finite value of η' and proceed the integration from this point. To seek solutions in the neighborhood of $\eta'=0$, $\theta(\eta')$ and $y(\eta')$ are expanded in the following power series in η'

$$\theta(\eta') = \theta_c + \theta_1\eta' + \theta_2\eta'^2 + \theta_3\eta'^3 + \cdots$$

$$y(\eta') = y_1\eta' + y_2\eta'^2 + y_3\eta'^3 + y_4\eta'^4 + \tag{5.5.22}$$

Substituting the above perturbation series into Eqs. 5.5.19 and 5.5.15 and equating terms of similar powers in η', the coefficients θ_n and y_n can readily be determined. These coefficients are extremely lengthy and can only be expressed in repeated parametric forms as

$$\theta_0 = -(j+1)/2 \qquad (5.5.23)$$

$$y_1 = -E_1/(C_1 + A_1\theta_0) \qquad (5.5.24)$$

$$\theta_1 = \theta_0^2 \left(A_2 + B_1\theta_0 + C_2/\theta_0 + E_2/(y_1\theta_0) \right)/C_1 \qquad (5.5.25)$$

$$y_2 = -y_1\theta_1/\theta_0 \qquad (5.5.26)$$

$$\theta_2 = \theta_0^2 \left(A_3 + (B_1 - 1)\theta_1 + B_2\theta_0 + \left[C_1\theta_1^2/\theta_0^2 - C_2\theta_1/\theta_0 \right. \right.$$
$$\left. \left. + C_3 \right]/\theta_0 + E_3/(y_1\theta_0) \right)/\left(C_1 + E_1/(2y_1) \right) \qquad (5.5.27)$$

$$y_3 = y_1 \left(\theta_1^2/\theta_0^2 - \theta_2/(2\theta_0) \right) \qquad (5.5.28)$$

$$\theta_3 = \theta_0^2 \left(A_4 + (B_1 - 2)\theta_2 + B_2\theta_1 + B_3\theta_0 + \left[C_1(2\theta_1\theta_2/\theta_0^2 \right. \right.$$
$$\left. - \theta_1^3/\theta_0^3 \right) + C_2(\theta_1^2/\theta_0 - \theta_2/\theta_0) - C_3\theta_1/\theta_0 + C_4 \left]/\theta_0 \right. \qquad (5.5.29)$$
$$\left. + \left(E_1\theta_1\theta_2/(3\theta_0^2) - E_2\theta_2/(2\theta_0) + E_4 \right)/(y_1\theta_0) \right)/\left(C_1 + 2E_1/(3y_1) \right)$$

$$y_4 = y_1 \left(7\theta_1\theta_2/(2\theta_0^2) - 3\theta_1^3/\theta_0^3 - \theta_3/\theta_0 \right)/3 \qquad (5.5.30)$$

where the coefficients in the above equations are as follows

Defining

$$S_1 = -\frac{(1+\eta_{CT}^2)}{2}$$

$$S_2 = -\frac{(1-\eta_{CT}^2)^2}{4}$$

$$S_3 = -\frac{(1-\eta_{CT}^2)(1-\eta_{CT}^4)}{16}$$

$$S_4 = \frac{(1-\eta_{CT}^2)^2(3+6\eta_{CT}^2+15\eta_{CT}^4)}{128}$$

$$P_0 = \frac{-(\gamma-1)}{\eta_{CT}-S_1}$$

$$P_1 = -\left(1-\frac{2P_0 S_2}{\eta_{CT}-S_1}\right)$$

$$P_2 = -\left(\frac{S_2}{\eta_{CT}-S_1} - P_0\left(\frac{3S_3}{\eta_{CT}-S_1} + \frac{4S_2^2}{(\eta_{CT}-S_1)^2}\right)\right)$$

$$P_3 = -\left(\frac{2S_3}{\eta_{CT}-S_1} + \frac{2S_2^2}{(\eta_{CT}-S_1)^2} - P_0\left[\frac{4S_4}{\eta_{CT}-S_1} + \frac{12S_2 S_3}{(\eta_{CT}-S_1)^2} + \frac{8S_2^3}{(\eta_{CT}-S_1)^3}\right]\right)$$

$$\psi_0 = \frac{\gamma+1}{\gamma-1}$$

$$\psi_1 = \frac{\psi_0(S_1-\eta_{CT})}{\gamma-1}$$

$$\psi_2 = \psi_0\left(\frac{S_2}{\gamma-1} + \frac{(S_1-\eta_{CT})^2}{(\gamma-1)^2}\right)$$

$$\psi_3 = \psi_0\left(\frac{S_3}{\gamma-1} + \frac{2S_2(S_1-\eta_{CT})}{(\gamma-1)^2} + \frac{(S_1-\eta_{CT})^3}{(\gamma-1)^3}\right)$$

$$\psi_4 = \psi_0\left(\frac{S_4}{\gamma-1} + \frac{2S_3(S_1-\eta_{CT})}{(\gamma-1)^2} + \frac{S_2^2}{(\gamma-1)^2} + \frac{3S_2(S_1-\eta_{CT})^2}{(\gamma-1)^3} + \frac{(S_1-\eta_{CT})^4}{(\gamma-1)^4}\right)$$

$$\mathcal{V}_0 = \frac{\ddot{?}}{?+1}$$

$$\mathcal{V}_1 = \frac{\ddot{?}}{?+1}$$

$$\mathcal{V}_2 = \frac{\dot{?}}{?+1}$$

$$\mathcal{V}_3 = \frac{\ddot{?}}{?+1}$$

$$a_0 = 2 + (j+1)\mathcal{V}_0$$

$$a_1 = (j+1)\mathcal{V}_1$$

$$a_2 = (j+1)\mathcal{V}_2$$

$$a_3 = (j+1)\mathcal{V}_3$$

$$\alpha_0 = a_0^2$$

$$\alpha_1 = 2a_0 a_1$$

$$\alpha_2 = a_1^2 + 2a_0 a_2$$

$$\alpha_3 = 2(a_0 a_3 + a_1 a_2)$$

$$b_0 = a_0 \phi_0$$

$$b_1 = a_0 \phi_1 + a_1 \phi_0$$

$$b_2 = a_0 \phi_2 + a_1 \phi_1 + a_2 \phi_0$$

$$b_3 = a_0 \phi_3 + a_1 \phi_2 + a_2 \phi_1 + a_3 \phi_0$$

$$J = 2 + (J-1)(j+1)$$

the A's and B's are given by

$$A_1 = -\beta_0 P_0/4$$

$$A_2 = -\frac{1}{2} + J\frac{\phi_0}{2} - (\beta_0 P_1 + \beta_1 P_0)/4 + (j+1) + 2/\gamma_0$$

$$A_3 = J\phi_1/2 - (\beta_0 P_2 + \beta_1 P_1 + \beta_2 P_0)/4 + 2(q_{cr} - S_1)/(\gamma+1)$$

$$A_4 = J\phi_2/2 - (\beta_0 P_3 + \beta_1 P_2 + \beta_2 P_1 + \beta_3 P_0)/4 - 2S_2/(\gamma+1)$$

$$B_1 = -1/2$$

$$B_2 = \frac{-J}{P_0 Q_0} + \frac{2S_2}{\eta_{cr} - S_1}$$

$$B_3 = \frac{J}{P_0 Q_0}\left(\frac{P_1}{P_0} + \frac{a_1}{a_0}\right) + \frac{2S_2}{\eta_{cr} - S_1}\left(\frac{3S_3}{S_2} + \frac{2S_1}{\eta_{cr} - S_1}\right)$$

Further, by defining

$$R_0 = 1/\zeta_1$$

$$R_1 = -2R_0 \zeta_2/\zeta_1$$

$$R_2 = R_0\left(4\zeta_2^2/\zeta_1^2 - 3\zeta_3/\zeta_1\right)$$

$$R_3 = R_0\left(-4\zeta_4/\zeta_1 + 12\zeta_2\zeta_3/\zeta_1^2 - 8\zeta_2^3/\zeta_1^3\right)$$

$$t_0 = \alpha_0 R_0$$

$$t_1 = \alpha_0 R_1 + \alpha_1 R_0$$

$$t_2 = \alpha_0 R_2 + \alpha_1 R_1 + \alpha_2 R_0$$

$$t_3 = \alpha_0 R_3 + \alpha_1 R_2 + \alpha_2 R_1 + \alpha_3 R_0$$

$$g_0 = p_0 R_0$$

$$g_1 = p_0 R_1 + p_1 R_0$$

$$g_2 = p_0 R_2 + p_1 R_1 + p_2 R_0$$

$$g_3 = p_0 R_3 + p_1 R_2 + p_2 R_1 + p_3 R_0$$

$$u_0 = t_0 \phi_0$$

$$u_1 = t_0 \phi_1 + t_1 \phi_0$$

$$u_2 = t_0 \phi_2 + t_1 \phi_1 + t_2 \phi_0$$

$$u_3 = t_0 \phi_3 + t_1 \phi_2 + t_2 \phi_1 + t_3 \phi_0$$

$$v_0 = p_0 \phi_0$$

$$v_1 = p_0 \phi_1 \quad p_1 \phi_0$$

$$v_2 = p_0 \phi_2 + p_1 \phi_1 + p_2 \phi_0$$

$$v_3 = p_0 \phi_3 + p_1 \phi_2 + p_2 \phi_1 + p_3 \phi_0$$

$$\omega_0 = v_0 P_0$$

$$\omega_1 = v_0 P_1 + v_1 P_0$$

$$\omega_2 = v_0 P_2 + v_1 P_1 + v_2 P_0$$

$$\omega_3 = v_0 P_3 + v_1 P_2 + v_2 P_1 + v_3 P_0$$

the C's and E's are given by

$$C_1 = -u_0/4 + g_0/4 - (j+1)(\gamma-1)\omega_0/8$$

$$C_2 = (\gamma-1)g\eta_{cr}t_0/4 - u_1/4 + g_1/4 - (j+1)(\gamma-1)\omega_1/8$$

$$C_3 = (\gamma-1)g\eta_{cr}t_1/4 - u_2/4 + g_2/4 - (j+1)(\gamma-1)\omega_2/8$$

$$C_4 = (\gamma-1)g\eta_{cr}t_2/4 - u_3/4 + g_3/4 - (j+1)(\gamma-1)\omega_3/8$$

$$E_1 = (j+1)(\gamma-1)\eta_{cr}t_0/4$$

$$E_2 = (j+1)(\gamma-1)\eta_{cr}t_1/4$$

$$E_3 = (j+1)(\gamma-1)\eta_{cr}t_2/4$$

$$E_4 = (j+1)(\gamma-1)\eta_{cr}t_3/4$$

For the non-reacting case, the coefficients of Eqs. 5.5.23 to 5.5.30
reduce to simpler forms given by

$$A_1 = D_1/(4(\gamma+1))$$

$$A_2 = -\frac{1}{2} + (2+(\gamma-1)(j+1))/(\gamma+1) + (3D_1+4)/(4(\gamma+1))$$

$$A_3 = (1-(\gamma-1)(j+1))/(\gamma+1)$$

$$A_4 = 0$$

$$B_1 = -\tfrac{1}{2}$$

$$B_2 = 2(2+(\gamma-1)(j+1))/D_1$$

$$B_3 = -8(2+(\gamma-1)(j+1))/D_1^2$$

$$C_1 = D_1(D_1+j(\gamma-1))/(4(\gamma+1)^2)$$

$$C_2 = (-D_1^2 + D_1(6-(\gamma-1)(2j+1)) + 4j(\gamma-1))/(4(\gamma+1))$$

$$C_3 = \left[D_1(-6 + (\gamma-1)(j+1)) + 4(2-(\gamma-1)(2j+1)) \right]/(4(\gamma+1)^2)$$

$$C_4 = -(2 - (\gamma-1)(j+1))/(\gamma+1)^2$$

$$E_1 = -(\gamma-1)(j+1)D_1^2/(8(\gamma+1))$$

$$E_2 = -(\gamma-1)(j+1)D_1/(\gamma+1)$$

$$E_3 = -2(\gamma-1)(j+1)/(\gamma+1)$$

$$E_4 = 0$$

$$D_1 = \gamma(j+3) + j - 1$$

From Eq. 5.5.23, we note that the coefficient $\theta_0 = -(j+1)/2$ which yields the time exponent $N = 2/5$, $1/2$ and $2/3$ for spherical, cylindrical and planar strong blast waves as in the classical self-similar solution.

For given geometry " j ", the Chapman-Jouguet Mach Number " η_{cj} ", and the specific heat ratio γ , the perturbation coefficients θ_m's and y_m's are first determined. Using the perturbation expressions given by Eq. 5.5.22, θ and y are determined at some small value of $\eta' = \eta'^{*}$ where $\eta'^{*} << 1$. With $\theta(\eta'^{*})$ and $y(\eta'^{*})$ as starting values, Eqs. 5.5.19 and 5.1.15 can then be integrated numerically using the Runge-Kutta method. From our experience, it was found that using the Runge-Kutta method, the step size h must be small as compared to η'^{*} in the early phases of the integration otherwise large errors are generated. It was found that using $h \le .05\eta'^{*}$ gave good results.

To determine the shock trajectory the identity

$$\dot{R}_s = \frac{dR_s}{dt}$$

is used and expressing the above equation in dimensionless parameters y and θ we get

$$\frac{\dot{R}_{CI}t}{R_o} = -\frac{1}{2}\int_0^{\eta'} y\frac{\frac{1}{J+1}}{\Theta\eta'^{\frac{1}{2}}}d\eta'$$

(5.5.31)

As the solution for $y(\eta')$ and $\Theta(\eta')$ is being determined, the integral in Eq. 5.5.31 can simultaneously be carried out numerically yielding the shock trajectory.

For small values of η', an analytical expression for the shock trajectory can be obtained by substituting the expansion for $y(\eta')$ into Eq. 5.5.31. Evaluating the integral, we get

$$\frac{\dot{R}_{CI}t}{R_o} = 2y_1^{\frac{1}{J+1}}\eta'^{\frac{J+3}{2(J+1)}}\left[\frac{1}{J+3} + \frac{T_1\eta'}{3J+5} + \frac{T_2\eta'^2}{5J+7} + \frac{T_3\eta'^3}{7J+9} + \right]$$

(5.5.32)

where

$$T_1 = y_2(j+2)/(y_1(j+1))$$

$$T_2 = (2j+3)\left(y_3/y_1 - jy_2^2/(2y_1^2(j+1))\right)/(j+1)$$

$$T_3 = (3j+4)\left(y_4/y_1 - jy_2y_3/(y_1^2(j+1))\right.$$

$$\left. + j(2j+1)y_2^3/(6y_1^3(j+1)^2)\right)/(j+1)$$

and the y_m's are given previously by Eqs. 5.5.24, 5.5.26, 5.5.28 and 5.5.30.

Looking at the extreme complexities of the various coefficients θ_m and y_n given in the preceeding pages, one cannot help but ask whether all these are necessary since the method after all is only approximate. We have tried various methods to obtain the starting values for θ and y in the simultaneous integration of Eqs. 5.5.18 and 5.5.15 and found all of them to be unsatisfactory. It should be pointed out that the integration of Eqs. 5.5.18 and 5.5.15 is stable only in the forward direction of increasing η', hence iterating for the correct starting values by going backwards to recover the boundary conditions at $\eta'=0$ does not work in this case. Another obvious method is to use the perturbation solution given in Section 5.2 to yield the starting values for $\theta(\eta'^*)$ and $y(\eta'^*)$ since the perturbation solution is extremely accurate for $\eta'^* \ll 1$. However the approximations in the perturbation scheme are not consistent with those in the method of Porzel and although the starting values might be more accurate, the use of them to start the integration of Eqs. 5.5.18 and 5.5.15 results in oscillations. However these oscillations damp out rapidly and a smooth curve for $\theta(\eta')$ and $y(\eta')$

can be obtained. Hence if one tolerates some oscillations in the initial period, the perturbation solution could be used to start the integration. In the authors' opinion the relationships for the coefficients θ_m and y_n although complex need to be obtained only once. Since they are consistent with the approximations of the method and yield good results, we feel that the use of them is justified.

It should be noted in the method of Porzel just described, the only approximation involved is the form for the solution of the density. Based on only one assumed form for the density profile, the particle velocity and the pressure profiles are determined exactly from the basic conservation equations. If the power law form for the density profile assumed is exact, as in the case of strong spherical

blast in a medium with $\gamma = 7$, then the velocity as well as the pressure profiles are also exact. From numerical solutions, we see that the density profiles for various values of γ and shock strengths can closely be approximated by a simple power law. Hence the method should yield extremely accurate results.

The present method satisfies conservation of total mass and total energy, however if the solutions for ψ , ϕ and f given by Eqs. 5.5.5, 5.5.8, and 5.5.12 are substituted into the differential equation of energy conservation (i.e., Eq. 5.4.3) it is found that the energy equation is not satisfied. This is due to the approximate forms of the profiles, and for the particular case of $\gamma = 7$, $j = 2$, $\eta' = 0$ in which the profiles are in fact the exact solution, the energy equation is also satisfied. However since quantities such as the shock trajectory and the shock strength - shock radius relationships depend on the integrated total energy and that is conserved, accurate results can be obtained in spite of the fact that the energy profile is in error.

5.6 Shock Propagation in Solid Media

In this Section we shall demonstrate the use of Porzel's
method described in the previous Section to account for non-similar
effects arising from the equation of state. We shall treat the problem
of strong shock propagation in a solid medium. For sufficiently strong
shocks, the material strength of the media can be neglected as compared
to the dynamic pressure involved typically of the megabar range. Under
this condition, the shocked states can be approximated to behave as a
compressible inviscid medium and the hydrodynamic equations given in
Chapter II can be used with the exception of the equation of state
which for solid media is quite complex in general. A full description
of the various equations of state for solid media is given by Rice,
McQueen and Walsh in their review article in the Advances of Solid
State Analysis. We shall not go into a discussion on that, but rather
use the simplified form for analytical work derived by Rae.

For an arbitrary equation of state the basic non-similar
equations can be written as

$$(\phi-\xi)\frac{\partial \psi}{\partial \xi} + \psi\frac{\partial \phi}{\partial \xi} + j\frac{\psi\phi}{\xi} = \theta\eta_s\frac{\partial \psi}{\partial \eta_s} \tag{5.6.1}$$

$$(\phi-\xi)\frac{\partial \phi}{\partial \xi} + \theta\eta^s + \frac{1}{\psi}\frac{\partial f}{\partial \xi} = \theta\eta_s\frac{\partial \phi}{\partial \eta_s} \tag{5.6.2}$$

$$(\phi-\xi)\left(\frac{\partial g}{\partial \xi} - \frac{f}{\psi^2}\frac{\partial \psi}{\partial \xi}\right) + 2\theta g = \theta\eta_s\left(\frac{\partial g}{\partial \eta_s} - \frac{f}{\psi^2}\frac{\partial \psi}{\partial \eta_s}\right) \tag{5.6.3}$$

where
$$\theta = \frac{R_S \ddot{R}_S}{\dot{R}_S^2} \tag{5.6.4}$$

$$\eta_S = 1/m_S \tag{5.6.5}$$

and
$$g(\xi, \eta_S) = e(r,t)/\dot{R}_S^2 \tag{5.6.6}$$

In the above equations η_S is used as the other independent variable instead of $\eta = 1/m_S^2$ used before because of convenience as we shall see later. One can write the energy integral

$$E_0 = \int_0^{R_S} (e - e_0 + u^2/2)\rho k_j r^j dr \tag{5.6.7}$$

which transforms to

$$1 = y I / \eta_S^2 \tag{5.6.8}$$

where

$$I = \int_0^1 (g - g_0 + \frac{\phi^2}{2}) 4 \xi^j d\xi \tag{5.6.9}$$

$$y = (R_S/R_0)^{j+1} \tag{5.6.10}$$

and
$$R_0 = (E_0/(\rho_0 C_0^2 k_j))^{\frac{1}{j+1}} \tag{5.6.11}$$

The shock strength - shock radius relationship can be obtained by the differentiation Eq. 5.6.10 with respect to η_S as

$$\frac{dy}{dm_S} = -(j+1)y/(\theta \eta_S) \tag{5.6.12}$$

For solid media under high pressures, the equations of state are generally derived from experimental shock wave data. The nature

of these experiments in general is to accelerate a metal plate to high velocities by solid explosives and let it impact onto a target material. The shock wave and the particle velocity in the target material are the two usual parameters measured and the shock Hugoniot determined from these data. For most solids, it was found from experimental shock Hugoniots that a linear relationship exists between the shock velocity and the particle velocity. This relationship is generally written as

$$\dot{R}_s = C + S u_1 \tag{5.6.13}$$

where C and S are the experimentally determined constants. Using the above equation the Mie-Gruneisen equation of state as derived by Rae is

$$\frac{e - e_o}{c^2} = \frac{p}{2 c^2 (S-1) \rho} - \frac{1}{2(S-1)} \frac{(\rho - \rho_o)}{(S \rho_o - (S-1)\rho)} \tag{5.6.14}$$

and in terms of the non-dimensional parameters used, it becomes

$$g - g_o = \frac{1}{2(S-1)} \left[\frac{f}{\psi} - \frac{(\psi - 1) \eta_s^2}{S - (S-1)\psi} \right] \tag{5.6.15}$$

In the above equation the Gruneisen factor is assumed to be constant having its limiting value of $2(S-1)$ at $\dot{R}_s \rightarrow \infty$. As pointed out by Rae, Eq. 5.6.15 ceases to be valid in the limit of very high pressure and also at low pressure. It is however a good approximation in the intermediate pressure range where the linear relationship between the shock velocity and the particle velocity applies. For the sake of convenience, Eq. 5.6.15 is used in the entire range of pressures bearing in mind its limitations. A more accurage form of the Mie-Gruneisen equation of state valid for a much wider range of pressures has been derived by Tillotson. With minor modifications Tillotson's

form can be incorporated into the non-similar methods described in this Chapter.

Using the equation of state given by Eq. 5.6.15, we can see that the departure from similarity arises from the finite shock Mach No. term on the right hand side. For strong shocks where $\eta_s \rightarrow 0$, this non-similar term vanishes and Eq. 5.6.15 reduces to a form similar to that for a perfect gas.

Using Eq. 5.6.13, the boundary conditions at the shock front can readily be obtained from the Rankine-Hugoniot relationships which can be written as

$$1 = \psi(1,\eta_s)\left(1 - \phi(1,\eta_s)\right) \tag{5.6.16}$$

$$f(1,\eta_s) - \frac{p_o}{\rho_o \dot{R}_s^2} = \phi(1,\eta_s)$$

$$g(1,\eta_s) - e_o/\dot{R}_s^2 = \frac{1}{2}\left(f(1,\eta_s) + \frac{p_o}{\rho_o \dot{R}_s^2}\right)\left(1 - \frac{1}{\psi(1,\eta_s)}\right) \tag{5.6.17}$$

Substituting Eq. 5.6.13 into the above equations, we obtain the following relationships for transition across a shock wave in a solid media

$$\psi(1,\eta_s) = \frac{S}{S-1+\eta_s} \tag{5.6.18}$$

$$\phi(1,\eta_s) = \frac{1-\eta_s}{S} \tag{5.6.19}$$

$$f(1,\eta_s) = \frac{1-\eta_s}{S} \tag{5.6.20}$$

To obtain non-similar solutions to the propagation of shock wave in solids, any one of the non-similar methods described in this Chapter can be used based on the above formulation. The quasi-similar method

of Oshima was used by Rae and the method of Porzel by Bach and Lee.
We shall present the analysis using the method of Porzel below since
it yields better results for the distribution of the various properties
behind the shock. As far as the shock trajectory is concerned, the
quasi-similar method, the method of Porzel and the simple quasi-steady
of Rae yield very close results.

Using the method of Porzel, the density profile is again
assumed to be a simple power law of the form

$$\psi = \psi(1,\eta_s) \xi^{g(\eta_s)} \qquad (5.6.21)$$

where the exponent $g(\eta_s)$ determined from the mass integral is given
as

$$g(\eta_s) = (j+1)(\psi(1,\eta_s)-1) \qquad (5.6.22)$$

From the continuity equation we obtain the particle velocity profile
to be

$$\phi(\xi,\eta_s) = \phi(1,\eta_s)\xi(1 - Ⓐ \ln\xi) \qquad (5.6.23)$$

where

$$Ⓐ = \frac{-\theta\eta_s}{\phi(1,\eta_s)\psi(1,\eta_s)} \frac{d\psi(1,\eta_s)}{d\eta_s} \qquad (5.6.24)$$

From the momentum equation we obtain the pressure profile to be

$$f(\xi,\eta_s) = f(1,\eta_s) + f_2(\xi^{g+2}-1) + f_3(\xi^{g+2}[(g+2)\ln\xi-1]+1)$$

$$+ f_4\left(2-\xi^{g+2}[(g+2)^2\ln^2\xi -2(g+2)\ln\xi +2]\right)$$

$$(5.6.25)$$

where

$$f_2 = \frac{\psi(1,\eta_s)}{(\bar{g}+2)}\left((1-\bar{\omega})\phi(1,\eta_s)(1-\phi(1,\eta_s)) - \theta\left(\phi(1,\eta_s) - \eta_s\frac{d\phi(1,\eta_s)}{d\eta_s}\right)\right) \tag{5.6.26}$$

$$f_3 = \frac{\psi(1,\eta_s)}{(\bar{g}+2)^2}\left[\theta\left(\bar{\omega}\phi(1,\eta_s) - \eta_s\frac{d}{d\eta_s}(\bar{\omega}\phi(1,\eta_s))\right) - \bar{\omega}\phi(1,\eta_s) - \bar{\omega}^2\phi^2(1,\eta_s) + 2\bar{\omega}\phi^2(1,\eta_s)\right] \tag{5.6.27}$$

$$f_4 = \frac{\psi(1,\eta_s)\bar{\omega}^2\phi^2(1,\eta_s)}{(\bar{g}+2)^3} \tag{5.6.28}$$

These profiles are identical in form to those given in the previous
Section for a perfect gas since they are obtained from the continuity
and momentum equations only. Substituting the density and pressure
profiles into the equation of state, the distribution of internal
energy can be obtained.

Substituting the various profiles into the energy integral
and solving for $d\theta/d\eta_s$ we get

$$\frac{d\theta}{d\eta_s} = \frac{2\phi(1,\eta_s)-1}{\eta_s} + \frac{(d_1+2\eta_s)(1+\eta_s)}{5\eta_s^2} + \frac{2\phi(1,\eta_s)(j+1)(s-1)}{\eta_s}$$

$$+ \frac{2\theta(1+(j+1)(s-1))}{d_1+2\eta_s} + \oint\left\{\frac{\phi(1,\eta_s)(d_1+2\eta_s)^2}{5\eta_s^2}\right.$$

$$- \frac{(d_1+2\eta_s)\phi(1,\eta_s)}{\eta_s^2\psi(1,\eta_s)} + \frac{(j+1)(s-1)\phi^2(1,\eta_s)(d_1+2\eta_s)}{\eta_s^2}$$

$$\left. - \frac{2(j+1)(s-1)(d_1+2\eta_s)^2}{ys}\right\} - \frac{2(j+1)(s-1)(d_1+2\eta_s)^2 G(\eta_s)}{\theta s} \tag{5.6.29}$$

where

$$d_1 = s(j+3) - 2 \qquad\qquad (5.6.30)$$

$$
\begin{aligned}
G(\eta_s) = \frac{1}{2(s-1)(s-1+\eta_s)(j+1)} &\left\{ ln\left(\frac{s-1+\eta_s}{\eta_s}\right) + \frac{(1-\eta_s)^2}{s(s-1+\eta_s)} \right. \\[2mm]
&- \frac{2\,s(s-1)(1-\eta_s)}{\eta_s(s+1-\eta_s)(s+2(1-\eta_s))} + \frac{4s(s-1)^2(1-\eta_s)^2}{\eta_s^2(s+1-\eta_s)(s+2(1-\eta_s))(s+3(1-\eta_s))} \\[2mm]
&- s(s+1-\eta_s)\sum_{k=1}^{\infty}\left(\frac{s-1}{s-1+\eta_s}\right)^k \frac{1}{k(s+k(1-\eta_s))(s+(k+1)(1-\eta_s))} \\[2mm]
&- 12s\frac{(s-1)^2(1-\eta_s)^3}{\eta_s^2}\sum_{k=1}^{\infty}\left(\frac{s-1}{s-1+\eta_s}\right)^k \cdot \\[2mm]
&\left. \frac{1}{(s+k(1-\eta_s))(s+(k+1)(1-\eta_s))(s+(k+2)(1-\eta_s))(s+(k+3)(1-\eta_s))} \right.
\end{aligned}
$$

$$(5.6.31)$$

To obtain $\theta(\eta_s)$ and $y(\eta_s)$ we have to integrate Eqs. 5.6.29 and 5.6.12 simultaneously with the boundary conditions $y(0) = 0$, $\theta = \theta_0$ at $\eta_s = 0$ as before. As in the perfect gas case, Eqs. 5.6.19 and 5.6.12 are singular at $\eta_s = 0$, so we must determine θ and y at some small value of η_s to start the numerical integration. In this case however, we cannot assume expansions for θ and y in the form given before by Eq. 5.5.22 since the function $G(\eta_s)$ has a $ln\,\eta_s$ term (see Eq. 5.6.31) and hence the previous form does not satisfy the differential equations (i.e., Eqs. 5.6.19 and 5.6.12).

Rather than solving for the proper starting form for y and θ the following procedure is adopted.

Noting that the cohesive contributions in the Mie-Gruneisen equation of state are small under very high pressures, the non-similar term in Eq. 5.6.15 is assumed to be negligible as compared to the first term for small but finite η_s . Eq. 5.6.15 then reduces to

$$ g = \frac{f}{2(S-1)y} \tag{5.6.32} $$

which is identical in form to that for a perfect gas when $2(S-1)$ is replaced by $\gamma-1$. Hence by assuming the solid medium to behave like a perfect gas with $\gamma = 2S-1$, the value of θ and y for some small value of η_s can be determined as in the previous Section. With these as starting values, Eqs. 5.6.19 and 5.6.17 are then integrated numerically. The solution for θ and y obtained using this procedure demonstrates a slight oscellation but rapidly damps out to give a smooth monotonic function of η_s .

The oscillations produced when the transition from the perfect gas to the Mie-Gruneisen equation of state is made is a direct result of the mismatch in the boundary conditions at the shock front. For small η_s when the medium was assumed to behave as a perfect gas, the boundary conditions used are those given by Eqs. 2.2.25 to 2.2.27 in Chapter II with $\gamma = 2S-1$. These values obtained differ from those for a solid medium when the boundary conditions are determined by Eqs. 5.6.18 to 5.6.20. The values obtained using the different relationships only agree in the limit as $\eta_s \to 0$. To obtain a better solution for $\theta(\eta_s)$ and $y(\eta_s)$ for small values of η_s , an approach similar to Rae's "quasi-steady" method can be used. The equation of state is first written as

$$g = \frac{f}{(\gamma(\eta_s)-1)\psi} \tag{5.6.33}$$

with γ allowed to vary with η_s such that the boundary conditions at the shock front as determined by Eqs. 5.6.18 to 5.6.20 are recovered at all times. For any values of η_s, the boundary values for $\psi(1)$, $\phi(1)$ and $f(1)$ from Eqs. 5.6.18 to 5.6.20 are then equated to their corresponding values across a strong shock wave in a perfect gas as follows:

$$\psi(1) = \frac{s}{s-1+\eta_s} = \frac{\gamma(\eta_s)+1}{\gamma(\eta_s)-1} \tag{5.6.34}$$

$$\phi(1) = f(1) = \frac{1-\eta_s}{s} = \frac{2}{\gamma(\eta_s)-1} \tag{5.6.35}$$

Solving for $\gamma(\eta_s)$ from the above relationships we obtain

$$\gamma(\eta_s) = \frac{\psi(1)+1}{\psi(1)-1} = \frac{2}{\phi(1)} - 1 = \frac{2}{f(1)} - 1 \tag{5.6.36}$$

$$\gamma(\eta_s) = \frac{2s-1+\eta_s}{1-\eta_s} \tag{5.6.37}$$

With the equation of state as given by equation 5.6.33, solutions for $\theta(\eta_s)$ and $y(\eta_s)$ for small values of η_s are next obtained in a manner similar to that for the perfect gas described in the preceeding Section. Evaluating the energy integral using Eq. 5.6.33 for the equation of state and solving for $d\theta/d\eta_s$, we get

$$\frac{d\theta}{d\eta_s} = \frac{2\phi(1,\eta_s) - 1}{\eta_s} + \frac{(j+1)(\gamma-1)\phi(1,\eta_s)}{\eta_s}$$

$$+ \frac{(d_1 + 2\eta_s)(1+\eta_s)}{s\eta_s^2} + \theta\left(\frac{2 + (j+1)(\gamma-1)}{d_1 + 2\eta_s}\right)$$

$$+ \frac{1}{\theta}\left[\frac{(j+1)(\gamma-1)(d_1 + 2\eta_s)\phi^2(1,\eta_s)}{2\eta_s^2}\right.$$

$$\left. + \frac{(d_1 + 2\eta_s)^2\phi(1,\eta_s)}{s\eta_s^2} - \frac{(d_1 + 2\eta_s)\phi(1,\eta_s)}{\eta_s^2\,\psi(1,\eta_s)}\right]$$

$$- \frac{(\gamma-1)(j+1)(d_1 + 2\eta_s)^2}{\theta\,y\,s}$$

$$(5.6.38)$$

where d_1 is defined previously by Eq. 5.6.30. Together with Eq. 5.6.12 for $dy/d\eta_s$, a pair of differential equations is obtained for $\theta(\eta_s)$ and $y(\eta_s)$. Eqs. 5.6.38 and 5.6.12 now permit the solution of θ and y for small values of η_s to be of the form

$$\theta = \theta_0 + \theta_1\eta_s + \theta_2\eta_s^2 + \cdots$$

$$(5.6.39)$$

$$y = y_1\eta_s + y_2\eta_s^2 + y_3\eta_s^3 + \cdots$$

The coefficients θ_n and y_n can readily be evaluated by substituting Eq. 5.6.39 into Eqs. 5.6.38 and 5.6.12. The resultant expressions for them are given below as

$$\theta_0 = -(j+1)/2$$

$$(5.6.40)$$

$$\theta_1 = \theta_0\left(\frac{A_1\theta_0 + C_1 + D_1/y_1}{C_0 - D_0/y_1}\right)$$

$$(5.6.41)$$

$$\theta_2 = \frac{\theta_0^2}{C_0}\left[A_2 + C_2/\theta_0 + D_2/(y_1\theta_0) + C_2\theta_1^2/\theta_0^2 \right.$$

$$\left. + B_0\theta_0 - C_1\theta_1/\theta_0^2 + D_1\theta_1/\theta_0^2 - \theta_1 \right] \tag{5.6.42}$$

$$y_1 = \frac{-D_0}{A_0\theta_0 + C_0} \tag{5.6.43}$$

$$y_2 = -2\theta_1 y_1/\theta_0 \tag{5.6.44}$$

$$y_3 = y_1\left(3\theta_1^2/\theta_0^2 - \theta_2/\theta_0 \right) \tag{5.6.45}$$

where

$$A_0 = d_1/s$$

$$A_1 = (s(3j+4)-2j)/s$$

$$A_2 = 2(j+1)/s$$

$$B_0 = 2(1+(j+1)(s-1))/d_1$$

$$C_0 = d_1(d_1+j(s-1))/s^2$$

$$C_1 = \left[d_1(j+2) + (2-d_1)(d_1+j(s-1)) \right]/s^2$$

$$C_2 = \left[(2-d_1)(j+2) - 2(d_1+j(s-1)) \right]/s^2$$

$$D_0 = -2(j+1)(s-1)d_1^2/s$$

$$D_1 = -2(j+1)d_1(d_1 S + 2(S-1))/S$$

$$D_2 = -2(j+1)(d_1^2 + 2Sd_1 + 4(S-1))/S$$

and d_1' is as given before by Eq. 5.6.30. For any arbitrary small value of η_S, the values $\theta(\eta_S)$ and $y(\eta_S)$ are obtained from Eqs. 5.6.39 to 5.6.45. Using these as starting values, the original equation for $d\theta/d\eta_S$ (i.e., Eq. 5.6.29) and Eq. 5.6.12 can then be integrated numerically. We found that using the starting values obtained by this procedure gave negligable oscillations initially since the boundary conditions at the front are now matched. Detailed results from this calculation can be found in the paper by Bach and Lee.

5.7 Asymptotic Motion of Detonation Waves

We have thus far demonstrated three non-similar methods for describing the motion of a detonation wave initiated by the instantaneous release of a finite quantity of energy E_0 . All these methods give a fairly accurate prediction of the detonation motion for strong detonations (i.e., $\eta' << 1$) but failed to describe the asymptotic behavior as $\eta' \to 1$ (i.e., $\eta \to \eta_{cj}$). In this Section, we shall investigate this asymptotic regime. For non-reacting blast wave, the asymptotic decay law has been studied by a large number of investigators, particularly by the Los Alamos group in connection with nuclear blast effects (e.g., Penny, Bethe, Brinkley, Kirkwood), by Whitham and Lighthill, and in the Soviet Union by Landau and Sedov. Recently, Levin and Chernyi gave the analysis for the asymptotic motion of detonation waves and pointed out the interesting possibility that for spherical and cylindrical detonation, Chapman-Jouguet condition can be met at a finite shock radius. For planar detonation, the Chapman-Jouguet condition is met at infinite shock radius, analogous to the non-reacting blast where the acoustic limit is only approached at $R_s \to \infty$. The approach to Chapman-Jouguet at a finite radius is an important result, since by relating this radius with the initiation energy and using some physical arguments might lead us to the development of a quantitative theory for the prediction of the critical energy for the direct initiation of cylindrical or spherical detonations in a given explosive. We have been studying this asymptotic problem following similar lines as Levin and Chernyi and found that although the mathematics indicate such a possibility for cylindrical or spherical decaying waves to approach Chapman-Jouguet conditions at a finite radius, it is not obvious that this possibility is indeed the unique solution. To prove the uniqueness of the solution we have to carefully analyse the

approximations used in taking the various limits as well as the details of
the flow structures of the decaying and the self-similar Chapman-Jouguet
solution. At present we have not completed this study to our satisfaction
but feel that the importance of the asymptotic behavior warrants an
exposition of the analysis to demonstrate this possibility of decay to
Chapman-Jouguet detonations at a finite radius for cylindrical and
spherical symmetry.

Following Chernyi, we first derive the relationships at the
wave front as $\eta' \to 1$. The boundary conditions at the front are given
previously as

$$\psi(1,\eta') = \frac{\gamma+1}{\gamma+\eta'\eta_{cr} - S} \tag{5.1.22}$$

$$\phi(1,\eta') = \frac{1 - \eta'\eta_{cr} + S}{\gamma+1} \tag{5.1.23}$$

$$f(1,\eta') = \frac{\gamma + \eta'\eta_{cr} + \gamma S}{\gamma(\gamma+1)} \tag{5.1.24}$$

where $\quad S = \left[(1-\eta')(1-\eta'\eta_{cr}^2) \right]^{1/2} \tag{5.1.25}$

we define $\quad \epsilon = 1-\eta' \quad , \quad \eta' = 1-\epsilon \tag{5.7.1}$

and in the asymptotic regime when $\quad \eta \to \eta_{cr} \; , \; \eta' \to 1 \quad ,$
$\epsilon \ll 1 \quad$. Expanding the boundary conditions in powers of ϵ ,
we obtain

$$\frac{U}{U_{cj}} - \frac{p}{p_{cj}} = 1 + \frac{(1-\eta_{cj})}{\gamma+\eta_{cj}}\left[\left(\frac{1+\eta_{cj}}{1-\eta_{cj}}\right)^{\frac{1}{2}}\epsilon^{\frac{1}{2}} + \frac{(\gamma\eta_{cj}+1)\epsilon}{(\gamma+\eta_{cj})(1-\eta_{cj})} + \cdots \right] \quad (5.7.2)$$

$$\frac{U}{U_{cj}} = 1 + \left(\frac{1+\eta_{cj}}{1-\eta_{cj}}\right)^{\frac{1}{2}}\epsilon^{\frac{1}{2}} + \frac{1+\eta_{cj}}{2(1-\eta_{cj})}\epsilon + \cdots \quad (5.7.3)$$

$$\frac{p}{p_{cj}} = 1 + \frac{\gamma(1-\eta_{cj})}{\gamma+\eta_{cj}}\left[\left(\frac{1+\eta_{cj}}{1-\eta_{cj}}\right)^{\frac{1}{2}}\epsilon^{\frac{1}{2}} + \frac{\epsilon}{1-\eta_{cj}} + \cdots \right] \quad (5.7.4)$$

In the above expression, the subscript CJ denotes conditions at a Chapman-Jouguet detonation front. To obtain the variation of entropy at the front in the asymptotic regime, we find an expression for p/ρ^γ as

$$\frac{p}{\rho^\gamma} = \frac{(p/p_{cj})}{(\rho/\rho_{cj})^\gamma} \cdot \frac{p_{cj}}{\rho_{cj}^\gamma} \quad (5.7.5)$$

and using Eqs. 5.7.2 and 5.7.4, we get

$$\frac{p}{\rho^\gamma} = \frac{p_{cj}}{\rho_{cj}^\gamma}\left[1 + \frac{\gamma(\gamma-1)(1-\eta_{cj})^2}{2(\gamma+\eta_{cj})^2}\epsilon + \cdots \right] \quad (5.7.6)$$

From the above equation, we see that to the order of $\epsilon^{\frac{1}{2}}$, the entropy remains constant at the front and is equal to its value at Chapman-Jouguet conditions.

To obtain the decay law, that is the variation of ϵ with shock

radius R_s' , we go back to the basic conservation equations. Using the momentum and the energy equation given in the previous Section 5.4

$$(\phi - \xi)\frac{\partial \phi}{\partial \xi} + \theta\phi + \phi \frac{\partial f}{\partial \xi} = -2\theta\eta'\frac{\partial \phi}{\partial \eta'} \qquad (5.4.2)$$

$$(\phi - \xi)\frac{\partial f}{\partial \xi} + \gamma f \frac{\partial \phi}{\partial \xi} + \gamma j \frac{f\phi}{\xi} + 2\theta f = 2\theta\eta'\frac{\partial f}{\partial \eta'} \qquad (5.4.3)$$

and evaluating them at the front, we get

$$(\phi(1)-1)\frac{\partial \phi}{\partial \xi}\Big|_{\xi=1} + \frac{1}{f(1)}\frac{\partial f}{\partial \xi}\Big|_{\xi=1} = -\theta\phi(1) + 2\theta\eta'\frac{\partial \phi(1)}{\partial \eta'} \qquad (5.7.7)$$

$$(\phi(1)-1)\frac{\partial f}{\partial \xi}\Big|_{\xi=1} + \gamma f(1)\frac{\partial \phi}{\partial \xi}\Big|_{\xi=1} = -2\theta f(1)$$
$$- \gamma j f(1)\phi(1) + 2\theta\eta'\frac{\partial f(1)}{\partial \eta'} \qquad (5.7.8)$$

Since $\phi(1) - 1 = -1/f(1)$, from the conservation of mass across the front, addition of Eqs. 5.7.7 and 5.7.8 yields

$$S\frac{\partial \phi}{\partial \xi}\Big|_{\xi=1} = \theta\left[2\eta'\left(\frac{\partial \phi(1)}{\partial \eta'} + \frac{\partial f(1)}{\partial \eta'}\right) - \phi(1) - 2 f(1)\right]$$
$$- \gamma j f(1)\phi(1) \qquad (5.7.9)$$

Using the boundary conditions given by Eqs. 5.1.22 to 5.1.25 to evaluate the derivatives, Eq. 5.7.9 can be written as follows after some algebraic manipulating.

$$S \frac{\partial \phi}{\partial \xi}\bigg|_{\xi=1} = \frac{-\theta}{S(\gamma+1)} \left\{ (3 + \eta' \eta_{cr}) S + 3 - \eta' \right.$$

$$\left. - \eta' \eta_{cr}^2 - \eta'^2 \eta_{cr}^2 \right\}$$

$$- \frac{j}{(\gamma+1)^2} (1 - \eta' \eta_{cr} + S)(\gamma + \eta' \eta_{cr} + \gamma S) \tag{5.7.10}$$

Solving for θ in the above equation, we get

$$\theta = \frac{-jS}{\gamma+1} \cdot \frac{(1 - \eta' \eta_{cr} + S)(\gamma + \eta' \eta_{cr} + \gamma S)}{(3 + \eta' \eta_{cr}) S + 3 - \eta' - \eta' \eta_{cr}^2 - \eta'^2 \eta_{cr}^2}$$

$$\frac{- (\gamma+1) S^2 \frac{\partial \phi}{\partial \xi}\big|_{\xi=1}}{(3 + \eta' \eta_{cr}) S + 3 - \eta' - \eta' \eta_{cr}^2 - \eta'^2 \eta_{cr}^2} \tag{5.7.11}$$

In the limit as $\eta' \to 1$ and $S \to \left[(1-\eta')(1-\eta_{cr}^2) \right]^{1/2}$ the above equation reduces to

$$\theta = -(1-\eta')^{1/2} \frac{j(\gamma+\eta_{cr})}{2(\gamma+1)} \left(\frac{1+\eta_{cr}}{1+\eta_{cr}} \right)^{1/2} - \frac{(\gamma+1)(1-\eta')}{2} \frac{\partial \phi}{\partial \xi}\bigg|_{\xi=1, \eta' \to 1} \tag{5.7.12}$$

Let us now consider the planar case first. For planar symmetry, and the first term in Eq. 5.7.12 vanishes leaving

$$\theta = -\frac{(\gamma+1)(1-\eta')}{2} \frac{\partial \phi}{\partial \xi}\bigg|_{\substack{\xi=1 \\ \eta' \to 1}} \tag{5.7.13}$$

The slope of the particle velocity at the front in the limit as given previously in Chapter III on the propagation of Chapman-Jouguet planar detonations by Eq. 3.1.6 is

$$\frac{\partial \phi}{\partial \xi}\Big|_{\xi=1,\,\eta' \to 1} \longrightarrow \frac{2}{\gamma+1} \tag{5.7.14}$$

Substituting the above equation into Eq. 5.7.13, we get

$$\theta_{\eta' \to 1} \longrightarrow -(1-\eta') \tag{5.7.15}$$

From the definition of θ

$$\theta = R_s \ddot{R}_s / \dot{R}_s^2 = \frac{R_s}{\dot{R}_s} \frac{d\dot{R}_s}{dR_s}$$

and the identity

$$R_s \frac{d}{dR_s} = \theta M_s \frac{d}{dM_s} = -2\theta \eta' \frac{d}{d\eta'}$$

we can write Eq. 5.7.15 as

$$\theta = -\frac{R_s}{2\eta'} \frac{d\eta'}{dR_s} \simeq -\frac{R_s}{2} \frac{d\eta'}{dR_s} \tag{5.7.16}$$

since $\eta' \simeq 1$. Substituting Eq. 5.7.16 into Eq. 5.7.15 and noting that $\epsilon = 1-\eta'$ and $d\eta' = -d\epsilon$, we get

$$\frac{R_s}{2} \frac{d\epsilon}{dR_s} = -\epsilon \tag{5.7.17}$$

Integrating the above equation yields

$$\epsilon = 1-\eta' = \left(R_{s\circ}/R_s\right)^2 \tag{5.7.18}$$

where $R_{s\circ}$ is an arbitrary constant of integration. Since $\eta' = \dot{R}_{cj}^2/\dot{R}_s^2$, where $\dot{R}_{cj}$ is the Chapman-Jouguet detonation velocity, we can write Eq. 5.7.18 as

$$\left[1 - \left(\frac{R_{so}}{R_s}\right)^2 \right]^{\frac{1}{2}} dR_s = \dot{R}_{cJ} dt$$

Since $R_{so}/R_s \ll 1$, we can expand the square bracket and taking the first term only upon integration yields

$$\dot{R}_{cJ}(t - t_o) = R_s \left[1 + \frac{1}{2}\left(\frac{R_{so}}{R_s}\right)^2 + \cdots \right] \tag{5.7.19}$$

Substituting Eq. 5.7.18 into Eqs. 5.7.2 and 5.7.4 we get the asymptotic decay laws for a planar Chapman-Jouguet detonation as follows

$$\frac{\rho}{\rho_{cJ}} = 1 + \frac{(1 - \eta_{cJ})}{\gamma + \eta_{cJ}} \cdot \left(\frac{1 + \eta_{cJ}}{1 - \eta_{cJ}}\right)^{\frac{1}{2}} \left(\frac{R_{so}}{R_s}\right) + \cdots \tag{5.7.20}$$

$$\frac{u}{u_{cJ}} = 1 + \left(\frac{1 + \eta_{cJ}}{1 - \eta_{cJ}}\right)^{\frac{1}{2}} \cdot \frac{R_{so}}{R_s} + \cdots \tag{5.7.2}$$

$$\frac{p}{p_{cJ}} = 1 + \frac{\gamma(1 - \eta_{cJ})}{\gamma + \eta_{cJ}} \left(\frac{1 + \eta_{cJ}}{1 - \eta_{cJ}}\right)^{\frac{1}{2}} \frac{R_{so}}{R_s} + \cdots \tag{5.7.22}$$

Eqs. 5.7.19 to 5.7.22 are identical to those given by Levin and Chernyi. From Eq. 5.7.19 we see that a planar detonation wave tends towards an asymptote

$$R_s - \dot{R}_{cJ} t = const. \tag{5.7.23}$$

as it approaches a Chapman-Jouguet wave. For a non-reacting planar blast wave, the asymptotic law as given by Sedov is

$$C_o(t - t_o) = R_s \left[1 - \left(\frac{R_{so}}{R_s}\right)^{\frac{1}{2}} - \frac{1}{8} \frac{R_{so}}{R_s} \ln\left(\frac{R_s}{R_{so}}\right) + \cdots \right] \tag{5.7.24}$$

From Eq. 5.7.24, we see that the decay of a planar blast to an acoustic wave has no asymptote. The blast trajectory always intersects the straight line $R_S - C_o t$ = constant for any large value of the constant.

For cylindrical and spherical symmetry, $j \neq 0$ and the first term in Eq. 5.7.12 remains

$$\theta = -j\left(\frac{\gamma \cdot \eta_{cT}}{2(\gamma+1)}\right)\left(\frac{1-\eta_{cT}}{1+\eta_{cT}}\right)^{\frac{1}{2}}(1-\eta')^{\frac{1}{2}} - (\gamma+1)\frac{(1-\eta')}{2}\frac{\partial\phi}{\partial\xi}\Big|_{\xi=1,\eta'\to1} \qquad (5.7.12)$$

From Eq. 5.7.12 given above, we see that the first term on the right hand side vanishes as $\eta' \to 1$ like $(1-\eta')^{1/2}$. However in Chapter III, it was shown that for the self-similar solutions of cylindrical or spherical Chapman-Jouguet detonations, the slope of the particle velocity at the front is infinite and behaves like $(1-\xi)^{-\frac{1}{2}}$ as $\xi \to 1$. Hence it seems reasonable to assume that the second term of Eq. 5.7.12 (i.e., $\frac{\gamma+1}{2}(1-\eta')\frac{\partial\phi}{\partial\xi}\Big|_{\xi=1,\eta'\to1}$) must behave like $(1-\eta')^{\frac{1}{2}}$ as $\eta' \to 1$ although we have to carefully look into this further and exercise great care in the taking of the limits of both ξ and η' as they approach unity. With the assumption that the second term behaves as $(1-\eta')^{\frac{1}{2}}$ as $\eta' \to 1$, we can write Eq. 5.7.12 as

$$\theta = -N(1-\eta')^{\frac{1}{2}} \qquad (5.7.25)$$

where N is some constant depending on the behavior of the limits of the second term of Eq. 5.7.12. Using Eq. 5.7.16, we can write Eq. 5.7.25 as

$$\theta = -\frac{R_S}{2}\frac{d\eta'}{dR_S} = -N(1-\eta')^{\frac{1}{2}} \qquad (5.7.26)$$

Integrating the above equation yields

$$(1-\eta_o')^{\frac{1}{2}} - (1-\eta')^{\frac{1}{2}} = N \ln \frac{R_s}{R_{so}}$$

or

<div style="text-align: right">(5.7.27)</div>

$$\epsilon^{\frac{1}{2}} = \epsilon_o^{\frac{1}{2}} - N \ln \frac{R_s}{R_{so}}$$

where $R_s = R_{so}$ at $\eta' = \eta_o'$. From the above equations we see that as $\eta' \to 1$ and $\epsilon \to 0$, the detonation becomes a Chapman-Jouguet wave and we have

$$R_{s\infty} = R_{so} \, e^{\frac{(1-\eta_o')^{\frac{1}{2}}}{N}}$$

<div style="text-align: right">(5.7.28)</div>

where $R_{s\infty}$ is the radius when the detonation becomes a Chapman-Jouguet detonation wave. It should be remembered that Eq. 5.7.28 is valid only when η_o' is very close to unity itself. In practice $R_{s\infty}$ can be obtained by extrapolation as $\eta_o' \to 1$ using various values of R_{so} and η_o' from some non-similar solution to determine the corresponding $R_{s\infty}$. Since Eq. 5.7.28 is only valid for sufficiently small values of $1-\eta_o'$, the non-similar method used must be accurate in this regime. We have found that both the perturbation and the quasi-similar method is quite inaccurate for $\eta' \sim 1$ but the method of Porzel yields excellent results in this regime.

The corresponding asymptotic decay laws for cylindrical and spherical detonations can be obtained by substituting Eq. 5.7.27 into Eqs. 5.7.2 to 5.7.4 as demonstrated in the planar case.

CHAPTER VI

ASYMPTOTIC SELF-SIMILAR MOTION

6.1 General Considerations

The initial conditions necessary for the existence of self-similar solutions are in general quite impossible to fulfill in practice. For example the constant energy self-similar solution for strong blast waves requires an idealized point, line or planar energy source of infinite power density, the self-similar solution for piston driven shocks requires the piston to have an infinite acceleration at the initial instant, and the self-similar solution for the explosion of a gas sphere into a vacuum requires special initial distributions of the fluid states in the sphere. If these idealized initial conditions are not met, and self-similar solutions exist, they cannot be valid initially but may give an approximate description of the asymptotic behavior when the influence of the initial conditions of the motion becomes vanishingly small. For example if a blast wave is generated by the release of energy in a finite time τ and in a finite volume of radius R_i , then the constant energy self-similar solution can only be used to describe the motion at late times $t \gg \tau$ and at a shock radius $R_s \gg R_i$, providing of course the shock strength still remains sufficiently strong to neglect counter-pressure effects. It should be pointed out that even when the conditions $t \gg \tau$ and $R_s \gg R_i$ are satisfied, the self-similar solution cannot be uniformly valid in space from r = 0 to r = R_s . The mass that has been subjected to the initial non-similar motion can never acquire the self-similar form. Hence in practice the self-similar profiles are only valid in the neighbourhood of the shock front and cannot describe the flow in the region near the center. As a result, the energy scaling principle is not valid even though the blast

- 275 -

trajectory and flow near the shock front may adequately be described by
the self-similar motion since taking the energy integral from r = 0 to
r = R_s includes mass that bears the memory of the initial non-similar
motion.

To illustrate the influence of the initial non-similar condi-
tions on the asymptotic self-similar motion, consider an experiment on
the propagation of a cylindrical blast wave generated by a linear spark
discharge or an exploding wire. For diagnostics, we measure say the
blast trajectory and the shock pressure variation with radius. By
matching the experimental blast trajectory (or shock pressure vs shock
radius) at late times with a theoretical one obtained from the self-
similar constant energy solution, we can determine the equivalent blast
energy E_o. The equivalent blast energy determined in this manner will
be less than the discharge energy E_d (i.e., the energy stored in the
capacitor $\frac{1}{2}CV^2$ less the resistive losses of the leads). This
energy difference $\Delta E = E_d - E_o$ will be greater the longer the dis-
charge time τ, which can easily be changed experimentally by altering
the discharge circuit parameters. The energy difference ΔE can be
interpreted as the fraction of the discharge energy that remains in the
mass bearing the memory of the non-similar initial motion while the
equivalent blast energy is the fraction of the discharge energy that
goes to the self-similar flow. The energy integral can thus be written
as

$$E_d = \int_o^{R_N} (\rho e + \rho\frac{u^2}{2}) k_j r^j dr + \int_{R_N}^{R_s} (\rho e + \rho\frac{u^2}{2}) k_j r^j dr$$

or in the similarity coordinates

$$\frac{E_d}{\rho_o c_o^2 k_j} = \int_0^{\xi_N} \left(\frac{f}{\gamma-1} + \frac{u_o \phi^2}{2}\right) \xi^j d\xi + \int_{\xi_N}^1 \left(\frac{f}{\gamma-1} + \frac{u_o \phi^2}{2}\right) \xi^j d\xi \qquad (6.1.1)$$

where R_N or $\xi_N = R_N/R_S$ is the boundary separating the non-similar from the self-similar region of the flow field. Since R_N, hence ξ_N, is unknown and can only be determined with an exact numerical solution of the problem, the energy integral therefore cannot provide the scaling constant for the blast trajectory. With a sufficiently rapid discharge and a vanishingly small source volume (i.e., $\tau \to o$, $R_i \to O$) the non-similar region becomes relatively small and the first integral on the right hand side of Eq. 6.1.1 can be neglected since $\xi_N \sim o$. Under this condition the energy integral can then be used to obtain the scaling constant A (i.e., $R_S = A t^N$). In practice, the shock strength must remain sufficiently strong at large shock radii where the non-similar initial conditions have negligible influence on the shock motion otherwise non-similar effects from another source (i.e., counter-pressure) begin to come in and there will be no limiting self-similar regime at any time for the propagation of the shock wave (except the limiting acoustic form).

In general, if the initial motion is non-similar and asymptotically approaches a self-similar motion, it is evident that the initial conditions, which dictate the early time non-similar motion, cannot be used to determine the self-similar solution for the motion at later times. The asymptotic self-similar solution must be found from the basic equations of motion themselves. However the asymptotic self-similar solutions cannot be completely determined, but contain certain constants which bear the memory of the initial non-similar motion. Zeldovich called this type of

asymptotic solution, self-similar motion of "the second class". In
contrast, self-similar motions of the first class are those in which
the initial conditions can be used to completely and uniquely determine
the solution such as the point blast problem of Chapter IV. Important
examples of this second class of self-similar motions are the implosion
problem, the propagation of a planar strong shock wave near the vacuum
edge of a star and the "sharp blow" problem. In this Chapter we shall
investigate these asymptotic self-similar motions starting with the
"sharp blow" problem. This is a particularly interesting problem since
in principle, it belongs to the explosion problem of the first class of
self-similar motion in which the initial conditions can be used to deter-
mine the solution (i.e., θ from the energy integral). However it turns
out that the energy integral is infinite if a self-similar solution
exists for all times and hence cannot be used to find θ . The solution
is found instead from the consideration of the singularities of the basic
conservation equations, a method of solution typical for the so called
second class of self-similar problems.

6.2 The Sharp Blow Problem

For the theoretical model, we consider initially a semi-infinite slab of gas at uniform pressure A and density B occupying the positive r half-plane (i.e., $0 \leq r < \infty$). In the negative r half-plane $-\infty < r < 0$, we have a vacuum environment. At time $t = 0$, it is assumed that a sufficient amount of energy is released at $r = 0$ to generate a strong shock wave which subsequently propagates into the gas in the positive r half-plane. Since the energy is assumed to be released in a vanishingly small volume at $t = 0$, the thermodynamic states of the gas are very high. In fact the temperature as well as the sound speed are infinite according to this theoretical model. Therefore simultaneously with the shock motion to the right, the gas escapes at infinite speed to the left. Hence at any time t, the gas motion is bounded by the shock front $r = R_s$ and the escape front at $r = -\infty$. The theoretical model, just described, is highly idealized but we shall see later how the self-similar solution based on this idealized model represents the asymptotic behavior of some realistic models with non-similar conditions.

If the shock remains sufficiently strong, self-similar solutions exist for the conditions specified by the present theoretical model. The self-similar equations of motion derived previously in Chapter II for planar symmetry and uniform initial density (i.e., $j = 0$, $\omega = 0$) can be written as

$$(\phi - \xi)\psi' + \psi\phi' = 0 \tag{6.2.1}$$

$$(\phi - \xi)\phi' + \theta\phi + \frac{1}{\psi}f' = 0 \tag{6.2.2}$$

$$(\phi - \xi)f' + \gamma f\phi' + 2\theta f = 0 \tag{6.2.3}$$

where $\theta = \dfrac{R_s \ddot{R}_s}{\dot{R}_s^2}$ = constant. (6.2.4)

The solution of Eq. 6.2.4 yields the following form for the shock trajectory

$$R_s = A t^N \tag{6.2.5}$$

with $\quad N = \dfrac{1}{1-\theta}$ (6.2.6)

The flow is bounded by the shock $r = R_s$ and the escape front at $r = -\infty$ corresponding to the limits for the similarity variable $-\infty < \xi \leq 1$. At the shock front the boundary conditions are given by the limiting strong shock relationships as

$$\psi(1) = \frac{\gamma+1}{\gamma-1} \tag{6.2.7}$$

$$\phi(1) = f(1) = \frac{2}{\gamma+1} \tag{6.2.8}$$

At the escape front, we have both the pressure and the density equal to zero.

$$\psi(-\infty) = f(-\infty) = 0 \tag{6.2.9}$$

The problem reduces then to the task of seeking a continuous solution to Eqs. 6.2.1 to 6.2.3 satisfying the boundary conditions at the shock front $\xi = 1$ (i.e., Eqs. 6.2.7 and 6.2.8) and at the escape boundary $\xi = -\infty$ (i.e., Eq. 6.2.9).

The choice of the appropriate solution depends on the value of the parameter θ , which i is yet unknown. For the self-similar solutions of the first class (e.g., the constant energy blast wave solution) θ can be determined from the initial conditions through dimensional considerations

of the energy integral. Writing the energy integral for the present

problem, we have

$$E = \int_{-\infty}^{R_s} \left(\frac{b}{\gamma-1} + \frac{\rho u^2}{2}\right) dr = \rho_0 \dot{R}_s^2 R_s \int_{-\infty}^{1} \left(\frac{f}{\gamma-1} + \frac{\psi}{2}\phi^2\right) d\xi \qquad (6.2.10)$$

For the symmetrical planar blast problem treated in Chapter I^V, we note

that the limits of the integral are finite (i.e., $0 \le \xi \le 1$). In the

present problem, the integral is bounded between $-\infty < \xi \le 1$. Hence if

the solution is continuous in the region $-\infty < \xi \le 1$ (i.e., no singulari-

ties) and yields an energy integral which is finite, then Eq. 6.2.10 can

be used to determine θ . By demanding that self-similar solutions exist,

the energy integral must be time independent. Hence we have

$$R_s \dot{R}_s^2 = A^3 N^2 t^{2(N-1)+N} \qquad = \text{constant}$$

and the time exponent $2(N-1)+N$ must vanish yielding $N = \frac{2}{3}$ (i.e.,

$\theta = -\frac{1}{2}$). However if this value of $\theta = -\frac{1}{2}$ is used and the similarity

equations are integrated with the strong shock conditions at $\xi = 1$, we

encounter the singularity $(\phi - \xi)^2 - \gamma f/\psi$ somewhere in the flow field

$-\infty < \xi \le 1$ resulting in ψ', f' and ϕ' to be infinite. For the

symmetrical blast problem treated in Chapter IV, this value of $\theta = -\frac{1}{2}$

does not result in a singularity in the region of interest and the solu-

tion is continuous for $0 \le \xi \le 1$. Since there is no physical reason for

the existence of such a singularity in the present problem, the value of

$\theta = -\frac{1}{2}$ obviously does not yield the physically acceptable solution.

Hence the energy integral cannot be used to determine θ a priori in this

"sharp blow" problem and the criterion of a continuous, singularity free

solution in the region of interest, satisfying the prescribed boundary

conditions, must be used instead. In other words θ is not known before-

hand and trial values of θ must be used until a particular value of θ is found that gives a continuous solution in the region $-\infty < \xi \leq 1$.

The singularity that is encountered in this second class of self-similar problems is when $(\phi - \xi)^2 - \gamma f/\psi = 0$. As pointed out in Chapter II, the occurence of this singularity implies that one of the physical characteristics coincides with a constant ξ line. To illustrate this, let $\xi = \xi^*$ when $(\phi - \xi)^2 - \gamma f/\psi = 0$ and at the constant ξ^* line, we have

$$\frac{dr}{dt} = \xi^* \dot{R}_s \qquad (6.2.11)$$

Solving for ξ^* from $(\phi - \xi^*)^2 - \gamma f/\psi = 0$, we get

$$\xi^* = \phi \pm \left(\frac{\gamma f}{\psi}\right)^{1/2} \qquad (6.2.12)$$

and equating Eq. 6.2.11 and 6.2.12 yields

$$\xi^* = \frac{1}{R_s}\frac{dr}{dt} = \phi \pm \left(\frac{\gamma f}{\psi}\right)^{\frac{1}{2}} = \frac{u}{R_s} \pm \frac{c}{R_s}$$

or

$$\frac{dr}{dt} = u \pm c \qquad (6.2.13)$$

which simply shows that the constant ξ^* line coincides with one of the physical characteristics of the basic conservation equations. Illustrating this graphically, consider the r-t plane below
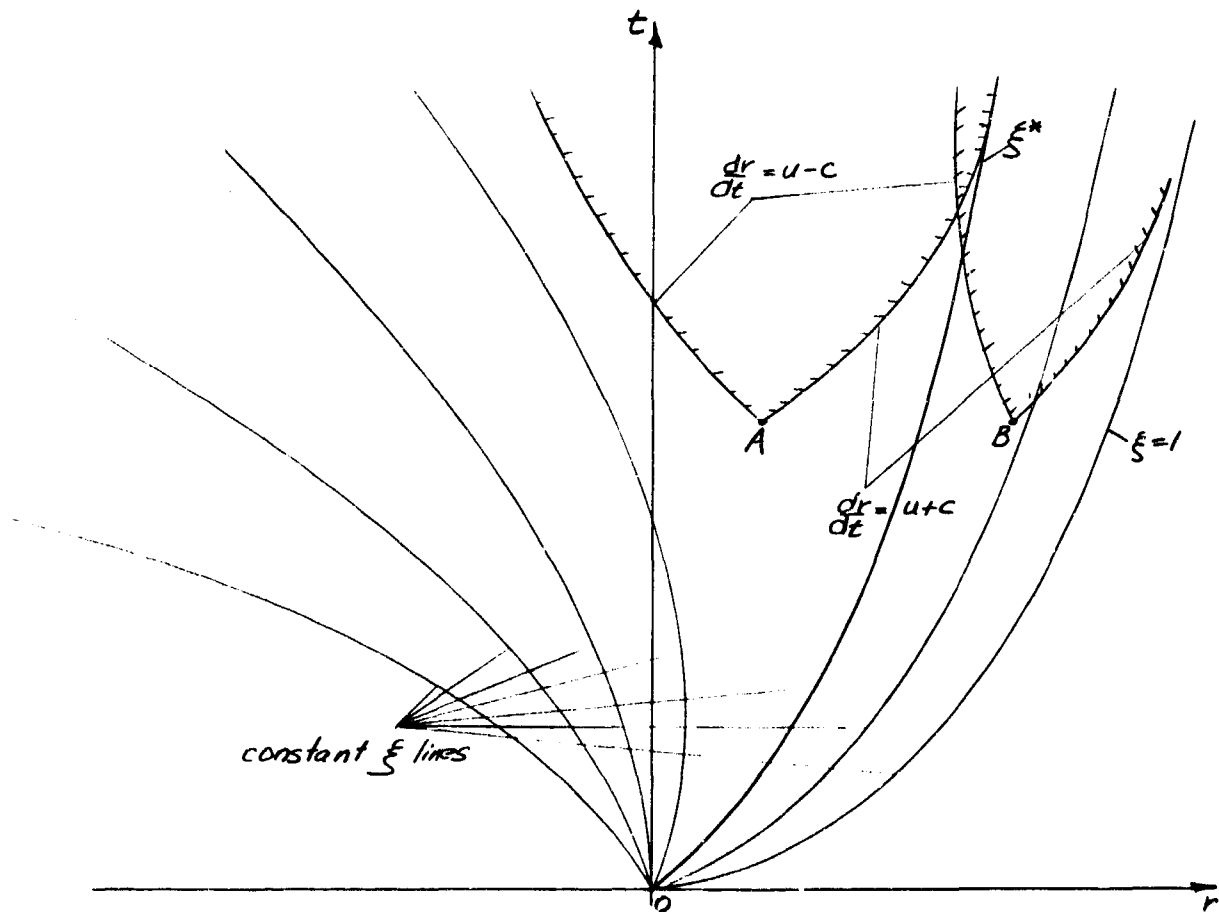
At the shock front $\xi = 1$, $(\phi \cdot \xi)^2 - \frac{\gamma f}{\gamma} = -\frac{(\gamma-1)}{\gamma+1} < 0$ and in the region $\xi^* < \xi < 1$, we have $(\phi \cdot \xi)^2 - \gamma f / \gamma < 0$. In the region $-\infty < \xi \leq \xi^*$, $(\phi \cdot \xi)^2 - \gamma f / \gamma > 0$ and at $\xi = \xi^*$, $(\phi \cdot \xi)^2 - \gamma f / \gamma = 0$. Any message in the flow field is transmitted into the corresponding region of influence which is bounded by the two characteristics $dr/dt = u \pm c$. Hence any disturbances generated at point B in the region $\xi^* < \xi < 1$ can influence the shock front upstream as well as the entire flow field downstream of B. However, disturbances generated at point A in the flow region $-\infty < \xi < \xi^*$ can only affect the flow region upstream to $\xi = \xi^*$ and downstream to $\xi \to -\infty$. Messages cannot be transmitted past the $\xi = \xi^*$

line upstream to influence the shock motion since the physical characteristic $\frac{dr}{dt} = u+c$ coincides with the ξ^* line. Since disturbances in the region $\xi^* < \xi < 1$ can ultimately be transmitted past the ξ^* line downstream to influence the entire flow field, it seems logical that the solutions for the two regions $\xi^* < \xi < 1$ and $-\infty < \xi < \xi^*$ must match along their common boundary ξ^*. From this physical consideration the criterion for determining the physically acceptable solution for this second class of self-similar problem is to guarantee the matching of solutions at the ξ^* boundary. In other words the parameter θ (or the time exponent N) must be so chosen such that the solution is continuous across the ξ^* boundary. It should be noted that the solution determined in this manner is independent of the initial conditions of the problem, even though they may be non-similar. The existence of the ξ^* line isolates a region behind the shock from the rest of the flow field. Hence even if the region $-\infty < \xi < \xi^*$ is non-similar, it cannot influence the self-similar region near the shock. The existence of the ξ^* line is a typical and necessary property of asymptotic self-similar motions originating from some non-similar initial flows.

Solving for the derivatives ψ', ϕ' and f' from the similarity equations (i.e., Eqs. 6.2.1 to 6.2.3) we get

$$\frac{d\psi}{d\xi} = \frac{-2\theta f + (\phi - \xi)\theta \phi \psi}{(\phi - \xi)[(\phi - \xi)^2 - \gamma f/\psi]} \tag{6.2.14}$$

$$\frac{d\phi}{d\xi} = \frac{-(\phi - \xi)\theta \phi + 2\theta f/\psi}{(\phi - \xi)^2 - \gamma f/\psi} \tag{6.2.15}$$

$$\frac{df}{d\xi} = \frac{-(\phi-\xi)\cdot2\theta f + \gamma\theta f \phi}{(\phi-\xi)^2 - \gamma f/\psi} \tag{6.2.16}$$

Hence we see that in order for ψ', ϕ' and f' to be finite as $\xi \to \xi^*$ and $(\phi-\xi)^2 - \gamma f/\psi \to 0$, the numerators of the above equations must simultaneously approach zero as well. In other words

$$-2\theta f + (\phi-\xi)\theta\phi\psi \to 0$$

$$-(\phi-\xi)\theta\phi + 2\theta f/\psi \to 0 \tag{6.2.17}$$

$$-2\theta f(\phi-\xi) + \gamma\theta f\phi \to 0$$

as $\xi \to \xi^*$. Substituting $(\phi^*-\xi^*)^2 = \gamma f^*/\psi^*$ into the above equations, we find that all three of them are simultaneously satisfied if

$$(\phi^*-\xi^*)\cdot\frac{2\theta}{\gamma} = \theta\phi^*$$

or $$\phi^* = \frac{2\xi^*}{2-\gamma} \tag{6.2.18}$$

Hence the method of solution for the present problem is to choose an arbitrary value of θ and proceed to integrate numerically the similarity equations with the strong shock conditions at $\xi = 1$. A convergent iteration procedure for θ is required that ultimately satisfies Eq. 6.2.18 at the singularity $(\phi-\xi)^2 - \frac{\gamma f}{\psi} = 0$. Due to the resulting indeterminancy of the slopes ψ', ϕ' and f' near the singularity ξ^*, numerical work can be facilitated if an analytical solution in the neighborhood of ξ^* is obtained by expanding the solution in powers of $(\xi-\xi^*)$. The numerical integration can then terminate close to the singularity and the analytical solution can be used to carry the integration through the singular

point $\xi = \xi^*$. The numerical value for the time exponent N(i.e., $R_S = At^N$) for different values of γ as computed by Rae is given below.

γ	N
1	0.500
1.1	0.568
1.4	0.600
5/3	0.6107
3	0.627
7	0.636
∞	0.642

Note that all values for N here are less than N = 2/3 which corresponds to the constant energy solution for the planar blast and is determined from the energy integral.

It is interesting to note that there exists a closed form solution for the "sharp blow" problem for the particular value of γ = 1.4. This can be found by first assuming a solution for the particle velocity ϕ of the form

$$\phi = a\xi + b \qquad (6.2.19)$$

where a and b are numerical constants and then proceed to determine the forms of the solutions for the density ψ and pressure f from the basic conservation equations. Substituting Eq. 6.2.19 into the continuity equation (i.e., Eq. 6.2.1) we get

$$\frac{d\psi}{\psi} + \frac{a\,d\xi}{(a-1)\xi + b} = 0 \qquad (6.2.20)$$

which can readily be integrated to yield

$$\psi = K\left[(a-1)\xi + b\right]^{\frac{-a}{a-1}} \qquad (6.2.21)$$

where K is a numerical integration constant. Substituting Eqs. 6.2.19 and 6.2.21 into the momentum equation (i.e., Eq. 6.2.2) we obtain

$$f' = -K\theta\left[(a-1)\xi + b\right]^{-\frac{a}{a-1}}(a\xi + b) - Ka\left[(a-1)\xi + b\right]^{-\frac{a}{a-1}+1} \qquad (6.2.22)$$

If the assumed forms of the solutions are exact, they must satisfy the energy equation as well. Using the particle velocity and the density profiles obtained, another expression for the pressure f can be found from the energy equation (i.e., Eq. 6.2.3) as follows

$$\frac{f'}{f} = -\frac{(\gamma\phi' + 2\theta)}{\phi - \xi} = -\frac{(\gamma a + 2\theta)a\xi}{(a-1)\xi + b} \qquad (6.2.23)$$

The above equation can be integrated to yield

$$f = k_1\left[(a-1)\xi + b\right]^{-\frac{(\gamma a + 2\theta)}{a-1}} \qquad (6.2.24)$$

and differentiating the above equation yields another expression for f' as

$$f' = -(\gamma a + 2\theta)k_1\left[(a-1)\xi + b\right]^{-\frac{(\gamma a + 2\theta)}{a-1} - 1} \qquad (6.2.25)$$

Eqs. 6.2.25 and 6.2.22 must be identical if the assumed form of the solution for ϕ is an exact solution of the basic equations. Eq. 6.2.22 can be expressed in a more convenient form using the identity

$$a\xi + b = \frac{a}{a-1}\left[(a-1)\xi + b\right] - \frac{b}{a-1}$$

as

$$f' = \frac{k\theta b}{a-1}\left[(a-1)\xi+b\right]^{-\frac{a}{a-1}} - k\left(a+\frac{\theta a}{a-1}\right)\left[(a-1)\xi+b\right]^{-\frac{a}{a-1}-1} \qquad (6.2.26)$$

In order for the two expressions for f' given by Eqs. 6.2.26 and 6.2.25, to be identical, we have for $k \neq 0$, either

$$\frac{\theta b}{a-1} = 0 \qquad \text{or} \qquad a+\frac{\theta a}{a-1} = 0 \qquad (6.2.27)$$

Since θ and b are non zero, we must have

$$\theta = -(a-1) \qquad (6.2.28)$$

Equating Eqs. 6.2.25 and 6.2.26, we get

$$-(\gamma a+2\theta)k_1\left[(a-1)\xi+b\right]^{-\frac{(\gamma a+2\theta)}{a-1}-1} = \frac{k\theta b}{a-1}\left[(a-1)\xi+b\right]^{-\frac{a}{a-1}} \qquad (6.2.29)$$

Since the exponents of the square bracketed terms in Eq. 6.2.29 must be identical, we can solve for a and using Eq. 6.2.28 we get the following result

$$a = -\frac{1}{\gamma-2} \qquad (6.2.30)$$

The solutions must satisfy the boundary conditions at the shock front $\xi = 1$. From Eqs. 6.2.19, 6.2.21 and 6.2.24, we get

$$\phi(1) = \frac{2}{\gamma+1} = a+b \qquad (6.2.31)$$

$$k = \psi(1)\left[a+b-1\right]^{\frac{a}{a-1}} = \frac{\gamma+1}{\gamma-1}\left[a+b-1\right]^{\frac{a}{a-1}} \qquad (6.2.32)$$

$$K_1 = f(1)\left[a+b-1\right]^{\frac{\gamma a + 2\theta}{a-1}} = \frac{2}{\gamma+1}\left[a+b-1\right]^{\frac{\gamma a + 2\theta}{a-1}} \tag{6.2.33}$$

From Eqs. 6.2.30 and 6.2.31, we obtain

$$b = \frac{3(\gamma-1)}{(\gamma+1)(\gamma-2)} \tag{6.2.34}$$

Equating the coefficients of $\left[(a-1)\xi + b\right]$ in Eq. 6.2.29 yields

$$\frac{k}{k_1} = \frac{-(\gamma a + 2\theta)(a-1)}{\theta b} \tag{6.2.35}$$

and substituting Eqs. 6.2.30 for a, 6.2.34 for b and 6.2.28 for θ, Eq. 6.2.35 becomes

$$\frac{k}{k_1} = \frac{(\gamma+1)(\gamma-2)}{3(\gamma-1)} \tag{6.2.36}$$

From Eqs. 6.2.32 and 6.2.33, we get also

$$\frac{k}{k_1} = -\frac{(\gamma+1)}{2} \tag{6.2.37}$$

Equating the two expressions for k/k_1 given respectively by Eqs. 6.2.36 and 6.2.37, we can solve for the value of γ as

$$\gamma = 7/5 = 1.4 \tag{6.2.38}$$

Using the value of $\gamma = 7/5$, the values for the constants a, b, K, K_1 and θ can be determined and the solutions for ϕ, f and ψ become

$$\phi = \frac{5}{6}(2\xi-1) \tag{6.2.39}$$

$$f = \frac{5}{6}\left(5-4\xi\right)^{-3/2} \tag{6.2.40}$$

$$\psi = 6 (5 - 4\xi)^{-5/2} \tag{6.2.41}$$

$$\theta = -2/3 \;, \quad N = 3/5 = .6000 \tag{6.2.42}$$

The above expressions give the exact solution for the present problem for the particular value of $\gamma = 7/5 = 1.4$. For other values of γ, closed form solutions cannot be obtained but the general behavior of the profiles is similar to that given by Eqs. 6.2.39 to 6.2.42.

The singularity ξ^{*} is found from the equation $(\phi \cdot \xi)^{2} - \gamma f/\psi = 0$ as

$$\xi^{*} = \phi^{*} \pm \left(\frac{\gamma f^{*}}{\psi_{*}} \right)^{1/2} \tag{6.2.43}$$

Substituting Eqs. 6.2.39 to 6.2.41 into the above expression yields

$$\xi^{*} = 5/4 \;, \quad -1/2 \tag{6.2.44}$$

Since the flow region is bounded by $-\infty \leq \xi \leq 1$, the solution for $\xi^{*} = 5/4$ can be discarded. For the solution to be regular at the singularity ξ^{*}, the condition

$$\phi^{*} = \frac{2\xi^{*}}{2 - \gamma} \tag{6.2.45}$$

must be satisfied. Using $\xi^{*} = -1/2$ in Eqs. 6.2.39 and 6.2.45, the value of ϕ^{*} obtained is identical. Hence the solution given by Eqs. 6.2.39 to 6.2.41 is continuous throughout the region $-\infty \leq \xi \leq 1$.

The solutions for ϕ, f and ψ given by Eqs. 6.2.39 to 6.2.41 are illustrated below
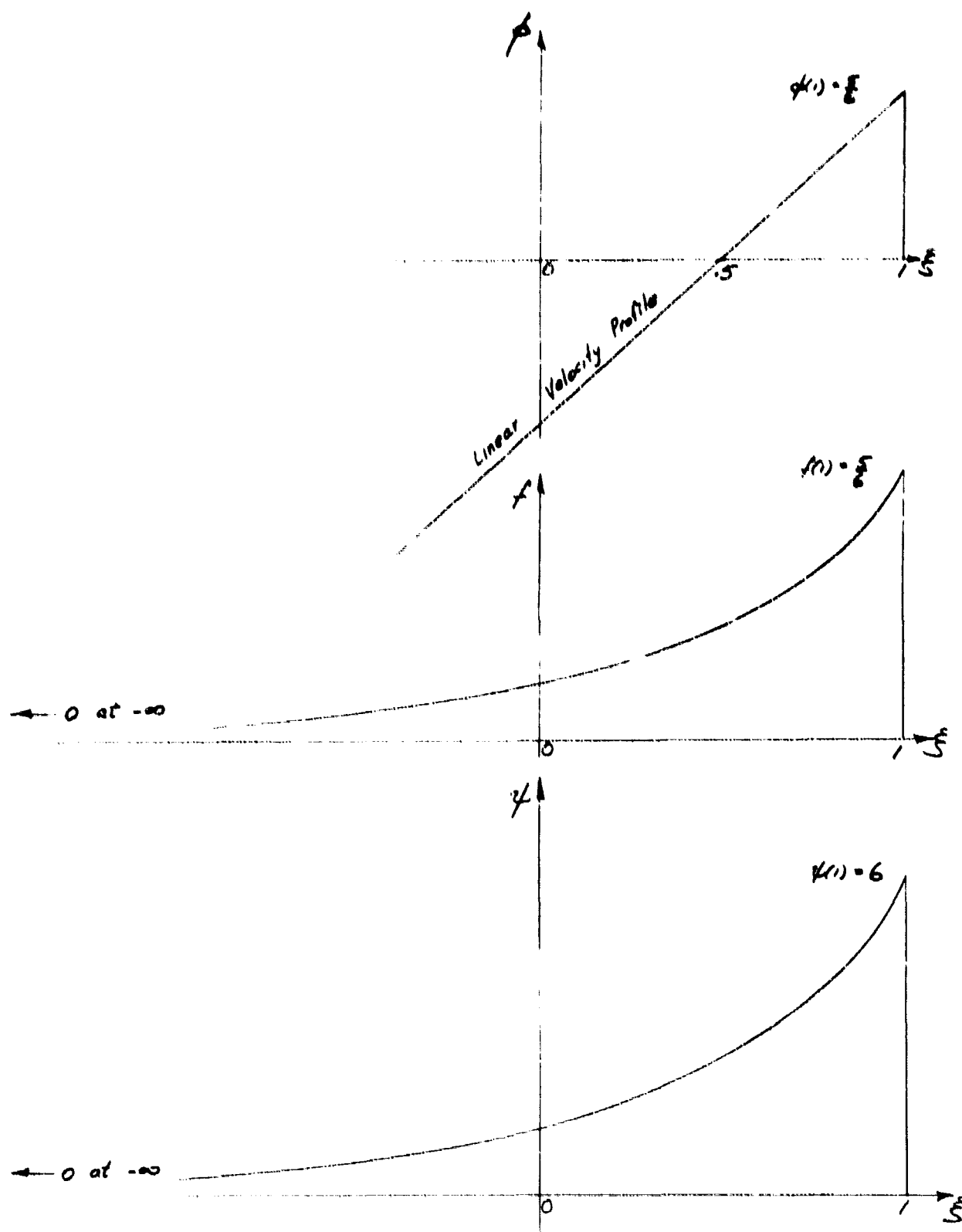
Since the solution (i.e., the time exponent N) is obtained from the basic equations themselves and not from the conservation of momentum and energy, let us now investigate the limitations on N imposed by the momentum and energy integrals. From the nature of the solution we see that part of the mass set in motion is carried by the shock to the right while the remaining part expands to the left into the vacuum environment. There exists a dividing boundary ξ' in which the particle velocity $\phi = 0$. The mass between this boundary and the shock is

$$M' = \int_{r'}^{R_s} \rho\, dr = \rho_0 R_s \int_{\xi'}^{1} \psi\, d\xi = \rho_0 R_s \cdot constant \qquad (6.2.46)$$

or
$$M' \sim t^N$$

For the particular case of $\gamma = 7/5$ where we have an exact solution, $\xi' = 1/2$ and

$$M' = .808\, \rho_0 R_s$$

where
$$R_s \cdot {}^{2/5}$$

From Eq. 6.2.46, we see that M' increases with time. Since both the particle velocities ahead of the shock and at the boundary ξ' are zero and the mass M' increases with time, the momentum in the volume bounded by the shock $\xi = 1$ and $\xi = \xi'$ must also increase with time. The momentum I' in this volume can be written as

$$I' = \int_{r'}^{R_s} \rho u\, dr = \rho_0 R_s \dot{R_s} \int_{\xi'}^{1} \psi\phi\, d\xi = constant \cdot t^{2N-1} \qquad (6.2.47)$$

and since I' increases with time the exponent N must be greater than 1/2. In other words

$$N > 1/2 \qquad (6.2.48)$$

The energy in the volume bounded by the shock and ξ' must decrease with time as M' increases with time since there is neither energy contribution from the mass coming in through the shock surface nor work being done on the gas by pressure forces at th boundary ξ' (i.e., $p'u'dt$ and the velocity $u'=0$). From the energy integral

$$ E' = \int_{r'}^{R_s} \left(\frac{p}{\gamma-1} + \frac{\rho u^2}{2}\right) dr = \rho_o \dot{R}_s^2 R_s \int_{\xi'}^{1} \left(\frac{f}{\delta-1} + \frac{\psi \phi^2}{2}\right) d\xi $$

$$ = \text{constant} \cdot t^{3N-2} \tag{6.2.49} $$

we see that the time exponent N must be less than 2/3, that is

$$ N < {}^2/_3 \quad . $$

for the energy E' to decrease with time. Therefore we see that N must have the range

$$ \frac{1}{2} < N < \frac{2}{3} \tag{6.2.50} $$

and the values of N for a range of $\gamma = 1$ to $\gamma = \infty$ given previously in the table fall within the prescribed range of Eq. 6.2.50.

Although the distributions of the fluid states behind the shock and the time exponent N of the shock trajectory are determined from the basic equations and boundary conditions, the solution is still incomplete. For example the proportionality constant A of the shock trajectory (i.e., $R_s = At^N$) which is determined by the initial conditions through the energy integral is as yet unknown. It cannot be obtained from the energy integral as in the blast wave problem since in this problem the integral diverges. In other words, the total energy bounded by the shock and the escape front in the self-similar motion is infinite. This is due to the kinetic energy near the vacuum edge being infinite since the particle velocity squared approaches infinity faster than the density goes to zero.

To illustrate this, let us seek the asymptotic solution near the vacuum boundary. Near the escape front, the pressure gradient is extremely small and neglecting it, the momentum equation becomes

$$(\phi - \xi)\phi' + \theta\phi = 0$$

which can be integrated immediately to yield

$$\phi = (1-\theta)\xi = \frac{\xi}{N} \tag{6.2.51}$$

Substituting this solution for ϕ into the continuity equation yields

$$\frac{d\psi}{\psi} = \frac{\theta}{1-\theta}\frac{d\xi}{\xi}$$

which can be integrated readily to give the asymptotic solution for the density ψ as

$$\psi = k\,|\xi|^{\frac{1-\theta}{\theta}} = k\,|\xi|^{-\frac{1}{1-N}} \tag{6.2.52}$$

In the above equation K is a constant of integration and the absolute value of ξ is used to guarantee a positive density always. Using now the asymptotic solutions for ϕ and ψ, the momentum equation yields the solution for the pressure f as

$$f = k_1\,|\xi|^{2-\frac{\gamma(1-\theta)}{\theta}} = k_1\,|\xi|^{2-\frac{\gamma}{1-N}} \tag{6.2.53}$$

k_1 is another integration constant and again the absolute value of ξ is used to ensure a positive pressure. The asymptotic solutions obtained are valid for general values of γ. Note that for the particular case of $\gamma = 7/5$ where we have the solutions in closed analytical forms given by Eqs. 6.2.36 to 6.2.41, they reduce, for large values of $|\xi|$, to the asymptotic forms given by Eqs. 6.2.51 to 6.2.53. From the asymptotic solutions, we see that since $\frac{1}{2} < N < \frac{2}{3}$, the kinetic energy $\phi^2\psi/2 \rightarrow 0$ as $\xi \rightarrow -\infty$. This leads to the divergence of the energy integral even though the solu-

tions for ϕ , ψ and f are continuous and singularity free. Hence

$$E = \int_{-\infty}^{R_s} \left(\frac{p}{\gamma-1} + \frac{\rho u^2}{2}\right) dr = \rho_0 \dot{R_s}^2 R_s \int_{-\infty}^{1} \left(\frac{f}{\gamma-1} + \phi \frac{\psi^2}{2}\right) dr = \infty$$

and explains why the energy integral cannot be used to evaluate the similarity exponent N for this problem. The fact that the self-similar solution for the "sharp blow" problem requires an infinite energy supply initially is quite interesting. In practice, the energy of the motion must be finite, but then the manner in which the energy is released initially is non-similar. Hence the self-similar solution represents an asymptotic solution and the infinite energy dilemma can be resolved by neglecting some mass near the vacuum edge that bears the memory of the starting process. In other words the asymptotic self-similar solution cannot be uniformly valid in the range $-\infty < \xi \leq 1$. This infinite energy dilemma is explained by Zeldovich and we will give the main aspects of it in the following discussion.

Let us first consider the following initial conditions. At time t = 0, a piston is pushed into the gas generating a shock wave. The piston path is such that the pressure at the piston face decreases to zero after a time interval τ , the piston is retracted and the gas expands to the left to vacuum and the shock propagates to the right into the gas at initial density ρ_0 . The pressure wave is given as
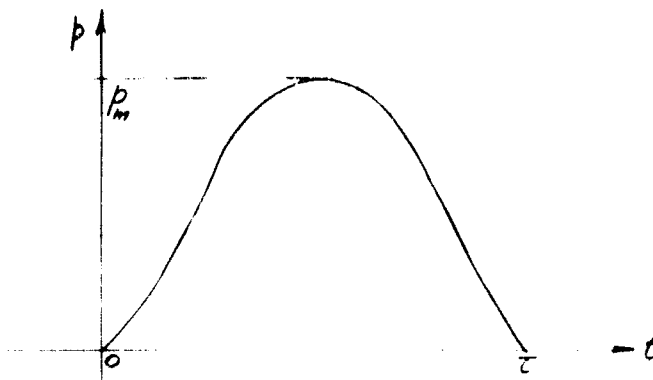
The momentum or impulse imparted to the gas by the piston is

$$\mathcal{J} = \int_0^\tau p\,dt = p_m\,\tau \int_0^I f\left(\tfrac{t}{\tau}\right) d\left(\tfrac{t}{\tau}\right) \qquad (6.2.54)$$

or $\qquad \mathcal{J} = a\,p_m\,\tau$

where $\qquad a = \int_0^I f\left(\tfrac{t}{\tau}\right) d\left(\tfrac{t}{\tau}\right)$

The energy imparted to the gas is equal to the work done by the piston

$$E = \int_0^\tau p\,u_p\,dt = \frac{b\,\tau\,p_m^{3/2}}{\rho_o^{1/2}} \qquad (6.2.55)$$

where

$$b = \int_0^I \frac{f\left(\tfrac{t}{\tau}\right) u_p\left(\tfrac{t}{\tau}\right)}{\left(\tfrac{p_m}{\rho_o}\right)^{1/2}} d\left(\tfrac{t}{\tau}\right)$$

and u_p is the piston velocity. For a square pressure pulse for example
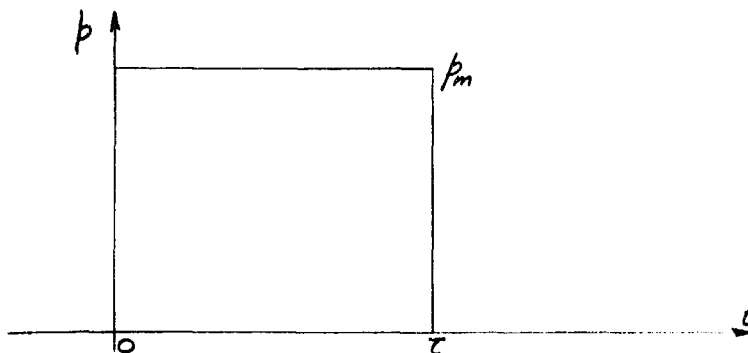
$a = 1$ and $b = \left(\tfrac{2}{\gamma+1}\right)^{1/2}$. The shock velocity is related to the pressure at the piston as

$$\dot{R}_S \sim \left(\tfrac{p_m}{\rho_o}\right)^{1/2}$$

and through the above relationship, the constant A of the shock path (i.e., $R_S \sim A t^N$) can be related to the initial conditions by the

expression below.

$$A \sim \left(\frac{p_m}{p_o}\right)^{\frac{1}{2}} \tau^{1-N} \tag{6.2.56}$$

If the asymptotic self-similar solution exists, then the parameter A must be finite as $\tau \to 0$. Therefore as $\tau \to 0$, p_m must approach infinity in the manner

$$p_m \to \tau^{-2(1-N)} \tag{6.2.57}$$

From Eq. 6.2.55, we note that the energy $E \sim p_m^{3/2} \tau$. Hence as $\tau \to 0$, $E \to \tau^{3N-2}$ and since $N < \frac{2}{3}$, the energy E in the self-similar motion is infinite. If the self-similar solution exists in the asymptotic limit as $\frac{t}{\tau} \to 0$, then it is evident that this self-similar solution cannot be uniformly valid in space encompassing all the mass set in motion from the shock to the escape boundary since the energy imparted to the gas is finite and uniform validity of the self-similar solution would signify infinite energy in the flow. We must then neglect a portion of the mass near the escape boundary that bears the imprint of the initial non-similar motion. To determine the mass that should be neglected, we have to solve the problem numerically and obtain the exact solution. However an accurate approximation can be made if we assume that the mass near the vacuum edge is adequately described by the asymptotic relationships obtained earlier as

$$\phi = \frac{\xi}{N} \tag{6.2.51}$$

$$\psi = k |\xi|^{-\frac{1}{1-N}} \tag{6.2.52}$$

$$f = K_1 |\xi|^{2 - \frac{\gamma}{1-N}} \tag{6.2.53}$$

Note that the constants K and K_1 in Eqs. 6.2.52 and 6.2.53 are related and the relationship can be obtained from the first integral as follows: As derived in Chapter II, the first integral is given as

$$\frac{\psi^{1 + \frac{\gamma(j+1)}{2\theta}} (\phi - \xi) \xi^j}{f^{\frac{j+1}{2\theta}}} = \text{constant}$$

and using the strong shock conditions at $\xi = 1$, the constant can be obtained and the first integral takes on the form

$$\frac{\psi^{1 + \frac{\gamma}{2\theta}} (\phi - \xi)}{f^{\frac{1}{2\theta}}} = \frac{-\left(\frac{\gamma-1}{\gamma+1}\right)\left(\frac{\gamma+1}{\gamma-1}\right)^{1 + \frac{\gamma}{2\theta}}}{\left(\frac{2}{\gamma+1}\right)^{\frac{1}{2\theta}}} \tag{6.2.58}$$

for the present planar geometry (i.e., $j = 0$). Using the asymptotic relationships for ψ and f , Eq. 6.2.58 yields the following expression for the constants K and K_1.

$$K_1 = \frac{K^\gamma}{\left(\frac{\gamma+1}{2}\right)\left(\frac{\gamma+1}{\gamma-1}\right)^\gamma (-K\theta)^{-2\theta}} \tag{6.2.59}$$

Note that θ is always negative since K_1 is positive. K can be found by integrating the similarity equations to a large negative value of ξ . For example for $\gamma = 1.4$, the value of $K = 3/16$ is obtained. In general K is a function of γ .

Let M_0 be the mass to be neglected and bounded by $-\infty < \xi \le \xi_*$.

$$m_o = \int_{-\infty}^{r_o} \rho \, dr = \rho_o R_s \int_{-\infty}^{\xi_o} \psi \, d\xi = \rho_o A t^N \int_{-\infty}^{\xi_o} \psi \, d\xi \qquad (6.2.60)$$

From the continuity equation, we have

$$\frac{d}{d\xi}(\phi \psi) = \xi \frac{d\psi}{d\xi}$$

and integrating by parts yields

$$\int_{-\infty}^{\xi_o} \psi \, d\xi = -\left[\psi(\phi - \xi) \right]_{-\infty}^{\xi_o} \qquad (6.2.61)$$

Using the asymptotic relationships for ψ and ϕ the mass integral can be determined and Eq. 6.2.60 can be written as

$$m_o = \rho_o A t^N \left(\frac{1-N}{N}\right) k \left| \xi_o \right|^{1 - \frac{1}{1-N}} \qquad (6.2.62)$$

For m_o to be time independent, we choose

$$\xi_o = -B t^{1-N} \qquad (6.2.63)$$

where $B > 0$ and Eq. 6.2.62 becomes

$$m_o = A K B^{\frac{-N}{1-N}} \cdot \frac{(1-N)}{N} \rho_o \qquad (6.2.64)$$

Neglecting m_o in the energy integral, we have

$$E_s = \rho_o A^3 N^2 t^{3N-2} \int_{\xi_o}^{1} \left(\frac{f}{\gamma - 1} + \frac{\psi \phi^2}{2} \right) d\xi \qquad (6.2.65)$$

As shown in Chapter IV, the integral in the above equation can be expressed

as

$$\int_{\xi_0}^{1}\left(\frac{f}{\gamma-1}+\frac{\psi\phi^2}{2}\right)d\xi = \frac{-N}{3N-2}\left[(\phi-\xi)\left(\frac{f}{\gamma-1}+\frac{\psi\phi^2}{2}\right)+f\phi\right]_{\xi_0}^{1}$$

Using the strong shock conditions at $\xi = 1$ and the asymptotic solutions near the vacuum edge we get

$$E_S = \rho_0\frac{A^3}{2}K\left(\frac{1-N}{2-3N}\right)B^{\frac{2-3N}{1-N}} \qquad (6.2.66)$$

Hence we see that by neglecting a small amount of mass m_0 , the energy integral can now be made time independent as the self-similar solution demands.

Let us now look at the momentum integral

$$\Pi = \int_{r_0}^{R_S}\rho u\,dr = \rho_0 R_S\dot{R}_S\int_{\xi}^{1}\psi\phi\,d\xi \qquad (6.2.67)$$

From the momentum equation

$$(\phi-\xi)\phi'+\theta\phi+\frac{1}{\psi}f' = 0,$$

and integrating, we get

$$f\Big|_{\xi_0}^{1} + \int_{\xi}^{1}\psi(\phi-\xi)\phi'd\xi +\theta\int_{\xi_0}^{1}\psi\phi\,d\xi = 0 \qquad (6.2.68)$$

From before we see that

$$\frac{d}{d\xi}\left[\psi(\phi-\xi)\right] = \psi$$

which when integrated by parts yields

$$\int_{\xi_0}^{1}\psi(\phi-\xi)\phi'd\xi = \psi\phi(\phi-\xi)\Big|_{\xi_0}^{1} + \int_{\xi_0}^{1}\psi\phi\,d\xi$$

Substituting the above equation into Eq. 6.2.68 yields

$$\left. f\right|_{\xi_o}^{\prime} + 4\phi(\phi-\xi)\Big|_{\xi_o}^{\prime} + (1+\theta)\int_{\xi_o}^{\prime} 4\phi\, d\xi = 0$$

Hence

$$\int_{\xi_o}^{\prime} 4\phi\, d\xi = -\frac{1}{1+\theta}\left\{ \left. f\right|_{\xi}^{\prime} + 4\phi(\phi-\xi)\Big|_{\xi_o}^{\prime}\right\} \tag{6.2.69}$$

The right hand side of Eq. 6.2.69 is zero at the upper limit $\xi = 1$ and at the lower limit the pressure f is small as compared to the other term $\phi 4(\phi-\xi)$. Therefore

$$\int_{\xi_o}^{\prime} 4\phi\, d\xi = -k\theta\frac{(1-\theta)}{1+\theta}\, |\,\xi_o|^{\frac{1+\theta}{\theta}} \tag{6.2.70}$$

We note that as $|\xi_o| \to \infty$, that is when all the mass is taken into account and described by the self-similar solution, the integral vanishes. Substituting Eq. 6.2.63 into Eq. 6.2.70, the momentum integral becomes

$$\Pi = \rho_o \dot{R}_s R_s \int_{\xi_o}^{\prime} 4\phi\, d\xi = \rho_o A^2 k \frac{(1-N)}{2N-1} B^{\frac{1-2N}{1-N}} \tag{6.2.71}$$

Using Eqs. 6.2.64, 6.2.66 and 6.2.71, we can express the shock trajectory as

$$R_s(t) = G(r)\frac{\Pi^2}{\rho_o E_s}\left(\frac{t}{\pi^3 \rho_o E_s^2}\right)^N \tag{6.2.72}$$

where

$$G(r) = \frac{2(2-3N)}{2N-1}\left[\frac{(2N-1)^3}{4k(1-N)(2-3N)^2}\right]^{1-N}$$

For $\gamma = 1.4$ Rae found that $K = 3/16$, $N = 0.6$ and $(\alpha \gamma) = (\frac{\ }{\ })$.
Numerical solutions for this problem with different loading histories (i.e.,
$f(t/\tau)$ of the piston) are given by Zhukov and Kazhdan.

6.1 Planar Shock Propagation in a Non-Uniform Density Field

In this Section we shall consider the asymptotic self-similar motion of a planar shock wave in a non-uniform density field. Particularly we shall consider the case in which the density decreases in the direction of the shock motion as a simple power law of the distance. Similar to the propagation of acoustic waves in a decreasing density field treated by Lamb, the shock amplifies since the energy density of the shock increases as the mass decreases. In the limit as the initial density $\rho_0 \to 0$, the shock strength $M_s \to \infty$. The limiting shock motion can be described by a self-similar solution of the second class in which the physically acceptable solution is determined by demanding the solution to be regular at the singularity $(\beta\xi)^\delta \quad V/y = 0$. This asymptotic solution is of interest in astrophysical problems as in the description of the emergence of a shock wave at a stellar surface in a supernova explosion (Frank-Kamenetskii and Gandel'man). Due to the high amplification of the shock wave at the edge of the star as $\xi' \to 0$, the temperature and the particle velocity behind the shock are extremely high. In fact the calculations by Colgate and Johnson indicate that the ejected mass from the star can acquire relativistic velocities and its kinetic energy can correspond to that of cosmic rays. There are other theories for the origin of cosmic rays in the universe and the shock wave theory is generally referred to as the hydrodynamic model. This asymptotic solution for the shock motion at the edge of a star has also been obtained by Sakurai. This solution is identical in many respects to the asymptotic self-similar solution for a strong converging shock wave obtained by Guderley and Butler. In the present problem, anticipation of the shock arises from the decrease in the initial density ρ_0 while for collapsing shock waves, the amplification is due to the area convergence.

We shall formulate the problem in a more general manner by considering a tube of length X_0, containing initially a gas with the density field described by a simple law

$$f_0 = \beta x^\delta \tag{6.3.1}$$

At time $t = 0$, a finite energy F_0 per unit area is released instantaneously at $x = X_m$, generating a strong planar blast wave. At later times the shock propagates in the direction of decreasing density towards the origin. We shall study first the initial phases of the shock motion in the vicinity of $x = X_m$ by a perturbation scheme and then the final asymptotic motion near the origin $x = 0$. In this way we can demonstrate the forgetfulness of the asymptotic motion on the initial conditions.

The theoretical model described simulates the following experimental situation.

Primary
Discharge

Secondary
Discharge
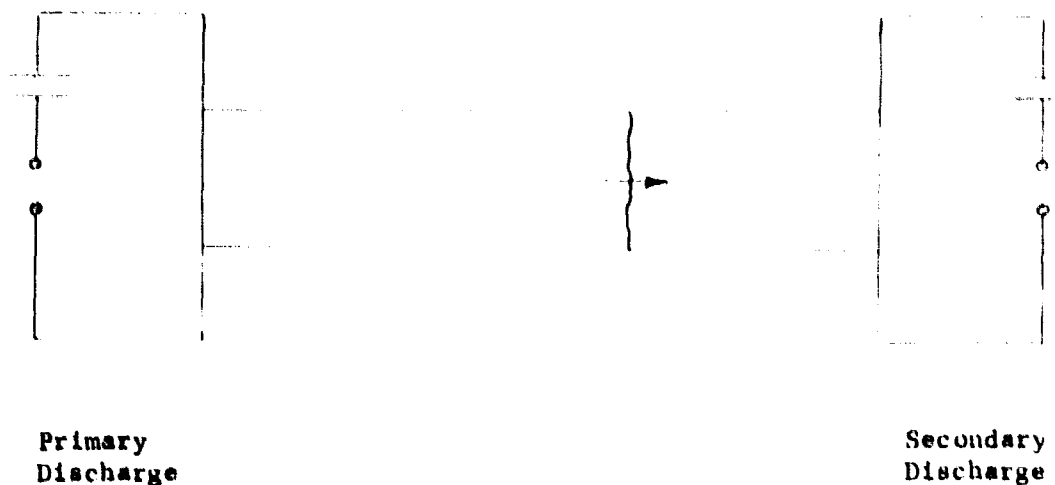
Consider a constant area tube filled with a cold gas initially. A strong planar blast is initiated at one end of the tube by discharging the primary low inductance capacitor bank. The secondary capacitor bank is charged to a voltage that is insufficient to break down the cold gas. As the blast reaches the other end, the hot ionized gas short out the electrodes and

the secondary bank fires, releasing its energy into the plasma generating
a secondary blast wave which propagates back into the flow processed by the
primary blast. The primary blast is used to shape the density field. The
sketch below illustrates the situation.
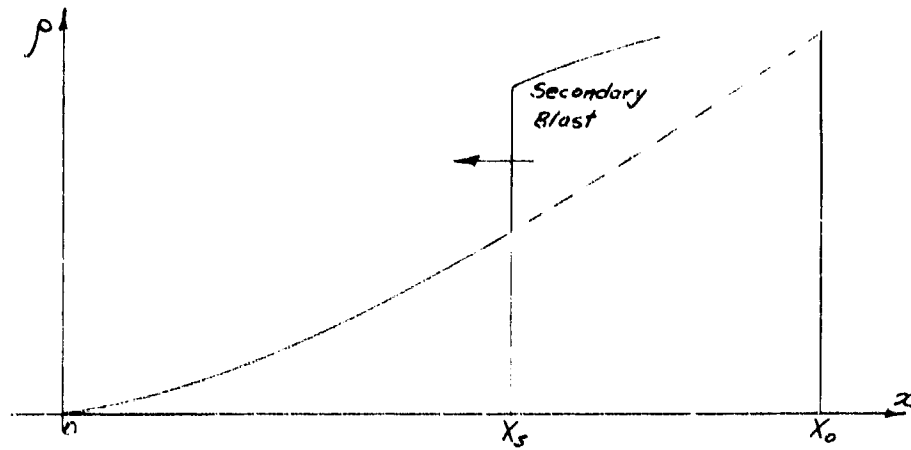
In reality the temperature and the particle velocity generated by the
primary blast is time dependent but these effects can be included into
the problem quite readily. For the present study we shall consider an
isothermal stationary medium with the density profile given by the simple
power law of Eq. 6.3.1.

The basic conservation equations for the planar one-dimensional
motion behind the blast are given as

$$\frac{\partial \rho}{\partial t} + \frac{\partial (\rho u)}{\partial x} = 0 \tag{6.3.2}$$

$$\frac{\partial u}{\partial t} + u \frac{\partial u}{\partial x} + \frac{1}{\rho} \frac{\partial p}{\partial x} = 0 \tag{6.3.3}$$

$$\left(\frac{\partial}{\partial t} + u \frac{\partial}{\partial x} \right) \frac{p}{\rho r} = 0 \tag{6.3.4}$$

With reference to the shock wave, we can express the initial density profile as

$$\rho_o = B X_s^{\delta}$$

(6.3.5)

where $X_s(t)$ is the instantaneous shock position, B and δ are numerical constants to be specified. For the analytical study we will transform Eqs. 6.3.2 to 6.3.4 using the following parameters

$$\psi(\xi, \eta) = \frac{\rho(x,t)}{\rho_o}$$

$$\phi(\xi, \eta) = \frac{u(x,r)}{\dot{X}_s}$$

$$f(\xi, \eta) = \frac{p(x,t)}{\rho_o \dot{X}_s^2}$$

(6.3.6)

$$\xi = \frac{x - X_o}{X_s - X_o}$$

$$\chi = \frac{X_s - X_o}{X_o}$$

Using Eq. 6.3.6, Eqs. 6.3.2 to 6.3.5 transform to the following

$$(\phi - \xi) \frac{\partial \psi}{\partial \xi} + \psi \frac{\partial \phi}{\partial \xi} + \frac{\delta \psi \chi}{1 + \chi} = -\chi \frac{\partial \psi}{\partial \chi}$$

(6.3.7)

$$(\phi - \xi) \frac{\partial \phi}{\partial \xi} + \theta \phi + \frac{1}{\psi} \frac{\partial f}{\partial \xi} = -\chi \frac{\partial \phi}{\partial \chi}$$

(6.3.8)

$$(\phi - \xi) \frac{\partial \sigma}{\partial \xi} + \left(2\theta - \frac{(\gamma-1)\delta\chi}{1+\chi}\right)\sigma = -\chi \frac{\partial \sigma}{\partial \chi} \qquad (6.3.9)$$

$$\rho_o = B\chi_o^\delta(1+\chi)^\delta \qquad (6.3.10)$$

where
$$\theta = \frac{(X_s - X_o)\ddot{X}_s}{\dot{X}_s^2} = \frac{\chi\ddot{\chi}}{\dot{\chi}^2} \qquad (6.3.11)$$

$$\sigma = \frac{f}{\gamma r} \qquad (6.3.12)$$

Using the continuity equation (i.e., Eq. 6.3.7) the energy equation (i.e., Eq. 6.3.9) can be expressed in a more convenient form as

$$(\phi - \xi)\frac{\partial f}{\partial \xi} + \gamma f \frac{\partial \phi}{\partial \xi} + \left(2\theta + \frac{\gamma\delta\chi}{1+\chi}\right)f = -\chi \frac{\partial f}{\partial \chi} \qquad (6.3.13)$$

The flow is bounded at all times by the shock $\chi = X_s$ and the wall $\chi = X_o$ (i.e., $0 \le \xi \le 1$). At time t = 0, the shock is at the wall $X_s = X_o$ and at some later time t = t_o, the shock reaches the origin $X_s = 0$. So the range for χ will be $0 \ge \chi \ge -1$. Conserving the total energy at any instant we have

$$E_o = \int_{X_s}^{X_o} \left(\frac{p}{\gamma-1} + \frac{\rho u^2}{2}\right)dx - \int_{X_s}^{X_o} \rho_o e_o dx \qquad (6.3.14)$$

Since we have assumed an isothermal atmosphere (i.e., T_o = constant), the initial internal energy e_o becomes

$$e_o = \frac{P_o}{(\gamma-1)\rho_o} = \frac{C_o^2}{\gamma(\gamma-1)} \qquad = \text{constant}$$

In terms of the dimensionless parameter defined by Eq. 6.3.6, the energy integral becomes

$$E_o = \rho_o X_o^3 \dot{X}^2 \chi I(\chi) - B\frac{C_o^2}{\gamma(\gamma-1)(\delta+1)}X_o^{\delta+1}\left[1-(1+\chi)^{\delta+1}\right] \qquad (6.3.15)$$

We can simplify the above equation by defining a characteristic time t^* and a characteristic sound speed C^* which can be formed from the initial parameters of the problem. Defining t^* and C^* as follows:

$$t^{*^2} = \frac{BX_o^{\delta+3}}{E_o} \qquad (6.3.16)$$

$$C^{*^2} = \frac{C_o^2 t^{*^2}}{X_o^2} = \frac{BX_o^{\delta+1}C_o^2}{E_o} \qquad (6.3.17)$$

We can now normalize t with respect to t^*. Defining a non-dimensional time τ as

$$\tau = t/t^* \qquad (6.3.18)$$

and using Eqs. 6.3.16 and 6.3.17, the energy integral (i.e., Eq. 6.3.15) reduces to the following

$$1 = \dot{\chi}^2 \chi(1+\chi)^\delta I(\chi) - \frac{C^{*^2}}{\gamma(\gamma-1)(\delta+1)}\left[1-(1+\chi)^{\delta+1}\right] \qquad (6.3.19)$$

where $\qquad I(\chi) = \int_1^0 \left(\frac{f}{\gamma-1} + \frac{1}{2}\phi^2\right)d\xi$

Henceforth, the dot of χ (i.e., $\dot{\chi}$ etc.) is differentiation with respect to τ. In terms of τ, the expression for θ, given by Eq. 6.3.11, remains unchanged as before.

$$\theta = \frac{\chi \ddot{\chi}}{\dot{\chi}^2}$$

The boundary conditions to be satisfied at the shock front $\xi = 1$ are given by the Rankine-Hugoniot relationships as

$$\psi(1,\chi) = \frac{\gamma+1}{\gamma-1+2\eta} \tag{6.3.20}$$

$$\phi(1,\chi) = \frac{2}{\gamma+1}(1-\eta) \tag{6.3.21}$$

$$f(1,\chi) = \frac{2}{\gamma+1} - \frac{(\gamma-1)\eta}{\gamma(\gamma+1)} \tag{6.3.22}$$

where
$$\eta = \frac{1}{m_s^2} = \frac{c_0^2}{\dot{x}_s^2} \tag{6.3.23}$$

In Eq. 6.3.23, where η is defined, the χ_s has differentiation with respect to real time t. In terms of τ we have

$$m_s = x_0 \frac{d(\chi_s/x_0)}{d\tau} \frac{d\tau}{dt} \cdot \frac{1}{c_0} = \frac{\dot{\chi}}{c^*}$$

and hence
$$\eta = \frac{c^{*2}}{\dot{\chi}^2} \tag{6.3.24}$$

where $\dot{\chi}$ in the above expression denotes differentiation with respect to τ.

For the initial motion of the blast wave, we seek solutions in the form of a power series in χ since when $\chi_s \sim x_0$, $\chi \sim 0$ and the

shock is close to the wall χ_0 . We therefore write the following pertur-
bation expressions for the dependent variables

$$\phi(\xi,\chi) = \sum_0^\infty \phi^{(n)}(\xi)\chi^n = \phi^{(o)} + \phi^{(\prime)}\chi + \cdots$$

$$f(\xi,\chi) = \sum_0^\infty f^{(n)}(\xi)\chi^n = f^{(o)} + f^{(\prime)}\chi + \cdots \qquad (6.3.25)$$

$$\psi(\xi,\chi) = \sum_0^\infty \psi^{(n)}(\xi)\chi^n = \psi^{(o)} + \psi^{(\prime)}\chi + \cdots$$

To find the appropriate perturbation form for the shock strength $\dot{\chi}(\chi)$,
we note from the energy integral that the left hand side is finite. There-
fore as $\chi \to o$, $\dot{\chi}^2 \to \frac{1}{\chi}$ since $I(\chi) \to$ finite and the second term on
the right hand side of Eq. 6.3.19 vanishes. The perturbation expression
for $\dot{\chi}^2$ therefore has the form

$$\dot{\chi}^2 = \frac{1}{\chi}\sum_0^\infty F_n \chi^n = \frac{F_0}{\chi} + F_1 + F_2 \chi + \cdots \qquad (6.3.26)$$

From the above expression, the expansion for $\theta(\chi)$ is found to be

$$\theta(\chi) = \sum_0^\infty \theta_n \chi^n = \theta_0 + \theta_1 \chi + \theta_2 \chi^2 + \cdots \qquad (6.3.27)$$

with

$$\theta_0 = -\frac{1}{2}$$

$$\theta_1 = \frac{F_1}{2F_0}$$

$$\theta_2 = \frac{F_2}{F_0} - \frac{1}{2}\left(\frac{F_1}{F_0}\right)^2$$

Substituting the above perturbation expressions into the conservation
equations, the energy integral and the boundary conditions and equating
terms of the same order in χ yields

Zeroth Order in χ

$$(\phi^{(0)} - \xi)\psi^{(0)'} + \psi^{(0)}\phi^{(0)'} = 0 \qquad (6.3.28)$$

$$(\phi^{(0)} - \xi)\phi^{(0)'} + \frac{1}{\psi^{(0)}} f^{(0)'} = -\theta_0 \phi^{(0)} \qquad (6.3.29)$$

$$(\phi^{(0)} - \xi)f^{(0)'} + \gamma f^{(0)}\phi^{(0)'} = -2\theta_0 f^{(0)} \qquad (6.3.30)$$

$$F_0 = 1/I^{(0)} \qquad (6.3.31)$$

$$I^{(0)} = \int_1^0 \left(\frac{f^{(0)}}{\gamma-1} + \frac{\phi^{(0)2}}{2}\psi^{(0)}\right) d\xi \qquad (6.3.32)$$

$$\theta_0 = -1/2$$

with the boundary conditions at the front $\xi = 1$ given as

$$\phi^{(0)}(1) = f^{(0)}(1) = \frac{2}{\gamma+1} \qquad (6.3.33)$$

$$\psi^{(0)}(1) = \frac{\gamma+1}{\gamma-1} \qquad (6.3.34)$$

First Order in χ

$$(\phi^{(0)} - \xi)\psi^{(1)'} + \psi^{(0)}\phi^{(1)'} = -\left[\psi^{(1)}(\phi^{(0)'}+1) + \delta\psi^{(0)} + \phi^{(1)}\psi^{(0)'}\right] \qquad (6.3.35)$$

$$(\phi^{(0)} - \xi)\phi^{(1)'} + \frac{1}{\psi^{(0)}} f^{(1)'} = -\left[\phi^{(1)}(1+\theta_0+\phi^{(0)'}) + \theta_1\phi^{(0)} - \frac{\psi^{(1)} f^{(0)'}}{\psi^{(0)2}}\right] \qquad (6.3.36)$$

$$(\phi^{(0)} - \xi)f^{(1)'} + \gamma f^{(0)}\phi^{(1)'} = -\left[f^{(1)}(1+2\theta_0+\gamma\phi^{(0)'}) + 2\theta_1 f^{(0)} + \phi^{(1)} f^{(0)'} + \gamma\delta f^{(0)}\right] \qquad (6.3.37)$$

$$F_1 = \frac{1}{I^{(0)}}\left[\frac{C^{*2}}{\gamma(\gamma-1)} + F_0 I^{(1)} + \delta F_0 I^{(0)}\right] \tag{6.3.38}$$

$$I^{(1)} = \int_1^0 \left(\frac{f^{(1)}}{\gamma-1} + \frac{\phi^{(0)^2}}{2}\psi^{(1)} + \phi^{(0)}\phi^{(1)}\psi^{(0)}\right)d\xi \tag{6.3.39}$$

$$\theta_1 = \frac{F_1}{2F_0}$$

and the boundary conditions at $\xi = 1$ given as

$$\phi^{(1)}(1) = \frac{-2C^{*2}}{F_0(\gamma+1)} \tag{6.3.40}$$

$$f^{(1)}(1) = \frac{(\gamma-1)}{2\gamma}\phi^{(1)}(1) \tag{6.3.41}$$

$$\psi^{(1)}(1) = \frac{2C^{*2}(\gamma+1)}{F_0(\gamma-1)^2} \tag{6.3.42}$$

We can carry out to higher orders in χ. The above perturbation scheme here is a simple coordinate perturbation method identical to that for blast waves with counter-pressure effects described in Chapter V.

Using the definition for $\dot{\chi}$, the shock trajectory becomes

$$\tau = C_0|\chi|^{3/2}\left[1 + C_1\chi + \cdots\right] \tag{6.3.43}$$

where

$$C_0 = \frac{2}{3(-F_0)^{1/2}}$$

$$C_1 = \frac{-3}{10}\frac{F_1}{F_0}$$

It is seen that the present zeroth order solution is in fact the constant energy planar strong blast solution. The non-similar effects from the initial density gradient and counter-pressure effects appear only in the first and higher order solutions. The method of solution here is identical to that described earlier in Chapter V where the perturbation solution for blast waves with counter-pressure effects was obtained.

It should be pointed out that even in the absence of counter-pressure effects (i.e., $C^{*^2}= O$), self-similar solutions do not exist for the present problem. This is due to the presence of the characteristic length X_o in the problem which leads to the time dependent terms $(1+\chi)^\delta$ in energy integral (i.e., Eq. 6.3.19) and $\delta \psi \chi (1+\chi)^{-1}$ in the continuity equation (i.e., Eq. 6.3.7). The self-similar solution only holds in the limit as $\chi \to o$, in which case we get the constant energy solution for planar blasts. Note that the initial density non-uniformity does not appear in the limiting self-similar solution as $\chi \to o$. This is due to the fact that in the present problem the density is finite and non-zero at the wall (i.e., $\rho(\text{wall})= \rho_o X_o^\delta$) while in the problem studied earlier in Chapter IV, the density is infinite or zero at the origin (i.e., $\rho_o = B r^\omega$, $\rho(\text{or}_1\quad) \to \infty$ or 0 as $r \to o$). Hence the effect of an initial non-uniform density field affects the solution immediately in the latter case for $\rho_o = B r^\omega$.

The present perturbation solution is only valid close to the wall and becomes progressively inaccurate as the shock advances towards the origin. Let us now investigate the asymptotic motion of the shock as it approaches the origin $\chi = o$. For the terminal motion of the shock, $X_s \ll X_o$ and considering only small distances behind the shock as well (i.e., $x \ll X_o$), the characteristic length X_o no longer comes into the problem. Hence if the shock wave is sufficiently strong near the origin,

as is generally the case after being continuously amplified as it propagates in a direction of decreasing density, then counter-pressure effects can be neglected. Under these conditions, a self-similar solution can exist for the asymptotic shock motion.

Since $x_s \ll x_0$ and $\tau \ll x_0$, we redefine the independent variables ξ and χ as

$$\chi' = \frac{x_s}{x_0} = 1 + \chi$$

$$\xi' = \frac{x_s}{x} = \frac{1 + \chi}{1 + \chi\xi}$$

(6.3.44)

In terms of the above defined variables, the basic conservation equations become

$$\xi'(1 - \phi\xi')\frac{\partial u}{\partial \xi'} - \xi'^2 u \frac{\partial \phi}{\partial \xi'} + \delta u = -\chi' \frac{\partial u}{\partial \chi'}$$

(6.3.45)

$$\xi'(1 - \phi\xi')\frac{\partial \phi}{\partial \xi'} + \theta\phi - \frac{\xi'^2}{4}\frac{\partial f}{\partial \xi'} = -\chi' \frac{\partial \phi}{\partial \chi'}$$

(6.3.46)

$$\xi'(1 - \phi\xi')\frac{\partial f}{\partial \xi'} - \gamma f \xi'^2 \frac{\partial \phi}{\partial \xi'} + (2\theta' + \delta)f = -\chi' \frac{\partial f}{\partial \chi'}$$

(6.3.47)

where $\quad \theta' = \frac{1 + \chi}{\chi}\theta = \frac{\chi'\ddot{\chi}'}{\dot{\chi}'^2}$

(6.3.48)

Note that the above equations are exact in that no approximations have been

- 114 -

io. Only a simple transformation of coordinates from (ξ, χ) to (ξ', χ') is involved.

As $\chi_n \to 0$, the shock strength $\zeta_s \to \infty$ since the density $\rho_s \to 0$. Assuming that $\chi'^2 \to \infty$ like χ^{-n} as $\chi' \to 0$, we write for the terminal shock motion

$$\dot{\chi}'^2 = \frac{G_0}{\chi'^\alpha} \tag{6.3.49}$$

where G_0 and α are positive constants. From the definition of θ' and Eq. 6.3.49, we get

$$\theta' = -\alpha/2 \tag{6.3.50}$$

and for the asymptotic motion near the origin the basic equations reduce to the following:

$$(1-\phi\xi')\frac{d\psi}{d\xi'} - \xi'\psi\frac{d\phi}{d\xi'} + \frac{3\psi}{\xi'} = 0 \tag{6.3.51}$$

$$(1-\xi'\phi)\frac{d\phi}{d\xi'} + \frac{\theta\phi}{\xi'} - \frac{\xi'}{\psi}\frac{df}{d\xi'} = 0 \tag{6.3.52}$$

$$(1-\xi'\phi)\frac{df}{d\xi'} - \gamma f\xi'\frac{d\phi}{d\xi'} + \frac{(2\theta'+\delta)f}{\xi'} = 0 \tag{6.3.53}$$

From Eq. 6.3.49, we obtain

$$\frac{d\chi'}{d\tau} = \dot{\chi}' = -\sqrt{G_0}\,\chi'^{-\alpha/2} \tag{6.3.54}$$

where the negative root for $\dot{\chi}'^2$ is taken since $\dot{\chi}'$ is negative when the shock advances in the direction of decreasing χ'. Integrating Eq. 6.3.54

yields the following expression for the shock trajectory

$$ \gamma = \left(\frac{2}{n+2} r_0 t_0 \right)^{n+2} (\ldots \quad \cdot)^{\frac{n}{n+2}} \tag{6.3.55} $$

and in terms of dimensional parameters, we have

$$ X_s = X_s (\ldots \ldots \ldots) (\ldots \frac{\epsilon}{\epsilon_0} r^{\ldots} \tag{6.3.56} $$

where t_c (or τ_c) is the time when $X_s = 0$. When t_c is taken to be zero as was done in the work of Frank-Kamenetskii and Sakurai, we have the familiar form for the shock trajectory as $X_s \sim (t)^N$ where $N = \frac{2}{n+2}$.

Solving for the derivatives ϕ' etc. from Eqs. 6.3.51 to 6.3.53, we get

$$ \frac{d\psi}{d\xi} = \frac{-[(1-\phi\xi')(\theta\phi\psi + (1-\phi\xi)\frac{d\psi}{\xi'}) + \xi'(2\theta - \delta(\delta-1))]}{(1-\xi')[(1-\phi\xi')^2 - \xi'^2\gamma f/4]} \tag{6.3.57} $$

$$ \frac{d\phi}{d\xi} = \frac{-[\frac{\theta\phi}{\xi} + (2\theta+\delta)\frac{f}{4}]}{[(1-\phi\xi')^2 - \xi'^2\gamma f/4]} \tag{6.3.58} $$

$$ \frac{df}{d\xi} = \frac{-[(1-\phi\xi')(2\theta+\delta)\frac{f}{\xi} + \gamma\theta f\phi]}{[(1-\phi\xi')^2 - \xi'^2\gamma f/4]} \tag{6.3.59} $$

The boundary conditions at the shock front $\xi' = 1$ are given by the strong shock relationships as

$$ \psi(1) = \frac{\gamma+1}{\gamma-1} \quad , \quad \phi(1) = f(1) = \frac{2}{\gamma+1} $$

As in the "sharp blow" problem, treated in the previous Section, the method

of determining the physically acceptable solution is to find the appropriate value of θ' that gives solutions for ϕ, f and ψ that satisfy the boundary conditions at the shock $\xi' = 1$ and is regular at the singularity $\cdots$. With θ' known, α and N are readily found to be

$$\theta' = -\gamma/\alpha \quad , \quad N = \frac{\overline{m}}{\alpha + \overline{m}}$$

The value of N corresponding to different values of γ and δ are tabulated below

δ	$\gamma = 5/3$	$\gamma = 7/5$	$\gamma = 6/5$
3.25	0.590	-	-
2	0.696	0.718	0.752
1	0.816	0.831	0.855
0.5	0.877	0.906	0.920

Note that as in the case of the "sharp blow" problem the present asymptotic solution is independent of initial conditions. The value of G_0 carries the information from the initial motion of the shock and cannot be determined in the asymptotic self-similar solution. To find G_0, we must solve the complete problem numerically.

Let us now investigate the distributions of pressure, density and the particle velocity as the shock approaches the origin (i.e., $X_S \to O$). As $X_S \to O$, $\xi' \to O$ and Eqs. 6.3.51 to 6.3.53 reduce to the following limiting forms

$$\frac{d\psi}{d\xi'} = -\frac{\delta\psi}{\xi'} \tag{6.3.60}$$

$$\frac{d\phi}{d\xi} = \frac{-\theta'\phi}{\xi'} \tag{6.3.61}$$

$$\frac{df}{d\xi'} = -\left(\frac{2\theta' + \delta}{\xi'}\right) f \tag{6.3.62}$$

Integrating the above equations yields

$$\psi = C_1 \xi'^{-\delta} \tag{6.3.63}$$

$$\phi = C_2 \xi'^{1-\theta'} \tag{6.3.64}$$

$$f = C_3 \xi'^{-(2\theta'+\delta)} \tag{6.3.65}$$

where C_1, C_2 and C_3 are constants of integration. In terms of dimensional variables, Eqs. 6.3.63 to 6.3.65 can be expressed as

$$\rho = \beta \psi = B C_1 x^{\delta} \tag{6.3.66}$$

$$u - \dot{X}_s \phi = -\left(\sqrt{G_o} \frac{X_o^{\frac{\alpha+2}{2}}}{t^*} C_2\right) x^{\theta'} \tag{6.3.67}$$

$$p = \rho_o \dot{X}_s^2 f = \left(B \frac{X_o^{\alpha+2} G_o}{t^{*2}} C_3\right) x^{2\theta'+\delta} \tag{6.3.68}$$

From the above equations, we see that as $X_s \rightarrow O$, the density distribution is proportional to the original density profile $\rho_o = B x^{\delta}$. The particle velocity u tends to infinity as $x \rightarrow O$ since $\theta' = -\alpha/2$. The pressure approaches zero as $x \rightarrow O$ since in general $2\theta' + \delta > O$. However both the momentum ρu and the kinetic energy $\rho u^2/2$ tend to zero as $x \rightarrow O$. It is interesting to note that yet another self-similar solution exists for the subsequent expansion of the gas to the vacuum after $t > t_c$.

6.4 Converging Shock Waves

In this Section we shall consider another important asymptotic motion, that of a converging cylindrical or spherical shock wave in the vicinity of its center of symmetry. The asymptotic self-similar solution for the final phases of collapse was first obtained by Guderley and later by Butler. The existence of the self-similar solution requires the absence of a characteristic length (i.e. $R_S << R_0$) and also the shock front to be of infinite strength (i.e., $M_S \to \infty$, $\eta \to 0$). Hence this solution is valid only in the immediate neighborhood of the center of convergence when both of these conditions can be realized in practice. As in the planar problem treated in the previous Section, we shall first consider the initial phases of the collapse when $R_S \sim R_0$ where the solutions are dependent on the initial conditions and then we will analyse the asymptotic motion for the final phases of collapse where the initial conditions do not appear. In this way a better physical insight to the problem can be achieved.

We shall consider a spherical or cylindrical chamber of radius R_0 containing a test gas at initial pressure p_0 and initial density ρ_0 .
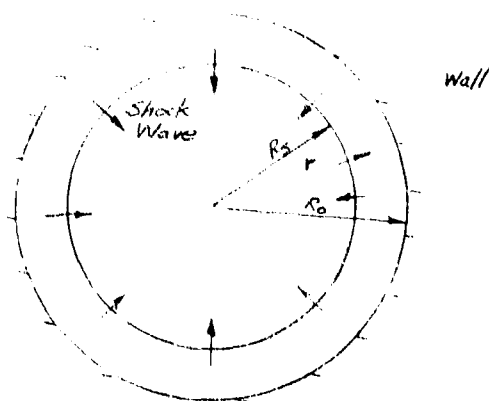
At time $t = 0$ a finite quantity of energy E_0 or, for the cylindrical case E_0 per unit length is released instantaneously at R_0 generating a strong shock wave. At subsequent times, the shock wave collapses toward the center of the axis of symmetry.

Neglecting viscous and heat transfer effects, and assuming a perfect gas with constant specific heat ratio γ, the conservation equations governing the adiabatic motion of the shocked-gas can be written as follows:

Conservation of mass

$$\frac{\partial \rho}{\partial t} + \frac{\partial (\rho u)}{\partial r} + j \rho \frac{u}{r} = 0 \tag{6.4.1}$$

Conservation of momentum

$$\frac{\partial u}{\partial t} + u \frac{\partial u}{\partial r} + \frac{1}{\rho}\frac{\partial p}{\partial r} = 0 \tag{6.4.2}$$

Conservation of energy

$$\left(\frac{\partial}{\partial t} + u \frac{\partial}{\partial r}\right)\frac{p}{\rho^\gamma} = 0 \tag{6.4.3}$$

where j = 1 for cylindrical symmetry

= 2 for spherical symmetry

The boundary conditions at the shock front $r = R_s$ are given by the standard Rankine-Hugoniot relationships for a normal shock in a perfect gas as follows

$$\frac{\rho_1}{\rho_0} = \frac{\gamma + 1}{\gamma - 1 + 2/M_s^2} \tag{6.4.4}$$

$$\frac{u_1}{\dot{R}_s} = \frac{2}{\gamma + 1}\left(1 - \frac{1}{M_s^2}\right) \tag{6.4.5}$$

$$\frac{p_1}{\rho_0 \dot{R}_s^2} = \frac{2}{\gamma + 1} - \frac{(\gamma - 1)}{\gamma(\gamma + 1)} \cdot \frac{1}{M_s^2} \tag{6.4.6}$$

where M_s is the shock Mach number defined as

$$M_s = |\dot{R}_s|/c_0 = |\dot{R}_s|\left(\frac{\rho_o}{\gamma p_o}\right)^{\frac{1}{2}} \tag{6.4.7}$$

The subscript '1' denotes conditions immediately behind the shock front while R_s and c_0 are the shock velocity and the sound speed of the undisturbed medium, respectively. In the present problem, it is more convenient to use a set of non-dimensional variables similar to that used in blast wave studies, Rae (1963).

$$\phi(\xi, x_s) = u(r,t)/\dot{X}_s(t) \tag{6.4.8}$$

$$f(\xi, x_s) = p(r,t)/(\rho_o \dot{X}_s^2(t)) \tag{6.4.9}$$

$$\psi(\xi, x_s) = \rho(r,t)/\rho_o \tag{6.4.10}$$

where

$$\xi = (r-R_o)/(R_s-R_o) \tag{6.4.11}$$

$$X_s = R_s - R_o \tag{6.4.12}$$

and

$$x_s = X_s/R_o = (R_s-R_o)/R_o \tag{6.4.13}$$

Equations 6.4.1 to 6.4.3 transform to the following equations, respectively.

$$(\phi-\xi)\frac{\partial \psi}{\partial \xi} + \psi \frac{\partial \phi}{\partial \xi} + j\frac{\phi\psi x_s}{1+x_s\xi} = -x_s\frac{\partial \psi}{\partial x_s} \tag{6.4.14}$$

$$(\phi-\xi)\frac{\partial \phi}{\partial \xi} + \theta\phi + \frac{1}{\psi}\frac{\partial f}{\partial \xi} = -x_s\frac{\partial \phi}{\partial x_s} \tag{6.4.15}$$

$$(\phi-\xi)\left(\frac{\partial f}{\partial \xi} - \frac{\gamma f}{\psi}\frac{\partial \psi}{\partial \xi}\right) + 2\theta f = -x_s\left(\frac{\partial f}{\partial x_s} - \frac{\gamma f}{\psi}\frac{\partial \psi}{\partial x_s}\right) \qquad (6.4.16)$$

where the parameter θ is defined as

$$\theta = x_s \ddot{x}_s / \dot{x}_s^2 \qquad (6.4.17)$$

and $\dot{x}_s$, $\ddot{x}_s$ denote first and second derivatives of x_s with respect to time t. A more convenient form of the energy equation can be obtained by eliminating ψ from Equations 6.4.14 and 6.4.16. Re-arranging the resultant equation one obtains

$$(\phi-\xi)\frac{\partial f}{\partial \xi} + \gamma f\frac{\partial \phi}{\partial \xi} + 2\theta f + \gamma j \frac{f\phi x_s}{1+x_s\xi} = -x_s\frac{\partial f}{\partial x_s} \qquad (6.4.18)$$

The region governed by Equations 6.4.14 to 6.4.18 is bounded by the shock front at $\xi = 1$ and by the chamber wall at $\xi = 0$. The shock originates at the chamber wall $x_s = 0$ and collapses to the center at $x_s = -1$.

Unlike the asymptotic solution for the final phases of collapse, the energy integral provides a useful relationship in the early phases of motion since the flow boundaries are finite (i.e., $1 \geqslant \xi \geqslant 0$). Conserving the total energy at any instant of time, one obtains the relationship:

$$E_0 = \int_{R_s}^{R_0}\left(\frac{p}{\gamma-1} + \frac{\rho u^2}{2}\right)k_j r^j dr - \int_{R_s}^{R_0}\frac{p_0}{\gamma-1}k_j r^j dr \qquad (6.4.19)$$

where the numerical constant k_j is defined as

$$k_1 = 2\pi, \quad j = 1 \quad \text{for cylindrical symmetry}$$

$$k_2 = 4\pi, \quad j = 2 \quad \text{for spherical symmetry}$$

The second integral on the right-hand side of Equation 6.4.19 represents the initial internal energy of the medium. Evaluating this integral and expressing the resultant equation in terms of the previously defined dimensionless variables, one obtains

$$E_o = \rho_o k_j R_o^{j+3} \dot{x}_s^2 x_s \left\{ I(x_s) - \frac{c_o^2 (1 - (1+x_s)^{j+1})}{R_o^2 \gamma(\gamma-1)(j+1) x_s \dot{x}_s^2} \right\} \quad (6.4.20)$$

where
$$I(x_s) = \int_1^0 \left(\frac{f}{\gamma-1} + \frac{\psi^2}{2}\right)(1+x_s\xi)^j d\xi \quad (6.4.21)$$

If the initiation energy E_o is large compared to the initial internal energy of the medium, the second term on the right-hand side of Equation 6.4.20 can be neglected. However, in contrast to the classical strong blast wave problem similarity solutions cannot be obtained here even under this condition due to the presence of the characteristic length R_o which results in the integral $I(x_s)$ being dependent on the shock position x_s. From Equation 6.4.20, it is seen that in the present problem, departure from similarity arises from both time-dependent boundary conditions when the initial internal energy of the medium cannot be neglected as compared to E_o, and also from the presence of a characteristic length R_o.

In the subsequent analysis, it is more convenient to seek an appropriate characteristic time so that the time variable t can be made non-dimensional. Defining a characteristic time t_j^* as

$$t_j^* = \left(\frac{\rho_o k_j R_o^{j+3}}{(j+1)E_o} \right)^{\frac{1}{2}}, \quad (6.4.22)$$

t_j^* can be interpreted as an order of magnitude of the total time of collapse.

In the subsequent analysis, the non-dimensional time variable τ where

$$\tau = t/t_j^* \quad (6.4.23)$$

will be used. The shock velocity $\dot{R}_s$ or $\dot{X}_s$ now becomes

$$\dot{R}_s = \dot{X}_s = R_0 \dot{x}_s = \frac{R_0}{t_j^*} \frac{dx_s}{d\tau}$$

Equations 6.4.14 to 6.4.18 remain unchanged except that $\dot{x}_s$ now represents differentiation with respect to τ . The energy integral (i.e., Equation 6.4.20) can be rewritten as

$$1 = x_s \dot{x}_s^2 (j+1) I(x_s) - c_j^{*2} \frac{(1 - (1+x_s)^{j+1})}{\gamma(\gamma-1)} \tag{6.4.24}$$

where c_j^* is the characteristic sound speed defined as

$$c_j^{*2} = c_0^2 t_j^{*2} / R_0^2 \tag{6.4.25}$$

If the initiation energy is very large (i.e., $E_0 \rightarrow \infty$), $t_j^* \rightarrow 0$ and $c_j^{*2} \rightarrow 0$ and the shock wave remains strong throughout its collapse. For example, in a spherical implosion chamber of radius 3 cm. containing air at 10 mm. Hg. initial pressure, an initiation energy of 10 joules gives a value of $t_2^* = 12.5 \times 10^{-6}$ sec. and $c_2^{*2} = 0.0196$. For hydrogen under identical conditions, $t_2^* = 0.346 \times 10^{-6}$ sec. while $c_2^{*2} = 0.0199$, approximately the same as that for air due to the higher sound speed in hydrogen.

For the initial phases of the collapse when $|x_s| \ll 1$, one may seek solutions to Equations 6.4.14 to 6.4.18 by assuming the following power series for the dependent variables ϕ , f and ψ.

$$\phi(\xi, x_s) = \sum_{n=0}^{\infty} \phi^{(n)}(\xi) x_s^n$$

$$f(\xi, x_s) = \sum_{n=0}^{\infty} f^{(n)}(\xi) x_s^n \tag{6.4.26}$$

$$\psi(\xi, x_s) = \sum_{n=0}^{\infty} \psi^{(n)}(\xi) x_s^n$$

An appropriate expansion for the shock velocity $\dot{x}_s$ can readily be obtained by inspection from the energy integral given by Equation 6.4.24. Since the left-hand side of Equation 6.4.24 is finite, $\dot{x}_s^2$ must be of the form

$$\dot{x}_s^2 = \frac{1}{x_s} \sum_{n=o}^{\infty} F_n x_s^n \qquad (6.4.27)$$

From Equation 6.4.27, one can readily determine the expansion for the parameter θ as:

$$\theta = \sum_{n=o}^{\infty} \theta^{(n)} x_s^n \qquad (6.4.28)$$

where the coefficients $\theta^{(o)}$, $\theta^{(\prime)}$, $\theta^{(2)}$ ..... are given as

$$\theta^{(o)} = -\frac{1}{2} \quad , \quad \theta^{(\prime)} = \frac{F_1}{2F_o} \qquad (6.4.29)$$

$$\theta^{(2)} = \frac{F_2}{F_o} - \frac{F_1^2}{2F_o^2} \qquad (6.4.30)$$

$$\theta^{(3)} = \frac{1}{2}\left(\left(\frac{F_1}{F_o}\right)^3 - \frac{3F_1 F_2}{F_o^2} + \frac{3F_3}{F_o} \right) \qquad (6.4.31)$$

Substituting the perturbation expressions given by Equations 6.4.26 to 6.4.31 into the conservation equations (Equations 6.4.14, 6.4.15 and 6.4.18) and into the energy integral (Equation 6.4.24), one obtains the following after equating coefficients of similar orders in x_s.

Zeroth Order

$$\left(\phi^{(o)} - \xi\right) \psi^{(o)\prime} + \psi^{(o)} \phi^{(o)\prime} = 0 \qquad (6.4.32)$$

$$\left(\phi^{(o)} - \xi\right) \phi^{(o)\prime} + \frac{1}{\psi^{(o)}} f^{(o)\prime} = -\theta^{(o)} \phi^{(o)} \qquad (6.4.33)$$

$$(\phi^{(o)} \xi) f^{(o)'} + \gamma f^{(o)} \phi^{(o)} = ? \quad \phi^{(o)}$$

$$(6.4.34)$$

$$F_o = 1/(j\omega I^{(o)})$$

$$(6.4.35)$$

where
$$I^{(o)} = \int_1^0 d\xi \left(\frac{f^{(o)}}{\gamma-1} + \phi^{(o)} \frac{\phi^{(o)'}}{2} \psi^{(o)} \right)$$

$$(6.4.36)$$

First Order

$$(\phi^{(o)} \xi) \psi^{(1)'} + \psi^{(o)} \phi^{(1)} = -\left[\psi^{(o)}(\phi^{(o)'} + 1) + \phi^{(1)} \psi^{(o)'} \right.$$
$$\left. + j \phi^{(o)} \psi^{(o)} \right]$$

$$(6.4.37)$$

$$(\phi^{(o)} \xi) \phi^{(1)'} + \frac{1}{\psi^{(o)}} f^{(1)'} = -\left[\phi^{(o)}(\phi^{(o)'} + 1 + \theta^{(o)}) + \theta^{(1)} \phi^{(o)} \right.$$
$$\left. - \psi^{(1)} f^{(o)'} / \psi^{(o)2} \right]$$

$$(6.4.38)$$

$$(\phi^{(o)} \xi) f^{(1)'} + \gamma f^{(o)} \phi^{(1)'} = -\left[f^{(o)}(\gamma \phi^{(o)'} + 1 + 2\theta^{(o)}) + 2\theta^{(1)} f^{(o)} \right.$$
$$\left. + \phi^{(1)} f^{(o)'} + \gamma j f^{(o)} \phi^{(o)} \right]$$

$$(6.4.39)$$

$$F_1 = -\left(\frac{\zeta_j \phi^{*2}}{\gamma(\gamma-1)} + F_o I^{(1)} \right) \cdot \frac{1}{I^{(o)}}$$

$$(6.4.40)$$

where
$$I^{(1)} = \int_{0}^{\xi^{(1)}} d\xi \left[j\frac{\xi}{S}\left(\frac{f}{\gamma-1} + \phi^{(0)}\frac{^2}{2}\psi^{(0)} \right) + \frac{f}{\gamma-1} + \phi^{(0)}\frac{^2}{2}\psi^{(0)} + \phi^{(0)}\phi^{(1)}\psi^{(0)} \right] \tag{6.4.41}$$

Second Order

$$(\phi^{(0)}\xi)\psi^{(1)\prime} + \psi^{(0)}\phi^{(1)\prime} = \left[\psi^{(1)}(\phi^{(0)\prime}+2) + \psi^{(0)}\phi^{(1)\prime} + \phi^{(1)}\psi^{(0)\prime} + \phi^{(0)}\psi^{(1)\prime} - j\xi\phi^{(0)}\psi^{(1)} + j(\phi^{(0)}\psi^{(1)} + \phi^{(1)}\psi^{(0)}) \right] \tag{6.4.42}$$

$$(\phi^{(0)}\xi)\phi^{(1)\prime} + \frac{1}{\psi^{(0)}}f^{(1)\prime} = -\left[\phi^{(0)}(\phi^{(0)\prime}+\theta^{(0)}+2) + \phi^{(1)}(\phi^{(0)\prime}+\theta^{(0)}) + \phi^{(0)}\theta^{(1)} - \psi^{(1)}f^{(0)\prime}/\psi^{(0)^2} + (\psi^{(1)}/\psi^{(0)} - \psi^{(1)})f^{(0)\prime}/\psi^{(0)^2} \right] \tag{6.4.43}$$

$$(\phi^{(0)}\xi)f^{(1)\prime} + \gamma f^{(0)}\phi^{(1)\prime} = -\left[f^{(1)}(\gamma\phi^{(0)\prime}+2\theta^{(0)}+2) + f^{(1)}(\gamma\phi^{(0)\prime}+2\theta^{(0)}) + 2\theta f^{(0)} + \phi^{(1)}f^{(0)\prime} + \psi^{(1)} \cdots - j\gamma\xi\phi^{(0)}f^{(0)} + \gamma j(\phi^{(0)}f^{(1)} + \phi^{(1)}f^{(0)}) \right] \tag{6.4.44}$$

$$F_2 = -\left(\frac{jC_j^{*2}}{2\gamma(\gamma-1)} + F_1 I^{(1)} + F_0 I^{(2)} \right) \cdot \frac{1}{I^{(0)}} \tag{6.4.45}$$

where $J^{(3)} = \int_1 \alpha \frac{\xi}{2} \left[\frac{f^{(3)'}}{\gamma-1} + \psi^{(1)}\frac{\phi^{(0)^2}}{2} + \psi^{(0)}\frac{\phi^{(1)^2}}{2} + \psi^{(0)}\phi^{(0)}\phi^{(1)} \right.$

$\qquad + \psi^{(1)}\phi^{(0)}\phi^{(0)} + j\xi\left(\frac{f^{(1)'}}{\gamma-1} + \psi^{(1)}\frac{\phi^{(0)^2}}{2} + \psi^{(0)}\phi^{(0)}\phi^{(1)} \right)$

$\qquad\qquad\qquad\qquad\qquad\qquad\qquad\qquad (6.4.46)$

$\qquad \left. + j(\frac{j-1}{2})\xi^2\left(\frac{f^{(0)'}}{\gamma-1} + \psi^{(0)}\frac{\phi^{(0)^2}}{2} \right) \right]$

Third Order

$(\phi^{(0)}-\xi)\psi^{(3)'} + \psi^{(3)}\phi^{(0)'} - \left[\psi^{(0)}(\phi^{(3)'}+3) + \psi^{(3)}\phi^{(0)'} + \psi^{(1)}\phi^{(2)'} \right.$

$\qquad + \phi^{(3)}\psi^{(0)'} + \phi^{(2)}\psi^{(1)'} + \phi^{(1)}\psi^{(2)'}$

$\qquad + j(\phi^{(0)}\psi^{(3)} + \phi^{(1)}\psi^{(2)} + \phi^{(2)}\psi^{(1)}) \qquad (6.4.47)$

$\qquad \left. - j\xi(\phi^{(0)}\psi^{(2)} + \phi^{(1)}\psi^{(1)}) + j\xi^2\phi^{(0)}\psi^{(1)} \right]$

$(\phi^{(0)}-\xi)\phi^{(3)'} + \frac{1}{\psi^{(0)}}f^{(3)'} - \left[\phi^{(3)}(\phi^{(0)'}+\theta^{(0)'}+3) + \phi^{(2)}(\phi^{(1)'}+\theta^{(1)}) \right.$

$\qquad + \phi^{(1)}(\phi^{(2)'}+\theta^{(2)}) + \phi^{(0)}\theta^{(1)}$

$\qquad - \psi^{(1)}f^{(2)'}/\psi^{(0)^2} + (\psi^{(1)^2}/\psi^{(0)} - \psi^{(1)})f^{(1)'}/\psi^{(0)^2} \quad (6.4.48)$

$\qquad - (\psi^{(1)^3}/\psi^{(0)^2} - 2\psi^{(1)}\psi^{(2)}/\psi^{(0)} + \psi^{(3)}) \times$

$\qquad\qquad\qquad\qquad\qquad\qquad\qquad \left. \times f^{(0)'}/\psi^{(0)^5} \right]$

$(\phi^{(0)}-\xi)f^{(3)'} + \gamma f^{(0)}\phi^{(3)'} = -\left[f^{(3)}(\gamma\phi^{(0)'}+2\theta^{(0)'}+3) + f^{(2)}(\gamma\phi^{(1)'}+2\theta^{(1)}) \right.$

$\qquad + f^{(1)}(\gamma\phi^{(2)'}+2\theta^{(2)}) + 2\theta^{(3)}f^{(0)}$

$\qquad + \phi^{(3)}f^{(0)'} + \phi^{(2)}f^{(1)'} + \phi^{(1)}f^{(2)'} \qquad (6.4.49)$

$\qquad + j\gamma(\phi^{(0)}f^{(3)} + \phi^{(1)}f^{(1)} + \phi^{(2)}f^{(0)})$

$\qquad \left. - j\gamma\xi(\phi^{(0)}f^{(1)} + \phi^{(1)}f^{(0)}) + j\gamma\xi^2\phi^{(0)}f^{(0)} \right]$

$$F_3 = -\left(\frac{j(j-1)C_j^{*^2}}{6\gamma(\gamma-1)} + F_0 I^{(3)} + F_1 I^{(2)} + F_2 I^{(1)} \right) \cdot \frac{1}{j+1} \tag{6.4.50}$$

where

$$
\begin{aligned}
I^{(3)} = \int_1^0 d\xi\Bigg(& \frac{f^{(1)}}{\gamma-1} + \psi\frac{(1)}{2}\phi^{(0)^2} + \psi\frac{(0)}{2}\phi^{(1)^2} + \psi^{(0)}\phi^{(0)}\phi^{(1)} \\
& + \psi^{(0)}\phi^{(1)}\phi^{(0)} + \psi^{(1)}\phi^{(0)}\phi^{(0)} + \psi^{(0)}\phi^{(0)}\phi^{(1)} \\
& + j\xi\Big[\frac{f^{(0)}}{\gamma-1} + \psi\frac{(0)}{2}\phi^{(0)^2} + \psi\frac{(0)}{2}\phi^{(0)^2} + \psi^{(0)}\phi^{(0)}\phi^{(0)} \\
& + \psi^{(0)}\phi^{(0)}\phi^{(0)}\Big] + j(j-1)\frac{\xi^2}{2}\Big[\frac{f^{(0)}}{\gamma-1} + \psi\frac{(0)}{2}\phi^{(0)^2} \\
& \qquad\qquad + \psi^{(0)}\phi^{(0)}\phi^{(0)}\Big]\Bigg)
\end{aligned}
\tag{6.4.51}
$$

The boundary conditions to be satisfied by the zeroth, first, second and third order equations at the shock front $\xi = 1$ can be determined by expanding the Rankine-Hugoniot relations. Substituting Equation 6.4.27 into Equations 6.4.4 to 6.4.6 and carrying out the expansions, one obtains for

Zeroth Order

$$\phi^{(0)}(1) = f^{2(0)}(1) = \frac{2}{\gamma+1} \tag{6.4.52}$$

$$\psi^{(0)}(1) = \frac{\gamma+1}{\gamma-1} \tag{6.4.53}$$

First Order

$$\psi^{(1)}(1) = \frac{-2C_j^{*^2}(\gamma+1)}{F_0(\gamma-1)^2} \tag{6.4.54}$$

$$\phi^{(1)}(1) = \frac{-2C_j^{*^2}}{F_0(\gamma+1)} \tag{6.4.55}$$

$$f^{(1)}(1) = \frac{(\gamma-1)\phi^{(1)}(1)}{2\gamma} \tag{6.4.56}$$

Second Order

$$\psi^{(2)}(1) = 2c_j^{*2}\frac{(\gamma+1)}{(\gamma-1)^2 F_0^{\,2}}\left(F_1 - \frac{2c_j^{*2}}{\gamma-1}\right) \tag{6.4.57}$$

$$\phi^{(2)}(1) = \frac{2c_j^{*2}F_1}{(\gamma+1)F_0^{\,2}} \tag{6.4.58}$$

$$f^{(2)}(1) = \frac{(\gamma-1)\phi^{(2)}(1)}{2\gamma} \tag{6.4.59}$$

Third Order

$$\psi^{(3)}(1) = -2c_j^{*2}\frac{(\gamma+1)}{(\gamma-1)^2 F_0^{\,3}}\left[\left(F_1 + \frac{2c_j^{*2}}{\gamma-1}\right)^2 - F_0 F_2\right] \tag{6.4.60}$$

$$\phi^{(3)}(1) = -\frac{2c_j^{*2}}{(\gamma+1)F_0^{\,3}}\left(F_1^{\,2} - F_0 F_2\right) \tag{6.4.61}$$

$$f^{(3)}(1) = \frac{(\gamma-1)\phi^{(3)}(1)}{2\gamma} \tag{6.4.62}$$

The zeroth order shock boundary conditions are simply those for an infinitely strong shock wave of limiting density ratio. The parameter c_j^{*2} appears in the first and higher order boundary conditions only. Hence for very large values of the initiation energy E_o where c_j^{*2} can be neglected, the first and higher order boundary conditions all become zero. The shock remains strong throughout its collapse under this condition. One should note that the determination of the boundary conditions for a higher order solution requires the complete solution of the lower order equations. For example, the first order boundary conditions can only be evaluated after the zero order solution is obtained and F_o determined

from the zero order energy integral (i.e., Equation 6.4.35).

From the differential equations for the zeroth order (i.e., Equations 6.4.32 to 6.4.34) its boundary conditions (i.e., Equations 6.4.32 and 6.4.33), and the value of $\theta^{(o)} = -1/2$, one observes immediately that the solution will in fact be the self-similar solution for strong planar blast waves. One would expect this result since the shock is initiated at the wall surface at R_o and for very short times after initiation, curvature effects are negligible and the flow is essentially planar.

With the zero order solution known, F_o can be evaluated from the energy integral (i.e., Equation 6.4.35) and the first order boundary conditions can now be determined. With these as starting values at the shock $\xi = 1$, the differential equations for the first order (i.e., Equations 6.4.37 to 6.4.39) can then be integrated numerically with a chosen value of $\theta^{(1)}$. The criterion for determining the correct solution is that the chosen value of $\theta^{(1)}$ gives a solution that satisfies the condition of zero particle velocity at the wall. An alternative criterion is that the assumed value of $\theta^{(1)}$ coincides with the value obtained from the first order energy integral. It was found that rapid convergence can be obtained using the "regula-falsi" method of iteration for $\theta^{(1)}$ based on the criterion of zero particle velocity at the wall ($\xi = o$, $\phi^{(1)}(o) = o$). The second criterion is also used to check the value of the $\theta^{(1)}$ obtained. The solutions for the second and higher orders are found in a similar manner.

The shock trajectory can be obtained from the definition of the shock velocity

$$\dot{x}_s = \frac{dx_s}{d\tau}$$

or

$$\tau = \int_0^{x_s} \frac{dx_s}{\dot{x}_s} \qquad (6.4.63)$$

Substituting the expansion for $\dot{x}_s^2$ in terms of x_q into the above equation, one obtains

$$\tau = -\int_0^{x_s} dx_s \left[\frac{F_0}{x_s} + F_1 + F_2 x_s + F_3 x_s^2 + \right]^{-\frac{1}{2}} \qquad (6.4.64)$$

Where the negative square root of $\dot{x}_s^2$ is taken since the shock velocity is directed towards the center of symmetry.

Integrating Equation 6.4.34 up to third order in x_s, the resultant expression for the shock trajectory becomes:

$$\tau = B_0 |x_s|^{\frac{3}{2}} \left(1 + B_1 x_s + B_2 x_s^2 + B_3 x_s^3 + \cdots \right) \qquad (6.4.65)$$

where

$$B_0 = \frac{2}{3\sqrt{|F_0|}}$$

$$B_1 = -\frac{3}{10} \frac{F_1}{F_0}$$

$$B_2 = \frac{3}{7} \left(\frac{3}{8} \frac{F_1^2}{F_0^2} - \frac{F_2}{2 F_0} \right)$$

$$B_3 = -\frac{1}{3} \left(\frac{5}{16} \left(\frac{F_1}{F_0} \right)^3 - \frac{3}{4} \frac{F_1 F_2}{F_0^2} + \frac{F_3}{2 F_0} \right)$$

The present analysis provides a fairly accurate and complete description of the initial phases of collapse of impulsively-generated implosions. For strong collapse where the initiation blast energy is large (i.e., $c_j^{*2} \longrightarrow 0$) the present perturbation scheme is simply a Taylor series expansion about the chamber wall $x_s = 0$ and the radius of convergence covers a significant portion of the total collapse. Counter-pressure effects become dominant for weak initiation and the validity of

the present second order solution is confined to the neighbourhood of wall whereby $|x_s| \ll 1$. A description of the complete collapse requires a numerical integration scheme. However, the present analysis provides an excellent method for determining the appropriate starting conditions for the numerical solution.

The coordinate perturbation method described here can be used to solve for the initial phases of collapse of shock waves generated by means other than an impulsive energy release. For example if the shock is initiated by a piston we simply redefine our independent variables ξ and x_s as

$$\xi = \frac{r - R_p}{R_s - R_p} \quad , \quad x_s = \frac{R_s - R_p}{R_p}$$

where R_p is the prescribed piston path. The rest of the analysis will be identical to that given above.

For collapsing shock waves in a detonating gas, we use the general boundary condition at the front given as

$$\psi(1) = \frac{\gamma + 1}{\gamma - S + \eta} \tag{6.4.66}$$

$$\phi(1) = \frac{1 + S - \eta}{\gamma + 1} \tag{6.4.67}$$

$$f(1) = \frac{\gamma + \eta + \gamma S}{\gamma(\gamma + 1)} \tag{6.4.68}$$

where

$$S = \left[(1 - \eta)^2 - k\eta \right]^{1/2} \tag{6.4.69}$$

$$k = 2q(\gamma^2 - 1) \tag{6.4.70}$$

$$q = Q/c_o^2 \tag{6.4.71}$$

$$\eta = 1/m_s^2 = c_o^2/\dot{R}_s^2 \tag{6.4.72}$$

in place of the relationships for the non-reacting case given by Eqs. 6.4.4 to 6.4.6. The energy integral will now include the chemical energy Q and Eq. 6.4.19 should be written as

$$E_o = \int_{R_s}^{R_o} \left(\frac{p}{\gamma-1} + \frac{\rho u^2}{2} \right) k_j \, r^j dr - \int_{R_s}^{R_o} \rho_o (e_o + Q) k_j \, r^j dr \tag{6.4.73}$$

which in terms of the dimensionless parameters becomes

$$1 = \dot{x}_s^2 x_s (j+1) I(x_s) - \beta_j^{*2} (1 - [1+x_s]^{j+1}) \tag{6.4.74}$$

where

$$\beta_j^{*2} = \frac{(e_o + Q) t_j^{*2}}{R_o^2} = \frac{\rho_o (e_o + Q) k_j R_o^{j+3}}{(j+1) E_o} \tag{6.4.75}$$

and $I(x_s)$, t_j^* are defined as before by Eq. 6.4.21 and 6.4.22 respectively. The rest of the perturbation analysis is identical as before and the equations for the different orders in x_s are as given by Eqs. 6.4.32 to 6.4.51. The term $c_j^{*2}/(\gamma(\gamma-1))$ in Eqs. 6.4.40, 6.4.45, 6.4.50 for F_1, F_2 and F_3 respectively must be replaced by β_j^{*2}. The zeroth order boundary conditions are identical as before, however the higher order terms will be changed to include the chemical energy release. These can readily be obtained by expanding the boundary conditions given by Eqs.

6.4.66 to 6.4.68 . For example the first and second order boundary conditions are given as

$$\psi^{(1)}(1) = \frac{\gamma+1}{\gamma-1}\left(\frac{\gamma A}{\gamma-1} - B\right) \tag{6.4.76}$$

$$\phi^{(1)}(1) = \frac{1}{\gamma+1}\left(\gamma A - (\gamma-1)B\right) \tag{6.4.77}$$

$$f^{(1)}(1) = \frac{1}{\gamma+1}\left(\gamma A + 2B\right) \tag{6.4.78}$$

where

$$A = -\left(\frac{\gamma^2-1}{\gamma}\right)\frac{\beta_j^{*2}}{F_0} \tag{6.4.79}$$

and

$$B = \frac{\gamma-1}{F_0}\cdot\beta_j^{*2} \tag{6.4.80}$$

$$\psi^{(2)}(1) = \frac{\gamma+1}{\gamma-1}\cdot\left(\frac{\gamma}{\gamma-1}A_1 + \left[B - \frac{\gamma A}{\gamma-1}\right]^2\right.$$
$$\left. + \frac{\gamma AB}{\gamma-1} + \frac{BF_1}{F_0}\right) \tag{6.4.81}$$

$$\phi^{(2)}(1) = \frac{1}{\gamma+1}\left(\gamma A_1 + \gamma AB + (\gamma-1)\frac{BF_1}{F_0}\right) \tag{6.4.82}$$

$$f^{(2)}(1) = \frac{1}{\gamma+1}\cdot\left(\gamma A_1 + \gamma AB - 2\frac{BF_1}{F_0}\right) \tag{6.4.83}$$

where

$$A_1 \cdot \left(\frac{\gamma^2-1}{\gamma}\right)\left(\frac{\xi^2}{2} + \beta_j^{*2}\right)\left[\frac{h_1}{h_0} + \frac{\ddot{R}}{\dot{R}}\right] + \left(\dot{u}^2\right)\left(\frac{\dot{R}^4}{\dot{R}_0}\right)$$ (6.4.84)

The solution for the various orders in ξ_s are obtained in an identical manner as described before. For a detonating gas the perturbation solution diverges rapidly and is valid only for $|\xi_s| < s_j$. This is due to the large magnitude of β_j^{*2} for a detonable medium. For example, for equi-molar acetylene-oxygen mixtures, at an initial pressure of 100 torr, the value of $\beta_j^{*2} \sim 60$ for $R_0 = 6$ cm and $E_d = 10$ joules.

For the final phases of collapse near the center of symmetry we redefine our variables as follows

$$\xi = \frac{r}{R_s}$$

$$r_s = R_s/R_0$$

$$\psi(\xi, r_s) = \rho(r,t)/\rho_0$$ (6.4.85)

$$\phi(\xi, r_s) = u(r,t)/\dot{R}_s(t)$$

$$f(\xi, r_s) = p(r,t)/(\rho_0 \dot{R}_s^2(t))$$

and the basic conservations (i.e., Eqs. 6.4.1 to 6.4.3) now become

$$(\phi - \xi)\frac{\partial \psi}{\partial \xi} + \psi \frac{\partial \psi}{\partial \xi} + \frac{\partial \psi}{\partial \xi} = \lambda \frac{\partial \psi}{\partial \xi} \tag{6.4.86}$$

$$(\phi - \xi)\frac{\partial \psi}{\partial \xi} + \psi \frac{\partial \psi}{\partial \xi} + \phi \psi = \lambda \frac{\partial \psi}{\partial \xi} \tag{6.4.87}$$

$$(\phi - \xi)\frac{\partial f}{\partial \xi} + \gamma f \frac{\partial \psi}{\partial \xi} + (2\theta + \gamma \psi)f = -\delta \frac{\partial f}{\partial \xi} \tag{6.4.88}$$

where

$$\theta = R_s \ddot{R}_s / \dot{R}_s^2 \tag{6.4.89}$$

The energy equation given above is of the same form as Eq. 6.4.18 in which the continuity equation has been used to eliminate the density ψ. The flow at all times is bounded by the shock front $r = R_s$ and the cavity wall $r = R_0$, hence $1 \leq \xi \leq R_0/R_s$. Initially at time $t = 0$ the shock is at the cavity wall $R_s = 0$ and at some time $t = t_c$, it arrived at the center of symmetry, hence $0 \leq R_s \leq 1$.

For the terminal motion near the center of convergence, $R_s \to 0$ (either $R_0 \to \infty$ and R_s finite or R_0 finite but the shock radius $R_s \to 0$) and the right hand terms of Eq. 6.4.86 to 6.4.88 vanish. The parameter $\theta \to \theta_0 =$ constant and for strong shocks, $\eta \to 0$ and the boundary conditions at the front given by Eqs. 6.4.66 and 6.4.68 reduce to

$$\psi(1) = \frac{\gamma+1}{\gamma-1} \tag{6.4.53}$$

$$\phi(1) = f(1) = \frac{2}{\gamma+1} \tag{6.4.52}$$

The basic equations for the terminal motion of the flow reduce to

$$\phi' = \frac{(2\gamma\phi + j\gamma\phi\psi/\xi)\phi - 2Q_o\gamma(\gamma+\xi)}{(\phi-\xi)^2 - \gamma\psi/\phi} \qquad (6.4.90)$$

$$f' = \psi(Q_o\phi + (\phi-\xi)\phi') \qquad (6.4.91)$$

$$\psi' = -(\psi\phi' + j\phi\psi/\xi)/(\phi-\xi) \qquad (6.4.92)$$

Before the above differential equations can be integrated, the value of Q_o must be known and for this second class of asymptotic self-similar motion, it cannot be determined from the initial conditions. Similar to the problems treated earlier in this Chapter, the solution is determined by seeking a value of Q_o that results in ϕ, f and ψ being continuous at the singularity $(\phi-\xi)^2 - \gamma\psi/\phi = 0$. From Eq. 6.4.90 we see that for regularity of the solution at $(\phi-\xi)^2 - \gamma\psi/\phi = 0$, we must have a value of Q_o that satisfies the condition

$$Q_o = \frac{\xi j f^* \phi^*/\psi^*}{2\xi^*(\phi^*(\phi^*-\xi^*) - f^*/\psi^*)} \qquad (6.4.93)$$

where the *superscript denotes conditions at the singularity. The values of Q_o for various values of γ and j are tabulated below

j = 1 : Cylindrical Symmetry

γ	θ_0	N	N (Butler)	N (Welsh)
1.2	0.0??21	0.86??63	0.861163	0.861163
1.4	0.19??3	0.855?22	0.855277	0.855323
5/3	0.22??54	0.815625	0.815625	0.815625
3	0.289214	0.775666		0.775667

j = 2 : Spherical Symmetry

γ	θ_0	N	N (Butler)	N (Welsh)
1.2	-0.320757	0.757142	0.757142	0.757142
1.4	-0.394361	0.717174	0.717173	0.717174
5/3	-0.452692	0.688377	0.688377	0.688377
3	-0.571314	0.636410		0.636411

From the definition of θ_0 , we can determine the form of the shock strength dependence on r_s and the shock trajectory. Integrating Eq. 6.4.89, we get

$$\dot{r}_s = -(F_0)^{1/2} r_s^{\theta_0}$$

$$(6.4.94)$$

where F_0 is a constant. The negative sign is chosen since the shock radius decreases with increasing time. Integrating Eq. 6.4.94 again yields

$$r_s = A\left(1 - \frac{t}{t_c}\right)^N$$

where

$$N = \frac{1}{1 - \theta_0}$$

$$(6.4.95)$$

and

$$A = \left[t_c \frac{(F_0)^{\frac{1}{2}}}{N}\right]^N$$

In the above equation, t_c is chosen such that when $r_s = 0$, $\tau = t_c$.

It should be noted that the constants r_o and t_c depend on the initial conditions and cannot be determined in the self-similar solution. They have to be found by matching this asymptotic self-similar solution to the exact numerical solution of the initial non-similar regime of the collapse processes.

For r_s finite but small (i.e., $r_s << 1$) we can seek corrections to this asymptotic self-similar solution to account for non-similar effects arising from counter-pressure or heat released by chemical reactions by a coordinate perturbation scheme in a small parameter $\epsilon(r_s)$. From an examination of the basic equations and the boundary conditions we find that if the self-similar solution for $r_s \to 0$ is to be recovered as $\epsilon \to 0$, then ϵ should have the form

$$\epsilon = r_s^\alpha \tag{6.4.96}$$

where $\alpha = -2\theta_o$ is a positive number since θ_o is negative. We can write the following perturbation expressions for the variables

$$r_s^2 = \frac{1}{\epsilon} \sum_0^\infty F_m \epsilon^n = \frac{1}{\epsilon}\left(F_o + F_1 \epsilon + \cdots \right) \tag{6.4.97}$$

$$\theta(r_s) = \sum_0^\infty \theta_m \epsilon^n = \theta_o + \theta_1 \epsilon + \cdots \tag{6.4.98}$$

$$\psi(\xi, r_s) = \sum_0^\infty \psi_m(\xi)\epsilon^n = \psi_o(\xi) + \psi_1(\xi)\epsilon + \cdots \tag{6.4.99}$$

$$\phi(\xi, r_s) = \sum_0^\infty \phi_m(\xi)\epsilon^n = \phi_o(\xi) + \phi_1(\xi)\epsilon + \cdots \tag{6.4.100}$$

$$f(\xi, r_s) = \sum_0^\infty f_n(\xi)\epsilon^n = f_o(\xi) + f_1(\xi)\epsilon + \cdots \tag{6.4.101}$$

From Eq. 6.4.97 and the definition of Θ (i.e., Eq. 6.4.99) the coefficients of Eq. 6.4.98 can be obtained as

$$\Theta_0 = -\alpha/2 \tag{6.4.102}$$

$$\theta_1 = \frac{\alpha}{2} \frac{F_1}{F_0} \tag{6.4.103}$$

Substituting these perturbation expressions into the basic equations and the boundary conditions and collecting the terms of the same order of magnitude in $\in$, we obtain for the zeroth order in $\in$, the self-similar solution described earlier and for the first order, we have

$$(\phi_0 - \xi) \psi_1' + \psi_0 \phi_1' = -\left[\psi_1 (\phi_0' + \alpha) + \phi_1 \psi_0' \right. \\ \left. + j(\phi_0 \psi_1 + \phi_1 \psi_0)/\xi \right] \tag{6.4.104}$$

$$(\phi_0 - \xi) \phi_1' + \frac{1}{\psi_0} f_1' = -\left[\phi_1 (\phi_0' + \theta_0 + \alpha) + \theta_1 \phi_0 \right. \\ \left. - \psi_1 f_0'/\psi_0^2 \right] \tag{6.4.105}$$

$$(\phi_0 - \xi) f_1' + \gamma f_0 \phi_1' = -\left[f_1 (\gamma \phi_0' + 2\theta_0 + \alpha) + 2\theta_1 f_0 \right. \\ \left. + \phi_1 f_0' + \gamma j(f_0 \phi_1 + f_1 \phi_0)/\xi \right] \tag{6.4.106}$$

The corresponding boundary conditions at the shock front $\xi = 1$ are given as

$$\psi_1(1) = \frac{\psi_0(1)(S_1 - 1)}{\gamma - 1} \beta \tag{6.4.107}$$

$$\phi_1(1) = \frac{(S_1 - 1)\beta}{\gamma + 1} \tag{6.4.108}$$

$$f_{(i)} = \frac{(\gamma S_i + i)\beta}{\gamma(\gamma + i)} \tag{6.4.109}$$

where

$$S_i = -(i + \frac{k}{2}) \tag{6.4.110}$$

$$\beta = \frac{c_o^2}{F_o R_o^2} \tag{6.4.111}$$

and $\psi_o(i)$ is given previously by Eq. 6.4.53. Note that the first order boundary conditions given above depend linearly on β, which is a constant and depends on the constant F_o. However F_o can only be found from the initial conditions through an exact numerical solution of the problem. To obtain a general perturbation solution independent of the numerical value of β, we can redefine the variables ψ_i, f_i and ϕ_i as

$$\psi_i = \psi_i^* \beta \quad , \quad \phi_i = \phi_i^* \beta \quad , \quad f_i = f_i^* \beta \tag{6.4.112}$$

Substituting Eq. 6.4.112   first order equations (i.e., Eqs. 6.4.104 to 6.4.106), we note that   also linearly dependent on β. Hence redefining F_i as

$$F_i/F_o = F_i^* \beta \tag{6.4.113}$$

then $\theta_i = \theta_i^* \beta$ where $\theta_i^* = \alpha F_i^*/2$. Similarly it can be seen that the second order variables are proportional to β^2 and so on for higher orders. For convenience we can non-dimensionalize time t with respect to t_c by defining

$$\tau = t/t_c \tag{6.4.114}$$

In terms of the redefined bariables, Eqs. 6.4.97 to 6.4.101 become

$$\dot{r_s}^2 = \frac{F_o^*}{\epsilon}\left[1 + F_1^* \beta \epsilon + F_2^* \beta^2 \epsilon^2 + \quad \right] \qquad (6.4.115)$$

where

$$F_o^* = F_o t_c^2 \qquad (6.4.116)$$

$$\theta = \theta_o + \theta_1^* \beta \epsilon + \qquad (6.4.117)$$

$$\psi = \psi_o + \psi_1^* \beta \epsilon + \qquad (6.4.118)$$

$$\phi = \phi_o + \phi_1^* \beta \epsilon + \qquad (6.4.119)$$

$$f = f_o + f_1^* \beta \epsilon + \qquad (6.4.120)$$

In terms of the new variables, the first order equations (i.e., Eqs. 6.4.104 to 6.4.106) remain unchanged and we simply replace ϕ_1 , ψ_1 , f_1 , θ_1 by ϕ_1^* , ψ_1^* , f_1^* and θ_1^* . The boundary values for $\psi_1^*(1)$ etc. at the shock are given as before by Eqs. 6.4.107 to 6.4.109 except β is absent. The solution is now universal and for any given value of β , the first order corrections can readily be found using Eqs. 6.4.115 to 6.4.120.

The first order solution is determined in an identical manner as the zeroth order self-similar solution. From Eqs. 6.4.104 to 6.4.106, we note the singularity for the first order equations is the same as the zeroth order (i.e., $(\phi_o - \xi)^2 - \gamma f_o / \psi_o = 0$). The corresponding regularity condition for the first order can be obtained from Eqs. 6.4.104 to 6.4.106 as

$$\frac{1}{Y_o}\left[\gamma f_1 \phi_o' + 2\theta_1 f_o + \phi_1 f_o' + \gamma j (f_o \phi_1 + f_1 \phi_o)/\xi\right]$$

$$-(\phi_o - \xi)\left[\phi_1(\phi_o' - \theta_o) + \theta_1 \phi_o - 4 f_o'/f_o^2\right] = 0 \qquad (6.4.121)$$

With the first order correction, the shock trajectory, the shock pressure p_1/p_o, density ρ_1/ρ_o, particle velocity u_1/C_o, and the variation of shock strength η with shock radius r_s are given by the following expressions:

$$(1 - \tau) = B_o \, r_s^{\frac{\alpha+2}{2}}\left[1 + B_1 \beta r_s^\alpha + \cdots\right] \qquad (6.4.122)$$

where

$$B_o = \frac{2}{\alpha+2}\left(F_o^*\right)^{-\frac{1}{2}} \qquad (6.4.123)$$

$$B_1 = \frac{-(\alpha+2)}{2(3\alpha+2)} F_1^* \qquad (6.4.124)$$

$$\frac{p_1}{p_o} = \frac{\gamma}{\eta}\left[\frac{2}{\gamma+1} + \frac{(\gamma S_1 + 1)}{\gamma(\gamma+1)} \beta r_s^\alpha + \cdots\right] \qquad (6.4.125)$$

$$\frac{\rho_1}{\rho_o} = \frac{\gamma+1}{\gamma-1}\left[1 + \frac{(S_1 - 1)}{\gamma-1} \beta r_s^\alpha + \cdots\right] \qquad (6.4.126)$$

$$\frac{u_1}{C_o} = -\eta^{-\frac{1}{2}}\left[\frac{2}{\gamma+1} + \frac{(S_1 - 1)}{\gamma+1} \beta r_s^\alpha + \cdots\right] \qquad (6.4.127)$$

$$\eta = \beta r_s^\alpha\left[1 + F_1^* \beta r_s^\alpha + \cdots\right] \qquad (6.4.128)$$

where

$$S_1 = -\left(1 + \frac{(1-\eta_{cj})^2}{2\eta_{cj}} \right)$$

and η_{cj} is the reciprocal of the Chapman-Jouguet detonation Mach No. squared.

From the above analysis we note that by extending the validity of the asymptotic self-similar solution to account for non-similar effects, we still fail to bring the initial conditions into the solution. An exact numerical solution is required to evaluate the constants E and F_1. The memory of the initial processes comes in through these constants.

For implosions in an initially non-uniform density field (i.e., $\rho_o = A r^\omega$), the asymptotic solution near the center of symmetry can be found in a manner identical to that given above. The basic equations will now contain an ω term. For a non-uniform density field, the planar case (i.e., $j = 0$) is not trivial and shock amplification can result due to the density decrease. The solution will be identical to that for the propagation of a shock wave near the vacuum edge of a star given in the previous Section.

6.5 Collapse of a Bubble in a Liquid

In this Section we shall consider the collapse of an empty spherical cavity in a liquid. Bubbles can be formed and grow if the pressure at a certain part of a flow field is below the vapor pressure of the liquid. When these bubbles are convected at a later time to a region of higher pressure, they collapse. The symmetrical collapse of these bubbles results in the generation of strong shock waves in the fluid leading to damage of submerged surfaces such as propeller blades. Although in reality, the inside of a bubble is not empty but contains a vapor we shall neglect the influence of the vapor on the collapsing motion of the bubble. This assumption is valid at least in the final phases of collapse when the pressure build up near the cavity wall is sufficiently high. Some conjectures have been made regarding the rate of condensation of the vapor being sufficiently rapid to influence the collapsing motion. At any rate, pulsating motion has been observed for fairly large bubbles indicating the strong influence of the inside vapor pressure on the bubble motion. On the other hand, cavitation damage indicates the generation of fairly strong shock waves and this suggests that a sufficient amount of focussing has been achieved. In this case it seems most likely that small bubbles actually terminate their collapse at $r = 0$. We shall neglect vapor pressure in our analysis and consider an empty cavity.

At an initial time $t = 0$, we assume a spherical cavity of radius R_0 in an infinite expanse of fluid at pressure p_∞. The pressure inside the cavity is zero. As a result of the pressure difference p_∞, the bubble begins to shrink. The initial motion of the collapse has been studied by Rayliegh and it is instructive to briefly review it again. For the initial motion, compressibility effects can be neglected because the motion is slow and the pressure rise low. Hence from the continuity equation for

an incompressible fluid $\overrightarrow{\nabla} \cdot \vec{u} = 0$, we get

$$\overrightarrow{\nabla} \cdot \vec{u} = \rho \left(\frac{\partial u}{\partial r} + \frac{2u}{r} \right) = 0$$

since the flow is spherically symmetric. Solving the above equation with the boundary condition that the particle velocity u at the cavity wall $R(t)$ equal to the velocity of the interface $\dot{R}(t)$ (i.e., $u(R) = \dot{R}$), we get the velocity distribution as

$$u(r) = \dot{R}(t) \left(\frac{R(t)}{r} \right)^{2} \tag{6.5.1}$$

From the momentum equation, we obtain

$$p = \int -\rho \left(\frac{\partial u}{\partial t} + u \frac{\partial u}{\partial r} \right) dr$$

Using Eq. 6.5.1 to evaluate the derivatives and integrating the above equation from the cavity wall R to infinity, we have

$$p = p_0 + \rho R \left(\frac{\ddot{R}R + 2\dot{R}^2}{r} \right) - \frac{\rho \dot{R}^2}{2} \left(\frac{R}{r} \right)^4 \tag{6.5.2}$$

Using the boundary condition at the cavity wall $r = R$, $p(R) = 0$, Eq. 6.5.2 becomes

$$0 = p_0 + \rho \left(\ddot{R}R + \frac{3}{2} \dot{R}^2 \right) \tag{6.5.3}$$

Solving the above differential equation under the initial condition $t = 0$, $\dot{R} = 0$, $R = R_0$, we obtain an equation for the velocity increase of the collapsing bubble with radius

$$\dot{R}^2 = \frac{2p_0}{3\rho} \left[\left(\frac{R_0}{R} \right)^3 - 1 \right] \tag{6.5.4}$$

Integrating the above equation with respect to time yields the trajectory of the collapsing bubble as

$$\left(\frac{2p_0}{3\rho} \right)^{\frac{1}{2}} \frac{t}{R_0} = \int_{R/R_0}^{1} \frac{z^2 dz}{(1 - z^3)^{\frac{1}{2}}} \tag{6.5.5}$$

The total collapse time τ may be obtained from Eq. 6.5.5 by integrating from zero to one. We obtain

$$\tau = B\left(\tfrac{5}{6}, \tfrac{1}{2}\right) R_0 \left(\tfrac{\rho}{6\rho}\right)^{\tfrac{1}{2}} \tag{6.5.6}$$

where $B(\alpha, \beta)$ the well known Beta function defined as

$$B(\alpha, \beta) = \frac{\Gamma(\alpha)\,\Gamma(\beta)}{\Gamma(\alpha+\beta)} \tag{6.5.7}$$

For the particular values $\alpha, \beta = \tfrac{5}{6}, \tfrac{1}{2}$

$$B\left(\tfrac{5}{6}, \tfrac{1}{2}\right) = \Gamma(\tfrac{1}{2})\Gamma(\tfrac{5}{6})/\Gamma(\tfrac{4}{3}) = \sqrt{\pi}\,\Gamma(\tfrac{5}{6})/\Gamma(\tfrac{4}{3})$$

so that the collapse time τ becomes

$$\tau = .915\, R_0 \left(\tfrac{\rho}{\rho_\infty}\right)^{\tfrac{1}{2}} \tag{6.5.8}$$

Using the above equation we can find the total time of collapse of a bubble of any given size initially. For example for a 1 mm radius bubble ($R_0 = 1$ mm) in water ($\rho = 1$ gm per cc, $\rho_\infty = 1$ atm) the total time of collapse is $\tau = .915 \times 10^{-4}$ sec. or about 1/10 of a millisecond. Of course this is only an approximate order of magnitude because compressibility effects become significant for the later part of the collapse and Eq. 6.5.5 is no longer valid. The pressure distribution can be obtained from Eq. 6.5.2 using Eq. 6.5.3 and the resultant form can be expressed as

$$\frac{p}{p_\infty} = \frac{1}{2}\left(\frac{\rho R^2}{p_\infty}\right)\left(\frac{1}{\xi} - \frac{1}{\xi^4}\right) + \left(1 - \frac{1}{\xi}\right) \tag{6.5.9}$$

where $\xi = r/R(t)$

The present problem contains a characteristic length R_0 and a characteristic velocity $(p_\infty/\rho)^{\tfrac{1}{2}}$. However in the asymptotic limit $R \to 0$, the length scale R_0 becomes too large and no longer characterizes the motion. Also from Eqs. 6.5.4 and 6.5.9 we note that the velocity $\dot{R}^2$, hence the pressure approaches infinity as $R \to 0$ and therefore the velocity scale

$(k/\rho)^{1/2}$ does not play a role in the asymptotic motion as $t \to 0$. The final phases of the collapse essentially forget the initial conditions since k and Λ do not appear as in the collapsing shock wave problem treated in the previous Section. The asymptotic motion suggests a similarity solution of the form

$$\phi(\xi) = u/\dot{R} \quad , \quad f(\xi) = p/(\rho \dot{R}^2)$$

since the only velocity and pressure scales are $\dot{R}$ and $\rho \dot{R}^2$ respectively. Similarity solutions of the above form for the asymptotic motion have been obtained by Hunter. Full compressibility effects were considered and the one dimensional non-steady gasdynamic equations were employed.

$$\frac{\partial \rho}{\partial t} + u \frac{\partial \rho}{\partial r} + \rho \frac{\partial u}{\partial r} + j \frac{\rho u}{r} = 0 \qquad (6.5.10)$$

$$\frac{\partial u}{\partial t} + u \frac{\partial u}{\partial r} + \frac{1}{\rho}\frac{\partial p}{\partial r} = 0 \qquad (6.5.11)$$

$$\frac{\partial S}{\partial t} + u \frac{\partial S}{\partial r} = 0 \qquad (6.5.12)$$

where S is the specific entropy. The equation of state used is the modified Tait form given as

$$\frac{p+B}{B} = \left(\frac{\rho}{\rho_0}\right)^\gamma \qquad (6.5.13)$$

where B is a constant of the order of 3 kilo bars, $\gamma \cong 7$ for water and ρ_0 is the density at zero pressure. From Eq. 6.5.13 we obtain the speed of sound as

$$c^2 = \left(\frac{\partial p}{\partial \rho}\right)_S = \frac{\gamma B}{\rho}\left(\frac{\rho}{\rho_0}\right)^\gamma = \frac{\gamma(p+B)}{\rho} \qquad (6.5.14)$$

For compressible motions in water, we can apply the isentropic approximation in general since the entropy change across even a fairly strong shock

wave is vanishingly small. For isentropic motion, Eqs. 6.5.10 to 6.5.12 can be reduced to the following pair of equations

$$\frac{\partial c^{-1}}{\partial t} + u\frac{\partial c^{-1}}{\partial r} + (\gamma-1)c^{-1}\frac{\partial u}{\partial r} + j(\gamma-1)c^{-1}\frac{u}{r} = 0 \qquad (6.5.15)$$

$$\frac{\partial u}{\partial t} + u\frac{\partial u}{\partial r} + \frac{1}{\gamma-1}\frac{\partial c^2}{\partial r} = 0 \qquad (6.5.16)$$

where u and c are the only two dependent variables to be determined. Once a solution for c^2 has been obtained the pressure and density distributions can be found from the equation of state and the relation for the sound speed with p and ρ.

Without restricting ourselves to the asymptotic final phases of the collapse at present, the boundary conditions for Eqs. 6.5.15 and 6.5.16 are given as

at the cavity wall $r = R$

$$u = \dot{R}$$
$$c^2 = \frac{\gamma B}{\rho_0} \qquad (6.5.17)$$

and at $r = \infty$

$$u = 0$$
$$c^2 = \frac{\gamma(\rho_0+B)}{\rho_\infty} \qquad (6.5.18)$$

We have considered for the final motion that $R \ll R_0$ and the bubble essentially originates at infinity. Since ρ_0 is of the order of 1 bar while B is 3 kilobars, ρ_∞ can be neglected in Eq. 6.5.18. Also ρ_∞ can be taken as B since the density changes in water under a few bars of pressures are negligibly small.

Transforming Eqs. 6.5.15 and 6.5.16 in the familiar blast wave coordinates we have

$$(\phi-\xi)\frac{\partial \epsilon}{\partial \xi} + (\gamma-1)\epsilon\frac{\partial \phi}{\partial \xi} + 2\theta\epsilon + j(\gamma-1)\frac{\epsilon\phi}{\xi} = 2\theta\eta\frac{\partial \epsilon}{\partial \eta} \qquad (6.5.19)$$

$$(\phi - \xi)\frac{\partial \phi}{\partial \xi} + \frac{1}{\gamma - 1}\frac{\partial \epsilon}{\partial \xi} + \theta\phi = 2\theta\eta\frac{\partial \phi}{\partial \eta} \tag{6.5.20}$$

where

$$\xi = \frac{r}{R}$$

$$\eta = \frac{\gamma B}{\rho_0} \cdot \frac{1}{\dot{R}^2}$$

$$\phi = \frac{u}{\dot{R}} \tag{6.5.21}$$

$$\epsilon = \frac{c^2}{\dot{R}^2}$$

$$\theta = \frac{R\ddot{R}}{\dot{R}^2}$$

and the corresponding boundary conditions become

$$\phi(1, \eta) = 1 \quad, \quad \epsilon(1, \eta) = \eta \tag{6.5.22}$$

We do not worry about the boundary conditions at $\xi = \infty$ because as will be shown later, the asymptotic motion is dependent and uniquely determined by the consideration of a small region of flow immediately in the wake of the cavity wall.

In the immediate neighborhood of the center of collapse, $\dot{R}^2 \to \infty$ and $\eta \to 0$. Assuming the derivatives of ϵ and ϕ with respect to η to remain finite as $\eta \to 0$, the right hand sides of Eqs. 6.5.19 and 6.5.20 vanish and we get

$$(\phi - \xi)\epsilon' + (\gamma - 1)\epsilon\phi' + 2\theta\epsilon + j(\gamma - 1)\frac{\epsilon\phi}{\xi} = 0 \tag{6.5.23}$$

$$(\phi - \xi)\phi' + \frac{1}{\gamma - 1}\epsilon' + \theta\phi = 0 \qquad (6.5.24)$$

The boundary conditions at the front $\xi = 1$ reduce to

$$\phi(1) = 1 \quad , \quad \epsilon(1) = 0 \qquad (6.5.25)$$

Solving for the derivatives ϵ' and ϕ' from Eqs. 6.5.23 and 6.5.24 we get

$$\epsilon' = \frac{\epsilon\left[(\gamma - 1)\theta\phi - (\phi - \xi)(2\theta + j(\gamma - 1)\phi/\xi)\right]}{(\phi - \xi)^2 - \epsilon} \qquad (6.5.26)$$

$$\phi' = \frac{\left[\frac{\epsilon}{\gamma - 1}(2\theta + j(\gamma - 1)\phi/\xi) - \theta\phi(\phi - \xi)\right]}{(\phi - \xi)^2 - \epsilon} \qquad (6.5.27)$$

From Eqs. 6.5.26 and 6.5.27 we see immediately that the slopes ϵ' and ϕ' are indeterminate at the cavity wall $\xi = 1$. Hence to start the integration it is necessary to find the solution in the neighborhood of the cavity wall $\xi = 1$ by expanding in power series of the form

$$\phi = 1 + a(\xi - 1)^{\alpha} + \cdots$$
$$\epsilon = b(\xi - 1)^{\beta} + \cdots \qquad (6.5.28)$$

Substituting the above expansions into Eqs. 6.5.26 and 6.5.27 we obtain

$$\alpha = \beta = 1$$

$$b = -\theta(\gamma - 1)$$

$$a = \frac{1}{\gamma}(1 - 2\theta - j(\gamma - 1))$$

and hence the solution near the wall can be written as

$$\phi = 1 + \frac{1}{\gamma}(1 - 2\theta - j(\gamma - 1))(\xi - 1) + \cdots$$

$$(6.5.29)$$

$$\epsilon = -\theta(\gamma - 1)(\xi - 1) + \cdots$$

Notice that θ is as yet unknown. If we select some specific value of θ and then using Eq. 6.5.29 to start the solution, proceed to integrate Eqs. 6.5.26 and 6.5.27 for $\xi > 1$, we find that the singularity $(\phi - \xi)^2 - \epsilon = 0$ is encountered for some $\xi = \xi^* > 1$. Hence, to complete this similarity solution, we must find a value of θ that will permit smooth crossing at the singularity $\xi = \xi^*$. From Eq. 6.5.26, the θ that permits this is the one that makes the numerator equal to zero at $\xi = \xi^*$ as well as yielding

$$\theta = \frac{j(\gamma-1)\phi(\phi-\xi)}{\xi[(\gamma-3)\phi + 2\xi]}\bigg|_{\xi=\xi^*} \qquad (6.5.30)$$

For example, from the paper by Akinsete and Lee, for $j = 2$ (spherical symmetry) and $\gamma = 7$ we have $\theta = -.80111$ and $\xi^* = 1.50094$.

We shall now attempt to obtain corrections to this similarity solution to account for finite η or $\dot{R}^2$ just prior to collapse by expanding the solution as

$$\phi(\xi,\eta) = \phi_0(\xi) + \phi_1(\xi)\eta + \cdots$$
$$\epsilon(\xi,\eta) = \epsilon_0(\xi) + \epsilon_1(\xi)\eta + \cdots \qquad (6.5.31)$$
$$\theta = \theta_0 + \theta_1 \eta + \cdots$$

Substituting the above equations into the original equations (Eqs. 6.5.19 and 6.5.20), the zero order solution ($\phi_0(\xi)$, $\epsilon_0(\xi)$ and θ_0) is found to be the similarity solution just discussed while the first order flow variables must now satisfy

$$\phi_1' = \frac{1}{D}\bigg[\frac{1}{\gamma-1}\Big((\gamma-1)\epsilon_1\phi_0' + 2\theta_1\epsilon_0 + \phi_1\epsilon_0' +$$
$$+ j\frac{(\gamma-1)}{\xi}(\phi_0\epsilon_1 + \phi_1\epsilon_0)\Big) - (\phi_0-\xi)\Big(\phi_1(\phi_0'-\theta_0) + \theta_1\phi_0\Big)\bigg] \qquad (6.5.32)$$

$$\epsilon'_1 = \frac{1}{D}\left[(\gamma-1)\epsilon_0\left(\phi_1(\phi'_0-\theta_0)+\theta_1\phi_0\right)-(\phi_0-\xi)\left(\epsilon_1\phi'_0(\gamma-1)\right.\right.$$

$$\left.\left.+2\theta_1\epsilon_0+\phi_1\epsilon'_0+j\left(\frac{\gamma-1}{\xi}\right)(\phi_0\epsilon_1+\phi_1\epsilon_0)\right)\right] \tag{6.5.33}$$

where

$$D = (\phi_0-\xi)^2-\epsilon_0 \tag{6.5.34}$$

The boundary conditions are found from Eq. 6.5.22 to be

$$\phi_0(1) = \epsilon_1(1) = 1 \quad , \quad \phi_1(1) = \epsilon_0(1) = 0 \tag{6.5.35}$$

Near the cavity wall ($\xi = 1$) ϕ_0 and ϵ_0 have the limiting forms given by Eq. 6.5.29. Also

$$D = (\phi_0-\xi)^2-\epsilon_0 \simeq \theta_0(\gamma-1)(\xi-1)$$

The numerator of Eq. 6.5.32, near $\xi = 1$ approaches

$$\phi'_0(1) + j\phi(1) = \frac{1}{\gamma}\left(1-2\theta_0-j(\gamma-1)\right) +j$$

and hence ϕ'_1 becomes (near $\xi = 1$)

$$\phi'_1(1) \longrightarrow \frac{\left[\frac{1}{\gamma}(1-2\theta_0-j(\gamma-1))+j\right]}{\theta_0(\gamma-1)(\xi-1)}$$

so that $\phi_1 \longrightarrow k \ln(\xi-1)$ near $\xi = 1$ unless the numerator $\frac{1}{\gamma}(1-2\theta_0-j(\gamma-1))+j = 0$. However θ_0 was determined from the similarity solution beforehand to yield smooth crossing at $\xi = \xi^*$ and therefore the numerator in question is not zero. Hence we are led to the conclusion that $\phi(\xi,\eta)$ behaves like

$$\phi = \phi_0(\xi) + k\eta \ln(\xi-1)$$

so that at $\xi = 1$, $|\phi(1,\eta)| = \infty$ unless $\eta = 0$ which does not satisfy the boundary conditions. This means that the perturbation series solution (Eq. 6.5.31) is not the proper one.

To see this better, let us return to the original equations (Eqs. 6.5.19 and 6.5.20) and examine the behavior of $\phi(\xi,\eta)$ and $\epsilon(\xi,\eta)$ near $\xi = 1$ by setting

- 354 -

$$\phi(\xi,\eta) = 1 + F_1(\eta)(\xi-1) + F_2(\eta)(\xi-1)^2 + \cdots$$

$$\epsilon(\xi,\eta) = \eta + G_1(\eta)(\xi-1) + G_2(\eta)(\xi-1)^2 + \cdots$$

(6.5.36)

and substituting the above equations into Eqs. 6.5.19 and 6.5.20. We get

$$\left[(F_1-1)(\xi-1) + \cdots \right]\left[G_1 + \cdots \right]$$
$$+ (\gamma-1)\left[\eta + G_1(\xi-1) + \cdots \right]\left[F_1 + 2F_2(\xi-1) + \cdots \right]$$
$$= -\left\{ \left[\eta + G_1(\xi-1) + \cdots \right]\left[2\theta + j(\tfrac{\gamma-1}{\xi})(1+F_1(\xi-1)+\cdots) \right] \right.$$
$$\left. -2\theta\eta\left[1 + (\xi-1)\tfrac{dG_1}{d\eta} + \cdots \right] \right\}$$

(6.5.37)

$$\left[(F_1-1)(\xi-1) + \cdots \right]\left[F_1 + \cdots \right] + \tfrac{1}{\gamma-1}\left[G_1 + 2(\xi-1)G_2 + \cdots \right]$$
$$= -\left\{ \theta(1 + F_1(\xi-1) + \cdots) - 2\theta\eta\left((\xi-1)\tfrac{dF_1}{d\eta} + \cdots \right) \right\}$$

(6.5.38)

a) Let us consider first $\eta \neq 0$. Taking lowest order of $\xi-1$ in Eq. 6.5.38 we have

$$G_1 = -\theta(\gamma-1)$$

(6.5.39)

and taking the zero order term in $(\xi-1)$ of Eq. 6.5.37 we obtain

$$(\gamma-1)\eta F_1 = -\eta(2\theta + j(\gamma-1)) + 2\theta\eta$$
$$= -\eta j(\gamma-1)$$

and since $\eta \neq 0$, one gets

$$F_1 = -j$$

(6.5.40)

It would therefore appear that if $\eta \neq 0$ the behavior of ϕ and ϵ near $\xi = 1$ is

$$\phi = 1 - j(\xi-1) + F_2(\xi-1)^2 +$$

$$\epsilon = \eta - \theta(\gamma-1)(\xi-1) + G_2(\xi-1)^2 +$$

(6.5.41)

b) We now let $\eta = 0$ and set $\theta(0) = \theta_0$. Taking the lowest order in $\xi - 1$ of Eq. 6.5.38 then gives

$$G_1 = -\theta_0(\gamma - 1)$$

which is the same form as given previously (Eq. 6.5.39). However upon examination of Eq. 6.5.37 we see that this time the lowest order is one instead of zero as it was in the $\eta \neq 0$ case. We therefore get

$$(F_1 - 1)G_1 + (\gamma - 1)G_1 F_1 = -G_1(2\theta_0 + j(\gamma - 1))$$

or

$$F_1 = \frac{1}{\gamma}(1 - 2\theta_0 - j(\gamma - 1)) \qquad (6.5.42)$$

and hence if $\eta = 0$, the behavior of ϕ and ϵ are

$$\phi = 1 + \frac{1}{\gamma}(1 - 2\theta_0 - j(\gamma - 1))(\xi - 1) + \cdots$$

$$\qquad (6.5.43)$$

$$\epsilon = -\theta_0(\gamma - 1)(\xi - 1) + \cdots$$

near $\xi = 1$ which is identical to the similarity solution form given earlier by Eq. 6.5.29.

Comparing the forms of ϕ given by Eqs. 6.5.41 and 6.5.43, we observe that if θ is a continuous function of η at $\eta = 0$, the slope of ϕ at the cavity wall is discontinuous at $\eta = 0$. Conversely, if θ is discontinuous in such a way that the slope of ϕ at the wall is continuous, then the slope of ϵ at the bubble wall has a jump at $\eta = 0$. The conclusion therefore is that ϕ or ϵ (or both) have a slope at the cavity wall which suffers a jump or discontinuity at $\eta = 0$.

It should be observed that the similarity solution obtained for $\eta = 0$ has a limited validity in any case since there is a forgetfulness in the solution of the initial conditions due to the singularity

$(\phi_0 - \xi)^2 - \epsilon_0 = 0$ at $\xi = \xi^*$. Further, this similarity solution is only valid at the point $R = 0$ and hence the range of validity is confined to the point of collapse itself. This is seen to be true since by the

analysis just performed, if we choose an $\eta \neq 0$ however small ($R \neq 0$),
the solution near the bubble wall is quite different in character. Hence,
we may then reasonably ask if the similarity solution itself has any phy-
sical meaning in the bubble problem just prior to collapse.

Attempts have been made by Holt and Schwartz, and Akinsete and
Lee to give this similarity solution meaning by stretching the ξ co-ordi-
nate using Lighthill's technique. The essence of the method is as follows:

Instead of perturbing the solution for ϕ and ϵ as given by
Eq. 6.5.31, we use the stretched co-ordinate S in place of ξ and write
the appropriate perturbation solution as

$$\phi(\xi,\eta) = \phi_0(S) + \phi_1(S)\eta + \phi_2(S)\eta^2 + \cdots$$

$$\epsilon(\xi,\eta) = \epsilon_0(S) + \epsilon_1(S)\eta + \epsilon_2(S)\eta^2 + \cdots \tag{6.5.44}$$

$$\theta(\eta) = \theta_0 + \theta_1\eta + \theta_2\eta^2 + \cdots$$

$$\xi = S + \xi_1(S)\eta + \xi_2(S)\eta^2 + \cdots \tag{6.5.45}$$

$$\eta = \eta$$

Using the relations

$$\frac{\partial}{\partial \xi} = \frac{1}{1 + \xi_1'\eta + \xi_2'\eta^2 +} \frac{\partial}{\partial S}$$

$$\frac{\partial}{\partial \eta} = \frac{\partial}{\partial \eta} - \frac{(\xi_1 + 2\xi_2\eta + \cdots)}{1 + \xi_1'\eta + \xi_2'\eta^2 +} \frac{\partial}{\partial S}$$

where the prime denotes differentiation with respect to S, one substi-
tutes Eqs. 6.5.44 and 6.5.45 into the original differential equations Eqs.
6.5.19 and 6.5.20 and equates like powers in η. The resultant zero and
first order equations are

$$(\phi_0 - S)\epsilon_0' + (\gamma-1)\epsilon_0\phi_0' = -\left[2\theta_0\epsilon_0 + j(\gamma-1)\frac{\epsilon_0\phi_0}{S}\right]$$

$$(\phi_0 - S)\phi_0' + \frac{1}{\gamma-1}\epsilon_0' = -\theta_0\phi_0$$

(6.5.46)

$$(\phi_0 - S)\epsilon_1' + (\gamma-1)\epsilon_0\phi_1' = -\left[\phi_1\epsilon_0' + (\gamma-1)\epsilon_1\phi_0' + 2\theta_1\epsilon_0 \right.$$

$$+ j(\frac{\gamma-1}{S})(\phi_0\epsilon_1 + \phi_1\epsilon_0)]$$

$$+ \xi_1\left[\epsilon_0'(1-2\theta_0) + j(\gamma-1)\frac{\epsilon_0\phi_0}{S^2}\right]$$

$$+ \xi_1'\left[(\gamma-1)\epsilon_0\phi_0' + \epsilon_0'(\phi_0-S)\right]$$

$$(\phi_0 - S)\phi_1' + \frac{1}{\gamma-1}\epsilon_1' = -\left[\phi_1(\phi_0'-\theta_0) + \theta_1\phi_0\right]$$

(6.5.47)

$$+ \xi_1\phi_0'(1-2\theta_0)$$

$$+ \xi_1'\left[\phi_0'(\phi_0-S) + \frac{\epsilon_0'}{\gamma-1}\right]$$

Before these equations can be solved, the boundary conditions at $\xi = 1$ must be imposed which are

$$\phi(1,\eta) = 1 \quad , \quad \epsilon(1,\eta) = \eta$$

When $\xi = 1$ at the cavity wall, we set $S = S_1$. Hence, from Eq. 6.5.45, we have

$$1 = S_1 + \xi_1(S_1)\eta + \xi_2(S_1)\eta^2 + \cdots$$

(6.5.48)

and we see that S_1 depends on η.

Expanding ξ_1, ξ_2, about $S_1 = 1$, we have

$$1 = S_1 + \eta\left[\xi_1(1) + (S_1-1)\xi_1'(1) + \cdots\right] + \eta^2\left[\xi_2(1) + \cdots\right] + \cdots$$

and setting $S_1 - 1 = \chi$ the above equation becomes

$$O = \chi + \eta \left[\xi_1(\cdot) + \chi \xi_1'(\cdot) + \quad \right] + \eta^2 \left[\xi_2(\cdot) + \chi \xi_2'(\cdot) \cdot \right] + \quad (6.5.49)$$

We may now readily obtain χ as a power series in η by substituting

$$S_1 - 1 = \chi = a_0 + a_1 \eta + a_2 \eta^2 + \cdot$$

into Eq. 6.5.49 and equating like powers of η yielding

$$S_1 = 1 - \xi_1(\cdot)\eta - (\xi_2(\cdot) - \xi(\cdot)\xi_1'(\cdot))\eta^2 + \cdots \quad (6.5.50)$$

From the boundary condition, the flow variables have values at the cavity wall $S = S_1$, ($\xi = 1$) given by

$$1 = \phi_0(S_1) + \phi_1(S_1)\eta + \cdots$$

$$\eta = \epsilon_0(S_1) + \epsilon_1(S_1)\eta + \cdot \quad (6.5.51)$$

and again expanding $\phi_0(S_1)$, $\epsilon_0(S)$ etc. about $S_1 = 1$ using the value for S_1, given by Eq. 6.5.50 we obtain the boundary conditions for the various orders as

$$\phi_0(1) = 1 \quad , \quad \epsilon_0(1) = 0 \quad (6.5.52)$$

$$\xi_1(\cdot)\phi_0'(\cdot) = \phi_1(\cdot)$$

$$\quad (6.5.53)$$

$$\epsilon_1(\cdot) - \xi_1(\cdot)\epsilon_0'(\cdot) = 1$$

Eqs. 6.5.46 are first integrated from $S = 1$ using the boundary conditions given by Eqs. 6.5.52. We recover the similarity solution for $\phi_0(S)$, $\epsilon_0(S)$ and θ_0 which is identical to that obtained and already discussed earlier in this section. As before, the solutions must be started at $S = 1$ due to the indeterminancy of the derivatives there. Then selecting a θ_0 that permits smooth crossing at $S = S^*$ gives the solution. Now, we proceed to solve the first order differential equations (Eq. 6.5.47) with the boundary equations given by Eq. 6.5.53. Unlike the previous situation, this time we have the variable $\xi_1(S)$ that we may

adjust at will in order that the resulting slopes of $\phi_1(s)$ and $\epsilon_1(s)$ at $s = 1$ be regular. In fact the function $\xi_1(s)$ may be as arbitrary as we wish just as long as the slopes of $\phi_1(s)$ and $\epsilon_1(s)$ are regular at $s = 1$. It can be seen however from the boundary condition (Eq. 6.5.53) that ϕ_1 and ϵ_1 depend on $\xi_1(s)$. At any rate, $\xi_1(s)$ is chosen to make the slopes of ϕ_1 and ϵ_1 be regular at $s = 1$ and the differential equations 6.5.47 are integrated and ∂_1 adjusted until smooth crossing is achieved at $s = s^*$ just as in the zero order case.

If we wish to obtain the second order solution, we continue in the same vein. This time we may adjust $\xi_2(s)$ so that ϵ_2 and ϕ_2 have regular slopes at $s = 1$ and then ∂_2 is varied until the integrated results give smooth crossing again at $s = s^*$. The resulting profiles ϕ, ϵ as functions of ξ and η are then found using Eqs. 6.5.44 and 6.5.45.

It is readily seen from the foregoing analysis that the resulting profiles for ϕ and ϵ as well as the independent variable $\xi = r/R$ are then given by the asymptotic series (Eqs. 6.5.44 and 6.5.45). Therefore, if the results are calculated to some given order in η, not only is there an uncertainty in the values of the flow variables but there also exists an uncertainty in the value of the independent variable $\xi = r/R$. It may well turn out that the similarity solution itself is the limiting solution to another problem entirely. Recall that the equation of state

$$(p+B)/B = (\rho/\rho_o)^\gamma$$

was assumed to hold right up to the time of collapse. The analytical consequences of this assumption gave us the strange behavior of the particle velocity not having a continuous slope at $R = 0$. Upon closer examination of the physical assumptions of the problem we see that at precisely the instant of collapse we have a finite density ρ_o collapsing at infinite speed at the centre. Surely this would cause some sort of additional im-

pulse to the problem resulting perhaps in a discontinuous behavior of the flow variables. The similarity solution therefore may represent a zero order process after collapse with no applicability to the solution prior to collapse at all.

From the foregoing remarks, it appears that we should exercise great caution and carefully consider the mathematical model before applying Lighthill's technique to a problem. Although there is no doubt that the technique offers a means of overcoming certain mathematical difficulties, nevertheless the resultant solution must have physical significance otherwise it becomes nothing more than a mathematical exercise. In the present bubble problem, the extreme difficulties in the experimental observations of the final phases of collapse results in the fact that we are still quite ignorant of the real physical situation. For this reason, we feel that further theoretical progress in this problem must await experimental verification of the similarity solution.

6.6 The CCW Method

Based on the works of Chester, Chisnell and Whitham on the
propagation of shock waves in a non-uniform channel, a very simple method
was developed which when applied to the strong converging shock problem
gave extremely accurate results. The CCW method was later applied to the
problem of shock motion near the vacuum edge of a star by Sakurai with
equal success. Recently Hayes also used the CCW method for a similar type
of problem, that is, the propagation of a shock wave in an exponential
atmosphere but found it to be less successful. Lee and Lee extended the
CCW method for converging detonation waves and found excellent agreement
with the experimental results. Alhborn and Huni's recent accurate measure-
ments of the trajectory of a converging cylindrical detonation wave also
found excellent agreement with the theoretical results based on the CCW
method. Hence it seems that in general, the CCW method can be applied to
this class of asymptotic problems with varying degrees of accuracy for
different problems. In view of its extreme simplicity and ease in obtain-
ing the solution, the CCW method is quite useful in obtaining a first
approximation to the correct solution. In this Section we will present
the CCW method and indicate how one can improve its accuracy by taking
higher order corrections.

The essence of the CCW method is to first write the basic con-
servation equations in characteristic form. Then the partial differential
equation for a particular characteristic is applied to the flow quantities
immediately behind the shock, or detonation front. Through the Rankine-
Hugoniot equations which relate these quantities to the shock strength
(i.e., M_S) and the initial states (i.e., ρ_o , p_o etc.) we can then
obtain the variation of the shock strength with its position. The success
of the CCW method of the problems discussed in this Chapter is due

to the fact that in all of these asymptotic problems, there exists a
limiting characteristic close behind the shock front. Its path is close
to that of the shock trajectory and tk states on this limiting charac-
teristic do not differ much from the states behind the shock front itself.
Hence the CCW approximation is quite adequate under these conditions.

We shall consider first the general case where the change of
shock strength can be due to both area change and variation of the initial
density ρ_o. The area change is caused by the cylindrical or spherical
geometry while the density variation is assumed to be given by the power
law form $\rho_o = Ar^\omega$. The case where both the area and the density varies
exponentially with distance is treated separately later because of its
special form. For $\rho_o = Ar^\omega$ and cylindrical or spherical symmetry the
basic conservation equations are given as

$$(\phi-\xi)\frac{\partial \psi}{\partial \xi} + \psi\frac{\partial \phi}{\partial \xi} + (j+\omega)\frac{\phi\psi}{\xi} = 2\theta\eta\frac{\partial \psi}{\partial \eta} \tag{6.6.1}$$

$$(\phi-\xi)\frac{\partial \phi}{\partial \xi} + \frac{1}{\psi}\frac{\partial f}{\partial \xi} + \theta\phi + \frac{\omega f}{\xi\psi} = 2\theta\eta\frac{\partial \phi}{\partial \eta} \tag{6.6.2}$$

$$(\phi-\xi)\frac{\partial f}{\partial \xi} + \gamma f\frac{\partial \phi}{\partial \xi} + 2\theta f + (\gamma j+\omega)\frac{f\phi}{\xi} = 2\theta\eta\frac{\partial f}{\partial \eta} \tag{6.6.3}$$

where

$$\theta = R_s\ddot{R}_s/\dot{R}_s^2 \quad , \quad \eta = c_o^2/\dot{R}_s^2 \tag{6.6.4}$$

Writing the above equations in characteristic form, we get the following
corresponding equations

$$(\phi - \xi)\frac{\partial S}{\partial \xi} - 2\theta\eta\frac{\partial S}{\partial \eta} + 2\theta S - \phi\frac{S\omega(\gamma-1)}{\xi} = 0 \qquad (6.6.5)$$

$$(\phi - \xi - \beta)\left[\frac{\partial \phi}{\partial \xi} - (\gamma f \psi)^{-\frac{1}{2}}\frac{\partial f}{\partial \xi}\right] - 2\theta\eta\left[\frac{\partial \phi}{\partial \eta} - (\gamma f \psi)^{-\frac{1}{2}}\frac{\partial f}{\partial \eta}\right]$$

$$+ \theta\left(\phi - \frac{2\beta}{\gamma}\right) + \frac{\beta}{\gamma\xi}\left(\beta\omega - \phi(\omega + \gamma j)\right) = 0 \qquad (6.6.6)$$

$$(\phi - \xi + \beta)\left[\frac{\partial \phi}{\partial \xi} + (\gamma f \psi)^{-\frac{1}{2}}\frac{\partial f}{\partial \xi}\right] - 2\theta\eta\left[\frac{\partial \phi}{\partial \eta} + (\gamma f \psi)^{-\frac{1}{2}}\frac{\partial f}{\partial \eta}\right]$$

$$+ \theta\left(\phi + \frac{2\beta}{\gamma}\right) + \frac{\beta}{\gamma\xi}\left(\beta\omega + \phi(\omega + \gamma j)\right) = 0 \qquad (6.6.7)$$

where $\quad S = f/\psi^{\gamma} \quad, \quad \beta^{2} = \gamma f/\psi$

Eq. 6.6.5 may be interpreted as a directional differential equation along a particle trajectory characteristic while Eqs. 6.6.6 and 6.6.7 correspond to the so-called negative and the positive characteristic directions. In the asymptotic problems treated earlier, there exists a positive character istic behind the shock. At this positive limiting characteristic we have

$$\phi^{*} + \beta^{*} = \phi(\xi^{*}) + \beta(\xi^{*}) = \xi^{*} \qquad (6.6.8)$$

so that evaluating Eq. 6.6.7 at $\xi = \xi^{*}$, the first term on the right hand side vanishes if ϕ and f are continuous at ξ^{*} and we can solve for θ yielding the following result

$$\theta = \left. \frac{-\beta(\beta\omega + \phi(\omega + \gamma_j))}{\gamma_\xi \left(\phi + \frac{2\beta}{\gamma} - 2\eta \left[\frac{\partial\phi}{\partial\eta} + (\gamma f \psi)^{\frac{1}{2}} \frac{\partial f}{\partial\eta} \right] \right)} \right|_{\substack{\xi = \xi^* \\ = \phi^* + \beta^*}} \tag{6.6.9}$$

If the limiting characteristic is close to the shock front (i.e., $\xi^* \simeq 1$) we can approximate $\phi(\xi^*)$ by $\phi(1)$ and $\beta(\xi^*)$ by $\beta(1)$ where $\phi(1)$, $\beta(1)$ are the values immediately behind the shock. Setting

$$\xi^* \simeq \phi(1) + \beta(1) \tag{6.6.10}$$

and substituting the above equation into Eq. 6.6.9 we get the following approximate relationship for θ.

$$\theta \simeq \frac{-\beta(1)\left[\omega\beta(1) + (\omega + \gamma_j)\phi(1) \right]}{\gamma(\phi(1) + \beta(1))\left[\phi(1) + \frac{2}{\gamma}\beta(1) - 2\eta \left(\frac{\partial\phi}{\partial\eta}(1) + (\gamma f(1)\psi(1))^{\frac{1}{2}} \frac{\partial f}{\partial\eta}(1) \right) \right]} \tag{6.6.11}$$

The values $\phi(1)$, $f(1)$, $\psi(1)$, $\beta(1)$ at the shock are given by the Rankine-Hugoniot relationships as

$$\psi(1) = \frac{\gamma + 1}{\gamma - S + \eta} \tag{6.6.12}$$

$$\phi(1) = 1 + \frac{S - \eta}{\gamma + 1} \tag{6.6.13}$$

$$f(1) = \frac{\gamma + \eta + \gamma S}{\gamma(\gamma + 1)} \tag{6.6.14}$$

$$\beta^2(1) = \gamma f(1) / \psi(1) \tag{6.6.15}$$

where

$$S = \left[(1-\eta)^2 - k\eta \right]^{\frac{1}{2}} \tag{6.6.16}$$

$$k = 2Q(\gamma^2-1)/c_o^2 \tag{6.6.17}$$

Using Eqs. 6.6.12 to 6.6.17, Eq. 6.6.11 yields a value for Θ for any shock strength η specified. Once $\Theta(\eta)$ is known, the shock trajectory and the variations of shock density, pressure and particle velocity with shock radius can readily be determined without actually solving for the details of the complete flow.

For strong shocks, Eq. 6.6.11 reduces to the following

$$\Theta_o = \frac{-\beta(1)\left[\omega\beta(1) + (\omega+\gamma j)\phi(1) \right]}{\gamma(\phi(1) + \beta(1))(\phi(1) + \frac{2}{\gamma}\beta(1))} \tag{6.6.18}$$

The boundary conditions $\phi(1)$, etc., at the shock take on their limiting values given by the expressions below

$$\phi(1) = f(1) = 2/(\gamma+1) \tag{6.6.19}$$

$$\psi(1) = (\gamma+1)/(\gamma-1) \tag{6.6.20}$$

$$\beta(1) = \left[-2\gamma(\gamma-1)/(\gamma+1)^2 \right]^{\frac{1}{2}} \tag{6.6.21}$$

Hence for any specified values of j , ω and γ , Θ_o can be obtained immediately from Eq. 6.6.18. A comparison of the results obtained from the CCW method and from the exact similarity solutions are given in the tables below

$j = 0$, Planar Symmetry

ω \ γ	1.2	1.4	5/3	3	7
0.5	-0.087450 / -0.091506	-0.103516 / -0.107625	-0.114097 / -0.118034	-0.130716 / -0.133975	-0.139017 / -0.141792
1.0	-0.170399 / -0.183013	-0.202135 / -0.215250	-0.223349 / -0.236068	-0.257181 / -0.267949	-0.274365 / -0.283485
1.5	-0.251210 / -0.274519	-0.298388 / -0.322876	-0.330154 / -0.354102	-0.381334 / -0.401924	-0.407629 / -0.425227

$j = 1$, Cylindrical Symmetry

ω \ γ	1.2	1.4	5/3	3	7
-0.5	-0.071688 / -0.071605	-0.087878 / -0.089445	-0.102476 / -0.107391	-0.139332 / -0.160254	-0.170219 / -0.213720
0	-0.161221 / -0.163112	-0.197143 / -0.197071	-0.226054 / -0.225425	-0.289214 / -0.294229	-0.336730 / -0.355462
0.5	-0.245871 / -0.254618	-0.299707 / -0.304696	-0.341562 / -0.343459	-0.428535 / -0.428203	-0.491373 / -0.497205
1.0	-0.328035 / -0.346124	-0.398752 / -0.412321	-0.452699 / -0.461493	-0.561630 / -0.562178	-0.638444 / -0.638947
1.5	-0.408769 / -0.437631	-0.495757 / -0.519946	-0.561262 / -0.579527	-0.690876 / -0.696152	-0.780592 / -0.780689

$j = 2$, Spherical Symmetry

ω \ γ	1.2	1.4	5/3	3	7
-1.0	-0.143397 / -0.143211	-0.172860 / -0.178890	-0.195827 / -0.214782	-0.240132 / -0.320508	-0.266723 / -0.427439
-0.5	-0.234586 / -0.234717	-0.287711 / -0.286516	-0.329825 / -0.332816	-0.413851 / -0.454483	-0.465546 / -0.569182
0	-0.320757 / -0.326223	-0.394361 / -0.394191	-0.452692 / -0.450850	-0.571314 / -0.588457	-0.647585 / -0.710924
0.5	-0.404167 / -0.417730	-0.496423 / -0.501766	-0.569119 / -0.568884	-0.717909 / -0.722432	-0.816700 / -0.852667
1.0	-0.485908 / -0.509236	-0.595713 / -0.609392	-0.681602 / -0.686918	-0.857275 / -0.856406	-0.976268 / -0.994909
1.5	-0.566579 / -0.600742	-0.693220 / -0.717017	-0.791534 / -0.804952	-0.991757 / -0.990381	-1.128881 / -1.136151
2.0	-0.646522 / -0.692249	-0.789519 / -0.824642	-0.899743 / -0.922986	-1.122838 / -1.124356	-1.276401 / -1.277894

Note: Each entry has the exact value of θ_O placed above the CCW result.

From the tables, we can see that the CCW method gives extremely
accurate results particularly for converging strong shock waves in a uni-
form density media. It should be noted that the CCW method can predict
only the shock trajectory and the variations of the shock states with shock
radius, no information on the flow structure can be obtained. If the
value of θ_0 determined by the CCW method is substituted back into the
similarity equations, and an integration is performed, we will find that
this approximate value of θ_0 although quite adequate for most experimental
purposes, is insufficiently accurate to yield solutions that are continuous
at the singularity $\xi = \xi^*$. Therefore the CCW method is restricted in
the sense that no information on the flow field behind the shock can be
obtained.

From the CCW method, the location of the limiting characteristic
ξ^*, which is approximated by $\phi(1) + \beta(1)$ is overestimated by a
substantial amount. For example, for converging spherical shock waves with
$\gamma = 1.4$ and $\omega = 0$, the exact similarity solution yields a value of $\xi^* =$
1.1296 while under the CCW approximation, $\xi^* = 1.2743$. This is due to the
fact that both ϕ and β decrease monotonically as we move away from the
shock front. However from Eq. 6.6.18, we see both the numerator and the
denominator are quadratic in ϕ and β, hence we would expect both to be
overestimated by evaluating the variables at the shock instead of at $\xi =$
ξ^*. This effect acts in a compensating manner resulting in an accurate
value for θ_0 for certain ranges of γ and ω.

We can obtain a better value of θ_0 by improving the estimate for
ξ^* as follows: we first expand the variables ϕ, f, ψ and β in a
Taylor series about the shock $\xi = 1$.

$$\phi = \phi_{(1)} + \epsilon \frac{\partial \phi_{(1)}}{\partial \xi} +$$

$$f = f_{(1)} + \epsilon \frac{\partial f_{(1)}}{\partial \xi} + \cdot$$

$$\psi = \psi_{(1)} + \epsilon \frac{\partial \psi_{(1)}}{\partial \xi} + \cdot \qquad (6.6.22)$$

$$\beta = \beta_{(1)} + \epsilon \frac{\partial \beta_{(1)}}{\partial \xi} + \cdot$$

where

$$\epsilon = \xi - 1 \qquad (6.6.23)$$

The quantities $\dfrac{\partial \phi_{(1)}}{\partial \xi}$, $\dfrac{\partial \psi_{(1)}}{\partial \xi}$, etc. may be formed from Eqs. 6.6.1 to 6.6.3 as

$$\frac{\partial \phi_{(1)}}{\partial \xi} = \frac{1}{D}\left[(\phi_{(1)} - 1)\left(2\theta\eta\frac{\partial \phi_{(1)}}{\partial \eta} - \theta\phi_{(1)} - \omega\frac{f_{(1)}}{\psi_{(1)}}\right) \right.$$
$$\left. + \frac{1}{\psi_{(1)}}\left(2\theta f_{(1)} + (\gamma_j + \omega)f_{(1)}\phi_{(1)} - 2\theta\eta\frac{\partial f_{(1)}}{\partial \eta}\right)\right] \qquad (6.4.24)$$

$$\frac{\partial f_{(1)}}{\partial \xi} = -\psi_{(1)}\left[(\phi_{(1)} - 1)\frac{\partial \phi_{(1)}}{\partial \xi} + \theta\phi_{(1)} + \omega\frac{f_{(1)}}{\psi_{(1)}} - 2\theta\eta\frac{\partial \phi_{(1)}}{\partial \eta}\right] \qquad (6.5.25)$$

$$\frac{\partial \psi_{(1)}}{\partial \xi} = \frac{-1}{\phi_{(1)} - 1}\left[\psi_{(1)}\frac{\partial \phi_{(1)}}{\partial \xi} + (j + \omega)\phi_{(1)}\psi_{(1)} - 2\theta\eta\frac{\partial \psi}{\partial \eta}\right] \qquad (6.5.26)$$

$$\frac{2}{\beta_{(1)}}\frac{\partial \beta_{(1)}}{\partial \xi} = \frac{1}{f_{(1)}}\frac{\partial f_{(1)}}{\partial \xi} - \frac{1}{\psi_{(1)}}\frac{\partial \psi_{(1)}}{\partial \xi} \qquad (6.5.27)$$

where $\qquad D = [(\phi_{(1)} - 1)^2 - \beta^2_{(1)}]$

and $\phi_{(1)}$, $\psi_{(1)}$, $f_{(1)}$ and $\beta_{(1)}$ are the shock jump conditions given by Eqs. 6.6.12 to 6.6.15. From the above relations, we see that to

the first order in $\in$, Eq. 6.6.22 may be written

$$\phi = \phi(1) + \in F_1(\eta, \theta) + \cdots$$

$$\psi = \psi(1) + \in F_2(\eta, \theta) + \cdots$$

$$f = f(1) + \in F_3(\eta, \theta) +$$

$$\beta = \beta(1) + \in F_4(\eta, \theta) +$$

(6.6.28)

where the F's are linear in θ . For $\eta \neq 0$, it is also seen (Eq. 6.6.9) that the quantities $\partial \phi / \partial \eta$ and $\partial f / \partial \eta$ must also be determined. In fact they may be found by taking the partial derivations of the expansions for ϕ and f with respect to η in Eq. 6.6.28 yielding, to first order in $\in$

$$\frac{\partial \phi}{\partial \eta} = \frac{\partial \phi(1)}{\partial \eta} + \in \frac{d F_1}{d \eta}$$

(6.6.29)

$$\frac{\partial f}{\partial \eta} = \frac{\partial f(1)}{\partial \eta} + \in \frac{d F_3}{d \eta}$$

Since F_1 and F_3 are linear in θ , one sees immediately that $\frac{\partial \phi}{\partial \eta}$ and $\frac{\partial f}{\partial \eta}$ to first order in $\in$ contain $\frac{d\theta}{d\eta}$ terms. At $\xi = \xi^*$, $\in^* = \xi^* - 1$ and the first order approximation of $\xi^* = \phi^* + \beta^*$ now becomes

$$\xi^* = \phi(1) + \beta(1) + \in^*(F_1 + F_4)$$

Since $\in^* = \xi^* - 1$, we then have

$$\xi^* = \frac{\phi(1) + \beta(1) - F_1 - F_4}{1 - F_1 - F_4}$$

(6.6.30)

and

$$\in^* = \frac{\phi(1) + \beta(1) - 1}{1 - F_1 - F_4}$$

(6.6.31)

We may now substitute Eqs. 6.6.28 and 6.6.29 with $\in = \in^*$ given by Eq. 6.6.31 into Eq. 6.6.9 yielding a more accurate determination of $\theta = \theta(\eta)$. For $\eta = 0$, the right hand side of Eq. 6.6.9 will contain terms

quadratic in θ in the numerator and denominator (since $F_1 \to F_4$ are linear in θ). Hence Eq. 6.6.9 becomes a cubic equation in θ which may easily be solved (numerically). For $\eta \neq 0$, the $\frac{\partial \phi}{\partial \eta}$ and $\frac{\partial f}{\partial \eta}$ terms in Eq. 6.6.9 will produce $\frac{d\theta}{d\eta}$ terms and the equation becomes a first order differential equation for θ with respect to η which is easily started from the solution of the cubic when $\eta = 0$.

There are other strategies for an improvement of the zero order θ . For example, we may use the θ_o determined by Eq. 6.6.10 for calculating F_1 , F_2 , F_3 , F_4 and $\frac{dF_1}{d\eta}$, $\frac{dF_3}{d\eta}$ for use in the right hand side of Eq. 6.6.9 and obtain an explicit expression for the new θ instead of the implicit one outlined above. We can also use the value of θ_o from Eq. 6.6.10 for calculating $\frac{dF_1}{d\eta}$ and $\frac{dF_3}{d\eta}$ eliminating the $\frac{d\theta}{d\eta}$ terms and obtain a cubic equation to solve at each η . Obviously the variations are endless.

If ϵ^* is small, we would expect that the resulting values of $\theta(\eta)$ would produce an improved result from the zero order solution. Actually this is not necessarily true. It has been found that where θ_o was fortuitously good, the θ obtained using first order corrections yielded a less exact result but still quite accurate. The value of ξ^* however improved considerably. Hence we conclude that the solution obtained exhibits an overall improvement although θ_o is slightly less accurate. This must be true since we are not only using the values of the variables at the shock, but their slopes at the shock as well.

In principle we can endlessly improve θ by taking more terms in the variable expansions (i.e., Eq. 6.6.22) about the shock. If terms up to ϵ^n are taken we must first solve an m'th order polynomial for ϵ^*. Then upon substitution into Eq. 6.6.9 an m'th order differential equation for θ with respect to η is obtained. It is seen however, that if $\eta > 2$.

the procedure would become somewhat unwieldy.

In some flow problems such as explosions in the atmosphere, where the density has an exponential behavior with altitude, it is seen that the geometry of the situation is somewhat intermediate between planar and spherical. We may represent this effect qualitatively by writing the basic conservation equations as

$$\frac{\partial \rho}{\partial t} + u\frac{\partial \rho}{\partial r} + \rho\frac{\partial u}{\partial r} + \rho\frac{u}{A}\frac{\partial A}{\partial r} = 0$$

$$\frac{\partial u}{\partial t} + u\frac{\partial u}{\partial r} + \frac{1}{\rho}\frac{\partial p}{\partial r} = 0 \qquad (6.6.32)$$

$$\frac{\partial p}{\partial t} + u\frac{\partial p}{\partial t} + \partial p\frac{\partial u}{\partial r} + \partial\frac{\rho u}{A}\frac{\partial A}{\partial r} = 0$$

where we assume that the flow is unidimensionally uniform but with the flow proceeding into a varying cross-sectional area.

Setting the density of the undisturbed medium to the ρ_∞, where

$$\rho_\infty = \rho_0 \, e^{\alpha r} \qquad (6.6.33)$$

and assuming that A has the form

$$A = A_0 \, e^{k\alpha r} \qquad (6.6.34)$$

it is seen that we must have $\alpha < 0$ and $k > 0$ in order to roughly correspond to the model considered - that is ρ_∞ decreases and A increases with altitude (or increasing r).

The variables of Eq. 6.6.32 are now made dimensionless by the transformations

$$\psi = \rho/\rho_\infty \; , \quad \phi = u/\dot{R}_s \; , \quad f = p/(\rho_0\dot{R}_s^2)$$

$$\xi = \alpha(r-R_s) \; , \quad R_s = R_s(t) \qquad (6.6.35)$$

yielding the transformed equations as

$$(\phi \cdot)\frac{\partial \psi}{\partial \xi} + \psi \frac{\partial \psi}{\partial \xi} + \psi(\cdots) \quad - \quad \frac{\partial \psi}{\partial \lambda}$$

$$(\phi \cdot)\frac{\partial \phi}{\partial \xi} + \phi \frac{\partial \psi}{\partial \xi} + \xi + \psi \quad - \quad \frac{\partial \phi}{\partial \lambda} \qquad (6.6.36)$$

$$\phi \frac{\partial \psi}{\partial \xi} + \psi \frac{\partial \psi}{\partial \xi} + \xi \psi + \cdots \quad - \quad \frac{\partial \psi}{\partial \lambda}$$

where

$$\gamma - \frac{\ddot{\lambda}}{\dot{\lambda}} \qquad (6.6.37)$$

Defining $\omega - 1/\dot{\lambda}^2$, we then have

$$\frac{1}{\lambda} \frac{\partial}{\partial \lambda} - \omega T \omega \frac{\partial}{\partial \tau} \qquad (6.6.38)$$

Hence we may also replace the right hand terms of Eq. 6.6.36 by $\omega T \omega \frac{\partial}{\partial \tau}$

For strong shocks we have the boundary conditions at the shock $\xi = 0$

$$\psi(0) = \frac{\mu+1}{\gamma-1} , \qquad \phi(0) - \phi(0) - \frac{2}{\gamma+1} \qquad (6.6.39)$$

and since the right hand sides of Eq. 6.6.36 are zero we obtain a similarity solution valid near the shock. The equations are integrated from the shock for $\xi > 0$. We encounter again a singularity at $\xi = \xi^*$ where

$$\phi(\xi^*) + \left(\psi(\xi^*)/\psi(\xi^*) \right)^{\frac{1}{2}} = 1 \qquad (6.6.40)$$

As before, this suggests that one chooses T until a smooth crossing is obtained. This regularity condition is best seen by writing the Eq. 6.6.36 in characteristic forms which read

$$(\phi \cdot)\frac{\partial S}{\partial \xi} - 2T\phi \frac{\partial S}{\partial \tau} + 2TS - \phi S(\gamma-1) = 0 \qquad (6.6.41)$$

$$(\phi - 1 - \beta)\left[\frac{\partial \phi}{\partial \xi} - (\gamma k \omega)^2 \frac{\partial^2 \phi}{\partial \xi^2}\right] - 2\tau\left(\frac{\partial \phi}{\partial \xi} - (\gamma k \omega)^2 \frac{\partial^2 \phi}{\partial \xi^2}\right)$$

$$+ \frac{\beta^2}{\delta} + \tau(\phi - 2\frac{\beta}{\delta}) - \frac{\phi \beta}{\delta}(1 + \gamma k) \quad = 0 \qquad (6.6.42)$$

$$(\phi - 1 + \beta)\left[\frac{\partial \phi}{\partial \xi} + (\gamma k \omega)^2 \frac{\partial^2 \phi}{\partial \xi^2}\right] - 2\tau\left[\frac{\partial \phi}{\partial \xi} + (\gamma k \omega)^2 \frac{\partial^2 \phi}{\partial \xi^2}\right]$$

$$+ \frac{\beta^2}{\delta} + \tau(\phi + 2\frac{\beta}{\delta}) + \frac{\phi \beta}{\delta}(1 + \gamma k) \quad = 0 \qquad (6.6.43)$$

where

$$\delta = \phi/4\gamma \quad , \quad \beta^2 = \gamma \phi/4 \qquad (6.6.44)$$

From Eq. 6.6.43, when $\phi + \beta - 1$ at $\xi = \xi^*$, we may solve for τ yielding

$$\tau = \left. \frac{-\left[\frac{\beta^2}{\gamma} + \frac{\phi \beta}{\delta}(1 + \gamma k)\right]}{\phi + \frac{2\beta}{\delta} - 2\tau\left[\frac{\partial \phi}{\partial \xi} + (\gamma k \omega)^2 \frac{\partial^2 \phi}{\partial \xi^2}\right]} \right|_{\xi = \xi^*} \qquad (6.6.45)$$

For strong shocks, we obtain as the zero approximation

$$\tau_0 = \frac{\frac{\beta(1)}{\gamma}(\beta(1) + \phi(1) + \gamma k \phi(1))}{\phi(1) + \frac{2}{\gamma}\beta(1)} \qquad (6.6.46)$$

Using $\phi^* + \beta^* = 1$, we may also approximate τ_0 by

$$\tau_0 = \frac{-\frac{\beta(1)}{\gamma}(1 + k\gamma)\phi(1)}{\phi(1) + \frac{2}{\gamma}\beta(1)} \qquad (6.6.47)$$

or

$$T_0 = \frac{-\frac{\beta(1)}{\gamma}\left(1 + \frac{\gamma k \phi(1)}{\phi(1) + \beta(1)}\right)}{\phi(1) + \frac{2}{\gamma}\beta(1)} \qquad (6.6.48)$$

The form given by Eq. 6.6.48 was used by Hayes in his recent work on shock motion in an exponential atmosphere.

BIBLIOGRAPHY

Chapter I PHYSICS OF EXPLOSIONS

1. Bach, G.G.,
Knystautas, R. and
Lee, J.H.
"Direct Initiation of Spherical Detona-
tions in Gaseous Explosives"
Proc. 12th Symposium (International) on
Combustion, Poitiers, July 1968,
The Combustion Institute, Pittsburgh,
853 (1969).

2. Belokon, V.A.,
Petrukhin, A.I. and
Proskuryakov, V.A.
"Entrance of a Strong Shock Wave into a
Wedge-Like Cavity"
Sov. Phys. - JETP 21. 33 (1965).

3. Bone, W.A.,
Fraser, R.P. and
Wheeler, W.H.
"A Photographic Investigation of Flame
Movements in Gaseous Explosions. Part 7.
The Phenomenon of Spin in Detonation"
Phil. Trans. Roy. Soc. (London),
235(A), 29 (1936).

4. Campbell, C. and
Woodhead, D.W.
"Striated Photographic Records of
Explosion Waves"
J. Chem. Soc. 130, 1572 (1927).

5. Campbell, C. and
Finch, A.C.
"Striated Photographic Records of
Explosion Waves, Part II. An Explana-
tion of the Striae"
J. Chem. Soc. 131, 2094 (1928).

6. Courant, R. and
Friedrichs, K.O.
Supersonic Flow and Shock Waves
Chap. 3, Sec. E, Interscience, 1948.

7. Denisov, Yu. N. and
Troshin, Ya. K.
"On the Mechanisms of Detonative
Combustion"
Proc. 8th Symposium (International) on
Combustion, Pasadena, 1960,
Williams and Wilkins Co., Bal'... re,
660 (1962).

8. Doring, W.
"Uber den Detonationsvorgang in Gasen"
Ann. Physik 43, 421 (1943).

9. Duff, R.E.
"Investigation of Spinning Detonation
and Detonation Stability"
Phys. Fluids 4, 1427 (1961).

10. Duff, R.E. and
Finger, M.
"Stability of a Spherical Gas Detonation"
Phys. Fluids 8, 764 (1965).

11. Fay, J.A.
"A Mechanical Theory of Spinning Detona-
tion"
J. Chem. Phys. 20, 942 (1952).

12. Jouguet, E.   La Mecanique des Explosifs
                                   Ed. Doin, Paris, 359 (1917).

13. Knystautas, R.   "An Experimental Study of Spherical
                                   Gaseous Detonation Waves"
                                   US AFOSR Rep. 69 - 1330 TR.

14. Knystautas, R. and   "Spark Initiation of Converging
    Lee, J.H.   Detonation Waves"
                                   AIAA J. $\underline{5}$, 1209 (1967).

15. Laffitte, P.   "L'Onde Explosive Spherique"
                                   Ann. de Phys., 10e Serie 4, 645 (1925).

16. Lee, J.H.,   "Two-Dimensional Unconfined Gaseous
    Lee, B.H.K. and   Detonation Waves"
    Shanfield, I.   Proc. 10th Symp. (International) on
                                   Combustion, Cambridge, 1964,
                                   The Combustion Institute, Pittsburgh,
                                   805 (1965).

17. Lee, J.H.,   "Direct Initiation of Cylindrical
    Lee, B.H.K. and   Gaseous Detonations"
    Knystautas, R.   Phys. Fluids $\underline{9}$, 221 (1966).

18. Lee, B.H.K.,   "Transmission of Detonation Waves Through
    Lee, J.H. and   Orifices"
    Knystautas, R.   AIAA J. $\underline{4}$, 365 (1966).

19. Lee, J.H.   "The Propagation of Shocks and Blast
                                   Waves in a Detonating Gas"
                                   Mechanical Engineering Research Labora-
                                   tory Rep. 65-1, McGill University (1965).

20. Manson, N. and   "Contribution to the Study of Spherical
    Ferrie, F.   Detonation Waves"
                                   Proc. 4th Symp. (International) on
                                   Combustion, MIT, 1952, Williams and
                                   Wilkins Co., Baltimore, 486 (1953).

21. Manson, N.   "Propagation des Detonations et des
                                   Deflagrations dans les Melanges Gaseux"
                                   Compt. Rend. $\underline{222}$, 46 (1946).

22. Urtiew, P.A. and   "Experimental Observations of the Trans-
    Oppenheim, A.K.   ition to Detonation in an Explosive Gas"
                                   Proc. Roy. Soc. $\underline{A295}$, 13 (1966).

23. Perry, R.W. and   "The Production and Stability of Converg-
    Kantrowitz, A.   ing Shock Waves"
                                   J. Appl. Phys. $\underline{22}$, 878 (1951).

24. Rae, W.J.   "Non-Similar Solutions for Impact-Generated
                                   Shock Propagation in Solids"
                                   Cornell Aero. Lab. Rep. AI-1821-A-2,
                                   NASA CR-54251 (1965).

25. Schott, G.L. "Observations of the Structure of Spinning Detonations"
Phys. Fluids $\underline{8}$, 850 (1965).

26. Sedov, L.I. Similarity and Dimensional Methods in Mechanics
Academic Press Inc., New York, 1959.

27. Shchelkin, K.I. and "Gas Dynamics of Combustion"
Troshin, Y.K. NASA TTF-231, 67 (1964).

28. Soloukhin, R.I. Shock Waves and Detonations in Gases
Mono Book Corp., Baltimore, 138 (1966).

29. Taylor, G.I. "The Dynamics of the Combustion Products Behind Plane and Spherical Detonation Fronts in Explosives"
Proc. Roy. Soc. $\underline{200(A)}$, 235 (1950).

30. Von Neumann, J. "Progress Report on Theory of Detonation Waves"
OSRD, 549, 1942; also Collected Works, 203, Vol. 6.

31. Dove, J.E. and "A Photographic Investigation of the
Wagner, H. Gg. Mechanisms of Spinning Detonation"
Proc. 8th Symp. (International) on Combustion, Pasadena, 1960, Williams and Wilkins Co., Baltimore, 589 (1962).

32. White, D.R. "Turbulent Structure of Gaseous Detonation"
Phys. Fluids $\underline{4}$, 465 (1961).

33. Zababakhin, E.I. "Cumulation of Energy and its Limits"
Soviet Phys. - Uspekhii $\underline{8}$, 295 (1965)

34. Zeldovich, Ya. B. and Theory of Detonation
Kompaneets, A.S. Academic Press, 1960.

35. Zeldovich, Ya. B. "An Experimental Investigation of
Kogarko, S.M. and Spherical Detonation of Gases"
Simonov, N.N. Soviet Phys. - Tech. Phys. (JETP) $\underline{1}$, 1689 (1956)

36. Zeldovich, Ya. B. "Theory of Propagation of Detonation Waves In Gaseous Systems"
NACA Tech. Memo. 1261, 1950.

37. Zeldovich, Ya. B. "Converging Cylindrical Detonation Wave"
Soviet Phys. - JETP $\underline{9}$, 550 (1959).

Chapter II   BASIC EQUATIONS, BOUNDARY CONDITIONS AND SIMILARITY
TRANSFORMATIONS

1. Korobeinikov, V.P.   "Teoriya Tochechnogo Vzryva (The Theory
    Mel'nikova, N.S. and   of Point Explosions)", Moscow, 1961,
    Ryazancv, Ye. V.   pp 3-330; Transl. U.S. Dept. of Commerce,
                               FPRS: 14, 334, Washington, D.C., July 1962

2. Lee, B.H.K.   "Non-Similar Solutions of Imploding Shocks
                               and Detonations"
                               Ph.D. Thesis, McGill University Report No.
                               66-1, (Dept. of Mechanical Engineering),
                               Montreal, Quebec (Feb 1966).

3. Lee, J.H.S.   "The Propagation of Shocks and Blast
                               Waves in a Detonating Gas"
                               Ph.D. Thesis, McGill University Report No.
                               65-1 (Dept. of Mechanical Engineering),
                               Montreal, Quebec (March 1965).

4. Lees, L. and   "Inviscid Hypersonic Flow over Blunt-
    Kubota, T.   Nosed Slender Bodies"
                              J. Aeronaut. Sci. $\underline{24}$, 195-202 (1957).

5. Mirels, H.   "Hypersonic Flow Over Slender Bodies
                               Associated with Power Law Shocks"
                               Advances in Applied Mechanics, Vol. III,
                               Academic Press, New York (1962).

6, Oswatitsch, K.   Gas Dynamics
                              (Transl. by Kuerti, G.), pp 168-172,
                               Academic Press, New York, 1956.

7. Rae, W.J.   "Analytical Studies of Impact-Generated
                               Shock Propagation Survey and New Results"
                               Cornell Aeronautical Laboratory Report
                               CAL No. A1-2456-A-1, Cornell University,
                               Buffalo, New York (June 1968).

8. Rae, W.J.   "Nonsimilar Solutions for Impact-Generated
                               Shock Propagation in Solids"
                               Cornell Aeronautical Laboratory Report
                               CAL No. AI-1821-A-2 (NASA Report No.
                               CR-54251), Cornell University, Buffalo,
                               New York (March 1965).

9. Rae, W.J. and   "Final Report on a Study of Meteoroid
    Kirchner, H.P.   Impact Phenomena"
                              Cornell Aeronautical Laboratory Report,
                               CAL No. RM-1655-M-4, Cornell University,
                               Buffalo, New York (Feb. 1963).

10. Sedov, L.I.   "Similarity and Dimensional Methods in
                               Mechanics"
                               Chapter IV, Academic Press, New York (1959)

11. Taylor, G.I.
"The Formation of a Blast Wave by a
Very Intense Explosion, I, Theoretical
Discussion"
Proceedings of the Royal Society (A)
Vol. 201, pp 159-174 (1950).

12. Zel'dovich, Ya. B. and
Raizer, Yu. P.
"Physics of Shock Waves and High
Temperature Hydrodynamic Phenomena"
(Edited by Hayes, W.D. and Probstein,
R.F.) Vols. I and II, Academic Press,
New York (1967).

Chapter III   ISENTROPIC SELF-SIMILAR MOTIONS

1. Glass, I.I.
"Shock Tubes, Part I: Theory and
Performance of Simple Shock Tubes"
UTIA Review No. 12 (May 1958).

2. Jouguet, E.
"Mechaniques des Explosifs"
O. Doin et Fils, Paris (1917).

3. Keller, J.B.
"Spherical, Cylindrical and One-
Dimensional Gas Flows"
Quart. Appl. Math. Vol. 14, No. 2,
p 171 (1956).

4. Lee, J.H.
Lee, B.K. and
Shanfield, I.
"Two-Dimensional Unconfined Gaseous
Detonation Waves"
Proc. of Tenth Symposium (International)
on Combustion, pp 805-815, Published by
the Combustion Institute, Pittsburgh,
Penn. (1954).

5. Lee, J.H.
"The Propagation of Shocks and Blast
Waves in a Detonating Gas"
Ph.D. Thesis, McGill University Report
No. 65-1 (Dept. of Mechanical Engineering),
Montreal, Quebec (March 1965).

6. Lee, J.H.
"Inviscid Hypersonic Flow of a Detonating
Gas"
Paper presented at the CASI Astronautics
Symposium, Toronto, Ontario (Feb. 1965).

7. Mirels, H. and
Mullens, J.F.
"Expansion of Gas Clouds and Hypersonic
Jets Bounded by a Vacuum"
AIAA Journal, Vol. 1, No. 3, p 596 (1963).

8. Sedov, L.I.
"Detonation in Media of Variable Density"
Proc. of Sixth Symposium (International)
on Combustion, pp 639-641, Rienhold Publish-
ing Corp., New York (1956).

9. Taylor, G.I.   "Dynamics of the Combustion Products Behind Planar and Spherical Detonation Fronts in Explosives" Proc. Roy. Soc. A, Vol. 200, 235   (1950).

Chapter IV NON-ISENTROPIC SELF-SIMILAR MOTIONS: THE STRONG BLAST WAVE PROBLEM

1. Korobeinikov, V.P., Mel'nikova, N.S. and Ryazanov, Ye. V.   "Teoriya Tochechnogo Vzryva (The Theory of Point Explosions)" Moscow, 1961, pp 3-330, Transl. U.S. Dept. of Commerce, FPRS: 14, 334, Washington, D.C. (July 1962).

2. Latter, R.   "Similarity Solution for a Spherical Shock Wave" J. Appl. Phys., Vol. 26, pp 954-960 (1955).

3. Lees. L. and Kubota, T.   "Inviscid Hypersonic Flow over Blunt-Nosed Slender Bodies" Journal of the Aeronautical Sciences Vol. 24, pp 195-202 (1957).

4. Lin, S.C.   "Cylindrical Shock Waves Produced by Instantaneous Energy Release" J. Appl. Phys. Vol. 25, No. 1, pp 54-57 (1954).

5. Mirels, H.   "Hypersonic Flow Over Slender Bodies Associated with Power Law Shocks" Advances in Applied Mechanics, Vol. III, Academic Press, New York (1962).

6. Sakurai, A.   "An Exact Solution of the Blast-Wave Problem" J. Phys. Soc. Japan Vol. 10, pp 827-828 (1955).

7. Sedov, L.I.   "Similarity and Dimensional Methods in Mechanics" Chapter IV, Academic Press, New York (1959).

8. Taylor, G.I.   "The Formation of a Blast Wave by a Very Intense Explosion, I, Theoretical Discussion" Proc. Roy. Soc. Series A, Vol. 201, pp 159-174 (1950). "II, The Atomic Explosion of 1945", Proc. Roy. Soc. Series A, Vol. 201, pp 175-186 (1950).

9. Taylor, J.L.   "An Exact Solution of the Spherical Blast-Wave Problem" Phil. Mag. Vol. 46, pp 317-320 (1955).

10. Von Neumann, J.   "The Point Source Solution"
                                   The Collected Works of J. Von Neumann,
                                   Vol. IV, Pergamon Press, New York (1961).

Chapter V   NON-SIMILAR SOLUTIONS FOR BLAST WAVES

1. Bach, G.G.,   "Direct Initiation of Spherical Detona-
    Knystautas, R. and   tions in Gaseous Explosives"
    Lee, J.H.   Proc. of the Twelfth Symposium (Interna-
                                   tional) on Combustion, pp 853-864, The
                                   Combustion Institute, Pittsburgh, Penn.
                                   (1969)

2. Bach, G.G. and   "Higher Order Perturbation Solutions for
    Lee, J.H.   Blast Waves"
                                   AIAA Journal, Vol. 7, No. 4, pp 742-744
                                   (1969).

3. Bach, G.G. and
    Lee, J.H.   "Shock Propagation in Solid Media"
                                   Paper No. 67-141 presented at the AIAA
                                   5th Aerospace Sciences Meeting in New
                                   York, January 1967.

4. Bach, G.G. and   "An Analytical Solution for Blast Waves"
    Lee, J.H.   AIAA Journal (In Press).

5. Bethe, H.A.,   "Blast Wave"
    Fuchs, K.,   Los Alamos Scientific Laboratory Report
    Hirshfelder, J.O.,   No. LA-2000 (Aug. 1947); (Available from
    Magee, J.L.,   CFSTI).
    Peierls, R.E. and
    Von Neumann, J.

6. Chernyi, G.G.   "Asymptotic Law of Propagation of a
                                   Plane Detonation Wave"
                                   Soviet Physics-Doklady, Vol. 12, No. 1,
                                   pp 21-22 (July 1967).

7. Korobeinikov, V.P.,   "Teoriya Tochechogo Vzryva (The Theory of
    Mel'nikova, N.S. and   Explosions)"
    Ryazanov, Ye. V.   Moscow, 1961, pp 3-330, Transl. U.S. Dept.
                                   of Commerce, FPRS: 14, 334, Washington,
                                   D.C. (July 1962).

8. Lee, B.H.K.   "Non-Similar Solutions of Imploding Shocks
                                   and Detonations"
                                   Ph.D. Thesis, McGill University Report No.
                                   66-1 (Dept. of Mechanical Engineering),
                                   Montreal, Quebec (Feb. 1966).

9   Lee, B.H.K.   "Non-Uniform Propagation of Imploding
                                   Shocks and Detonations"
                                   AIAA Journal, Vol. 5, No. 11, pp 1997-
                                   2003 (Nov. 1967).

10. Lee, J.H.

"The Propagation of Shocks and Blast
Waves in a Detonating Gas"
Ph.D. Thesis, McGill University Report
No. 65-1 (Dept. of Mechanical Engineer-
ing) Montreal, Quebec (March 1965).

11. Lee, J.H.

"Inviscid Hypersonic Flow of a Detonating
Gas"
Paper presented at the CASI Astronautics
Symposium, Toronto, Ontario (Feb. 1965).

12. Levin, V.A. and
    Chernyi, G.G.

"Asymptotic Laws of Behavior of Detonation
Waves"
PMM Vol. 31, No. 3, pp 393-405 (1967).

13. Oshima, K.

"Blast Waves Produced by Exploding Wire"
Aeronaut. Res. Inst., University of Tokyo,
Report No. 358 (July 1960).

14. Oshima, K.

"Blast Waves Produced by Exploding Wires"
Exploding Wires (Ed. by W.G. Chace and H.K.
Moore, Plenum Press, New York, 1962), Vol.
2, pp 159-180.

15. Porzel, F.B.

"Height of Burst for Atomic Bombs, Part I,
The Free Air Curve"
Los Alamos Scientific Laboratory Report
LA-1664 (May 1954). Declassified Sept. 1,
1960.

16. Rae, W.J.

"Non-Similar Solutions for Impact Generated
Shock Propagation in Solids"
Cornell Aeronautical Laboratory Report CAL
No. AI-1821-A-2 (NASA Report No. CR-54251)
Cornell University, Buffalo, New York
(March 1965).

17. Sakurai, A.

"On the Propagation and Structure of the
Blast Wave, Part I"
Journal of the Physical Society of Japan,
Vol. 8, No. 5, pp 662-669 (1953).

18. Sakurai, A.

"On the Propagation and Structure of the
Blast Wave, Part II"
Journal of the Physical Socity of Japan,
Vol. 9, No. 2, pp 256-266 (1954).

19. Sedov, L.I.

"Similarity and Dimensional Methods in
Mechanics"
Chapter IV, Academic Press, New York (1959).

20. Swigart, R.J.

"Third-Order Blast Theory and its Applica-
tion to Hypersonic Flow Past Blunt-Nosed
Cylinders"
Journal of Fluid Mechanics, Vol. 9, pp 613
620 (1960).

21. Zaker, T.A.   "Point Source Explosion of a Solid"
                                   Armour Research Foundation, Illinois Inst.
                                   of Tech. Report ARF 4132-6 (Nov. 1959).

Chapter VI   ASYMPTOTIC SELF-SIMILAR MOTION

1. Akinsete, V.A.   "Hydrodynamics of a Spherical Cavity
                                   Collapsing in a Liquid"
                                   Ph.D. Thesis, McGill University Report No.
                                   68-1 (Mechanical Engineering Dept.),
                                   Montreal, Quebec (April 1968).

2. Akinsete, V.A. and   "Non-Similar effects in the Collapsing of
    Lee, J.H.   an Empty Spherical Cavity in Water"
                                   The Physics of Fluids, Vol. 12, No. 2,
                                   pp 428-434 (1969).

3. Bach, G.G. and   "Initial Propagation of Impulsively
    Lee, J.H.   Generated Converging Cylindrical and
                                   Spherical Shock Waves"
                                   Journal of Fluid Mechanics Vol. 37, Part
                                   3, pp 513-528 (1969).

4. Bruschlinskii, K.V. and   "On Auto-Models in the Solution of
    Kazhdan, Ja. M.   Certain Problems of Gas Dynamics"
                                   Russian Mathematical Surveys, Vol. 18,
                                   No. 2, pp 1-22 (1963).

5. Chester, W.   "The Quasi-Cylindrical Shock Tube"
                                   Phil. Mag. Series 7, Vol. 45, pp 1293
                                   1301 (1954).

6. Chisnell, R.F.   "The Motion of a Shock Wave in a Channel
                                   With Applications to Cylindrical and
                                   Spherical Shock Waves"
                                   Journal of Fluid Mechanics, Vol. 2, pp 286-
                                   298 (1957).

7. Colgate, S.A. and
    Johnson, M.H.   "Hydrodynamic Origin of Cosmic Rays"
                                   Phys. Rev. Letters, Vol. 5, pp 235-238
                                   (1960).

8. Gandel'man, G.M. and   "Shock Wave Emergence at a Stellar Surface"
    Frank-Kamenetskii, D.A.   Soviet Physics, Doklady, Vol. 1, pp 223-226
                                   (1956).

9. Habashi, W.G.   "A Theoretical Investigation of the Propa-
                                   gation of Shocks and Imploding Blast Waves
                                   in a Decreasing Density Field"
                                   M.Eng. Thesis, McGill University, Dept. of
                                   Mechanical Engineering, Montreal, Quebec
                                   (April 1969).

10. ...ll, H. and   "Cavitation Bubble Collapse in Water With
     Swaile, N.J.   Finite Density Behind the Interface"
                            Physics of Fluids, Vol. 6, No. 4, pp 571-
                            577 (1963).

11. Hunter, C.   "On the Collapse of an Empty Cavity in
                            Water"
                            Journal of Fluid Mechanics, Vol. 10
                            pp 241-261 (1960).

12. Lamb, Sir Horace   "Hydrodynamics"
                            6th Edition, p 122, Dover Publications,
                            New York (1945).

13. Lee, B.H.K.   "Non-Similar Effects of Imploding Shocks
                            and Detonations"
                            McGill University Report No. 66-1
                            (Mechanical Engineering Dept.) Montreal,
                            Quebec (Feb. 1966).

14. Lee, B.H.K.   "Non-Uniform Propagation of Imploding
                            Shocks and Detonations"
                            AIAA Journal, Vol. 5, No. 11, pp 1997-
                            2003 (Nov 1967).

15. Rae, W.J. and   "Final Report on a Study of Meteoroid
     Kirchner, H.P.   Impact Phenomena"
                            Cornell Aeronautical Laboratory Report
                            RM-1655-M-4, Cornell University, Buffalo,
                            New York (Feb. 1963).

16. Rae, W.J.   "Analytical Studies of Impact-Generated
                            Shock Propagation Survey and New Results"
                            Cornell Aeronautical Laboratory Report
                            AL-2456-A-1. Cornell University, Buffalo,
                            New York (June 1968).

17. Sakurai, A.   "On the Problem of a Shock Wave Arriving
                            at the Edge of a Gas"
                            Communications in Pure and Applied Math
                            ematics, Vol. 13, pp 353-370 (1960).

18. Whitman, G.B.   "On the Propagation of Shock Waves Through
                            Regions of Non-Uniform Area in Flow"
                            Journal of Fluid Mechanics, Vol. 4,
                            pp 337-360 (1958).

19. Zel'dovich, Ya. B. and "Physics of Shock Waves and High Temper-
     Raizer, Yu. P.   ature Hydrodynamic Phenomena"
                            Vol. II, Edited by W.D. Hayes and R.F.
                            Probstein, Academic Press, New York (1967).

DOCUMENT CONTROL DATA - R & D

1. ORIGINATING ACTIVITY (Corporate author)	2a. REPORT SECURITY CLASSIFICATION
McGill University Department of Mechanical Engineering Montreal 110, P.Q., Canada	UNCLASSIFIED
	2b. GROUP

3. REPORT TITLE

THEORY OF EXPLOSIONS

4. DESCRIPTIVE NOTES (Type of report and inclusive dates)

Scientific   Interim

5. AUTHOR(S) (First name, middle initial, last name)

John H. Lee

Romas Knystautas

Glen G. Bach

6. REPORT DATE	7a. TOTAL NO. OF PAGES	7b. NO. OF REFS
November 1969	191	108

8a. CONTRACT OR GRANT NO. AF-AFOSR 1290-67	9a. ORIGINATOR'S REPORT NUMBER(S)
8. PROJECT NO. 9711-01	MERL 69-10
61102F	9b. OTHER REPORT NO(S) (Any other numbers that may be assigned this report)
681308	AFOSR 69-1090TR

10. DISTRIBUTION STATEMENT

1. This document has been approved for public release and sale; its distribution is unlimited.

11. SUPPLEMENTARY NOTES	12. SPONSORING MILITARY ACTIVITY
TECH, OTHER	AF Office of Scientific Research (SREP) 1400 Wilson Boulevard Arlington, Virginia

13. ABSTRACT

The report starts out by discussing the Physics of Explosions in terms of physical concepts and experimental observations. Close affinity between explosion and implosion phenomena and gaseous detonation combustion is shown. The bulk of the report then presents the ground work for the theoretical study of explosions outlining the governing equations, boundary conditions and solutions of specific problems.

DD FORM 1473 (1 NOV 65)

KEY WORDS	LINK A		LINK B		LINK C	
	ROLE	WT	ROLE	WT	ROLE	WT
Explosions						
Chemical Explosions						
Gaseous Detonations						
Diverging Detonations						
Imploding Detonations						
Detonation Structure						
Reactive Blast Waves						
Analytical Solutions						
Laser Sparks						